1995

Characterisation of waxy gas-condensates by high temperature capillary gas chromatography and oxidative degradation

Heath, David John

CHARACTERISATION OF WAXY GAS-CONDENSATES BY HIGH TEMPERATURE CAPILLARY GAS CHROMATOGRAPHY AND OXIDATIVE DEGRADATION

by

DAVID JOHN HEATH

A thesis submitted to the University of Plymouth
in partial fulfilment for the degree of

DOCTOR OF PHILOSOPHY

Department of Environmental Sciences
Faculty of Science

In collaboration with
British Gas plc

March 1995

DECLARATION

I hereby certify that the work described in this thesis is my own, except where otherwise acknowledged, and has not been submitted previously for a degree at this, or any other, University.

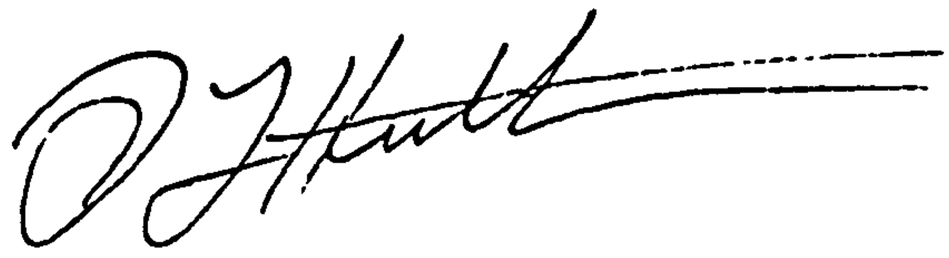

David John Heath

COPYRIGHT

To my Family

CHARACTERISATION OF WAXY GAS-CONDENSATES BY HIGH TEMPERATURE CAPILLARY GAS CHROMATOGRAPHY AND OXIDATIVE DEGRADATION

by
DAVID JOHN HEATH

ABSTRACT

High molecular weight (HMW) hydrocarbons (defined herein as C_{35+} compounds) are difficult to characterise by conventional analytical methods. Very few studies have reported precise and reproducible quantification of such compounds in fossil fuels. Nonetheless, such components have important effects on the physical and biological fate of fossil fuels in the geosphere. For example, the phase behaviour of waxy gas condensates is significantly affected by the varying proportions of HMW compounds. Similarly HMW compounds are amongst the most resistant petroleum components to biodegradation. The current study reports the development of reproducible quantitative high temperature capillary gas chromatography (HTCGC) methods for studying both these aspects of the chemistry of HMW hydrocarbons. In addition those hydrocarbons which remain unresolved when analysed by gas chromatography (so called unresolved complex mixtures UCMs) are also studied. UCMs may account for a large portion of the hydrocarbons in many fossil fuels yet very little is known about their composition. Knowledge of these compounds may be important in enhancing the prediction of phase behaviour. Oxidative degradation and GC-MS is used to elucidate the types of structures present within the UCM.

The concentrations of C_{35+} hydrocarbons in two unusually waxy gas condensates from high temperature wells in the North Sea were determined by HTCGC. The whole C_{35+} fraction comprised about 20% of the total hydrocarbons and consisted of compounds with carbon numbers extending up to and beyond C_{80}. By paying particular attention to sample dissolution and injection, good reproducibility and precision were obtained. For example, for authentic *n*-C_{20} to *n*-C_{60} alkanes a relative standard deviation of under 5% for manual injection, linear response factors (1.01 C_{20} to 0.99 C_{60}), and a linear calibration for 5 ng to 25 ng on-column were found. Limits of detection are reported for the first time for HMW *n*-alkanes. The limits were found to be as low as 0.8 ng for C_{20} to 1.87 ng for C_{60}. Tristearin is proposed as a suitable HTCGC internal standard for quantification since the FID response factor (1.1) was close to that of the HMW *n*-alkanes and response was linear. Importantly, when co-injected with the two waxy North Sea condensates, tristearin was adequately separated from the closest eluting alkanes, *n*-C_{59} and *n*-C_{60} under normal operating conditions. Qualitative characterisation of the HMW compounds in the waxy gas condensates and in synthetic wax blends (polywax 1000) using HTCGC-EI MS and HTCGC-CI MS produced molecular ions or pseudo molecular ions for *n*-alkanes up to *n*-C_{60}. The spectra of some HMW compounds contained fragment ions characteristic of branched compounds but detailed characterisation was very limited.

This study has also shown, for the first time, the significance of the unresolved complex mixture in gas condensates. UCM hydrocarbons accounted for over 20% of the total hydrocarbons in a waxy North sea condensate. The condensate was first distilled and the distillate UCMs isolated. These were found to be between 64 to 97% unresolved after molecular sieving (5Å) and urea adduction. The UCMs were oxidised using CrO_3/AcOH which produced 5-12% CO_2, and 55-83% dichloromethane-soluble products. Thus 65-94% of the original UCMs were accounted for as oxidation products. The remainder were thought to be water soluble acids which could not be determined in the presence of the AcOH reagent. Of the recovered oxidised products, 27-81% were resolved and these comprised mainly *n*-monocarboxylic acids (19-48%). The average chain length was found to be C_{12} indicating the average length of alkyl groups. Branched acids, ketones, ketoacids, *n*-dicarboxylic acids, branched dicarboxylic acids, lactones, isoprenoid acids, alkylcyclohexane carboxylic acids and toluic acids accounted for the majority of the remaining resolved products. The distillate UCMs all showed variations in amounts of products but not in composition. *Retro*-structural analysis suggested that the UCM in the gas condensate was mainly aliphatic and branched. The number of isomers of simple branched alkanes over the UCM molecular weight range (determined by cryoscopy) was calculated to be over 15000. Overall, oxidation provided structural information for about half of the UCM.

HTCGC was also used to measure the biodegradability of HMW alkanes in a waxy Indonesian oil. Traditional alkane isolation techniques (TLC and CC) discriminated against HMW compounds above C_{40} whereas adsorption onto alumina in a warm cyclohexane slurry provided an aliphatic fraction still rich in HMW compounds and suitable as a biodegradation substrate. A waxy Indonesian oil was subjected to 136 day biodegradation by *Pseudomonas fluorescens*. Extraction efficiencies of over 90% (RSD <5%) were obtained for *n*-alkanes up to C_{60} using continuous liquid-liquid extraction. Over 80% of the oil aliphatic fraction was degraded within 14 days. After 136 days only 14% of the original aliphatic fraction remained, yet surprisingly no decreases in the concentrations of compounds above C_{45} were observed. However, the use of a rapid screening biodegradation method proved conclusively that *Pseudomonas fluorescens* was capable of utilising *n*-alkanes up to C_{60} once the bacteria had acclimated to the HMW alkanes. This is the first report of bacterial utilisation of an *n*-alkane as large as C_{60}.

Preface

Gas chromatography is perhaps the single most important technique in routine use for the characterisation of hydrocarbon fluids. Modern capillary gas chromatography provides an efficient and quick method for identifying the many hundreds of compounds present in hydrocarbon fluids and is now widely applied throughout the petroleum industry. However, there remain at least two important limitations: (1) the analysis of high molecular weight compounds with boiling points greater than the operational temperature limit of conventional gas chromatography columns (*ca.* 310°C), and (2) the analysis of those mixtures of hydrocarbons which are not resolved into peaks (the so called unresolved complex mixtures UCMs). The scope of this Thesis is to address these limitations in the light of two contemporary fields of research.

Chapter 1 provides a general introduction to the importance of high molecular weight compounds (C_{35+}) in the prediction of phase behaviour of gas condensates and introduces the technique of high temperature capillary gas chromatography (HTCGC) for characterising high molecular weight hydrocarbons. The aim was to establish a quantitative and reproducible HTCGC (-MS) method for analysing the C_{35+} fraction. The results for two waxy gas condensates from high pressure and temperature wells in the North Sea are reported.

Chapter 2 gives an introduction to UCMs and summarises the few studies that have attempted previously to unravel the composition of this quantitatively important fraction (see **Rowland and Revill, 1995** for discussion). This chapter shows the quantitative significance of the UCM is in a North Sea condensate and attempts to elucidate the structures of unresolved hydrocarbons, using oxidative degradation (CrO_3/AcOH)

followed by conventional GC. Since current theories predict that even a low boiling point UCM will contain many hundreds of compounds, the gas condensate was first fractionated by vacuum distillation to provide a series of simpler UCM fractions which were oxidised and characterised. The results are presented and discussed in the context of possible precursor structures present in the UCM.

The second part of the Thesis (Chapter 3) is a study of the biological degradation of high molecular weight *n*-alkanes. Particular attention is paid to how these compounds may be altered while in the marine environment. The aims were: to isolate the aliphatic hydrocarbons of a waxy Indonesian crude oil and to study the rates of biodegradation of the *n*-alkanes up to hexacontane (C_{60}) using the quantitative HTCGC techniques developed in Chapter 1 to investigate the theory that Indonesian oils are the source of the tar balls and palaeo-tar balls found on the coasts of Australia **(McKirdy, 1994 and references therein)**. Particular emphasis was placed on validation of the techniques for reproducible recovery and analysis of C_{35+} *n*-alk1anes from the biodegradation medium. The results of the 136 day *in vitro* experiment are discussed. Such studies of high molecular weight waxes were not possible by GC prior to the advent of HTCGC.

Chapter 4 contains the experimental details to the methods used.

In Chapter Five, results from Chapters One, Two and Three are summarised and the final conclusions of the study given together with an appraisal of the techniques developed. Suggestions for further work are proposed.

CONTENTS

ACKNOWLEDGEMENTS

I would like to express my appreciation to Prof. Steve Rowland for his supervision and encouragement throughout the course of this study. I also owe a debt of gratitude to Dr C. Anthony Lewis who has given a great deal of his time and knowledge, providing support and ideas that have been invaluable and much appreciated.

I would also like to express my appreciation to the following people and organisations whose help contributed to making this work possible: my second supervisor Dr R. Lowry for his active encouragement, SERC and British Gas plc for funding and part funding this study, respectively, Mr Brian Moffatt my industrial supervisor and to the staff of the then PVT section, British Gas plc, London Research Station. Special thanks must go to the technical staff in the departments of Environmental Sciences and Biology, especially to Mr Ian Doidge for his time, patience and practical experience and also to Mr R. Srodzinski, Mr A. Arnold, Mr A. Tonkin, Mr R. Evens, Miss A. Goundry and Mrs J. Carter. Thanks are due to; Dr R. Moate (Electron Microscopy Centre, University of Plymouth) for use of the scanning electron microscope facility, Mr J. Carter (University of Bristol) for running the HTCGC-MS and Prof. J.R. Maxwell for allowing me to make use of the NERC mass spectrometry facility. Thanks to Dr D.M. McKirdy and Dr D. Padley (University of Adelaide) for kindly providing the Australian tar ball samples. A very special thanks for the help given by the members of the Petroleum and Environmental Geochemistry Group- Miss E.J. Wraige, Mr A.J. Revans, Mr D.A. Cooke, Mr K.V. Thomas, Mr R. Pemberton, Mr M.D. Ripley, Miss S. Neely and Miss H.F. Sturt. Thanks also to Miss N.G. Wilson for her advice on microbiology and to Mr E.M. Parsons for proof reading this thesis. Many of the ideas for this study have come from the work of other academics and I hope that I have acknowledged them accordingly. I would also like to say that I have been proud and fortunate to have worked with such good friends and colleagues (past and present) here at the University of Plymouth who have helped make the past seven years very enjoyable. Finally, a very special debt of gratitude is owed to my family for their support throughout all my education and to Ester for whom, in part, this work was completed.

ABBREVIATIONS AND SYMBOLS

AET	Atmospheric equivalent temperature
°C	Degrees Celsius
CC	Column chromatography
CI	Chemical ionisation
CFU	Colony forming unit
DCM	Dichloromethane
EI	Electron impact
EQS	Equations of State
FID	Flame ionisation detector
FIMS	Field ionisation mass spectrometry
GC	Gas chromatography
GC-MS	Gas chromatography-mass spectrometry
HMW	High molecular weight
hr	Hour
HTCGC	High temperature capillary gas chromatography
i.d.	Internal diameter
IR	Infrared
k_{bio}	Biological rate constant
KRI	Kovats retention indices
LMW	Low molecular weight
LOD	Limit of detection
mbbl	Million barrels
mg	Milligram (x 10^{-3} g)
ml	Millilitre (x 10^{-3} l)
m/z	Mass to charge ratio
μg	Microgram (x 10^{-6} g)
n.d.	Not determined
ng	Nanogram (x 10^{-9} g)
PTV	Programable temperature vapourisation injector
PVT	Pressure, volume and temperature (general term given covering reservoir fluid analyses)
RBF	Round bottom flask
RF	Relative response factor
RSD	Relative standard deviation
RT	Retention time
rpm	Revolutions per minute
SD	Standard deviation
SIM DIST	Simulated distillation
THF	Tetrahydrofuran
TIC	Total ion current chromatogram
TLC	Thin layer chromatography
UA	Urea adduct
UCM	Unresolved complex mixture
UCMox	Oxidised unresolved complex mixture
UNA	Urea non-adduct
UV	Ultraviolet spectroscopy
ZNA	Zeolite non-adduct

CHAPTER ONE

QUANTIFICATION OF THE C_{30+} FRACTION OF NORTH SEA GAS-CONDENSATES BY HIGH TEMPERATURE CAPILLARY GAS CHROMATOGRAPHY

Small amounts of high molecular weight (C_{30+}) hydrocarbons can have a significant effect on the phase behaviour of petroleum reservoir fluids. Until recently quantitative analysis of the C_{30+} hydrocarbon fraction has been beyond the scope of high resolution gas chromatography.

High temperature capillary gas chromatography is studied and shown to be a useful method for the quantitative determination of the high molecular weight hydrocarbons in the C_{30+} fraction of two waxy North Sea gas-condensates. The procedure shows good reproducibility (RSD <5%), linear FID response (1.00 to 0.99), and low limits of detection (0.8 - 1.9 ng) for C_{20-60} n-alkanes.

1.1 Introduction

1.1.1 General

Exploration of the North Sea by the oil and gas industry is expanding; a trend which is envisaged to continue into the late-1990's **(Quilan, 1991)**. Many of the new hydrocarbon finds hold considerable stocks of gas-condensate, adding to those condensate fields already under development and emphasising the importance of condensates as a future hydrocarbon reserve. For example, Bruce field, one of the largest being developed, was expected to reach peak production by 1994 with recoverable reserves estimated at 2.6 tcf of gas and 220 mbbl of condensate, and will produce 80,000 barrels of condensate per day **(Smith, 1991a)**. East Brae, a large gas/gas-condensate field already under development in the central North Sea, is estimated to yield 1.5 tcf of gas and 300 mbbl of liquids **(Smith, 1991b)**.

Discoveries in the central North Sea, particularly in the Norwegian Central Graben, have included high temperature and high pressure reservoirs in deep over pressurised Jurassic/Triassic plays **(Baller, 1991; Takla, 1992)**. These reservoirs are found at great depths, typically 3000 to 5000 metres, with high pressures up to 15,000 psi (higher in ultra high-pressure wells) and temperatures between 100 to 200°C. Development of these represented a major engineering challenge but is now under way. The high temperature and high pressure wells Embla and Lille-Frigg are estimated to hold recoverable reserves of 57 mbbl and 22 mbbl of condensate respectively **(Takla, 1992)**.

Gas condensates are defined by **Miles (1989)** as hydrocarbons which are in the gas phase at reservoir temperatures and pressures but which are liquids at the surface. They form during the later stages of catagenesis (the principal stage of oil formation), when the source rock hydrocarbons and remaining kerogen are converted to lighter hydrocarbons by the cracking of C-C bonds and methane becomes the dominant compound **(Tissot and Welte, 1984)**. Gas condensates can range in appearance from colourless to dark brown, with an average API of >45° **(Miles, 1989)** and generally comprise light hydrocarbons with boiling points in the gasoline range (C_5-C_{10}) **(Tříska**

et al., 1984).

The condensate produced from these high temperature and high pressure wells contains a greater proportion of high molecular weight (HMW) hydrocarbons (C_{30+} fraction) which results in condensates that are very waxy, comprising compounds with up to one hundred carbon atoms (**Moffatt pers. comm., 1991**). However this also means that a small reduction in reservoir pressure can precipitate substantial amounts of liquid hydrocarbons into the pores of the reservoir rock through a process known as retrograde condensation.

1.1.2 Retrograde condensation

A gas reservoir may be classed as a dry gas, wet gas or retrograde condensate gas reservoir (**Ahmed, 1989**). The differences between these can be represented best in the form of a phase diagram (Figure 1-1). For a single pure hydrocarbon there is a given pressure for every temperature at which the hydrocarbon fluid can exist as a liquid (Figure 1-1 A). In a hydrocarbon mixture, the system is no longer as simple and the single line representing the pressure - temperature relationship is replaced by a broad region in which the two phases, liquid and gas, can coexist (Figure 1-1 B). The Bubble Point curve represents the temperatures and pressures at which gas begins to leave the hydrocarbon fluid with decreasing pressure or increasing temperature while the Dew Point curve represents the pressures and temperatures at which liquid will start to form in the gas. The highest temperature at the phase envelope is called the cricondentherm, and the highest pressure is called the cricondenbar. At the critical point, properties of both gas and liquid mixtures are identical and the fluid is known as a supercritical fluid.

In the case of dry gas there are insufficient heavy hydrocarbons to produce a condensate even with a decrease in temperature (Figure 1-1 C).

For a wet gas (Figure 1-1 D), the temperature of the hydrocarbon mixture is above the critical condensing temperature and so a reduction in pressure will not cause condensation to occur until the temperature is reduced on reaching the surface (stock tank).

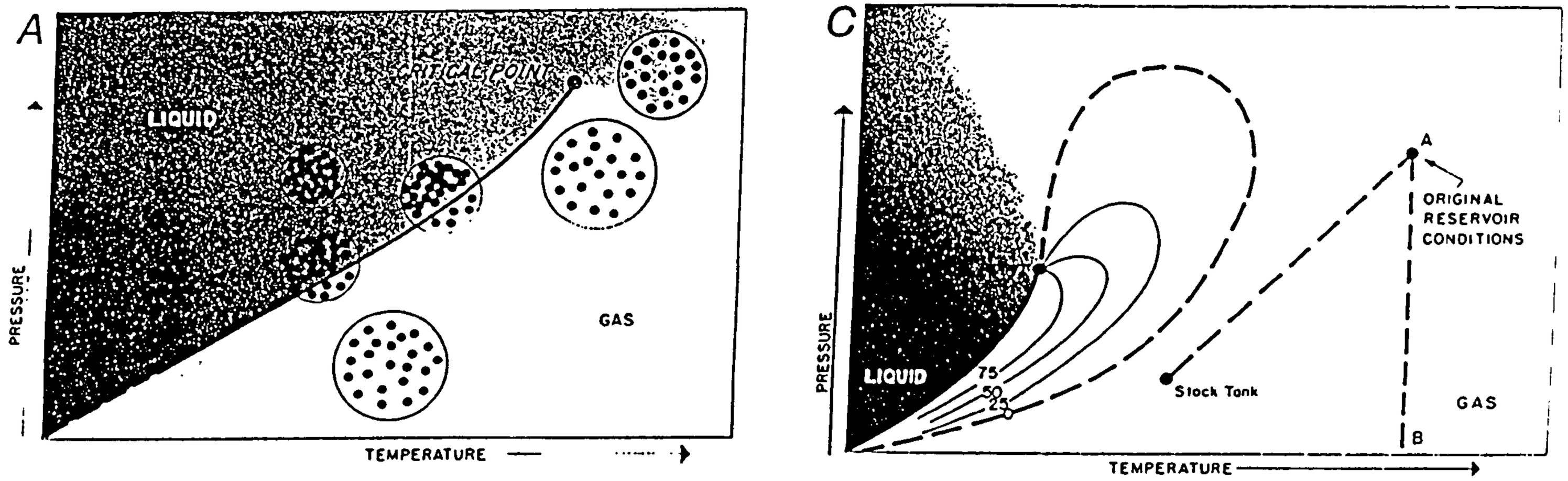

Figure 1-1 Phase diagram of: A) a pure hydrocarbon component, B) 50:50 mixture of two pure components, C) dry gas and D) wet gas (adapted from **Clark, 1969**).

In the case of a retrograde condensate, the hydrocarbon mixture exists between the critical point and the cricondentherm (Figure 1-2 a). So when pressure is decreased during production, instead of expanding (if a gas) or vaporizing (if a liquid), the reverse will happen. When pressure is reduced a condensate will form; this is known as retrograde condensation. The process is described more fully by **Clark (1969)** and is shown in Figure 1-2 b. Retrograde condensation is caused by forces acting on molecules of unlike sizes. As pressure drops (at constant temperature) below the dew point [A] (Figure 1-2 a) the attraction between light and heavy component molecules decreases because the light molecules gain more kinetic energy and start to move further apart. As this occurs the attraction between the heavy molecules becomes more effective; thus, these heavy molecules coalesce into a liquid. This process continues until a pressure is reached [B] where a maximum amount of liquid is formed. Further reduction in pressure permits the heavier hydrocarbons to gain more energy and overcome these forces and start to vaporise in the normal way until complete vaporisation occurs at pressure [C].

Clearly, if during production the reservoir pressure can be maintained above the dew point, retrograde behaviour will not occur and no condensate will be formed. Alternatively if a field is allowed to be depleted under its own natural energy, thus reducing the pressure in the reservoir, then retrograde behaviour may occur. This can be problematic because retrograde condensate will accumulate in the sand around the well bore and cause a reduction in permeability, gas flow and in producing pressures (Figure 1-2 c & d). If this happens then an alternative and usually costly depletion strategy is needed. Thus the accurate modelling of phase behaviour is crucial to planning a suitable depletion strategy for reservoirs.

1.1.3 Wax precipitation

Wax precipitation occurs when the solvating capacity of the gas and/or condensate for HMW hydrocarbons is reduced at lower temperatures **(Carnahan, 1989)**. Wax precipitation is a potential problem when hydrocarbon mixtures are transported by pipeline under water, in cold climates, or in processing plants where wax deposition may result in the plugging of pipes and process equipment **(Ashford *et al.*, 1990,**

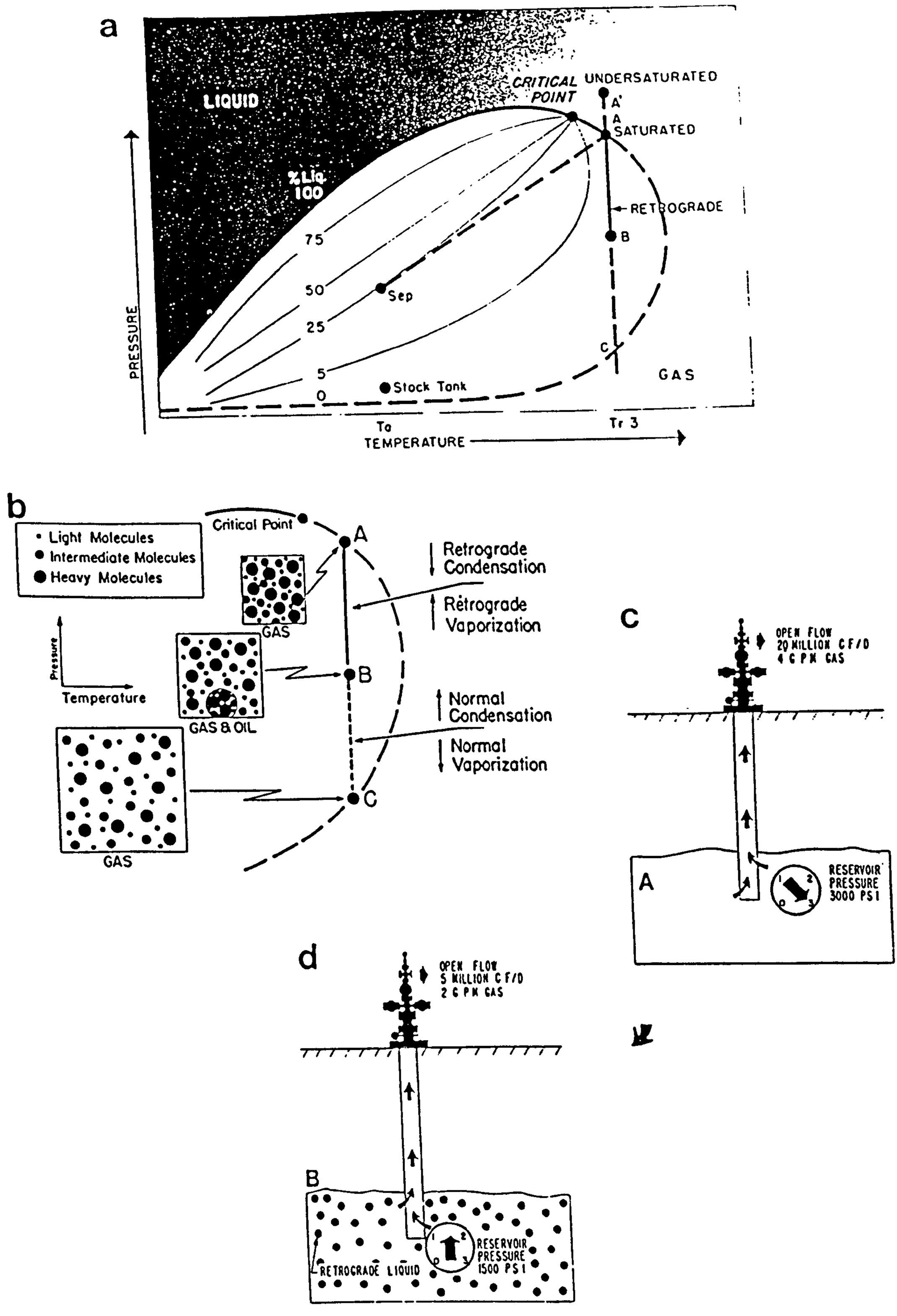

Figure 1-2 a) Phase diagram of retrograde condensate gas, b) the process of retrograde behaviour and c) the effect of retrograde condensation on reservoir performance (adapted from **Clark, 1969**).

Pedersen *et al.*, 1989). A gas chromatogram of a pipeline wax deposit is shown in Figure 1-3 (**Philp, 1994**). Most of the wax comprises hydrocarbons C_{30} to C_{50}.

Remedial action such as hot oiling and wire-line cutting to remove precipitated wax (**Tuttle, 1983; Ashford *et al.*, 1990**), or preventative methods using wax inhibitors like ethyl-vinyl-acetate (EVA) copolymers (**Gilby, 1983**) will increase the costs of production. If this is to be avoided it is necessary to determine the conditions under which wax precipitation takes place and to estimate the amount of wax that is likely to form. This will require a detailed knowledge of the hydrocarbon fluids.

1.1.4 Modelling phase behaviour

In the past, according to **Pedersen (1989)**, reservoir engineers, when designing production schemes, tended to rely more on experience than on the properties and composition characteristics of the hydrocarbon fluids produced. Today, because of the massive investment in the oil and gas industry, production systems and equipment undergo detailed engineering analyses and careful design to optimise production and minimise operating costs and investment.

The phase behaviour and physical properties (*i.e.* density, viscosity, and enthalpies) of gas condensates and oils are, according to **Pedersen (1989)** uniquely determined by the state of the system, *i.e.*, temperature, pressure, and composition. Traditionally, such data (so-called PVT data) have been acquired by distillation (C_{7+}) followed by detailed laboratory tests. While this level of analysis of oils and condensates is adequate for many purposes, it is costly and computer modelling of phase behaviour based on mathematical expressions known as equations of state (EQS), offer a rapid and less expensive approach to providing valuable physical data for the petroleum engineer **(Ahmed 1989).**

A representative mathematical description of a reservoir fluid is essential for modelling behaviour within the reservoir but such a description must be based on an accurate and full determination of the reservoir fluid composition since the prediction

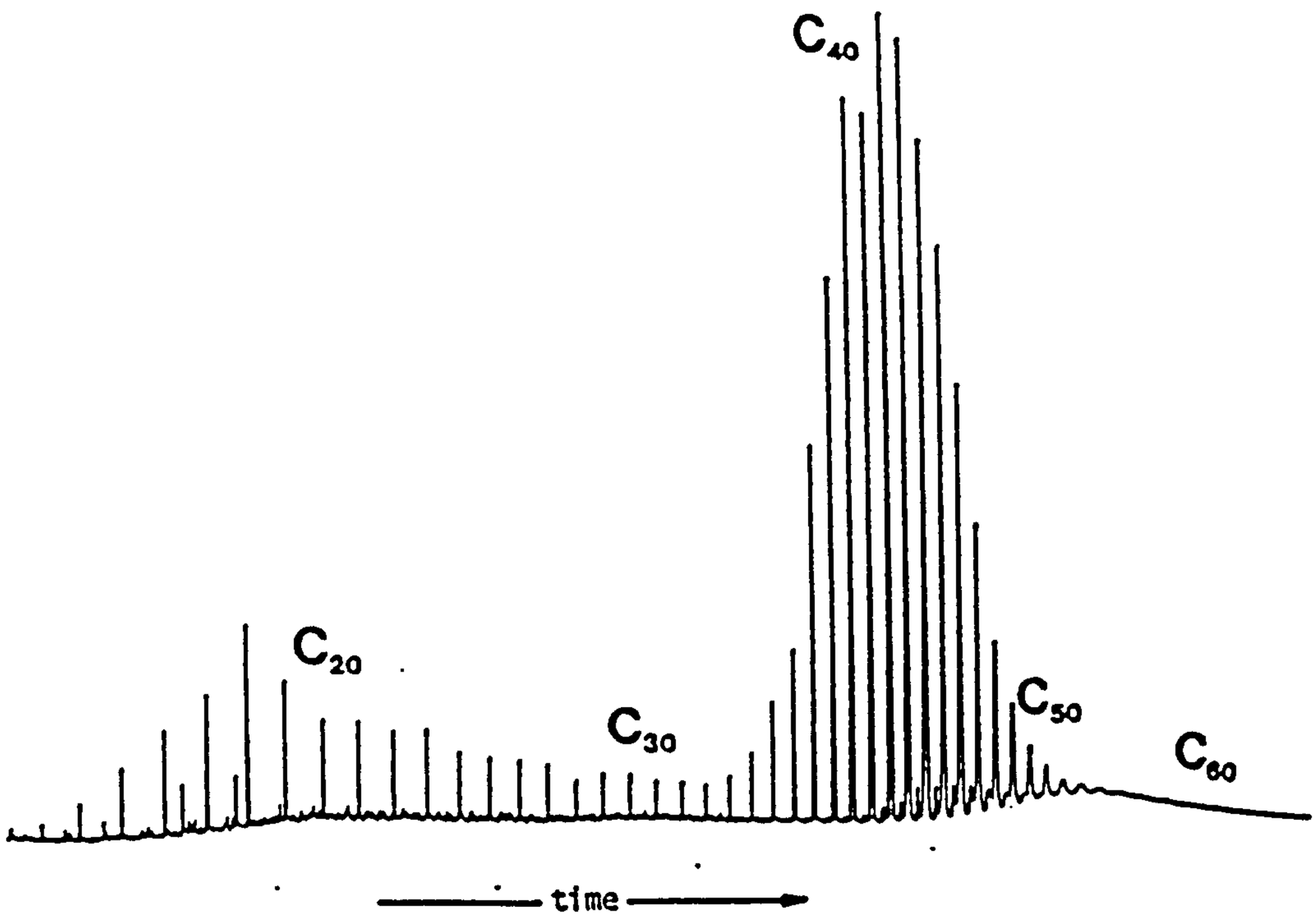

Figure 1-3 Capillary HTCGC of a crude oil wax deposit collected from a drill stem pipe (**Philp, 1994**).

of phase behaviour is very sensitive to both the quantity and description of the heaviest species present (**Whitson, 1983 and Pedersen *et al.*, 1989**). Unfortunately the latter are also the hydrocarbons that are amongst the most difficult to quantify with good analytical precession and accuracy (especially $>C_{35}$).

Experimental reservoir analysis involves taking pressurised fluids collected during well testing and measuring PVT properties using physical methods such as constant volume depletion (see **Pedersen *et al.*, 1989**), or predictively by entering composition, mole%, molecular weight, and density data into a PVT computer model based around a mathematical EQS.

According to **Moffatt (pers. comm., 1991)** it is possible to achieve the chemical analysis of pressurised fluids collected directly from the reservoir in a single operation by using a high pressure sampling valve followed by gas chromatography. Unfortunately it is not possible with present technology to calculate in a single operation, at pressure, physical fluid properties such as density from composition, pressure and temperature. If this was the case then all the information required by the petroleum engineer could be gathered from a single characterisation of the reservoir fluid. This would make the need for constant volume depletion redundant (**Moffatt pers comm., 1991**). The major limitations are that:

I) high pressure sampling valves have a pressure limit of 5,000 psi and require considerable maintenance when working close to their limits.

II) use of a single chromatography column to separate nitrogen, methane, ethane through to the heavier hydrocarbons is not possible with out a reduction in analytical accuracy.

III) <u>it is difficult to quantify HMW ($>C_{30}$) by GC.</u>

IIV) single phase analysis does not at present allow complementary measurements of properties such as specific gravity or molecular weight,

nor does it provide fluid density data.

At present, analysis of composition requires reducing the reservoir fluid to atmospheric pressure (*viz* to laboratory conditions). The gaseous and liquid hydrocarbons fractions are then analyzed separately. The data from analyses of both fractions are combined to yield the original reservoir fluid composition. Traditionally, data on composition in the oil and gas industry have only been reported up to a C_{7+} (boiling point > 69°C) fraction, the physical data being mainly based on the properties of low temperature fractional distillates and composition data from analysis by chromatographic techniques. However, this is inadequate for accurate modelling of the physical properties of hydrocarbon mixtures (**Pedersen *et al.*, 1989; Whitson, 1983**).

More recently, advances in gas chromatography and vacuum distillation have extended possibilities for the characterisation of components with boiling points up to 441°C (**Tříska *et al.*, 1984**). This is both straightforward and adequate for most condensates which are usually light, clear, mobile liquids containing compounds with up to about thirty carbon atoms. All these constituents may be eluted quantitatively from gas chromatographic columns. However, HMW hydrocarbons ($>C_{30}$, >boiling point 450°C) are considerably more difficult to analyze by chromatographic techniques and until recently have been beyond the scope of gas chromatography. Nonetheless these compounds may account for up to about **20%** of waxy condensates, many of which are sufficiently waxy to solidify at room temperature when stabilised. The gas industry has considerable interest in producing waxy condensates from HT/HP reservoirs waxy condensates and hence there is increasing interest in methods suitable for obtaining quantitative and qualitative information about these HMW compounds.

Several techniques are applicable to the analysis of HMW compounds (**Adlard, 1995**) but possibly the most important are Supercritical Fluid Chromatography (SFC), and High Temperature Capillary Gas Chromatography (HTCGC). Given the focus of the present research, only the latter will be discussed herein.

1.1.5 High Temperature capillary gas chromatography (HTCGC) and GC-simulated distillation (GC-SIMDIST)

Since 1986 HTCGC has become an established technique and has been widely applied (Table 1-1). The demarcation between "regular" capillary gas chromatography and HTCGC is somewhat arbitrary. Although several authors state that HTCGC starts at temperatures above 350°C, a more recent review by **Sandra (1990)** claims "280°C seems an acceptable choice". The upper limits of HTCGC are yet to be defined, and though higher temperatures (>450°C) may be attained by improving the thermal stability of both column support and stationary phase, the true working temperature limit will be that at which pyrolysis of the analyte and/or the column resolution becomes unacceptable. At present this limit is around 420-430°C.

It is difficult to separate the two techniques of high temperature capillary gas chromatography and capillary simulated distillation (GC-SIMDIST) because the roots of their development are closely intertwined and the actual difference between them is not clear cut. Simulated distillation is the standard method (**ASTM D-2887 & D-3710**) by which the distribution of initial, intermediate, and final boiling points of crude oil or heavy distillates are determined by gas chromatography (reviewed by **Bashall, 1987; Abbot, 1995**).

Prior to 1980, short (ca. 5 m) packed column gc with flame ionisation detection was used for the analysis of higher boiling fractions. The major drawback of this method was the low amounts of material that could be eluted from the column and the poor resolution. The latter is a particular disadvantage when structural information is required. For example, in the analysis of waxes (because information about branched and straight chain hydrocarbons is important in formulation and blending; **Barker, 1987**), for formulation of blends that become lubricating feedstock or finished products (**Bashall, 1987**), and investigation of mineral and vegetable oils (**Lawrence, 1983; Geeraert and Sandra, 1984**). Thus a need arose for a chromatographic method with good resolution but which was capable of eluting higher boiling point compounds.

Analysis	Reference	Chromatography	Comments
Anti-oxidants & Polymer Additives	Blum & Damasceno (1987)	Col: Glass capillary PS-089 (OH-terminated 5% phenyl methyl polysiloxane) coated. Temp. prog: to 420°C. Det: FID.	
	David & Sandra (1993)	Col: HP-1, 25 m x 32 μm i.d. Temp prog: 80 to 380°C (8°C/min), Carrier: He 150 kPa (constant flow). Inj: On-column Det: FID.	
Asphaltenes	Del Rio *et al.*, (1992)	Col: Al-clad, 3 m and 25 m x 0.32mm i.d., HT-5. Temp. prog: 60 - 440°C at 8°C/min (50 min hold). Inj: Split-splitless. Det: FID and MS.	
Biodegradation of *n*-alkanes	Hanstveit (1992)	Col: Chrompack Sim-Dist, 10 m x 0.32 mm i.d.. Temp. prog: 108 - 410°C. Carrier: He. Det: FID	
Crude oil	Lipsky and Duffy (1986) part 1 & 2	Col: Al-clad, 15 m x 0.2 mm i.d., bonded methylpolysiloxane (0.1 μm, film). Carrier: H_2 (20 psi). Temp. Prog: 60 - 430°C at 15°C/min, hold 430°C. Inj: PE PTV. Det: FID	Introduced Aluminium clad capillary columns.
Detergents	Sandra & David (1990)	Col: Al-clad, 10 m x 530 μm i.d & 10 m x 250 μm i.d. Temp. prog: Inj: On-column and split-splitless. Carrier: H_2. Det: FID.	
Lipids	Evershed *et al.*, (1992)	Col: Al-clad, 12 m x 0.22 mm i.d., SGE, BP-1 coated (0.1 μm film). Temp. prog: 50 - 330°C at 8°C/min. Inj: On-column. Det: MS.	

Table 1-1 Applications of high temperature capillary gas chromatography.

continued overleaf .....

Continued ....

Analysis	Reference	Chromatography	
Porphyrins	Zeng & Uden, (1994)		
Sedimentary Organic matter	Kohnen *et al.*, (1989)	Col: Al-clad, 25 m x 0.32 mm i.d; Chrompack, HT-5 coated (0.1 μm film thickness). Temp. prog: Ambient to 130°C at 20°C/min and then at 4°C to 350°C and finally at 6°C to 450°C. Carrier: H_2. Inj: On-column. Det: FID.	
Steroids	Evershed et al., (1987)	Col: 12 m x 0.22 mm i.d., BP-1 coated (0.1 μm, film). Temp prog: 150 - 350°C at 12°C/min. Inj: on-column Det: MS	
SIM-DIST	Luke & Ray, (1985)	Col: Glass 6 m x 0.32 μm OV-1 coated (0.15 μm). Carrier: H_2. Temp. Prog: 30 - 390°C at 10°C/min. Inj: On-column. Det: FID.	First reported use of capillary columns for HTCGC/SD. Eluted petroleum residues boiling up to 650°C (C_{70}). Quantitative study. A constant FID response for *n*-alkanes up to *n*-C_{60} using short columns.
	Trestianu *et al.*, (1985)	Col: Glass <15m a polar silicon phase. Carrier: H_2 Constant flow. Temp. Prog: 40 - 430 °C. Inj: On-column Det: FID.	Eluted compounds at the end of the temperature program, compounds with 100 - 120 carbon atoms and 130 - 140 carbon atoms at the end of the final isotherm (30 mins). Quantitative study similar to above.
	Noel, (1988)	Col: 5 m megabore HP-1. Carrier: He 30 ml/min. Inj: Split-splitless Det: FID.	
	Curvers & van de Engle, (1989)	Col: HP-1 Wide bore column, Carrier: He 20 ml/min. Temp. prog: 40 - 430°C at 10°C. Inj: PTV Det: FID.	
	Firor & Phillips, (1989)	Col: 5 m x 0.53 mm i.d., polyimide & Al-clad coated fused silica. Carrier: He 12 ml/min. Temp. Prog: 40 - 430°C at 6°C. Inj: modified on-column. Det: FID.	Compares the use of Polyimide and Al-cladding for column support.
	McCormack *et al.*, (1991)	Col: Al-clad, 12 m x 0.53 mm i.d., HT-5 coated (0.15 μm, film, SGE). Carrier: He 8-10 ml/min. Temp. Prog:40 - 400°C at 5°C/min. Inj: On-column. Det: FID.	

Continued overleaf .....

continued ....

Analysis	Reference	Chromatography	
	Thomson & Rynaski (1992)	Col: Al-clad 10 m x 0.53 mm i.d., (Mega-bore) HT-5, SGE, 0.015 μm, Film; Al-clad 6m x 0.53 mm i.d., carborane/ methylsilicone coated (Chrompak); and Chrompack, 10 m x 0.5 mm i.d., 0.15 μm HT-SIMDIST CB (wide bore metal column). Carrier: He 25ml/min. Temp. prog. 60 - 450°C at 10°C/min (hold 10 min). Inj: SPI PTV Det: FID.	Comparrison of HTCGC/SIM-DIST and SFC/SIM-DIST. Quatitative study similar to Luke and Ray (1985) and Trestainu (1985) which also investigates the effect of injection speed when using manual injection. Recommends a fast injection.
Reviews	Bashall (1987)		HTCGC/SIM-DIST.
	Baker (1988)		Review of methods for wax analysis including HTCGC.
	Barker (1989)		HTCGC, Injectors: On-column & PTV, Detectors.
	Huball (1990)		HTCGC, Injectors, Detectors, Sample integrity and Column stability.
	del Rio (1992)		Uses of HTCGC for the analysis of biomarkers.
	Peadon (1994)		HTCGC/SIM-DIST.
	Philp (1994)		HTCGC for the analysis of fossil fuels.
	Abbot (1995)		Overview of the technique of SIM-DIST. using HTCGC.
	Barker (1995)		Review of HTCGC for wax analysis.
Waxes	Giles (1987)	Column: BP-5, 15 m. Temp. prog: 100 to 350°C at 8°C/min. Carrier: N_2. Inj: Split-Splitless. Det: FID.	

1.1.5 (a) Column developments

The search for improved thermal stability of GC stationary phases has been an on-going challenge in gas chromatography since its early development. Initially, packed stainless steel columns were used for HTGC studies and in particular the Dexil (300-gc and 400-gc) series of polycarboranylene phases originally developed by the Olin corporation became popular. These could be operated at temperatures up to 400°C (**Novotny *et al.*, 1972; Pollock, 1972; Tullock, 1973**). Other commercially available phases were also used at high temperatures, including SE52 and OV-1. **Wood (1969)** used a stainless steel column packed with SE30 silicone phase at temperatures up to 400°C to study the triglycerides of various fats and oils. Triglycerides are a group of high boiling point esters that are found in the numerous fats and oils used in food products for example, the chocolate industry (**Geeraert and Sandra, 1984**), and the baking industry (**Wood, 1969**) and their analysis has gained widespread attention. The upper temperature range for triglyceride analysis is typically 380°C, which makes them accessible by the use of high-temperature GC columns.

Despite the fore-mentioned applications, packed stainless steel columns produced high column bleed at temperatures above 350°C and still lacked good enough resolution for many purposes. According to **Huball (1990)** analysts soon realized that the use of capillary columns offered several advantages over packed columns. These included better resolution, shorter conditioning times, less column bleed, lower elution temperatures (resulting in an expanded temperature range), shorter analysis times, and potentially longer column lifetimes. However, one of the key difficulties when trying to develop such high temperature capillary systems was that many of the commercial phases were unbonded gums which meant that they did not adhere well to the surface of the capillary wall. Despite attempts to modify their adhesion, they showed a lack of film stability when operated for prolonged periods at high temperatures (**Maskarinec and Olerich, 1980**).

Important developments for capillary columns came about in the late 70's through pioneering studies of **Mandani *et al.* (1976; 1977; 1978; 1981)** and **Blomberg and Wännman (1979a; 1979b)**. These workers developed methods for the *in situ*

production of efficient, thermally stable, insoluble silicone polymeric stationary phases from α,ω-hydroxypolymethylsiloxane type pre-polymers on treated glass surfaces of capillary columns. This produced good film stability, low levels of bleed and large film thicknesses. These early columns were improved later by **Grob and co-workers (1976)**, and **Sandra *et al.*, (1977)**, (who introduced polyimide coated fused silica in place of glass for the column), and **Lipsky and McMurray (1982)** all of whom not only contributed to producing the general commercial capillary columns available today but who also carried out the groundwork from which true HTCGC eventually emerged.

By the mid 80's advances in simulated distillation techniques led **Luke and Ray (1985)** concurrently with **Trestianu *et al.*, (1985)** to utilise short pyrex glass capillary columns (<10 m) coated with a non-polar methyl siloxane phase in an attempt to improve on the standard method of packed column simulated distillation (ASTM D 2887). The first report showed that it was possible to obtain quantitative SIM-DIST data on crude oil residues boiling up to 650°C (C_{70}). Using a dedicated high temperature chromatograph in conjunction with their short capillary column **Trestianu *et al.*, (1985)** showed that with operating temperatures of 430°C it was possible to elute, at the end of temperature programmed operation, *n*-alkanes *n*-$C_{100\text{-}120}$, and by extending the final isotherm (<30 min), $C_{130\text{-}140}$ compounds. Such columns were found to last for several months in routine use.

For many types of high boiling point mixtures eluting at temperatures above 340°C (eg triglycerides) simulated distillation was not capable of providing detailed structural resolution. Thus, it was still important to develop true high temperature capillary columns. It was soon recognised that the problem was not with the stationary phase, (the new phenyl polysiloxane phases had been shown to have good temperature stability up to 400°C; **(Geeraert and Sandra, 1984; Peaden *et al.*, 1982)**), but with the thermal instability of the outer column support. Polyimide is the most common support for glass and fused silica columns because of the greater flexibility it renders to the column. However, its maximum operating temperature is ca 370°C, which is more than adequate for general chromatographic use, but which at higher temperatures, begins to thermally degrade and become brittle. This leads to disruptions in the polymeric sheath

and soon segments of the outer surface of the synthetic glass are exposed to the atmosphere. Small fissures may then form in the fused silica which expand and weaken the capillary column.

The disadvantages of polyimide as a column support led to the search for alternatives. In work published in 1986, using an aluminium coating as a substitute for polyimide, with a bonded cross-linked methyl polysiloxane stationary phase, **Lipsky and Duffy (1986)**, introduced the earliest commercially-available HTCGC column (Figure 1-4). The aluminium sheathing retained the flexibility of fused silica while operating at temperatures extending to 400-440°C. Aluminium clad columns are now widely available from several commercial suppliers.

Other authors continued to use glass for specific HTCGC studies (*e.g.* **Blum and co-workers (1988)** for the analysis of porphyrins), and still more recent developments have included a return to stainless steel columns. The latter offers the advantages of strength and durability at high temperatures but the problem of de-activating the inner surface of the metal tubing had to be overcome: this has been approached in several ways.

Methods developed by **Vonk *et al.*, (1992)** and **Buyten *et al.*, (1990 a,b)** involve treating the metal surface with a series of bonded layers, and then finally with the high temperature phase. A second method involves depositing on the inner surface of a stainless steel column, a thin layer of fused silica which can then be coated like a conventional fused silica column (**Zou *et al.*, 1992**; **Restek Corporation, 1992**). The thermal stability of polyimide has also been increased (300-400°C) and it is now useful for many more HTCGC applications (**Chrompack, Raritan, New Jersey**).

The choice of column for a particular application (*i.e.* whether aluminium clad, high temperature polyimide or metal) remains with the analyst. Aluminium clad columns conduct electricity and need to be carefully installed into those detectors which are at high potential. High temperature polyimide overcomes this problem but the polyimide coating may become brittle above 400°C, giving it a limited life-time (**Barker, 1995**). Metal columns which are now much improved in terms of column bleed and resolution,

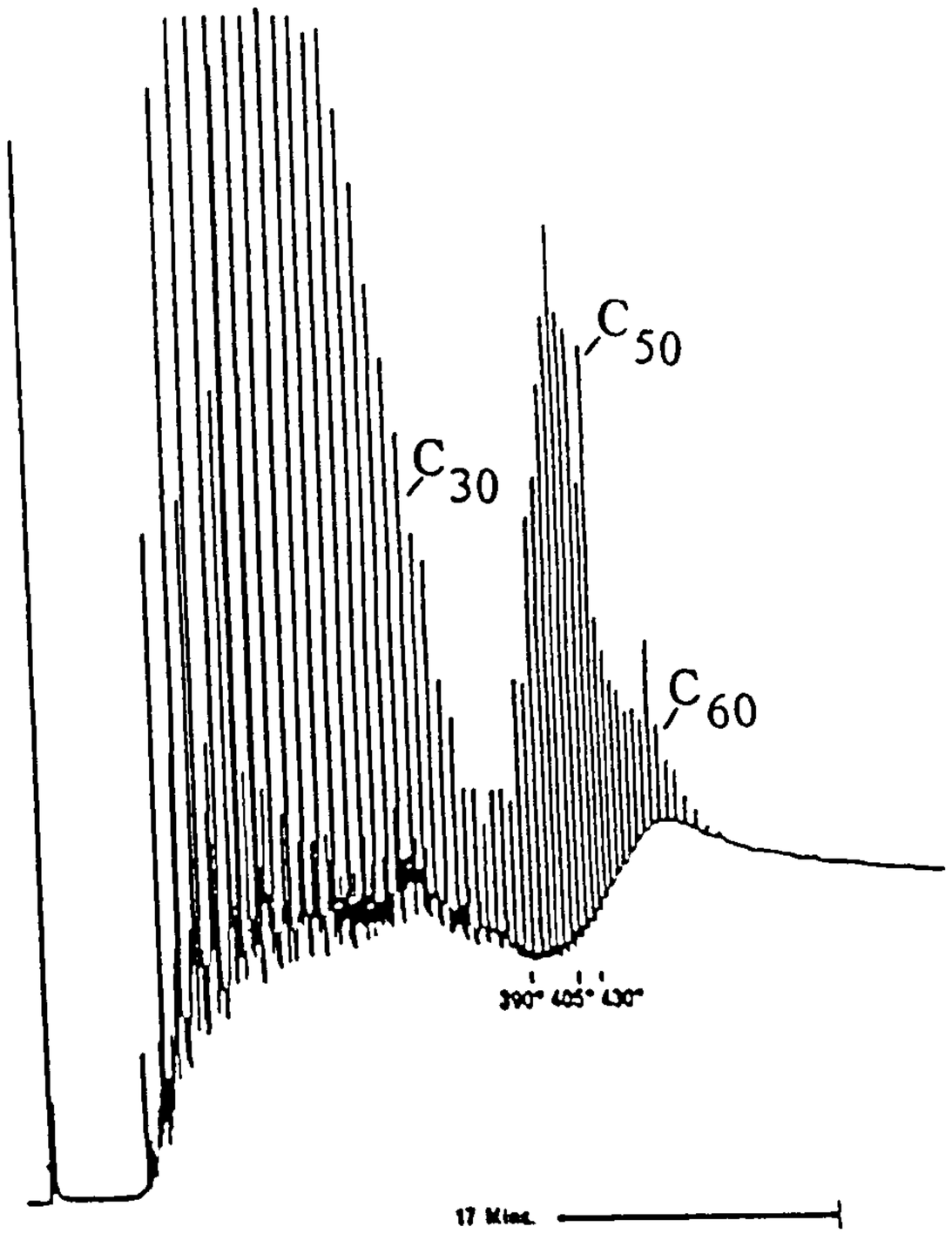

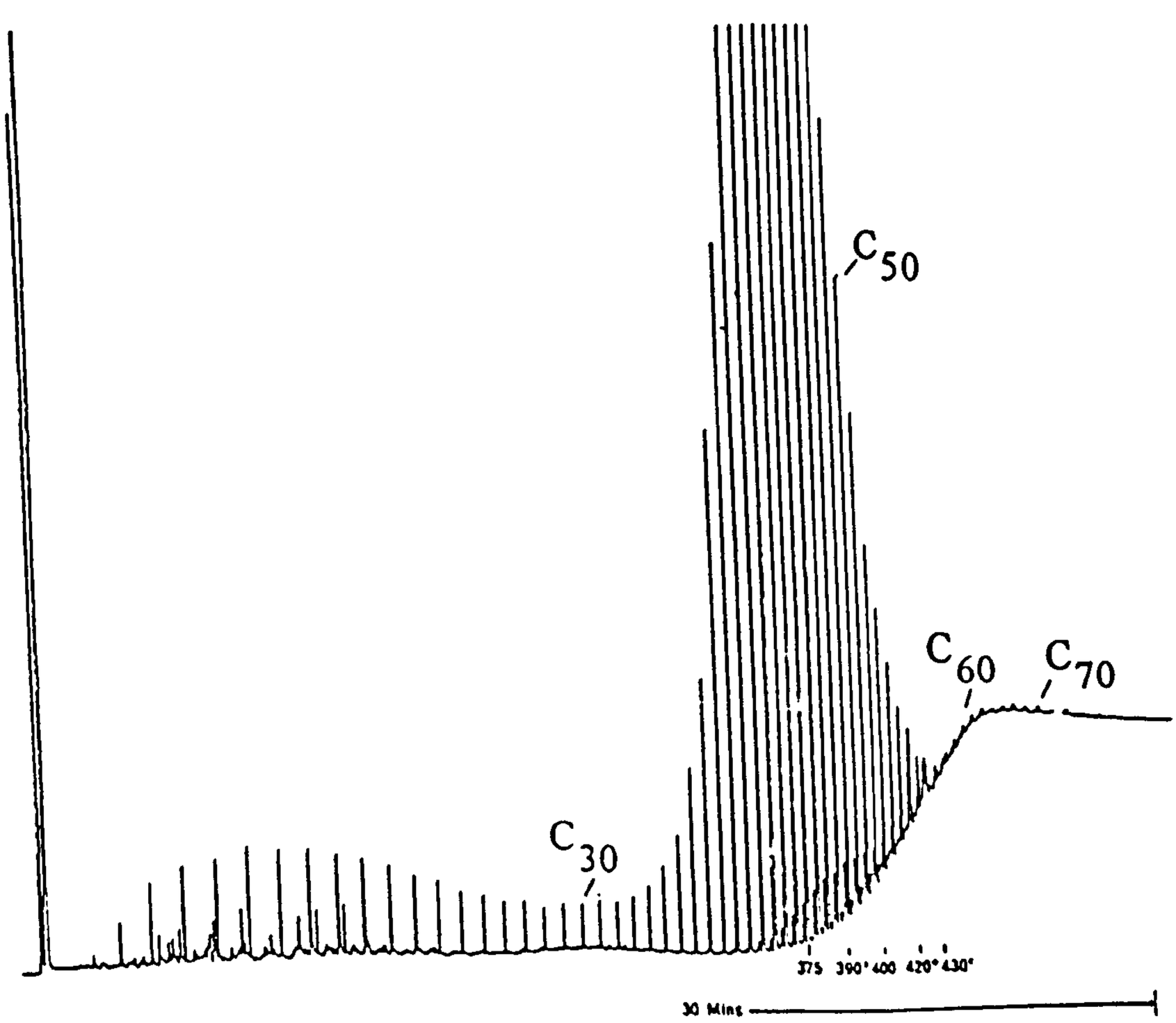

Figure 1-4 HTCGC of two crude oils using an aluminium clad capillary column (taken from Lipsky and Duffy, 1985).

offer the advantage of durability but lack flexibility. Fitting these columns requires careful attention and they are also conductive. Metal columns are at present more expensive than the other options and there are too few examples of the use of high temperature metal columns in the literature to evaluate their use properly. Aluminium clad columns still remain the most popular choice.

1.1.5 (b) Instrumentation developments - Gas Chromatograph

Besides the advances in high temperature capillary columns, developments in the manufacture of dedicated high temperature gas chromatographic instrumentation are important. A review by **Barker (1989)** reports that a great deal of the early work into HTCGC was severely hindered by the limitations of the available instrumentation, including imprecise temperature control of the injectors and detectors above 375°C; repeatability of the heating and cooling cycles (due to the high thermal mass of the oven insulation), and inaccurate flow/pressure control.

Many of these early problems were overcome with the introduction of low thermal mass ovens (with double skin air circulation and more efficient fans to reduce temperature gradients) and micro processor temperature control. **Trestianu *et al.*, (1985)** reported the first use of a special high temperature version of the Mega Series capillary gas chromatograph (Carlo Erba instruments). The new chromatograph was able to program temperature rises reproducibly up to 500°C and to achieve programming rates of at least 15°C/min above 400°C. Most major instrument companies have now either upgraded their existing range of chromatographs or introduced their own dedicated HT instruments.

1.1.5 (c) Instrumentation developments - Injectors

Until recently the on-column injector was the most popular injector used for HTCGC. On-column injection for capillary columns was an idea originally conceived by **Desty (1965)**. The initial design of the cool on-column injector was first introduced by **Schomburg *et al.*, (1977)** but later improved by **Grob and Grob (1978)**. The on-column injector (Figure 1-5 A) works by introducing a small amount of sample directly onto the cool column via a small long syringe needle pushed through a valve system.

A

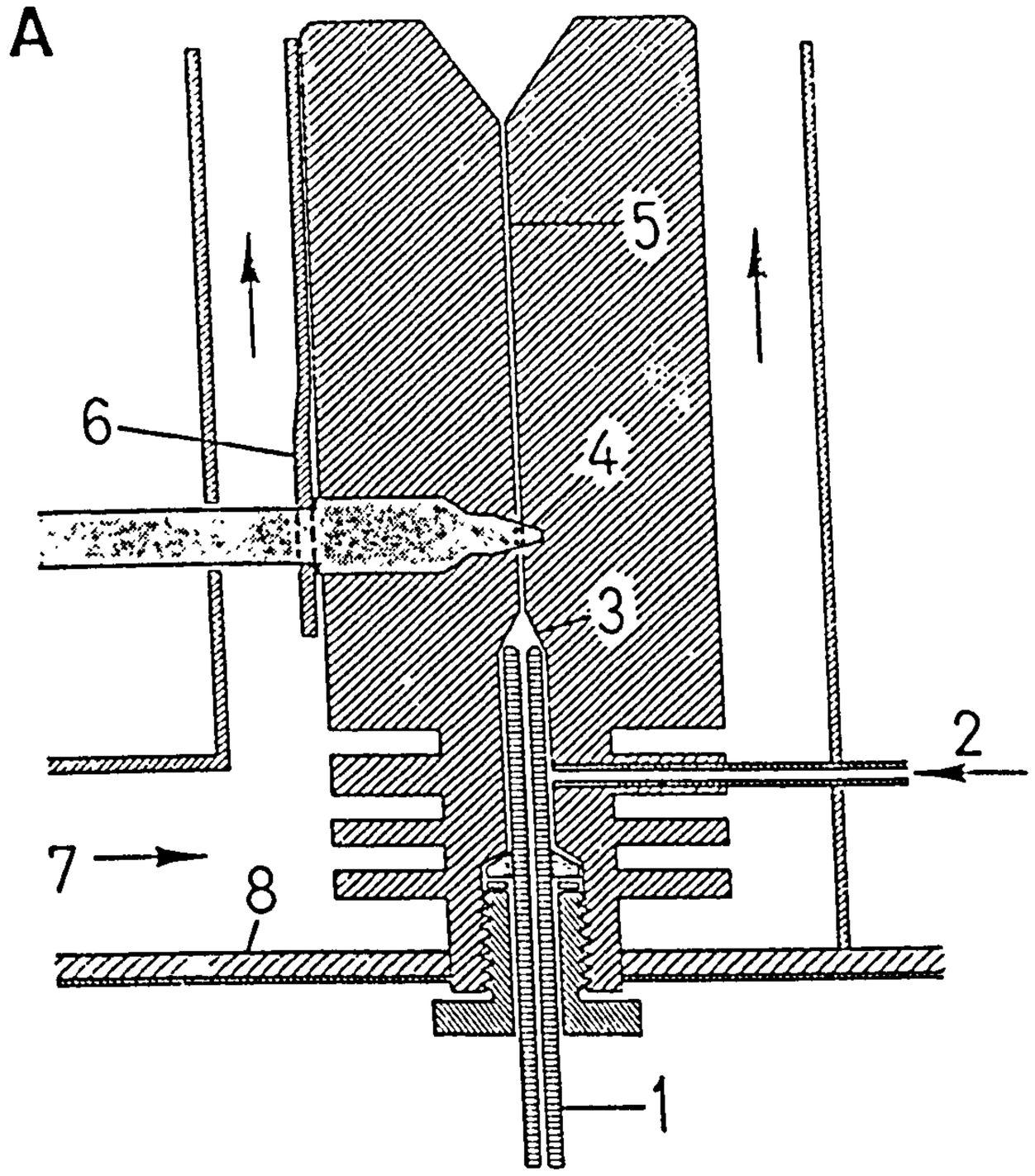

1: capillary column.
2: carrier entrance.
3: centring cone.
4: stop-cock valve.
5: channel replacing septum.
6: spring.
7: entrance of cooling air.
8: heat insulation.

B

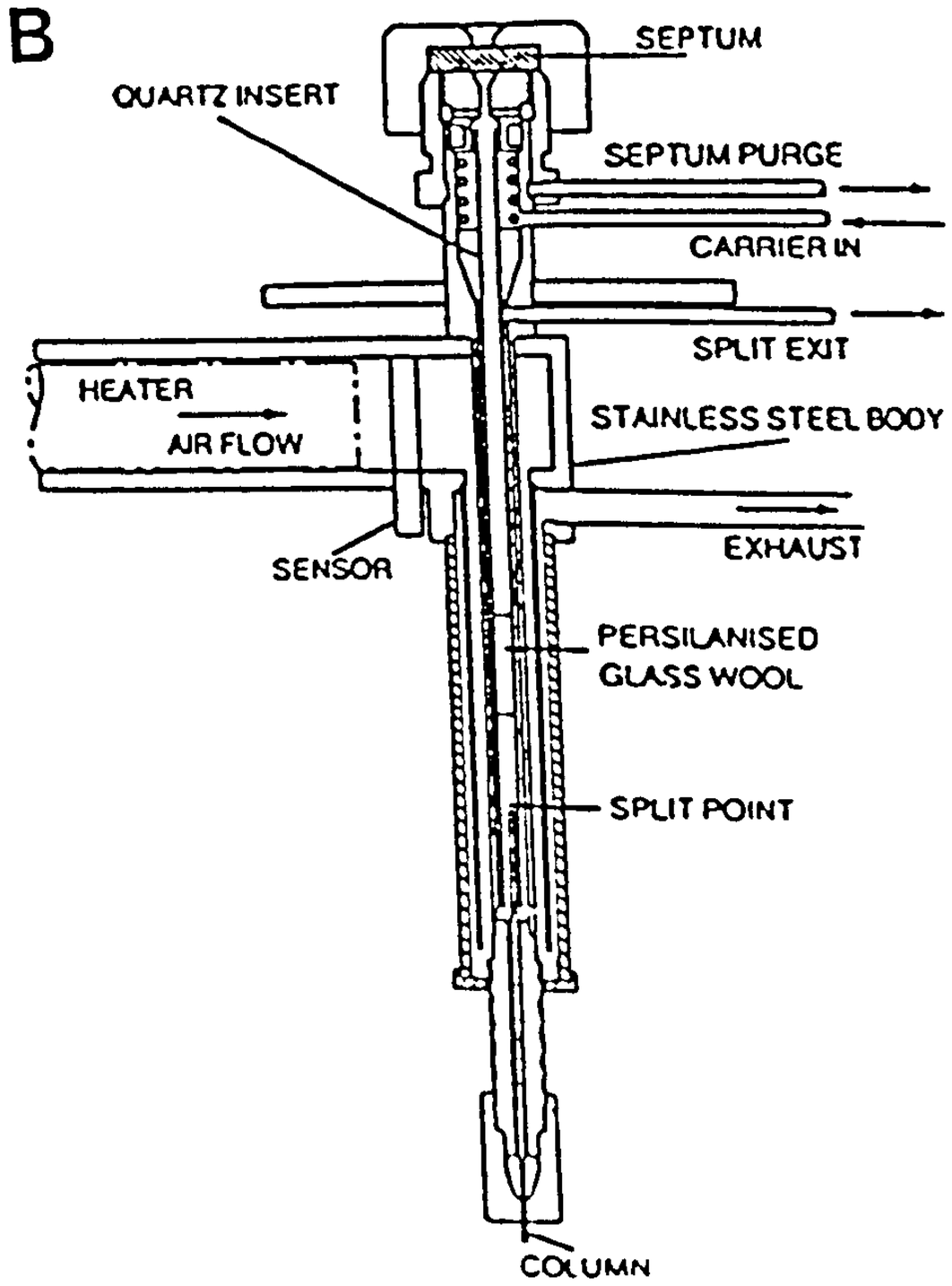

Figure 1-5 A) Schematic design of modified on-column injector (adapted from **Grob & Grob, 1978**) and B) programmable temperature vaporizer injector (adapted from **Schomberg, 1981**).

The sample is placed either directly onto the analytical column or onto a retention gap within the oven.

A second type of injector used more recently in HTCGC applications is that developed independently by **Poy (1981)** and **Schomburg (1981)** and is known as the programmable temperature vaporiser (PTV) injector (Figure 1-5 B). The method was originally commercialised by Dani Instruments, a company which was later purchased by Perkin Elmer who improved the design. A solution of the sample is injected, via a septum, into a narrow glass insert (tube) into which a capillary column protrudes, in a similar fashion to a traditional split/splitless injector. A glass or silanised quartz wool is placed inside the insert to retain non-volatile material and to help in forming a plug of condensed sample before volatilisation into the column (though, **Sandra and David (1989)** claim better results are obtained with the glass insert left empty). Here the PTV injector differs from a conventional injector, because the injector body is heated rapidly so that the sample components are eluted, each at its boiling point on to the column as a vapour.

The question of which is the best type of injector for HTCGC is a matter of opinion. Both techniques have been used successfully. Cool on-column injection is preferred by some authors (*e.g.* **Trestianu, 1986**) because the sample is injected directly onto the column in the oven so the sample will be heated at the same rate as the oven program temperature, and in the opinion of **Trestianu (1986)**, is the most nondiscriminating sampling system. In the case of the PTV injector the maximum column temperature is restricted to 440°C by the fact that the injector has to be approximately 10°C above the column temperature to elute quantitatively all the components **(Barker, 1989)**. Alternatively, many authors **(Tipler and Johnson, 1990; Barker, 1989)** prefer PTV injection because, it is a "universal" injection system which can be used for many modes of analysis (*e.g.* split injection, on-column injection, solvent flush), has low component discrimination, and ordinary syringe needles can be used so injection is readily automated.

1.1.5 (d) Carrier gas and flow control

Constant pressure or carrier gas flow regulation is also an important factor in HTCGC. Optimum carrier gas velocities are usually expressed in the form of van Deemter curves (Figure 1-6). The curves shown for the gases N_2, H_2 and He illustrate that there is an optimal flow that will result in the best column efficiency **(Rood, 1991)**, where the curve reaches its minimum. As temperature is increased the viscosity of the gas also increases causing a reduction in flow rate. In conventional chromatography the temperature increase from 40 to 300°C causes only a small change in viscosity and so the reduction in flow rate is not a serious problem. This is not the case for HTCGC were if the carrier gas is kept under a constant head pressure the flow rate is almost halved by the time the column is at temperature above 370°C.

Two schools of thought exist about constant flow or constant pressure. **Trestianu (1991)** states that the advantages of constant flow over constant pressure are that it provides better separating power of the capillary column, shorter analysis times (reduced by 25-30%) and provides a greater constancy of detector response. A study by **Grob and Tschour (1990)** suggests that keeping a constant pressure would be preferable to constant flow from the point of view of theoretical plate numbers. This is because flow regulators cause elevated gas velocities due to expansion of the gas within the column with the effect that at high temperatures the number of theoretical plates is reduced by a factor of two for hydrogen and a factor of five for helium. With constant inlet pressure these authors found that optimum plate numbers were equal at 60°C and 370°C for both hydrogen (0.2-0.25 bar) and helium (0.5 bar).

1.1.5 (e) Detectors

As in conventional GC the flame ionisation detector (FID) is probably the most commonly used detector for HTCGC and the design and operation of the FID is important for maintaining capillary chromatographic performance at high temperatures. Though the basic FID design is difficult to improve upon, most modern detectors have been redesigned to give a smaller detector volume for coping with low capillary column gas flows **(Barker, 1989)** and for HTCGC an important development made by **Berg and Hawkins (1992)** was the design of an inert flame tip consisting of a ceramic tube

with a ceramic cap (in place of a conventional metal cap) sheathed in a Kovar metal alloy tube to supply the polarising field such that the sample never comes into contact with the hot metal. This solved the problem whereby the conventional metal tip became active at high temperatures (>370°C), adsorbing hydrocarbon solutes and causing peak tailing. The ceramic flame tip also reduces baseline noise. Furthermore, metal or metal-clad HTCGC columns usually needed to be modified before installation into metal FID caps, by removal of a small portion of the metal column cladding to prevent electrical shorting of the metal flame tip on non-grounded instruments. The ceramic tip does away with the need for this modification. Many new GC ovens are capable of operation at up to 500°C. Because the maximum operating temperature of the FID is currently around 450°C and because an FID should be operated at least 10°C higher than the maximum oven temperature to reduce condensation of high molecular weight residues on the flame jet (which can lead to increased background noise), the full potential of modern high temperature columns may not be fully realised and there is a need for detectors to be redesigned for use at 500°C.

Mass spectrometers have not been widely used as detectors for HTCGC. **Evershed and Prescott, (1989)** successfully connected an aluminium clad fused silica column to a magnetic sector mass spectrometer and the resulting system was used to elute *n*-alkanes up to pentacontane. This also meant that thermal degradation of the analyte at high oven temperatures could be studied. They later reported that some high molecular weight acyl lipids (eg. steryl fatty acyl esters bearing a polyunsaturated acyl moiety) were susceptible to thermal degradation **(Evershed *et al.*, 1992). Evershed and co-workers (1990)**, also applied HTCGC-MS in a study to investigate lipids extracted from ancient ceramic pot shards and other materials of archaeological origin. **Gallegos *et al.*, (1991)**, using a standard J&W DB-1 capillary column (350°C end temperature) carried out GC-electron impact mass spectrometry, and were the first to couple HTCGC with field ionisation mass spectrometry (HTCGC-FIMS), to investigate porphyrins and iso- and cyclic hydrocarbons (C_{36}-C_{60}) in petroleum. The authors were able to obtain spectra for *n*-C_{50} and porphyrins. **Del Rio *et al.*, (1992)** used HTCGC-MS (60-400°C) to analyze flash pyrolysates of asphaltenes. They suggested that the thermal breakdown of these asphaltenes might be responsible for the production or release of naturally

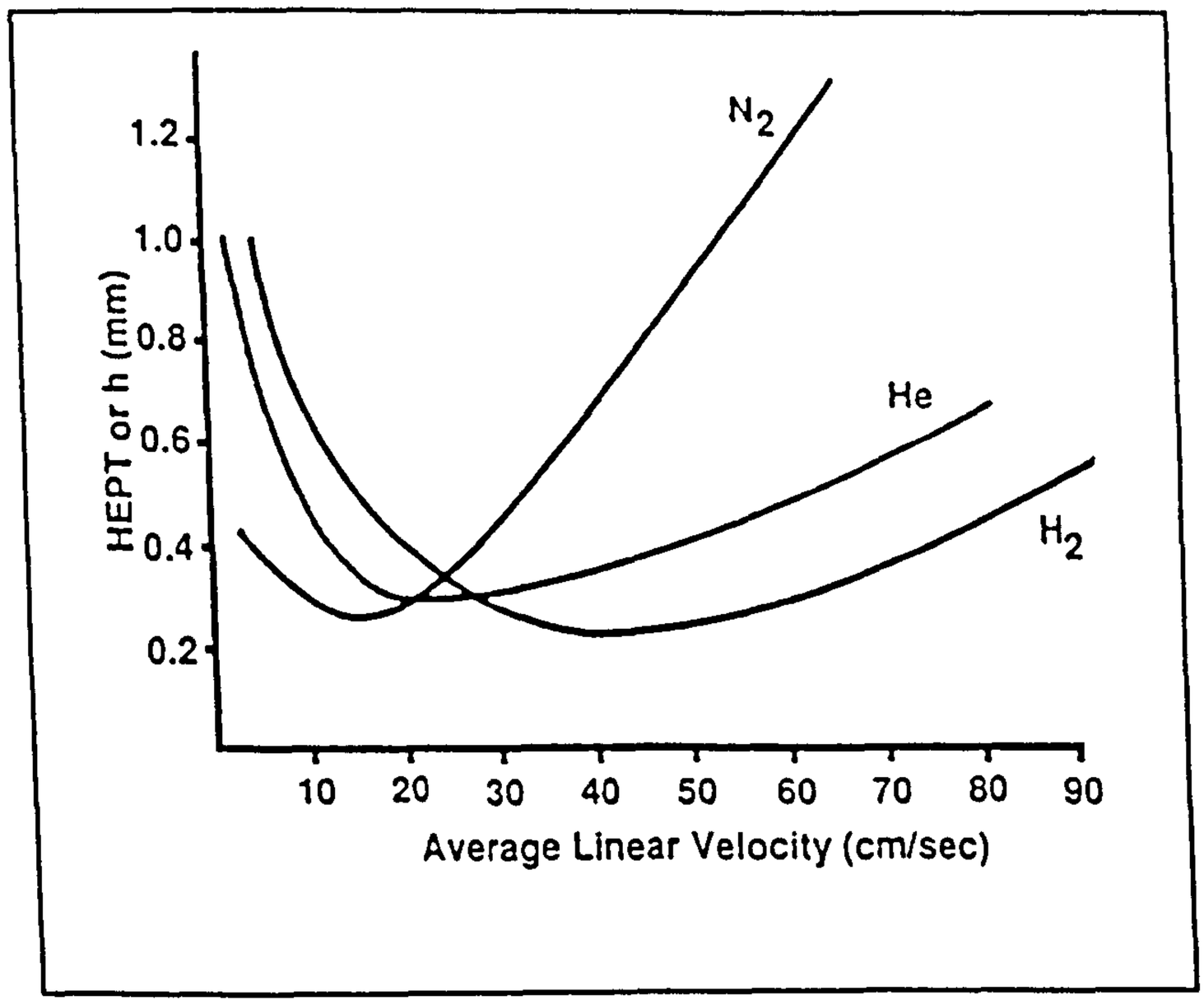

Figure 1-6 van Deemter curves (source: **Rood, 1991**).

occurring high molecular weight hydrocarbons in petroleum. HTCGC-MS was also used in studies of oligosaccharide in foodstuffs and in intestinal contents (**Hansson *et al.*, 1991; Carlsson and co-workers, 1992**). In the former study the authors successfully studied oligosaccharides with up to 12 sugar units (molecular weight >2000).

Other detectors that have been used with HTCGC include the alkali flame ionisation detector to study free base petroporphyrins (**Blum & Eglinton, 1989**) and inductively coupled plasma - mass spectrometry (ICP-MS) to study metallo porphyrins (**Pretorius, 1994; Ebdon *et al.*, 1994**).

1.3 Aims of study

The aim of the research described in this chapter was to establish a HTCGC (-MS) method for the quantification (or determination) and characterisation of the C_{30+} fractions of waxy gas condensates. The substrates used to develop the methods were two waxy condensates from high pressure, high temperature wells of the central North Sea. However the methods should be equally applicable to many other sample types.

1.3 Results and Discussion

1.3.1 Analysis of waxy gas condensates by high temperature capillary gas chromatography

Conventional and HTCGC gas chromatograms of two gas condensates from high pressure and temperature wells of the mid North Sea region are shown in Figure 1-7 A and Figure 1-8 A. Both conventional chromatograms show the predominance of low molecular weight compounds characteristic of gas condensates, but also show an abundance of higher molecular weight paraffinic compounds. The *n*-alkane distribution in both condensates maximises below *n*-C_{11}, followed by a continuous decrease of *n*-alkanes versus increasing number of carbon atoms extending out to *n*-C_{33}. Analysis of the same two condensates using a HTCGC column (12 m x 0.32 mm i.d., HT-5) at a temperature program of 50°C to 420°C at 10°C/min shows the presence of higher molecular weight ($>C_{33}$) compounds (Figure 1-7 B and Figure 1-8 B). Components including C_{50} are present in condensate U and including C_{70} in condensate W.

1.3.2 Determination of high molecular weight compounds (C_{30+})

Few studies have examined the quantitative aspects of HTCGC and those that have, have been confined to simulated distillation experiments (**Trestianu *et al.*, 1985; Luke and Ray, 1985; and Thompson and Rynaski, 1992**). Thus it was necessary in the present research to make a careful study of all aspects of the HTCGC technique, paying special attention to reproducibility, determination of response factors, linearity of response and limits of detection.

1.3.2 (a) Instrumentation and Solvents

The instrument used for HTCGC in this study was a dedicated Mega Series HTCGC chromatograph (Carlo Erba) fitted with a constant flow constant pressure control module as detailed in the experimental section. Helium, the carrier gas, was kept under constant pressure at the point of injection and then after a 5 second delay switched automatically to a constant flow of 3 ml/min. The chromatograph was fitted with an

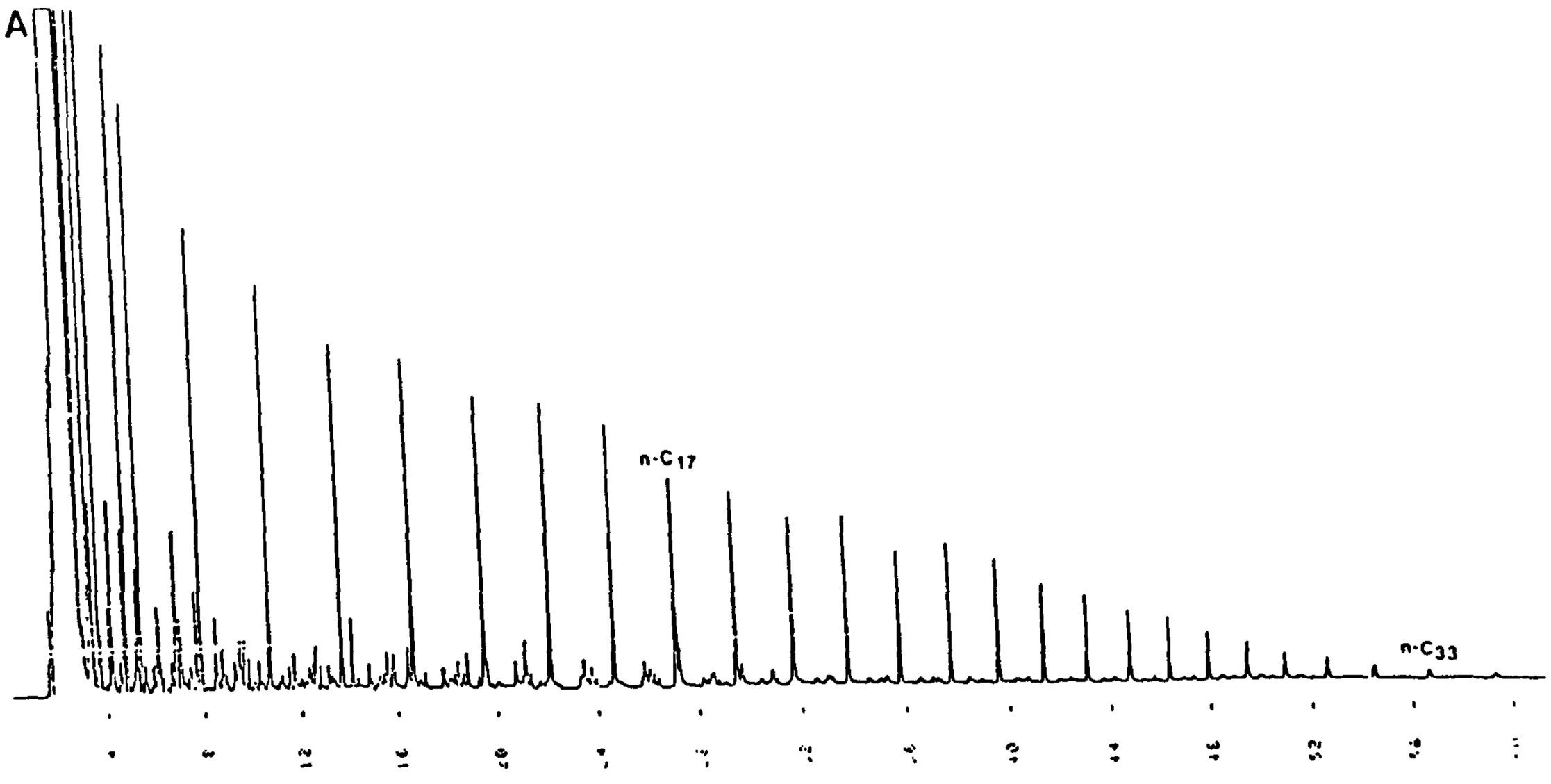

[GC: DB5 (J&W), 30 m x 0.32 mm i.d., 50-300°C @ 5°C/min (20 min), He carrier, FID]

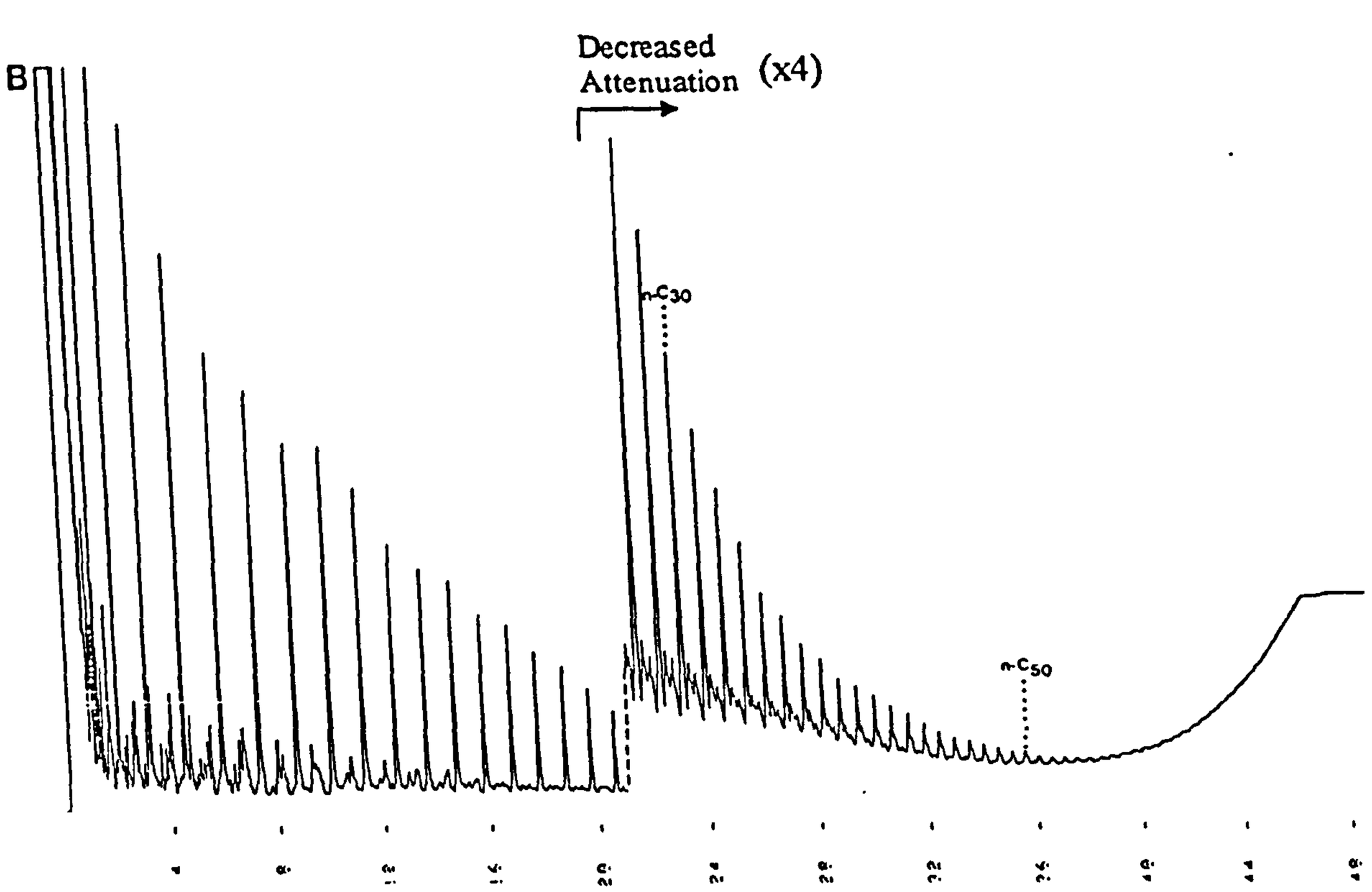

[GC: HT-5 (SGE), 12 m x 0.32 mm i.d., 50-410°C @ 10°C/min (10 min), He carrier, FID]

Figure 1-7 A) Gas Chromatogram of a Waxy North Sea gas-condensate (U) and B) HTCGC of the same gas condensate.

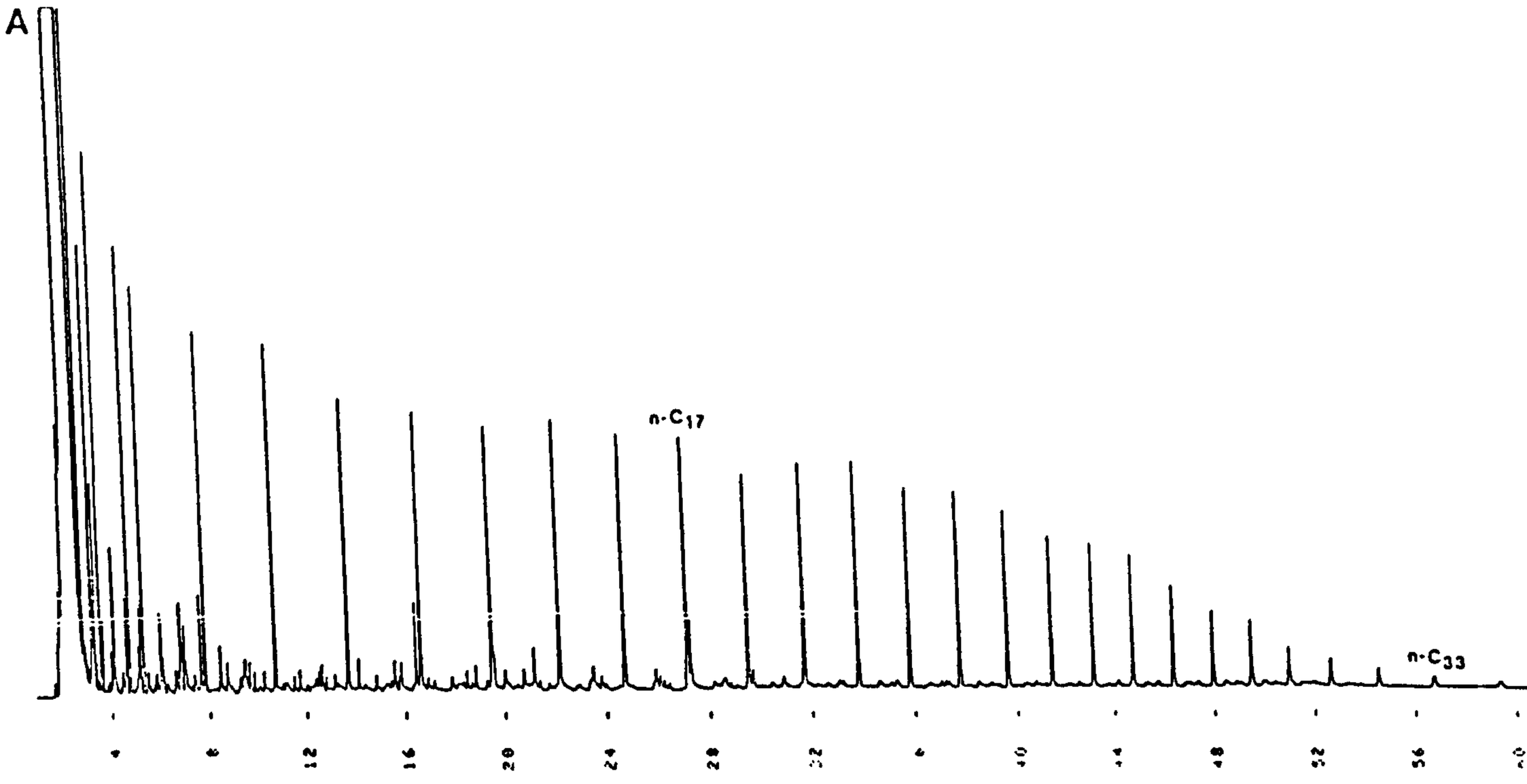

[GC: DB5 (J&W), 30 m x 0.32 mm i.d., 50-300°C @ 5°C/min (20 min), He carrier, FID]

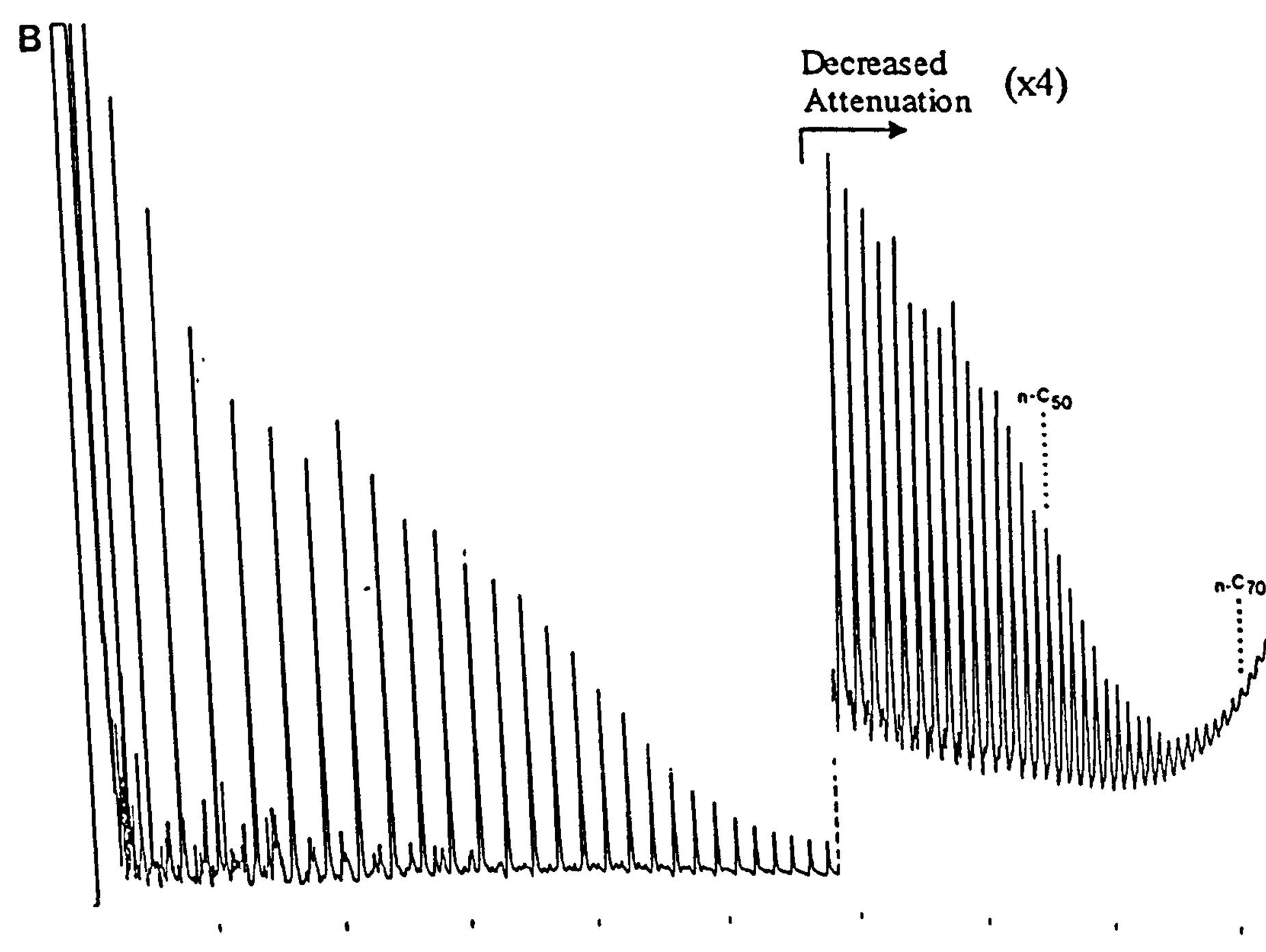

[GC: HT-5 (SGE), 12 m x 0.32 mm i.d., 50-410°C @ 10°C/min (10 min), He carrier, FID]

Figure 1-8 A) Gas Chromatogram of a Waxy North Sea gas-condensate (W) and B) HTCGC of the same gas condensate.

aluminium clad capillary column (SGE, HT-5, 12 m x 0.32 mm i.d., 0.1 μm, film). When the column was initially installed severe electrical noise was observed in the FID. This was thought to be because the column or detector was not at ground potential. Using the method developed by **Evershed and Prescott (1989)** the top three centimetres of the aluminium coating were removed by dissolving the aluminium in a 50% w/v aqueous sodium hydroxide solution.

In the literature several solvents are proposed for use in HTCGC analysis. The most common are tetrahydrofuran (THF), carbon disulphide (CS_2), iso-octane (2,2,4-trimethylpentane) and cyclohexane (see review by **Huball, 1990**).

Tetrahydrofuran did not dissolve the authentic higher molecular weight hydrocarbons (*e.g.* *n*-C_{60}), typical of those of the gas condensates efficiently because its low boiling point (65-67°C) prevented sufficient heating of the solution.

CS_2 was avoided for safety reasons while iso-octane was found to have a boiling point (b.p. 99-98°C) which made it difficult to remove from the sample by subsequent N_2 blow down.

Cyclohexane was found to be the most suitable solvent because its boiling point (b.p. 80.7°C, **CRC handbook**) allowed the solvent to be safely heated to above the measured cloud point of hexacontane (*n*-C_{60}, 53°C) and was easily removed when required.

1.3.2 (b) Injection reproducibility

To measure the precision of on-column injection, five injections of a *n*-C_{20}, *n*-C_{30}, *n*-C_{40}, *n*-C_{50} and *n*-C_{60} *n*-alkane mixture were made. Before injection it was necessary to heat the samples in order to dissolve the larger paraffins ($\geq$*n*-C_{40}). This was done by simply placing the sample vial on a hot area of the chromatograph. The results are shown in Table 1-2. The Relative Standard Deviation (%RSD) between injections was 7.4% (*n*-C_{20}) to 12.5% (*n*-C_{60}). The rather high RSD values were thought to be due to the uneven heating of the sample solution prior to injection which caused differences

Table 1-2 Peak areas for authentic *n*-alkanes using manual injection.

n-Alkane[a]	*n*-C_{20}	*n*-C_{30}	*n*-C_{40}	*n*-C_{50}	*n*-C_{60}
Peak Area[b]	96920	95348	74729	71166	58828
	106863	99748	83655	80515	66627
	111342	101635	89739	85437	66940
	118242	118212	86197	86607	72880
	113988	110041	94347	92723	82147
Mean	109471	104996.8	85733.4	83289.6	69484.4
SD(n-1)	8141.9	9110.9	7346.3	8051.2	8661.3
RSD%	7.4	8.7	8.6	9.7	12.5

[a]Concentration of each n-alkane = *c* . 25ng on-column

[b]Peak area measurements made using a Shimadzu C-R3A integrator.

Table 1-3 Peak areas for authentic *n*-alkanes using an improved manual injection technique.

n-Alkane[a]	*n*-C_{20}	*n*-C_{30}	*n*-C_{40}	*n*-C_{50}	*n*-C_{60}
Peak Area[b]	137942	102848	37531	54420	21530
	131289	96764	35148	50710	20079
	136259	104563	37877	54548	21570
	126819	98379	33782	48698	19261
	136252	98103	35870	52052	20762
Mean	133712	100131	36042	52086	20640
SD(n-1)	4588.5	3374.3	1697.1	2494.1	985.9
RSD%	3.4	3.4	4.7	4.8	4.8

[a]Concentration of each n-alkane = *c* . 23ng (n-C_{20}), 17ng (n-C_{30}), 7 ng (n-C_{40}), 9 ng (n-C_{50}), and 4 ng (n-C_{60}) on-column.

[b]Peak area measurements made using a Shimadzu C-R3A integrator.

in the sample volume. To avoid this, a small vial heater capable of maintaining a temperature of 55°C was developed (see Experimental). Ideally a heated auto-sampler such as that used by **Trestianu *et al.*, (1985)** would be preferable, but by keeping the injection method constant and using a fast injection speed (**Thompson and Rynaski, 1992**), injection reproducibility was much improved (Table 1-3). The RSD% for the standard *n*-alkanes ranged between 3.4% (n-C_{20}) and 4.8% (n-C_{60}).

1.3.2 (c) Calibration

FID response must vary at different concentrations of analyte (**Sewell and Clarke, 1987**). Yet there does not seem to have been any previous attempts to examine the linearity of HTCGC-FID response of HMW *n*-alkanes.

HTCGC peak areas obtained from examination of a calibration mixture comprising equal amounts of n-C_{20}, n-C_{40}, n-C_{50} and n-C_{60} (Figure 1-9) are shown in Table 1-4. The standard deviations were calculated from five repeat injections of the second and last data points and are shown in Table 1-4 and as error bars (± 1 x SD(n-1)) on the calibration curves for each pure *n*-alkane (Figure 1-10). Regression analysis produced good correlation coefficients of 0.999 (n-C_{20}), 0.997 (n-C_{40}), 0.998 (n-C_{50}) and 0.998 (n-C_{60}). Thus a good linear response is obtainable for the compounds over the concentrations used. To the author's knowledge, few if any such quantitative reproducibility data have been obtained previously for compounds as large as even n-C_{40}. Thus the analytical window for quantitative determination of hydrocarbons is expanded significantly by this study.

1.3.2 (d) Limit of detection

The limit of detection of HTCGC for the determination of the high molecular weight compounds is also important for quantitative analysis but has not been reported previously. The term limit of detection (LOD) is generally accepted to be the concentration of the analyte giving a signal (y) equal to the blank signal (y_B) plus two standard deviations of the blank (s_B) (**Miller and Miller, 1988**).

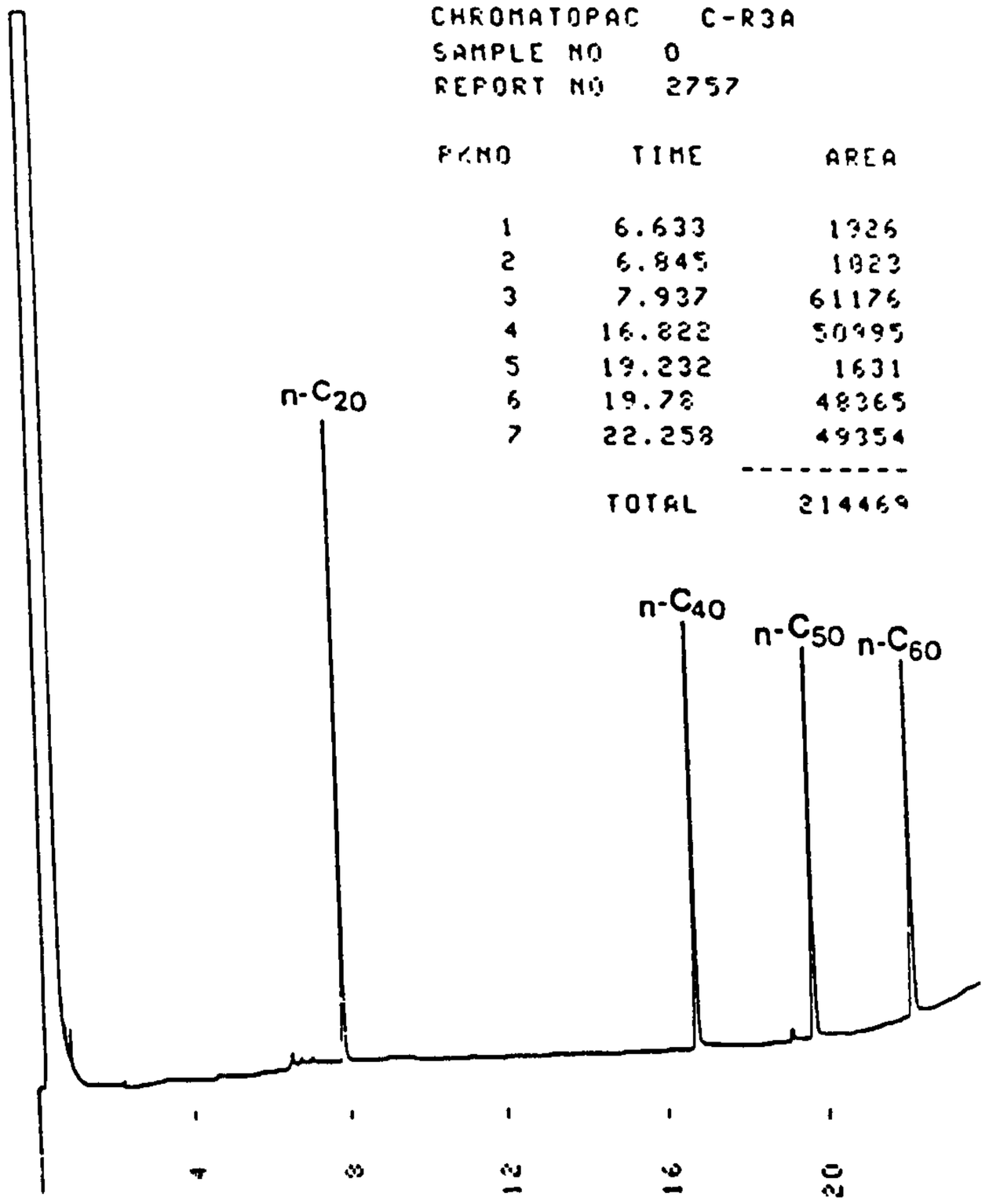

Figure 1-9 HTCGC of a *n*-alkane calibration standard (*n*-C_{20} (16.7 ng), *n*-C_{40} (15 ng), *n*-C_{50} (15.5 ng) and *n*-C_{60} (15 ng).

Table 1-4 Peak areas for known concentrations of *n*-alkanes *n*-C_{20}, *n*-C_{40}, *n*-C_{50}, and *n*-C_{60}.

n-Alkane					
n-C_{20}			*n*-C_{40}		
Conc. (ng)	Peak Area[1]	SD(n-1)[2]	Conc. (ng)	Peak Area	SD(n-1)
0	0		0	0	
5.55	21233	2433	5	18086	539
11.1	40860		10	30674	
16.65	61176		15	50995	
22.2	83502		20	71581	
27.75	102988	9357	25	92386	5371
n-C_{50}			*n*-C_{60}		
Conc. (ng)	Peak Area	SD(n-1)	Conc. (ng)	Peak Area	SD(n-1)
0	0		0	0	
5.15	18338	801	5	17963	766
10.3	29481		10	33497	
15.45	48365		15	49354	
20.45	66294		20	69137	
25.6	81708	2411	25	90393	4602

1 Peak areas measured using a Shimadzu C-R3A Integrator.
2 Standard deviation, n=3.

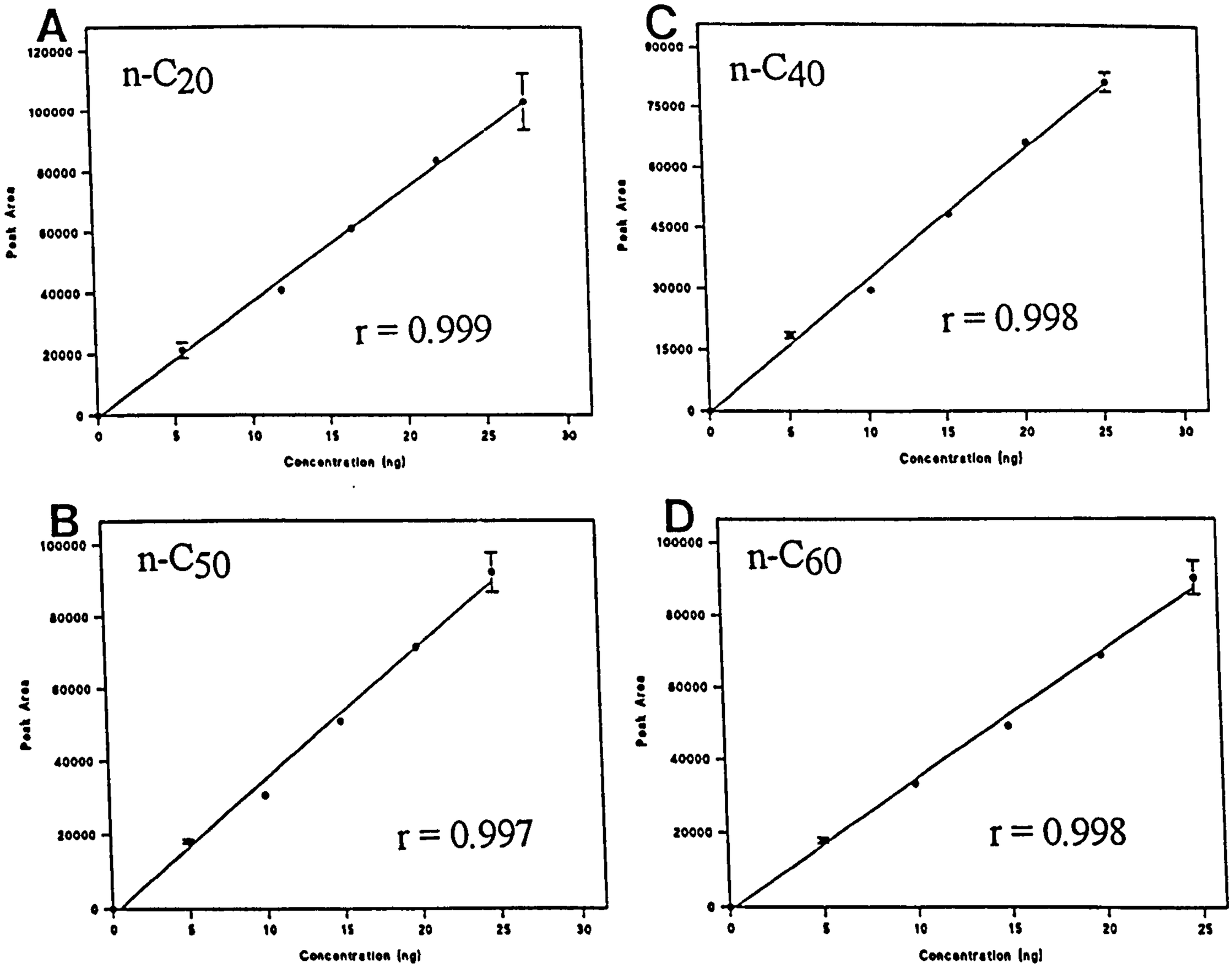

Figure 1-10 Calibration graphs for *n*-C_{20}, *n*-C_{40}, *n*-C_{50}, and *n*-C_{60}.

$$y - y_B = 3s_B \qquad [1]$$

Calculating the blank signal from chromatographic analysis using the Shimadzu C-R3A integrator is difficult and for this study a more acceptable method outlined by **Miller and Miller (1988)** was adopted. This method negates the need to actually measure the standard deviation of the blank by substituting with the statistic $s_{y/x}$.

$$s_{x/y}=\{\frac{\Sigma(y_i-y_i)^2}{n-2}\}^{1/2}$$

The term $s_{y/x}$ is similar to that which is used for the standard deviation of a set of repeat measurements, but measures the deviation in the y-residuals, *i.e.* y_i-$\hat{y}_i$ (Figure 1-11). The y_i values are the points on the calculated regression line corresponding to the x-values ("fitted" y-values), and are calculated from the regression equation. The calculated intercept of the regression line is used in place of the blank signal. These values can then be substituted into equation [1] to generate a y-value equivalent to the LOD. Knowing this, the LOD can be calculated from the regression line.

The above equations were entered into a computer spread-sheet package (Excel 5.0, Microsoft Corporation) and Table 1-5 shows the calculated LOD for *n*-C_{20}. The LOD's were 0.8 ng (*n*-C_{20}), to 4.72 ng (*n*-C_{50}) and for 1.87 *n*-C_{60} (Table 1-6). The higher value for *n*-C_{50} arising from the high variation of the difference between the measured signal and the regression line. With heated auto-injection the RSD between runs should be reduced and this would mean a much lower LOD. Even so these LOD's for $>n$-C_{40} HMW hydrocarbons are acceptable and within the range found for many analytes examined by conventional GC.

1.3.2 (e) Response factors

In the study carried out by **Thompson and Rynaski (1992)** the authors reported that when using a 15 m x 0.25 mm .i.d. high temperature capillary column relative response factors for *n*-alkanes with carbon numbers between C_{44-60} were unacceptable (*e.g.* *n*-C_{50}, 0.93 and *n*-C_{60}, 0.86). However, by using shorter megabore SIMDIST columns **Thompson and Rynaski (1992)** (6 m x 0.53 mm i.d.)-and in a separate study **Trestianu *et al.*, (1985)** (7 m x 0.6 mm i.d)-showed that it was possible to obtain the same relative FID response factors for *n*-alkanes up to *n*-C_{60} but the columns gave

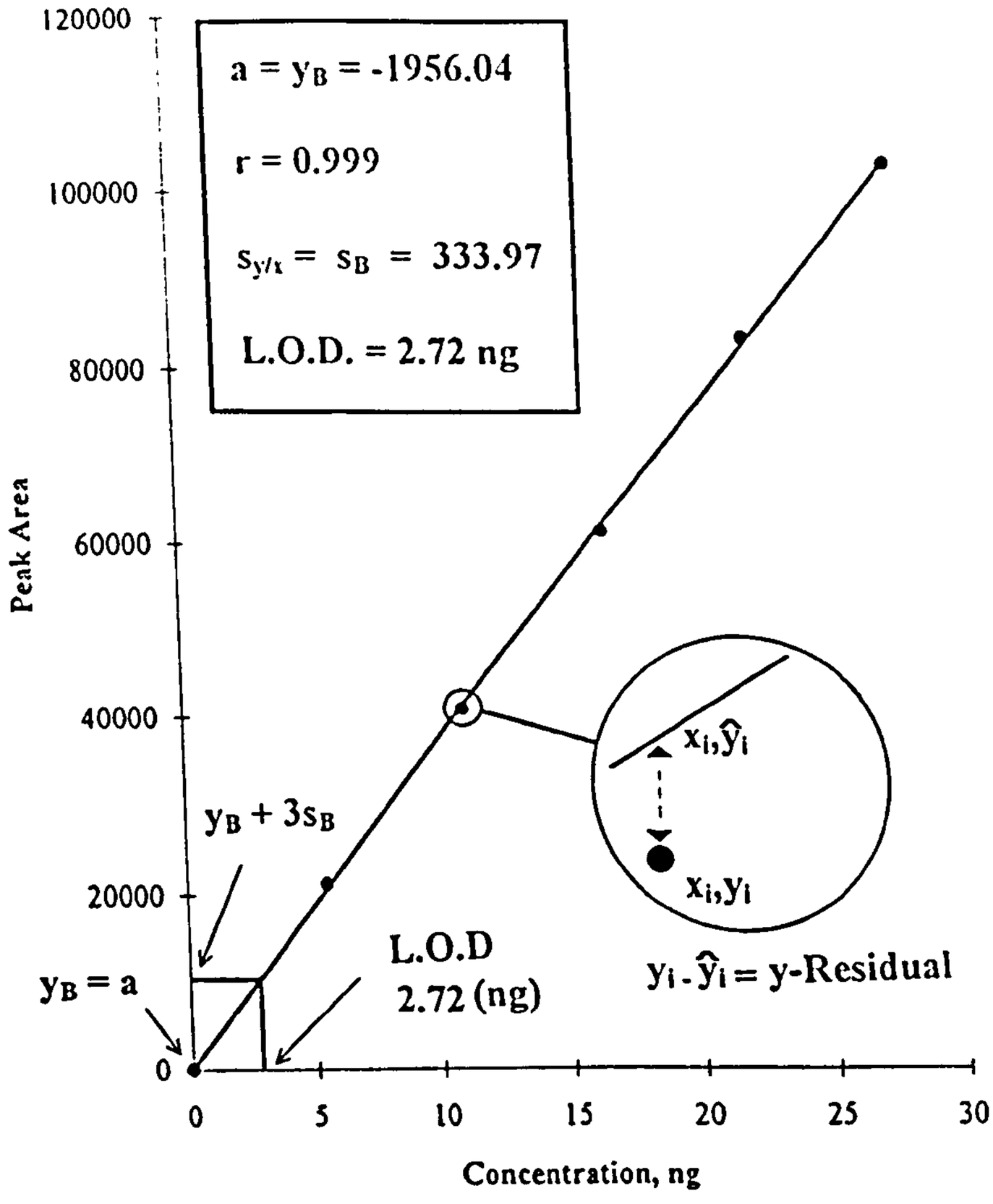

Figure 1-11 Graph showing how the limit of detection (L.O.D.) is calculated. (adapted from **Miller and Miller, 1986**).

Table 1-5 Calculation of the L.O.D.

x_i	x_i^2	y_i	$\hat{y}_i$	$\lvert y_i-\hat{y}_i \rvert$	$(y_i-\hat{y}_i)^2$
0.0	0.0	0.0	-1956.04	1956.04	3826092.48
5.55	30.80	21233	18427.45	2805.56	7871138.86
11.10	123.21	40860	38810.93	2049.07	4198687.86
16.65	277.22	61176	59194.42	1981.59	3926679.11
22.20	492.84	83502	79577.9	3924.10	15398560.81
27.75	770.06	102988	99961.39	3026.62	9160398.36
Σx_i^2 = 1694.14				$\Sigma(y_i-\hat{y})^2$ = 44381557.48	
$S_{y/x}$ = 3330.97				y = 8036.88	
Regression Line (y = mx + c)					
m = 3672.7					
c = -1956.04					
Limit of detection = 2.72 ng					

ref: Miller and Miller (1988)

Table 1-6 Summary of calibration results and the limits of detection for authentic *n*-alkanes (*n*-C_{20}, *n*-C_{40}, *n*-C_{50}, and *n*-C_{60}).

n-Alkane	*n*-C_{20}	*n*-C_{40}	n-C_{50}	n-C_{60}
n=	6	6	6	6
x-data min	0	0	0	0
x-data max	27.75	25	25.6	25
y-data min	0	0	0	0
y-data max	102988	92386	81708	90393
slope of line	3729.11	3672.78	3190.18	3550.54
y-intercept	-674.43	-1956.05	-216.49	-991.05
x-intercept	0.18	0.53	0.07	0.27
xy correlation	0.999	0.997	0.998	0.998
(correlation)2	0.998	0.994	0.996	0.997
LOD (ng)	0.8	2.39	4.27	1.87

Table 1-7 Response factors (RF) of *n*-alkanes relative to *n*-C_{20}.

Response Factors[1]			
n-C_{20}	*n*-C_{40}	*n*-C_{50}	*n*-C_{60}
1	0.94	0.95	0.93
1	0.83	0.79	0.91
1	0.93	0.87	0.90
1	0.91	0.87	0.89
1	0.99	0.87	0.97
mean	0.92	0.87	0.92
SD(n-1)	0.06	0.06	0.03

poorer resolution.

Response factors (RF) for the *n*-alkanes examined herein were calculated relative to squalane using the formula below;

$$RF = \frac{Area_X}{Area_{Reference}} \times \frac{Wt_{Reference}}{Wt_X}$$

Initially RF values for the *n*-alkanes were found to be low (Table 1-7) and similar to those reported by **Thompson and Rynaski, (1991)** using a smaller wide-bore column. Dissolution of *n*-C_{60} requires heating the sample to above 55°C and maintaining the temperature above the cloud point (*i.e.* that temperature at which the compound begins to precipitate on cooling). The cloud point of *n*-C_{60} in cyclohexane was found to be *ca.* 53°C. If the wax was not totally dissolved a true homogeneous mixture was hard to obtain and wax was found to collect on the glassware and could not be effectively removed even with continual rinsing with clean solvent. Heating the solution also causes a considerable expansion of the solvent, affecting the volumetrics.

To overcome these problems a system was developed (see Experimental) whereby the solvents and standard solutions were maintained at a constant temperature (55°C) just above the cloud point of *n*-C_{60} by heating in a water bath. It was found that very little *n*-C_{60} precipitated onto glassware during manipulation of the solutions and that which did was easily removed by rinsing with the warm solvent. Table 1-8 shows the reanalysis of a series of *n*-alkanes prepared in this fashion. The measured amounts in ng were calculated relative to squalane (31.85 mg). The results show a much improved RF for *n*-C_{40} (0.98), *n*-C_{50} (0.99) and *n*-C_{60} (0.99), and for which this "high resolution" chromatography column matched those from the values obtained by previous authors **(Trestianu et al., 1985; Luke and Ray, 1985; and Thompson and Rynaski, 1992)** using much shorter, lower resolution columns.

1.3.2 (f) Internal Standards

Simulated distillation calculations are usually performed using external standardization **(ASTM D 3710)** with LMW *n*-alkanes that elute before the analytes of interest. Typically samples examined by such techniques are heavy oils or residues remaining

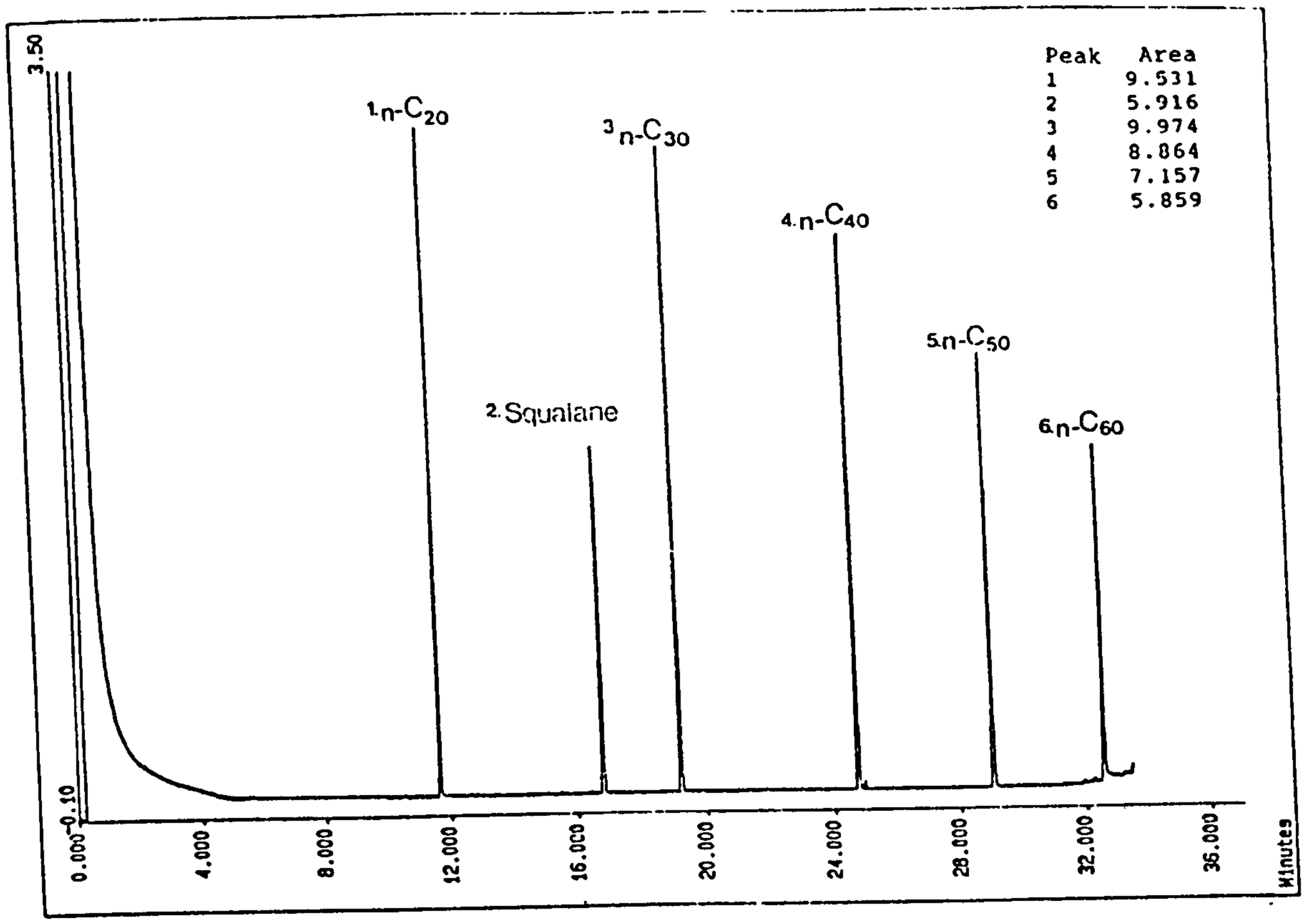

Figure 1-12 HTCGC of Squalane co-injected with a series of *n*-alkanes.

Table 1-8 Recalculated response factors for *n*-alkanes *n*-C_{20} to n-C_{60} relative to squalane.

n-Alkane	n-C_{20}	n-C_{30}	n-C_{40}	n-C_{50}	n-C_{60}
Actual amount (ng)	50.7	53.7	49.2	38.8	32.0
Measured amount (ng)	51.5	53.6	48.0	38.7	31.6
	52.7	52.0	48.0	37.0	31.9
	51.2	54.0	47.5	36.5	32.3
	50.2	53.1	47.2	37.4	28.5
	51.6	52.9	48.0	37.4	31.1
mean	51.4	53.1	47.7	37.4	31.1
%	101.5	98.9	97.0	96.4	97.1
SD(n-1)	0.896	0.760	0.371	0.815	1.507
[1]RF	1.01	1.13	0.98	0.99	0.99

1 Response factor calculated relative to Squalane (31.85 mg) using manual on-column injection.

after vacuum distillation of crude oils. This is not possible in the case of gas condensates because they contain large amounts of LMW compounds. In any case external calibration often leads to higher inaccuracies because of the variability of injections. Neither are *n*-alkanes suitable as internal standards since gas condensates usually contain large amounts of *n*-alkanes. Alternative compounds suitable as internal standards are therefore necessary.

When choosing an internal standard there are several criteria that should be adopted. According to **Sewell and Clarke (1987)** an internal standard should:

. be structurally similar to the compound(s) of interest.
. be completely resolved from other components of the sample.
. elute close to the compound(s) of interest.
. be stable and be obtainable in a high purity state.

There seems to be no mention in the literature of internal standards suitable for HTCGC internal standards (*e.g.* with boiling points greater than 525°C (*n*-C_{40})).

One group of compounds that have been the focus of many qualitative HTCGC studies are the triglycerides that occur in fats and oils **(Review by Geeraert and Sandra 1987; Evershed *et al.*, 1990)**. Typical structures of this group of compounds are shown in Figure 1-13. The number and length of side chains varies with a concomitant increase in boiling point. **Tremonia *et al.*, (1987)** used HTCGC to study triglycerides and found that they did not thermally degrade. Pure compounds are available commercially obviating the need for lengthy synthesis. Thus these compounds satisfy most of the above criteria for use as internal standards.

Figure 1-14 shows a chromatogram of a mixture *n*-C_{20}, *n*-C_{30}, *n*-C_{40}, *n*-C_{50} and *n*-C_{60} alkanes co-injected with the compounds tristearin, tribehenin and triarachnidin. Tristearin was chosen for further study because it elutes very close to *n*-C_{60}, which was the longest retained pure *n*-alkane available. The standard compounds *n*-C_{23}, *n*-C_{60} and tristearin (Table 1-9), were further investigated and compared. All three compounds

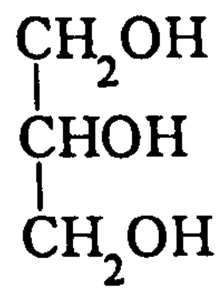

Glycerol

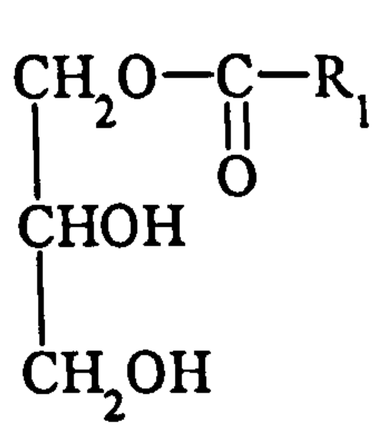

1-Monoacylglycerol

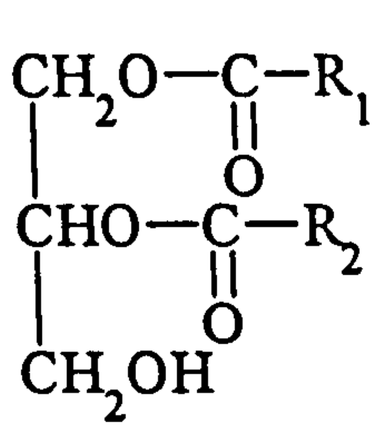

1,2-Diacylglycerol

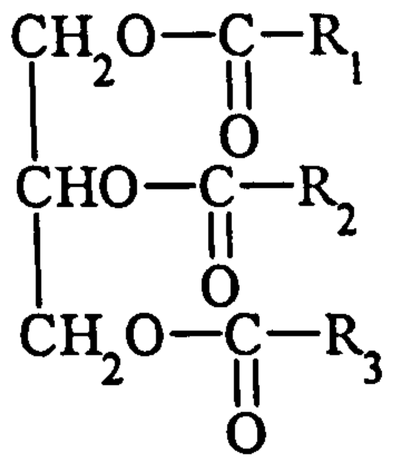

1,2,3-Triacylglycerol

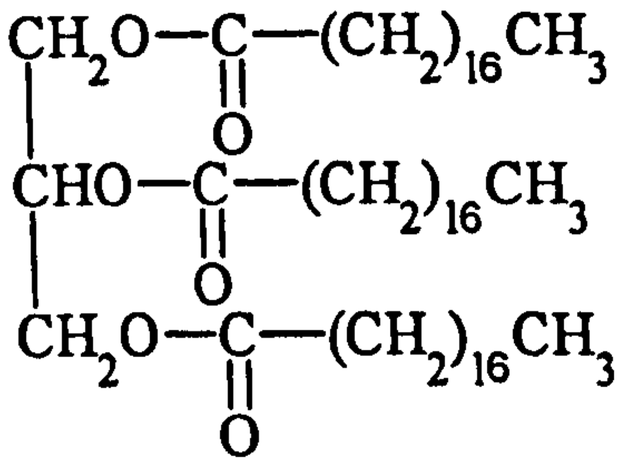

1,2,3-Trioctadecanoylglycerol
(Tristearin)

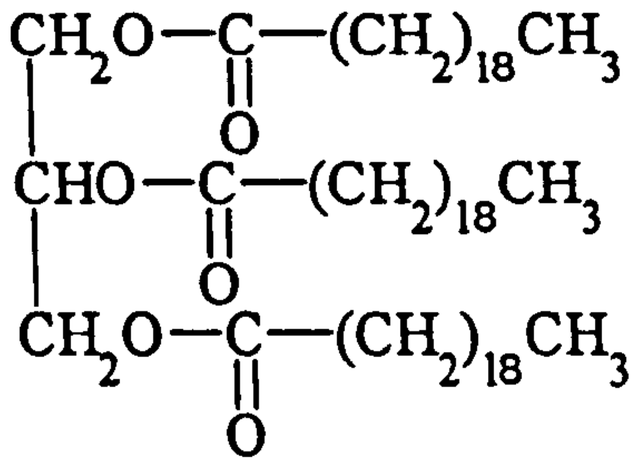

1,2,3-Trieicosanoylglycerol
(Triarachidin)

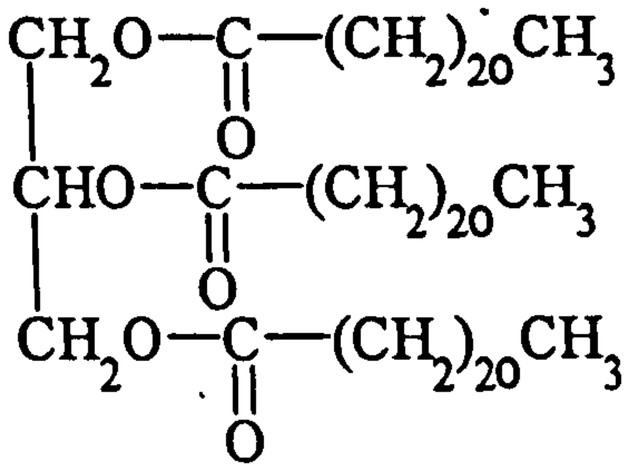

1,2,3-Tridocosanoylglycerol
(Tribehenin)

Figure 1-13 Structures of triglycerides.

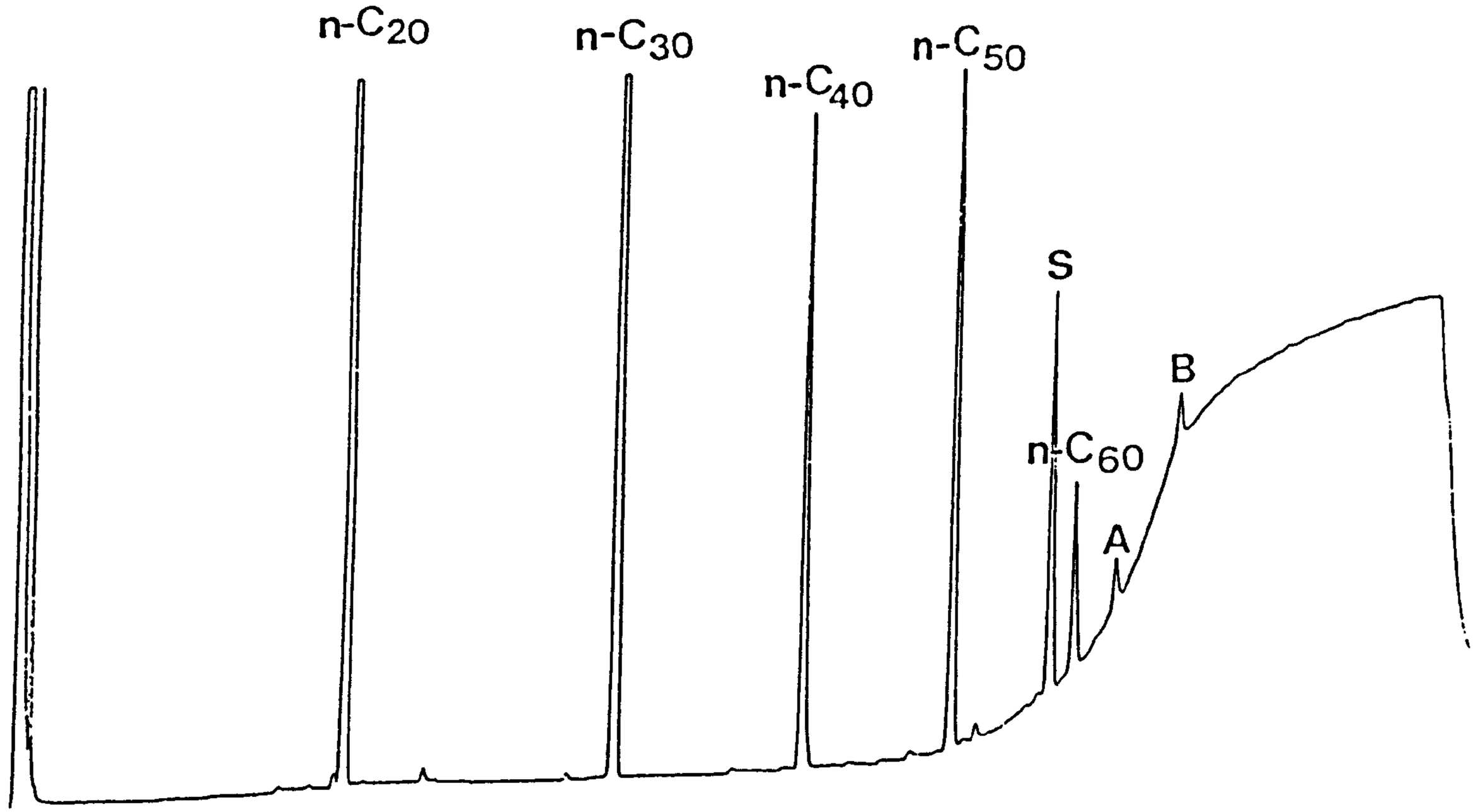

Figure 1-14 The triglycerides Tristearin (S), Tribehnin (B) and Triarachnidin (B) co-injected with a series of *n*-alkanes.

Table 1-9 Peak areas for known concentrations of *n*-C_{23}, Tristearin and *n*-C_{60}.

n-C_{23}			Tristearin			*n*-C_{60}		
Conc. (ng)	Peak Area[a]	SD(n-1)[b]	Conc. (ng)	Peak Area	SD(n-1)	Conc. (ng)	Peak Area	SD(n-1)
0.00	0.0		0.00	0.0		0.00	0.0	
6.35	2456	107	5.15	2288	69	6.13	2321	76
12.70	4646		10.30	4356		12.26	4489	
19.05	6295		15.45	5612		18.39	5765	
25.40	8554	190	20.60	7970	170	24.52	7764	182

1 Peak areas obtained using a Shimadzu C-R3A Intergrator.

2 n=3

gave a good linear calibration over the concentrations used (Figure 1-15) with correlation coefficients of 0.998 (n-C_{23}) and 0.996 (tristearin), and 0.995 (n-C_{60}), (Table 1-10). The limit of detection for each compound was calculated using the method described previously (1.3.2. d) and decreased from 1.9 ng for n-C_{23}, to 2.2 ng for tristearin to 2.8 ng for n-C_{60}. Tristearin had a slightly higher response factor (1.1) than n-C_{23}, while the average response factor for n-C_{60} was 0.97, slightly lower than expected but again within acceptable limits (*i.e.* equal response factors) for use in quantitative HTCGC.

Figure 1-16 (A) shows a partial chromatogram of condensate W co-injected with tristearin (6.5 ng) which elutes between n-C_{59} and n-C_{60}. Figure 4-25 (B) shows an expanded portion of the same region of chromatogram obtained with a slower oven temperature rate of 5°C/min. Using this program rate the resolution between the three peaks was improved to the point where tristearin was almost completely resolved from the analytes.

Choosing a internal standard is usually a compromise. In this study the triglyceride tristearin is obviously structurally dissimilar to the hydrocarbon determinands present in the gas condensates. However, tristearin is thermally stable and the present study shows that it gives a linear response, has a response factor that is close to that of n-hexacontane (C_{60}) and at a temperature program of 5°C/min is almost completely resolved from the other compounds present. It is available commercially in a pure form and obviates the need for in-house synthesis.

1.3.3 Determination of the C_{30+} Fraction of condensate U and W

Using the above method it is possible to calculate the amount of compounds present in the C_{30+} fraction the condensates U and W. Peak integration was carried out using the Shimdazu C-R3A integrator. Initially the drift setting on the integrator was set to zero. This enables peak detection to the baseline rather than valley to valley, thus taking into account the unresolved complex mixture underlying the resolved peaks (Figure 1-17 A). This UCM accounts for a significant portion (21%) of the chromatographic peak

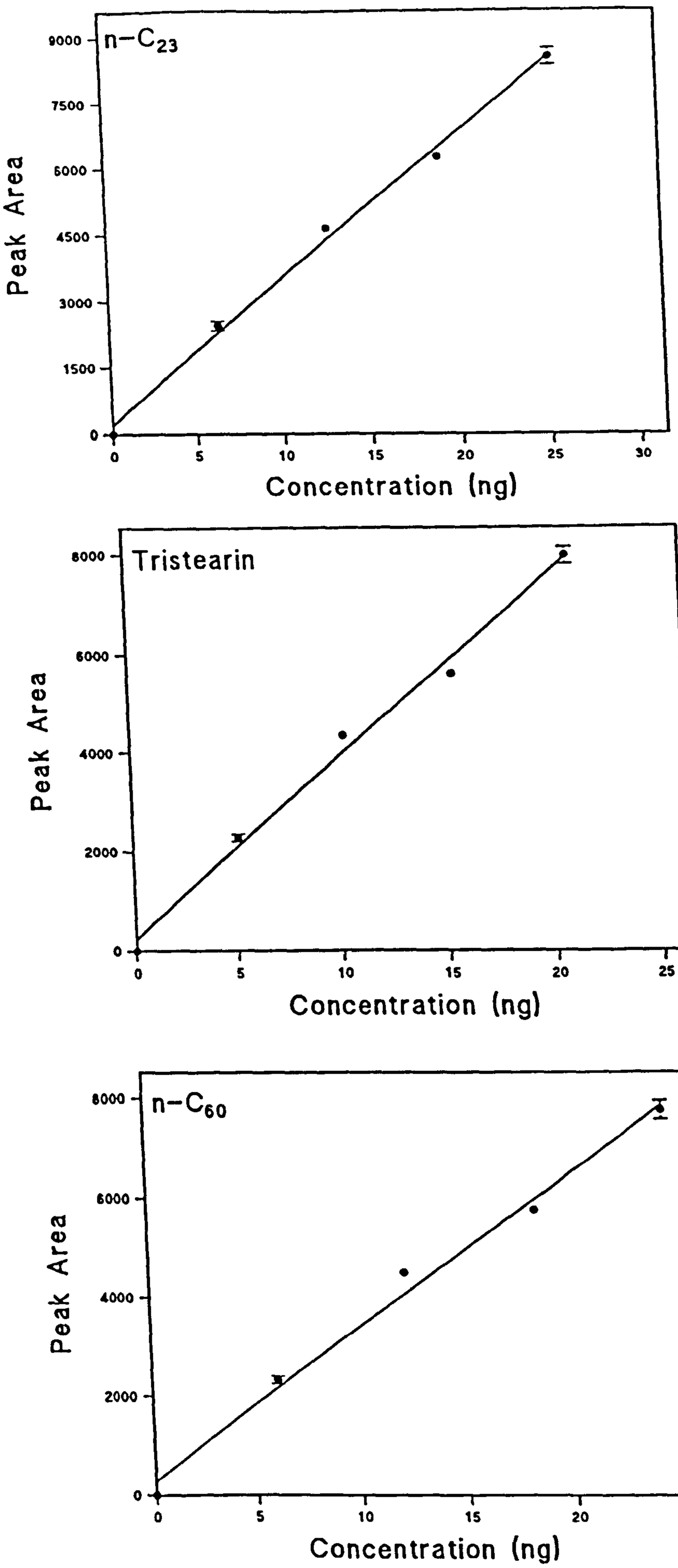

Figure 1-15 Calibration graphs for *n*-C_{23}, Tristearin and *n*-C_{60}.

Table 1-10 Summary of results from the calibration of *n*-C_{23}, Tristearin and *n*-C_{60}.

n-Alkane	*n*-C_{23}	Tristearin	*n*-C_{60}
n=	5	5	5
x-data min	0	0	0
x-data max	25.4	20.91	6.13
y-data min	0	0	0
y-data max	8554	7970	7764
slope of line	3729.1	369.64	309.5
y-intercept	200	215.01	273.4
x-intercept	-0.61	-0.58	-0.88
xy correlation	0.998	0.996	0.995
(correlation)2	0.996	0.992	0.991
R.F.	-	1.1	0.97
LOD (ng)	1.9	2.2	2.8

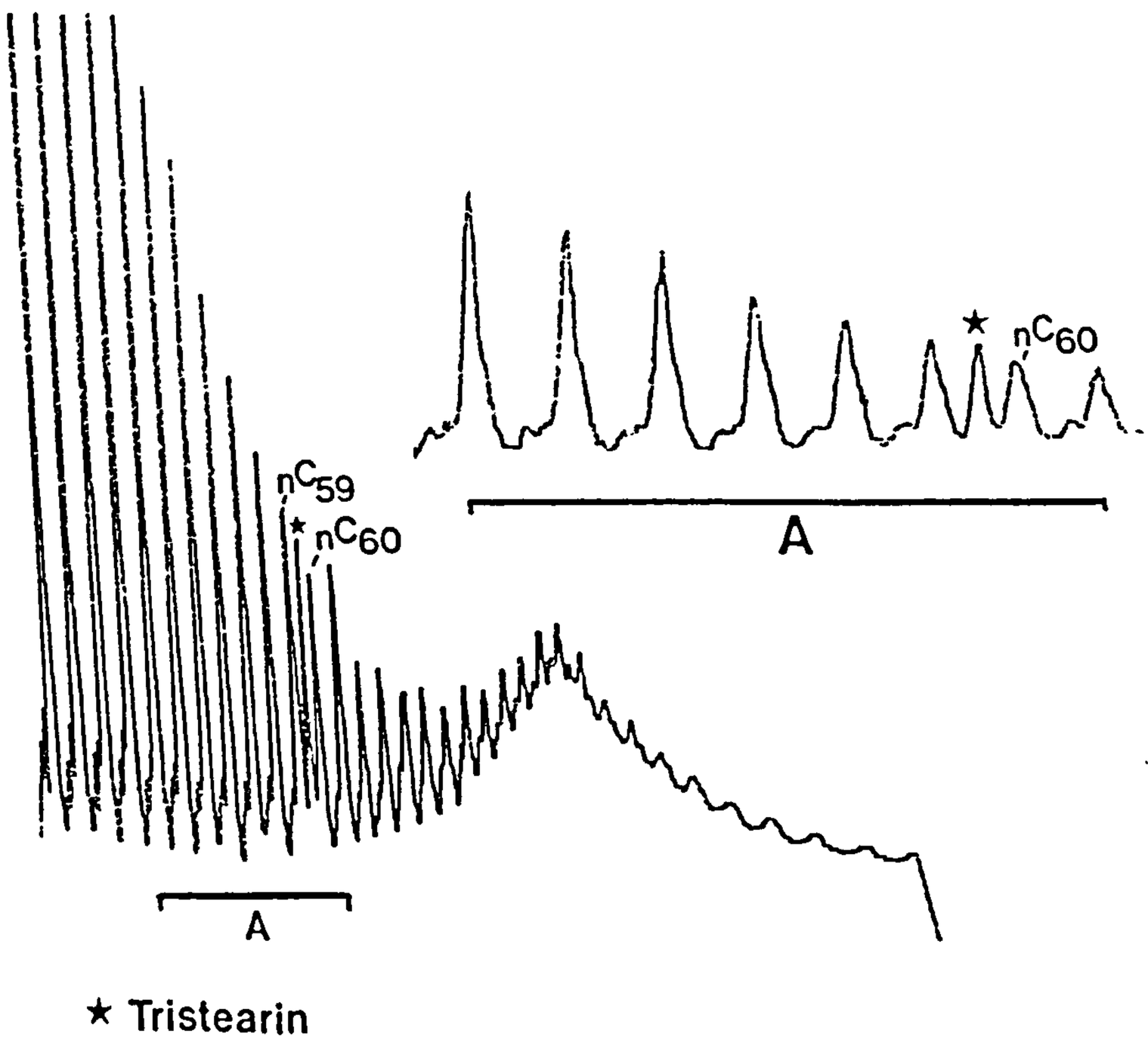

Figure 1-16 A) Partial chromatogram of condensate W co-injected with internal standard Tristearin, and B) expanded section.

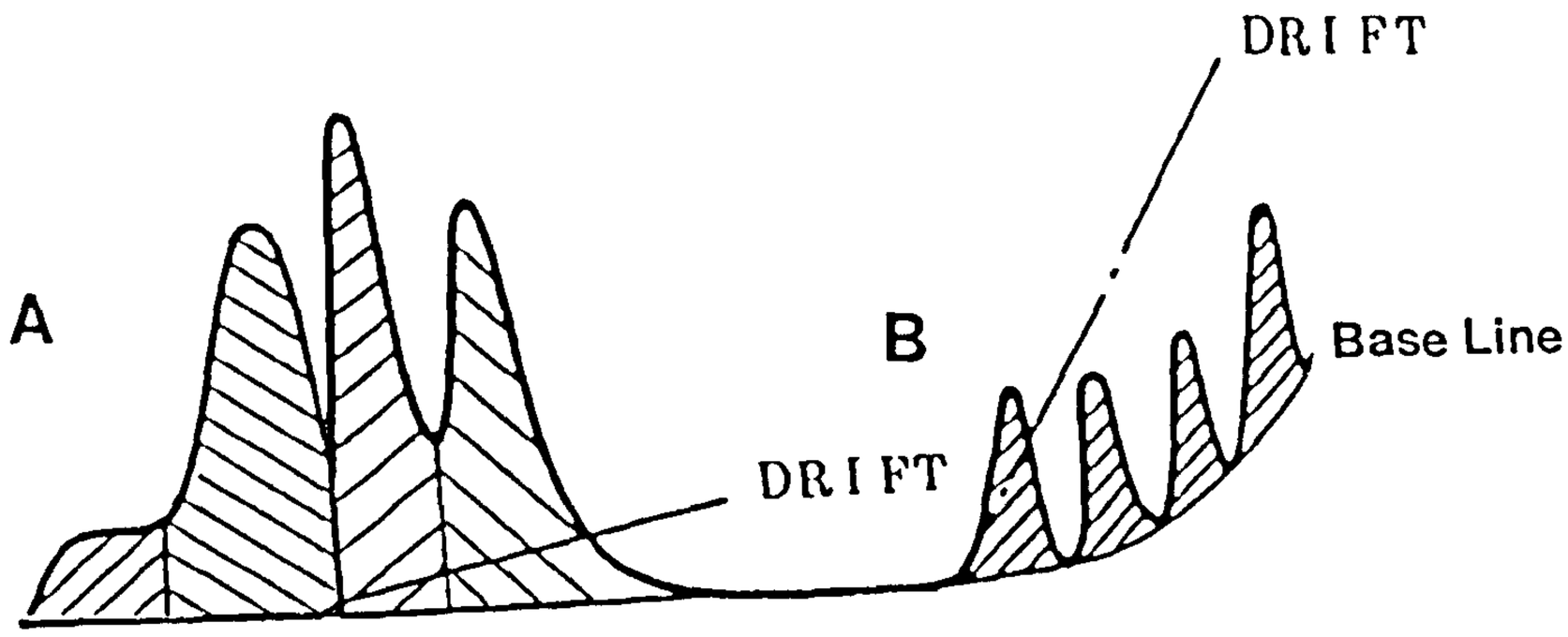

Figure 1-17 A) Integration with drift setting set to zero and B) integration with drift set to a high value.

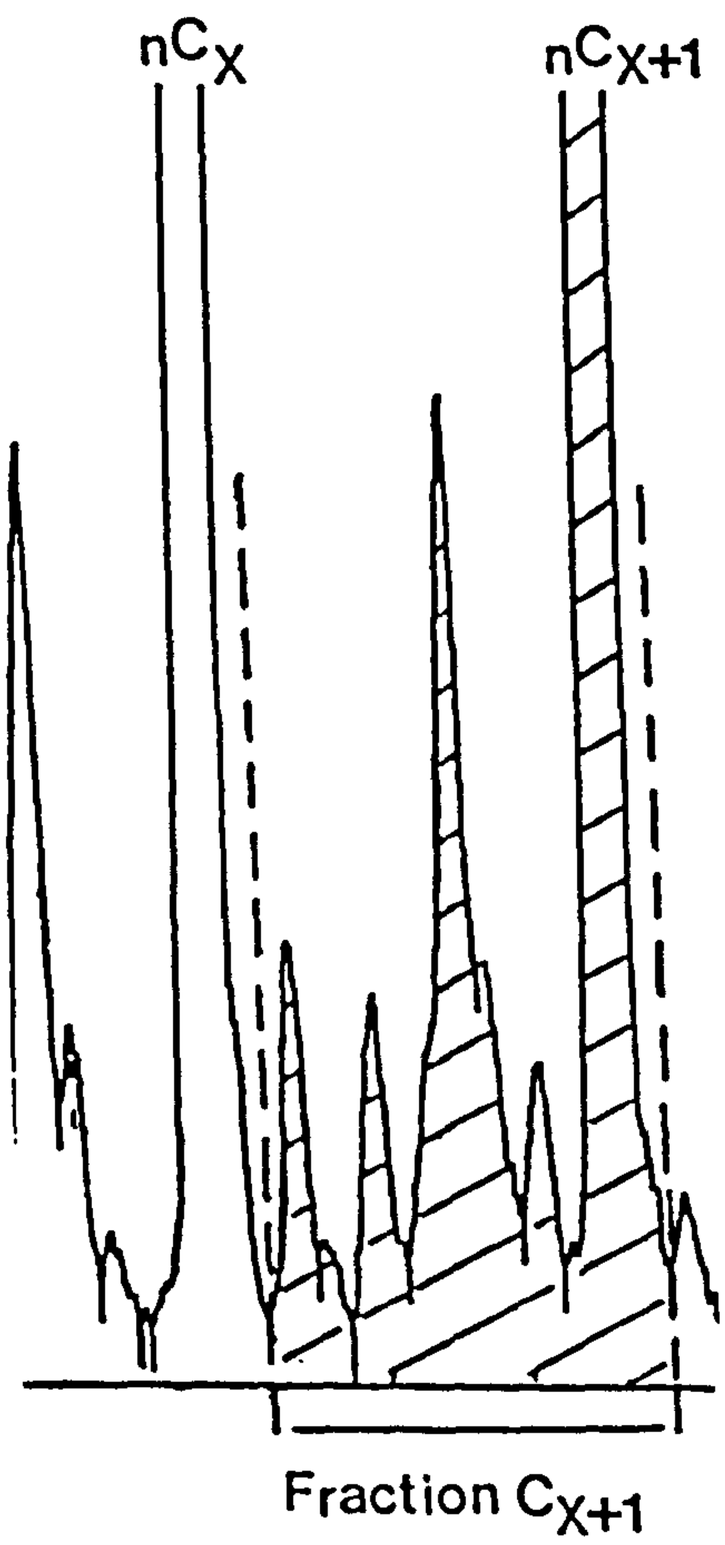

Figure 1-18 Integration of hydrocarbon fractions.

area (see Chapter 3). The drift was then increased towards the end of the chromatogram to account for the increase in the baseline from column bleed (Figure 1-17 B). This increase in base line can be overcome by using background subtraction but this facility depends on the instrument or integrator being used. In the case of the Shimadzu C-R3A integrator, background subtraction is not possible.

The area for each hydrocarbon fraction was measured between consecutive *n*-alkanes including the area of the later eluting *n*-alkane (Figure 1-18). This is a standard protocol used by most industries. The amount of each fraction on-column (ng) and the weight-weight% of each of the fractions can then be calculated from the area of the internal standard.

The use of cyclohexane as solvent precluded the accurate measurement of the light fractions ($<C_{12}$) present in the whole condensate, so direct comparison of these findings to those of other studies using conventional GC cannot be made. However, it is possible to compare the sets of results by normalizing the data to the C_{12+} fraction. The results are given in Table 1-11 and 1-12 and plotted in Figure 1-19. The quantitative results obtained using the high temperature GC for condensates U and W match closely those obtained by **British Gas (1992)** but importantly HTCGC also enables the determination of the components greater than C_{30} (Figure 1-19).

Figure 1-20 (A) shows the retention time of the *n*-alkanes C_{12} to C_{44} plotted against their natural boiling points (no boiling point data could be found for alkanes with carbon numbers greater than *n*-C_{44}). The correlation appears linear and gives a correlation coefficient of 0.9998. Closer examination shows that the actual boiling points deviate from the linearity of regression line at lower and higher retention times (Figure 1-20 B). A better model for the data is obtained when plotting the polynomial regression through the data ($r^2=1$ Figure 1-20 C). By extrapolation of the polynomial equation the boiling points for higher eluting *n*-alkanes can then be estimated from the regression equation (Figure 1-20 D) The extrapolated boiling points for condensates U and W are given in Tables 1-13 and 14. A simulated distillation curve can then be obtained by plotting the cumulative weight of each fraction against the boiling point.

Table 1-11 Comparison of results of the chromatographic analysis of condensate U (L.R.S = British Gas plc London Research Station using conventional GC and, H.T. = this study using HTCGC).

Analysis of Condensate U by GC and HTCGC[a]				
Fraction	L.R.S. wt.wt%	H.T. wt.wt%	Fraction	H.T. wt.wt%
C12	11.83	10.61	C39	0.22
C13	12.13	11.06	C40	0.18
C14	9.82	10.16	C41	0.15
C15	8.67	9.16	C42	0.12
C16	6.47	7.00	C43	0.11
C17	5.81	7.35	C44	0.09
C18	5.31	6.24	C45	0.07
C19	5.66	5.22	C46	0.07
C20	4.81	4.72	C47	0.06
C21	4.31	4.09	C48	0.06
C22	4.01	3.66	C49	0.04
C23	3.81	3.63	C50	0.03
C24	3.21	2.41	C51	0.03
C25	2.56	2.39	C52	0.03
C26	2.26	2.03	C53	0.03
C27	1.65	1.47	C54	0.02
C28	1.35	1.40	C55	0.02
C29	1.10	1.24	C56	0.02
C30		1.01	C57	0.01
C31		0.84	C58	0.01
C32		0.69	C59	0.01
C33		0.60	C60	0.01
C34		0.48	C61	0.01
C35		0.38	C62	0.01
C36		0.29	C63	0.01
C37		0.26	C64	0.004
C38		0.23		

a. Both set of data normalized to the C_{12+} fraction.

Table 1-12 Comparison of results of the chromatographic analysis of condensate W (L.R.S = British Gas London Research Station using conventional GC and, H.T. = this study using HTCGC).

Analysis of Condensate W by GC and HTCGC[a]				
Fraction	L.R.S. wt.wt%	H.T. wt.wt%	Fraction	H.T. wt.wt%
C12	11.830	10.612	C39	0.217
C13	12.130	11.057	C40	0.185
C14	9.825	10.155	C41	0.148
C15	8.672	9.156	C42	0.122
C16	6.466	7.001	C43	0.109
C17	5.815	7.346	C44	0.090
C18	5.313	6.240	C45	0.074
C19	5.664	5.217	C46	0.068
C20	4.812	4.722	C47	0.063
C21	4.311	4.087	C48	0.055
C22	4.010	3.657	C49	0.038
C23	3.810	3.631	C50	0.035
C24	3.208	2.413	C51	0.027
C25	2.556	2.387	C52	0.034
C26	2.256	2.026	C53	0.026
C27	1.654	1.474	C54	0.022
C28	1.353	1.395	C55	0.020
C29	1.103	1.236	C56	0.017
C30		1.005	C57	0.008
C31		0.836	C58	0.014
C32		0.692	C59	0.012
C33		0.595	C60	0.011
C34		0.480	C61	0.008
C35		0.380	C62	0.007
C36		0.294	C63	0.006
C37		0.255	C64	0.004
C38		0.228		

a. Both set of data normalized to the C12+ fraction.

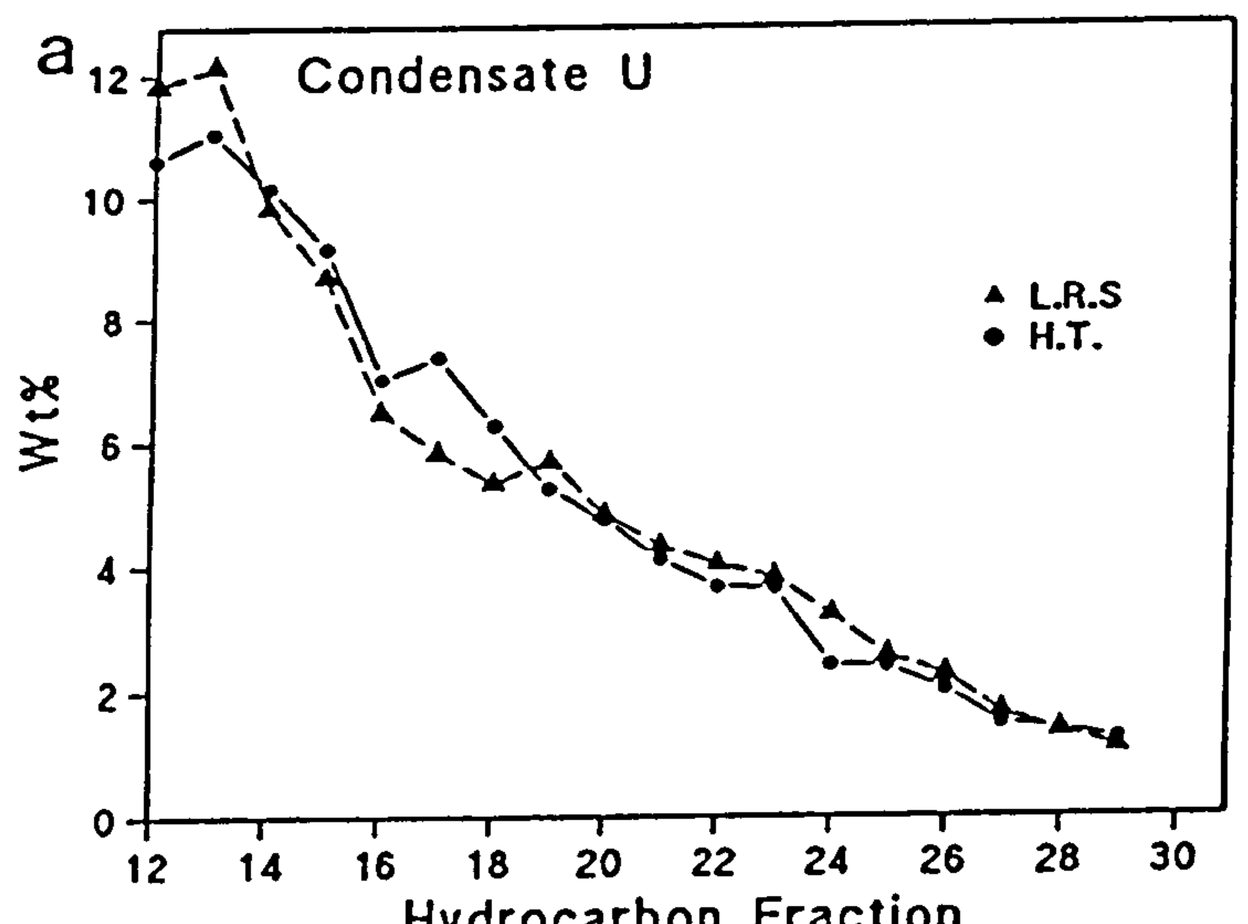

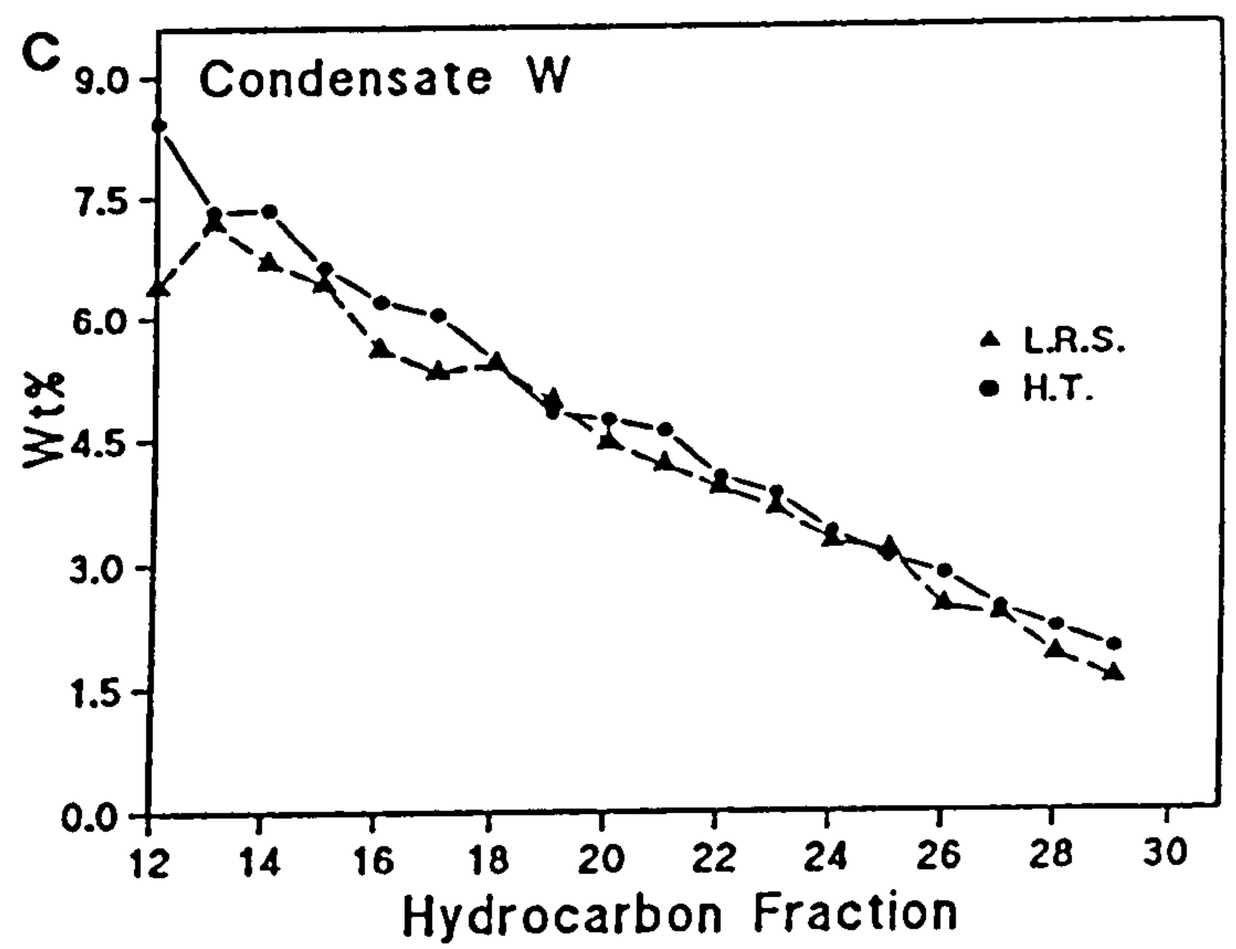

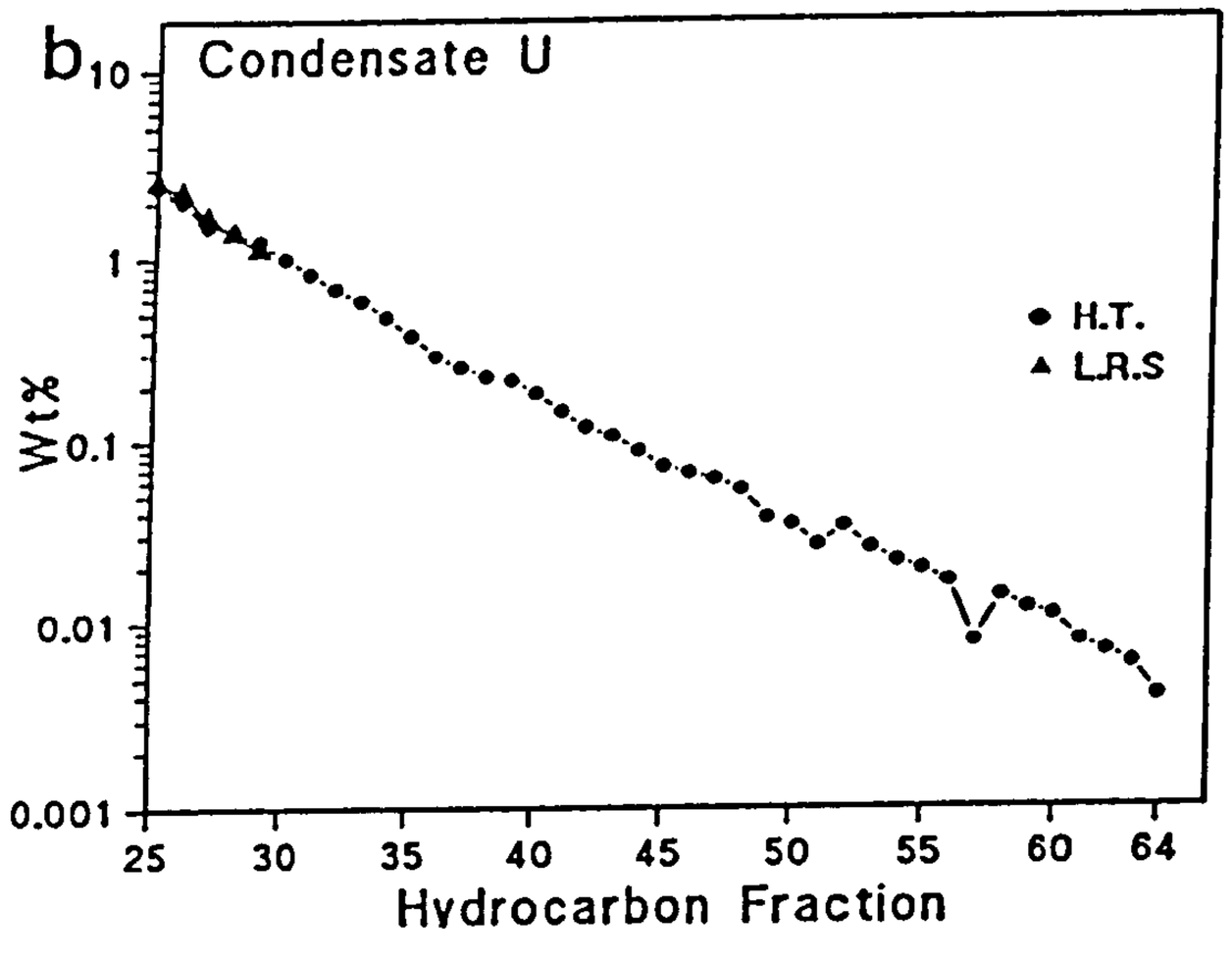

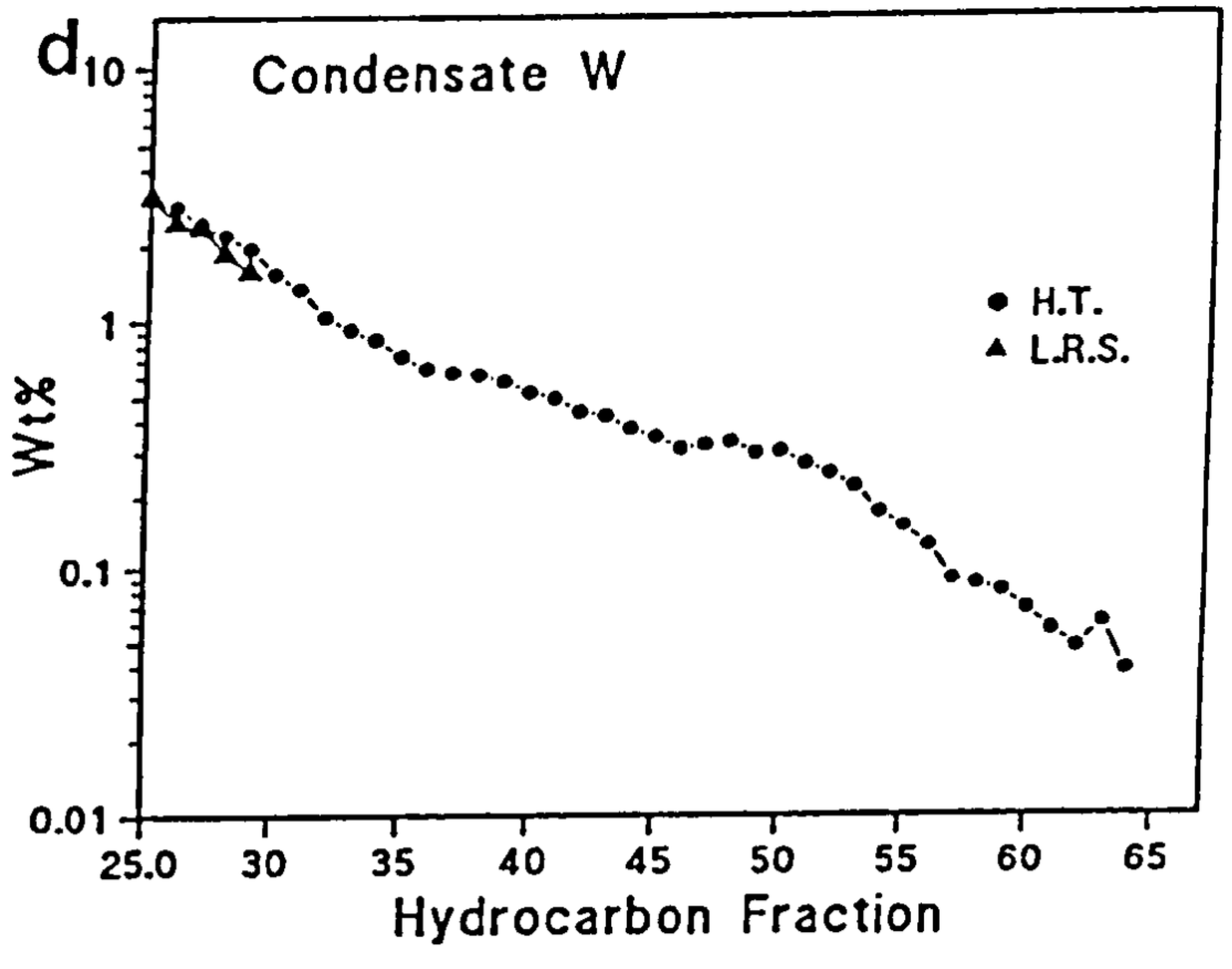

Figure 1-19 Weight against hydrocarbon fraction of condensate U & W calculated by conventional GC and HTCGC and B) extended analysis showing wt% of hydrocarbons C_{25} to C_{65} by HTCGC.
(L.R.S = London Research Station Analysis, H.T. = HTCGC Analysis)

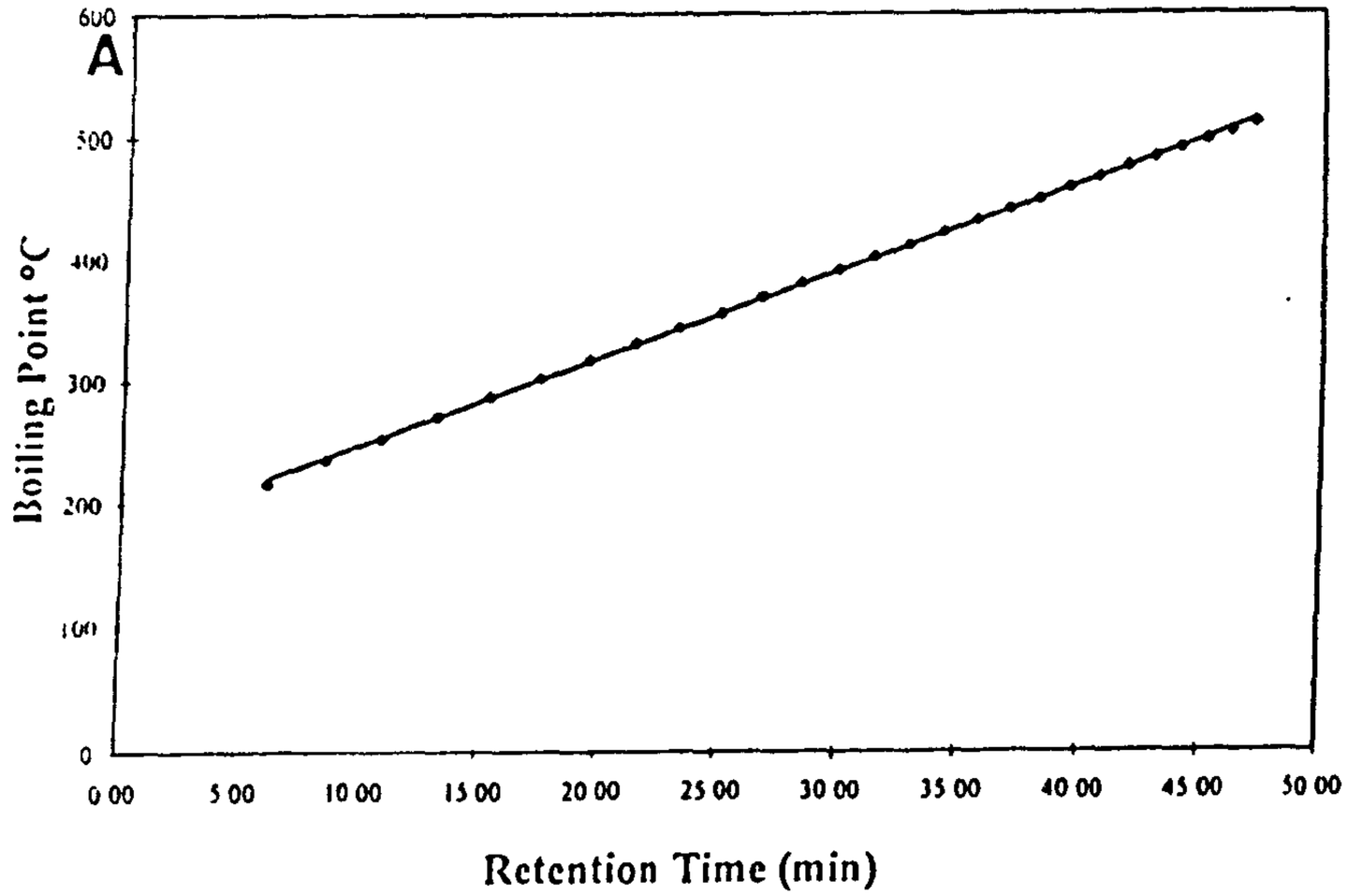

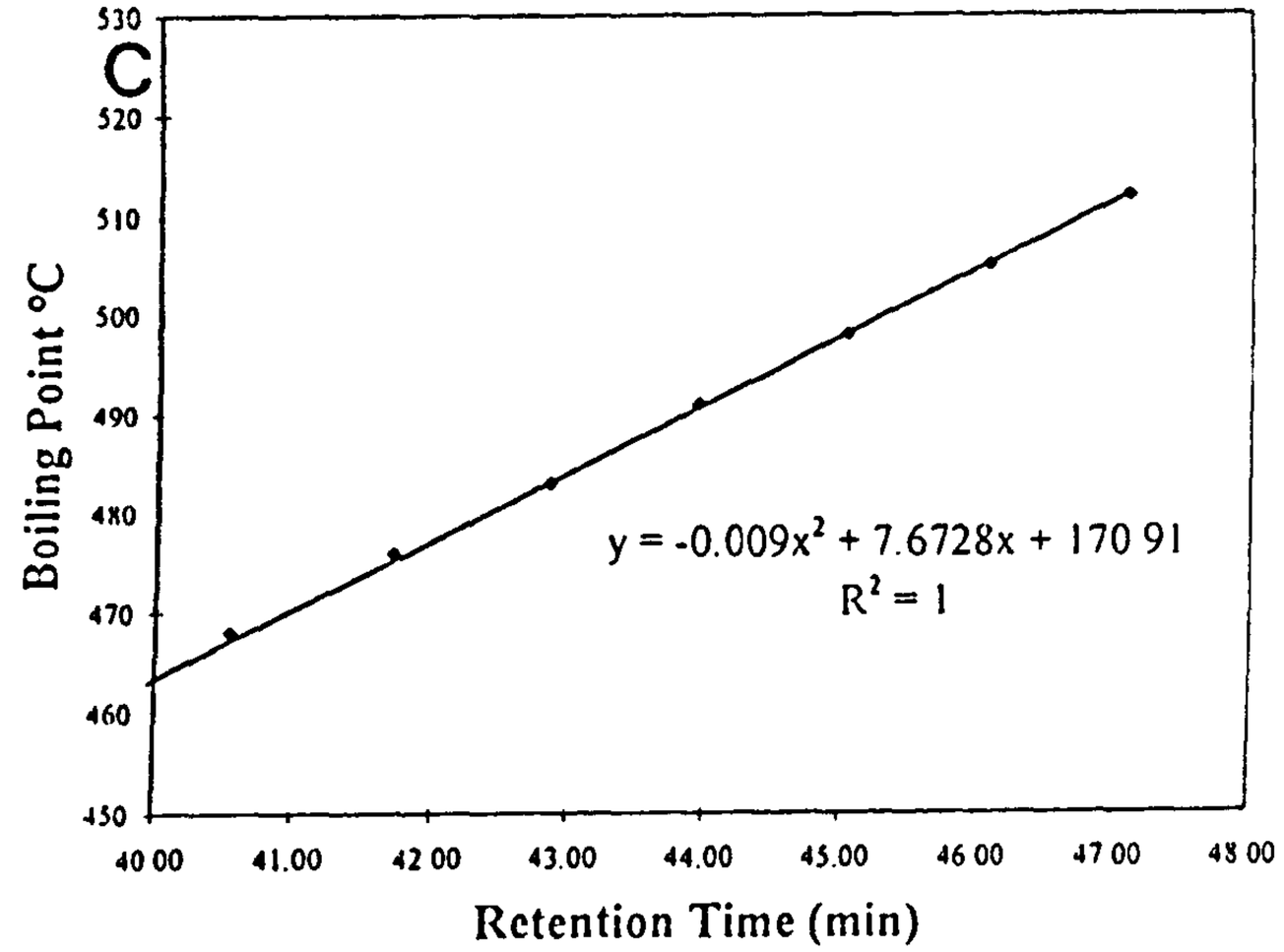

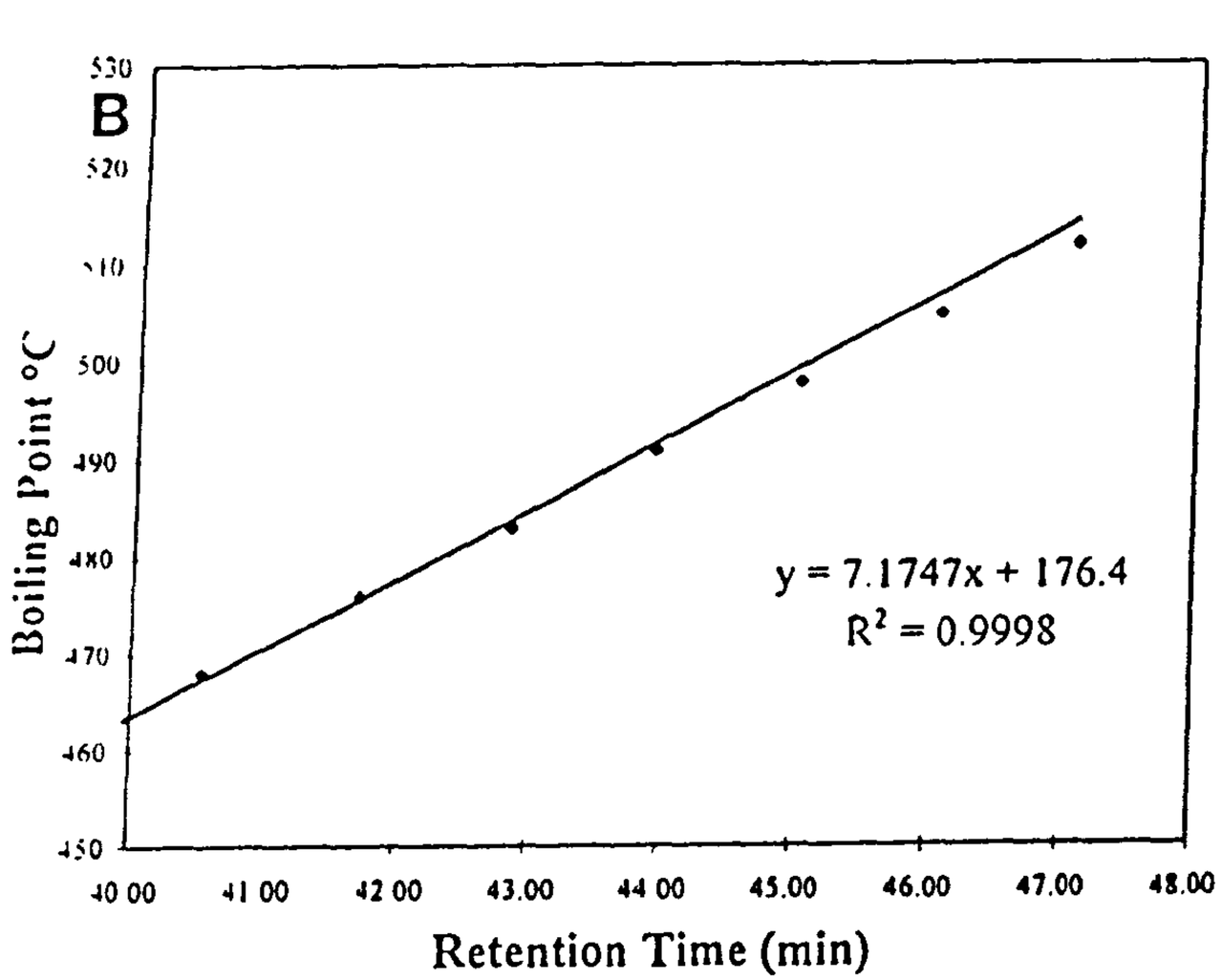

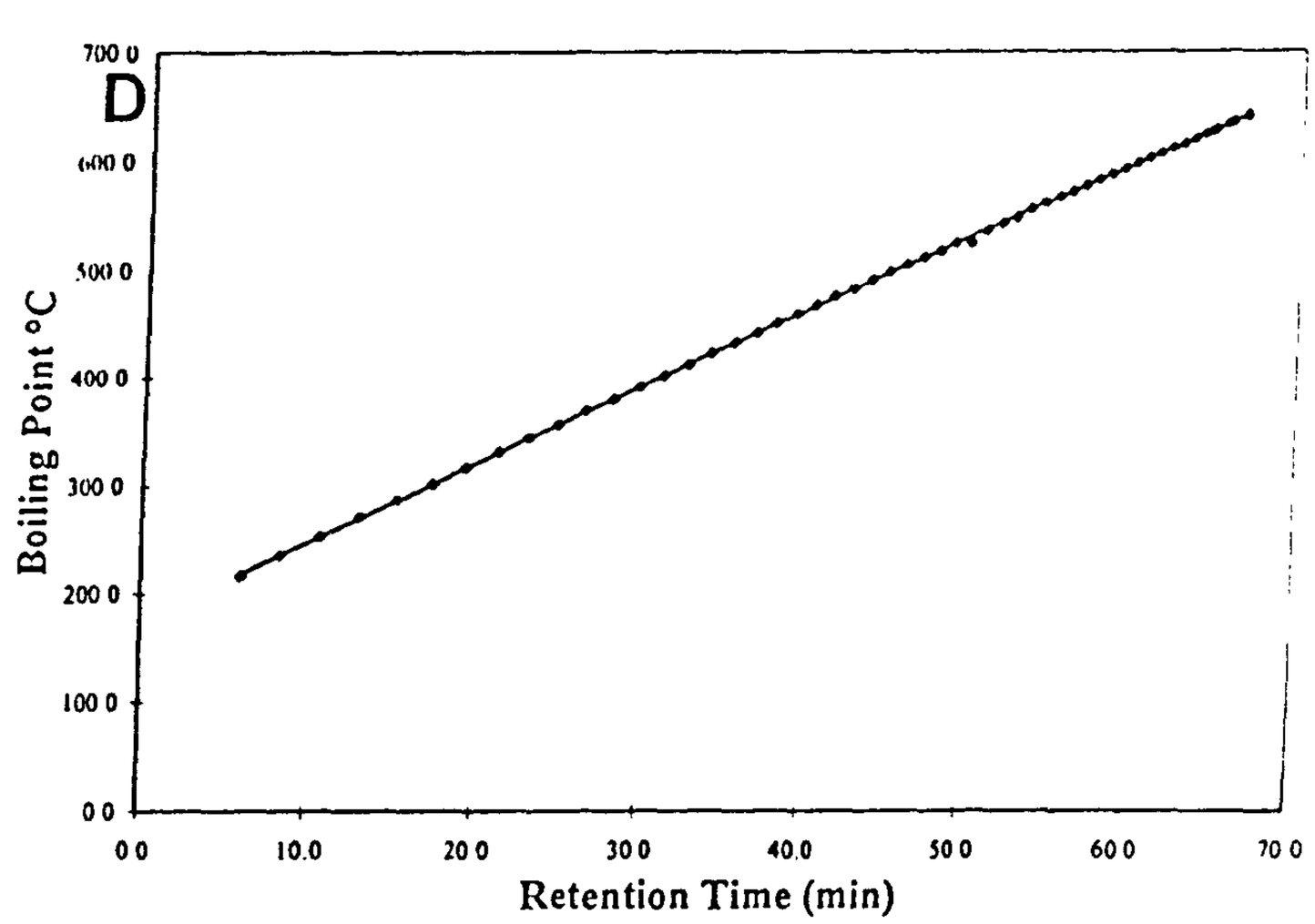

Figure 1-20 Graphs showing: A) Boiling point *vs* retention time for fractions C_{12} to C_{44}. B) Linear regression (retention time between 40 to 48 min). C) polynomial regression (retention time 40 to 48 min). D) Boiling point *vs* extrapolated retention time.

Table 1-13 Amount of each hydrocarbon fraction expressed as amount (ng) on-column and weight percent of the total condensate U.

HTCGC Analysis of Condensate U											
Fraction	R.T.	B.pt.	Area	ng[a]	Wt.Wt%	Fraction	R.T.	B.pt.	Area	ng	Wt.Wt%
C12	6.11	216	2423263	1273	3.96	C39	48.08	518	49520	26.0	0.08
C13	8.44	235	2524851	1326	4.13	C40	49.05	525	42148	22.1	0.07
C14	10.80	253	2318962	1218	3.79	C41	50.00	531	33867	17.8	0.06
C15	13.10	271	2090839	1098	3.42	C42	50.93	537	27938	14.7	0.05
C16	15.30	287	1598687	840	2.62	C43	51.83	543	24936	13.1	0.04
C17	17.42	302	1677424	881	2.74	C44	52.72	548	20533	10.8	0.03
C18	19.43	317	1425022	748	2.33	C45	53.58	544[b]	16893	8.9	0.03
C19	21.34	331	1191411	626	1.95	C46	54.43	550	15548	8.2	0.03
C20	23.18	344	1078333	566	1.76	C47	55.28	555	14367	7.5	0.02
C21	24.93	356	933296	490	1.53	C48	56.08	560	12564	6.6	0.02
C22	26.63	369	835197	439	1.37	C49	56.88	565	8740	4.6	0.01
C23	28.25	380	829163	435	1.36	C50	57.66	570	7894	4.1	0.01
C24	29.82	391	551072	289	0.90	C51	58.43	575	6216	3.3	0.01
C25	31.33	402	545017	286	0.89	C52	59.18	580	7820	4.1	0.01
C26	32.77	412	462689	243	0.76	C53	59.93	584	5927	3.1	0.01
C27	34.17	422	336479	177	0.55	C54	60.63	589	5057	2.7	0.01
C28	35.53	432	318611	167	0.52	C55	61.36	593	4473	2.3	0.01
C29	36.84	441	282331	148	0.46	C56	62.04	597	3811	2.0	0.01
C30	38.11	450	229586	121	0.38	C57	62.73	602	1920	1.0	0.00
C31	39.35	459	190804	100	0.31	C58	63.43	606	3121	1.6	0.01
C32	40.54	468	158023	83.0	0.26	C59	64.06	610	2788	1.5	0.00
C33	41.71	476	135970	71.4	0.22	C60	64.47	613	2403	1.3	0.00
C34	42.85	483	109528	57.5	0.18	C61	64.71	614	1882	1.0	0.00
C35	43.94	491	86741	45.6	0.14	C62	65.38	618	1614	0.8	0.00
C36	45.03	498	67209	35.3	0.11	C63	65.76	620	1347	0.7	0.00
C37	46.07	505	58331	30.6	0.10	C64	66.63	626	908	0.5	0.00
C38	47.08	512	52125	27.4	0.09	Total			22.5×10^6		37.60

a. Amount of each fraction on-column (1 µl) measured using internal standard.

b. Extrapolated boiling point values.

Table 1-14 Amount of each hydrocarbon fraction expressed as amount (ng) on-column and weight percent of the total condensate W.

HTCGC Analysis of Condensate W											
Fraction	R.T.	B.pt.	Area	ng[a]	Wt.Wt%	Fraction	R.T.	B.pt.	Area	ng	Wt.Wt%
C12	5.167	216	1488955	847	2.56	C39	46.94	518	101990	53.6	0.18
C13	7.367	235	1296125	868	2.23	C40	47.92	525	92103	48.4	0.16
C14	9.667	253	1300380	878	2.24	C41	48.87	531	86689	45.5	0.15
C15	11.93	271	1170369	937	2.01	C42	49.78	537	77038	40.5	0.13
C16	14.13	287	1095093	660	1.88	C43	50.70	543	74239	39.0	0.13
C17	16.25	302	1066147	839	1.83	C44	51.58	548	66087	34.7	0.11
C18	18.26	317	961199	582	1.65	C45	52.45	544[b]	61039	32.1	0.10
C19	20.18	331	850997	610	1.46	C46	53.43	550	54510	28.6	0.09
C20	22.02	344	835119	577	1.44	C47	54.13	555	56565	29.7	0.10
C21	23.78	356	811136	640	1.39	C48	54.93	560	58343	30.6	0.10
C22	25.48	369	711918	495	1.22	C49	55.75	565	52397	27.5	0.09
C23	27.1	380	676216	497	1.16	C50	56.52	570	53187	27.9	0.09
C24	28.67	391	597633	446	1.03	C51	57.28	575	47662	25.0	0.08
C25	30.18	402	542108	313	0.93	C52	58.78	580	43627	22.9	0.07
C26	31.63	412	507350	375	0.87	C53	58.78	584	38769	20.4	0.07
C27	33.02	422	434032	338	0.75	C54	59.51	589	30627	16.1	0.05
C28	34.39	432	389259	300	0.67	C55	60.23	593	26653	14.0	0.05
C29	35.7	441	345358	295	0.59	C56	60.90	597	22148	11.6	0.04
C30	37.0	450	274578	193	0.47	C57	61.58	602	16016	8.4	0.03
C31	38.21	459	239219	193	0.41	C58	62.27	606	15371	8.1	0.03
C32	39.4	468	184625	165	0.32	C59	62.93	610	14276	7.5	0.02
C33	40.57	476	164395	137	0.28	C60	63.59	613	12122	6.4	0.02
C34	41.7	483	150256	122	0.26	C61	64.22	614	10003	5.3	0.02
C35	42.8	491	128795	107	0.22	C62	64.86	618	8517	4.5	0.01
C36	43.88	498	114734	83.2	0.20	C63	65.47	620	10676	5.6	0.02
C37	44.93	505	110358	72.9	0.19	C64	66.08	626	6851	3.6	0.01
C38	45.94	512	108515	57.0	0.19	Total			23.3×10^6		30.22

a. Amount of each fraction on-column (1 µl) measured using internal standard.

b. Extrapolated boiling point values.

Such curves are shown for both condensate U and W in Figure 1-21. The distillation curves from this experiment do not show an initial boiling point (IBP) due to the large amount of LMW hydrocarbons ($< C_{12}$). These compounds are difficult to quantify using cyclohexane as the solvent. This would normally mean either distilling the condensate to remove the LMW material or using a solvent with a much lower boiling point than cyclohexane (which may cause problems with solvating the HMW components greater than *n*-C_{50}). This problem could also be overcome by using a much lower GC oven temperature (cryogenic cooling) and a pressurised sampling valve (see Introduction). The condensate could then be introduced directly on to the column without having to use a solvent carrier system.

1.3.4 Centrifugation of waxy gas condensates

Injection of large amounts of condensate (< 30 mg/ml) on to the HTCGC to increase the response of the HMW compounds resulted in overloading the column with the lower molecular weight components greater than *n*-C_{30}. Thus a method was needed for obtaining a high molecular weight fraction.

An obvious approach was to remove the lighter compounds by distillation (see Chapter 3). However, the quantitative and reproducible distillation of crude petroleum and condensates is not a trivial task and the necessary apparatus was still being commissioned at this stage of interest. Therefore alternatives were sought.

Traditionally centrifugation has been used as an industrial method for increasing the melting point of petroleum-derived waxes, in particular microcrystalline or petrolatum wax (**Warth, 1956**). The wax is separated from a high-viscosity lubricating fraction by mixing with solvent. The solvent used varies with the particular refinery method, for petrolatum wax naphtha is used, but often polar solvents such as benzene or dichloromethane are used in the production of microcrystalline wax, and are added to aid precipitation of the wax at a higher chill temperature. The wax solution is then cooled to -12°C before being centrifuged at 18,000 rpm.

A similar approach to that above was carried out herein on a micro-scale by

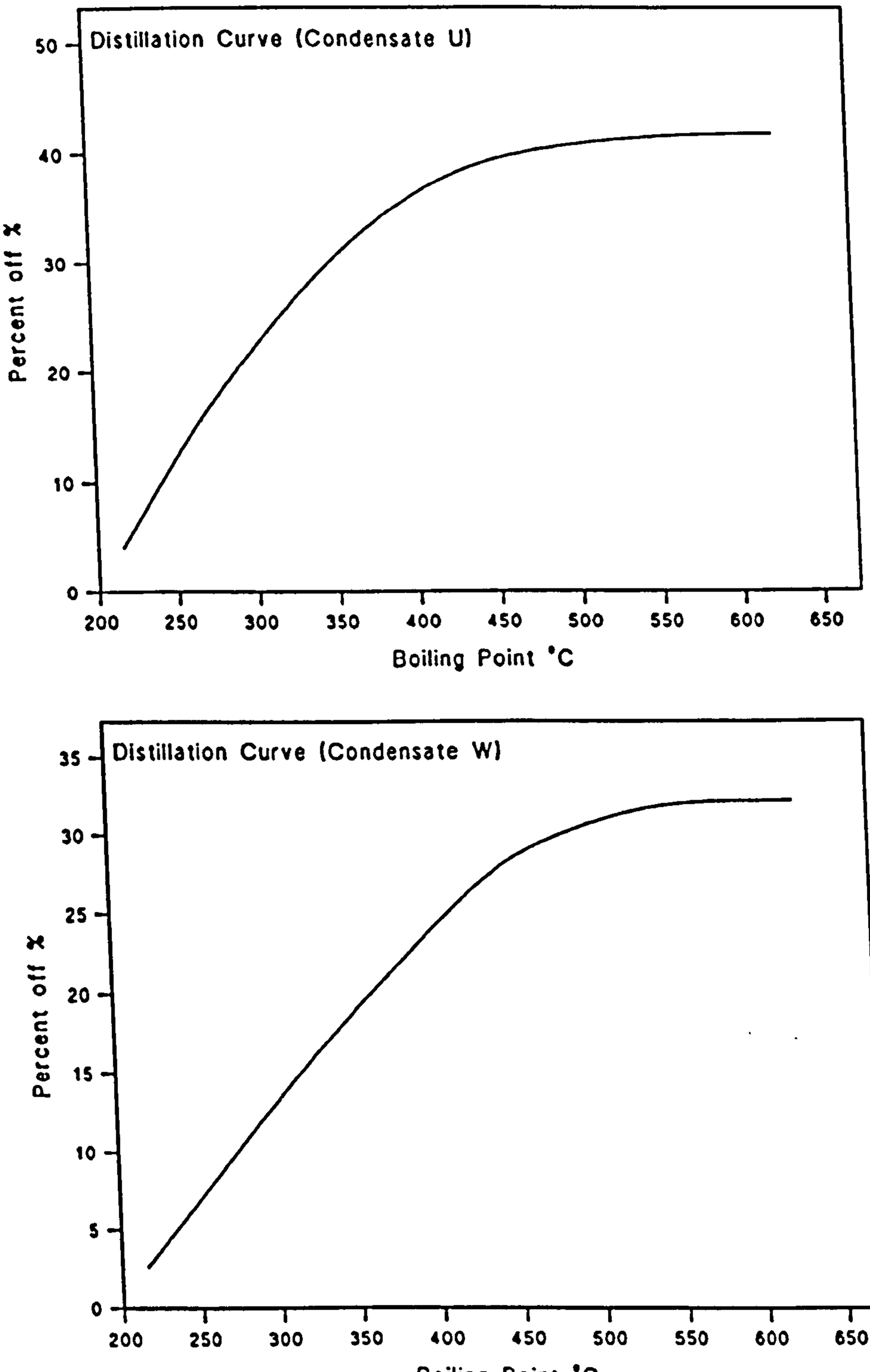

Figure 1-21 Simulated distillation curves for condensates U and W.

dissolving condensate in warm pentane and allowing the mixture to stand and cool before centrifuging the suspended material down at 2000 rpm to a waxy pellet (see Experimental) followed by repetitive addition of fresh solvent and centrifugation. The centrifuged solids were then analyzed by HTCGC. The results for the gas condensates U and W are shown in Figures 1-22 and 1-23. The resultant pellet for condensate U produced a series of compounds including n-alkanes ranging from *n*-C_{30} to greater than *n*-C_{70}, (maximising at around *n*-C_{42}) and between *n*-C_{25} to above *n*-C_{80} (maximising at *n*-C_{50}) in condensate W. Analysis of the supernatant by HTCGC shown in figures 1-22 [B] and 1-23 [B] revealed that centrifugation had removed the majority of material eluting after *n*-C_{40}. Even though a small amount of residual higher molecular weight compounds would be expected to remain because of their limited solubility in pentane, centrifugation appears to be a useful method for obtaining a high molecular weight fraction.

1.3.5 High temperature capillary chromatography mass spectrometry

High temperature capillary GC columns have been used only rarely with mass spectrometers. One reason for this is that many modern HTCGC columns are metal, or coated with a metal, and thus they conduct electricity. It then becomes impractical to install the column into a magnetic sector instrument where there are high potentials across the ion source (**Evershed and Prescott, 1989**). In the present study HTCGC-mass spectrometry was performed using a Finnigan quadruple mass spectrometer. The transfer line of GC-mass spectrometer had been modified so that it could be heated above 400°C. Unlike the magnetic sector instrument the ion source in the quadrupole instrument operates at ground potential, allowing the aluminium clad capillary column (SGE HT-5) to be inserted directly into the ion source without the necessity of removing the outer cladding (*cf.* **Evershed and Prescott, 1989**).

Figure 1-24 shows a total ion chromatogram obtained by HTCGC-MS of *n*-C_{20}, *n*-C_{40}, *n*-C_{50}, and *n*-C_{60}. Under EI conditions, molecular ions were only obtained for *n*-C_{20} (*m/z* 282) and *n*-C_{40} (*m/z* 562). The spectra of all four compounds (Figure 1-25) showed ions characteristic of alkanes (*viz* m/z 57+n*14) which exhibited an exponential decrease

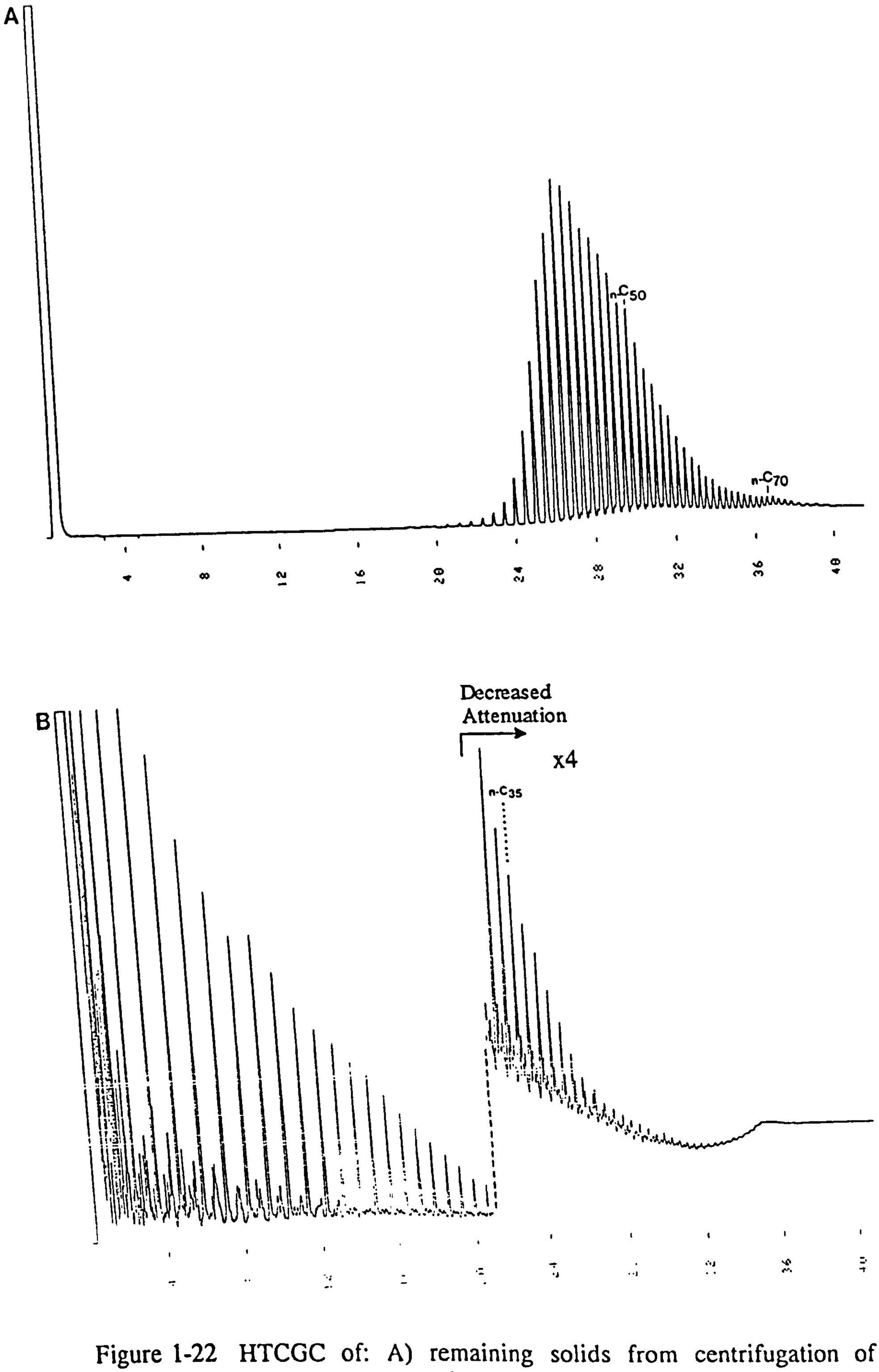

Figure 1-22 HTCGC of: A) remaining solids from centrifugation of condensate U and B) supernatant from centrifuged sample U.

[GC: HT-5 (SGE), 12 m x 0.32 mm i.d., 50-410°C @ 10°C/min (10 min), He carrier, FID]

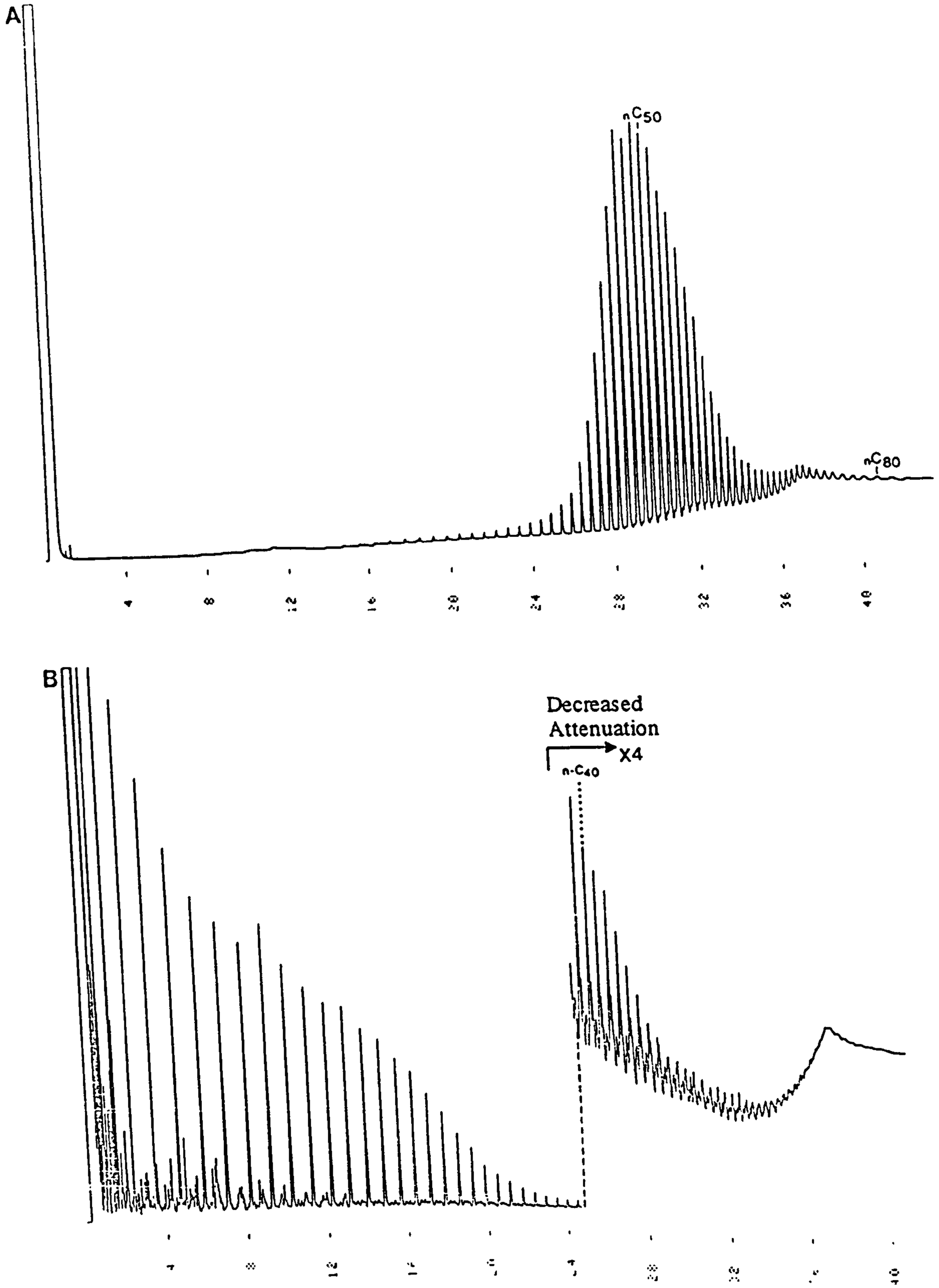

Figure 1-23 HTCGC of: A) remaining solids from centrifugation of condensate W and B) supernatant from centrifuged sample W.

[GC: HT-5 (SGE), 12 m x 0.32 mm i.d., 50-410°C @ 10°C/min (10 min), He carrier, FID]

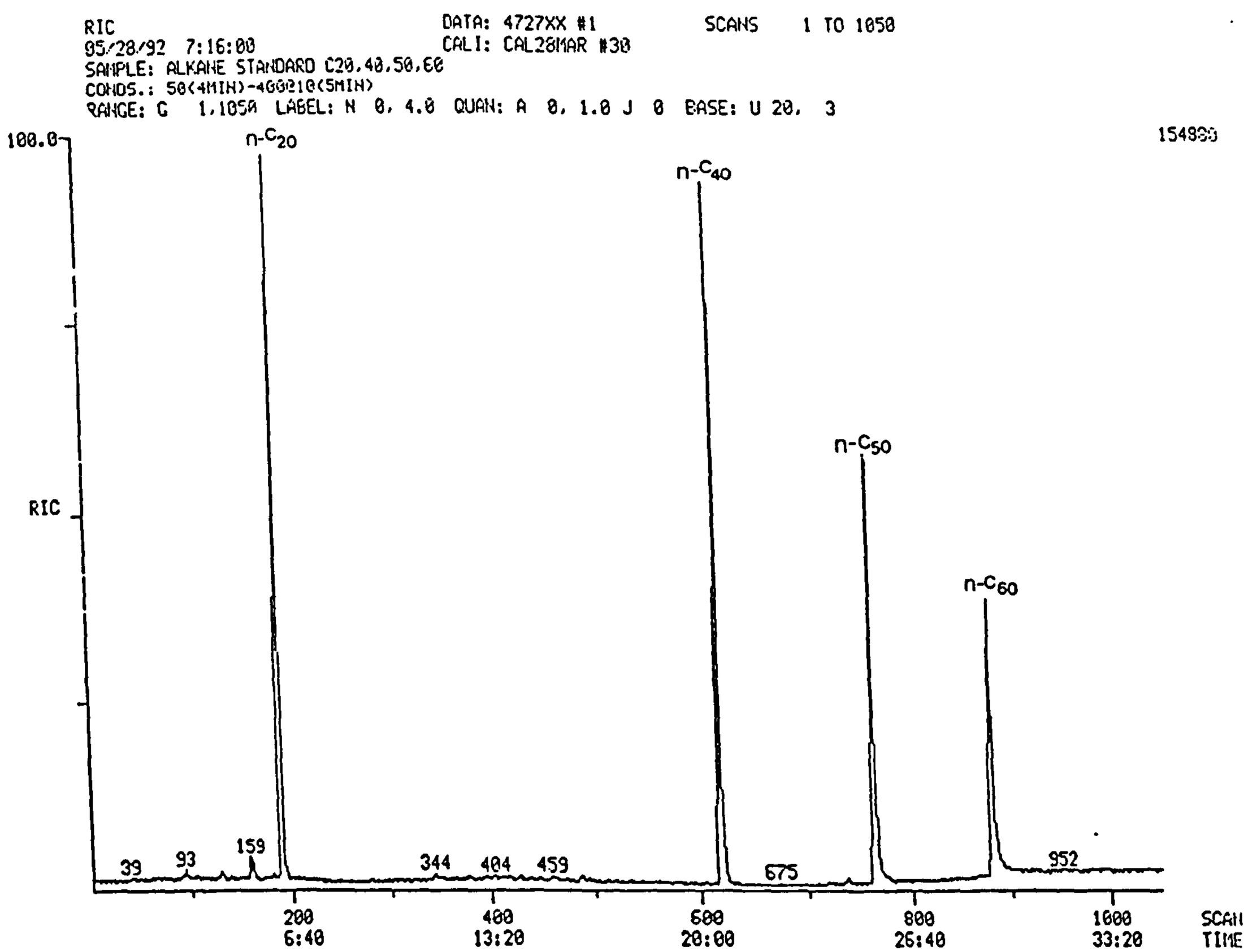

[GC: HT-5 (SGE), 12 m x 0.32 mm i.d., 50-410°C @ 10°C/min (10 min), He carrier, FID]

Figure 1-24 HTCGC-MS total ion current chromatogram of a mixture of (n-C_{20}, n-C_{40}, n-C_{50}, n-C_{60}) alkanes.

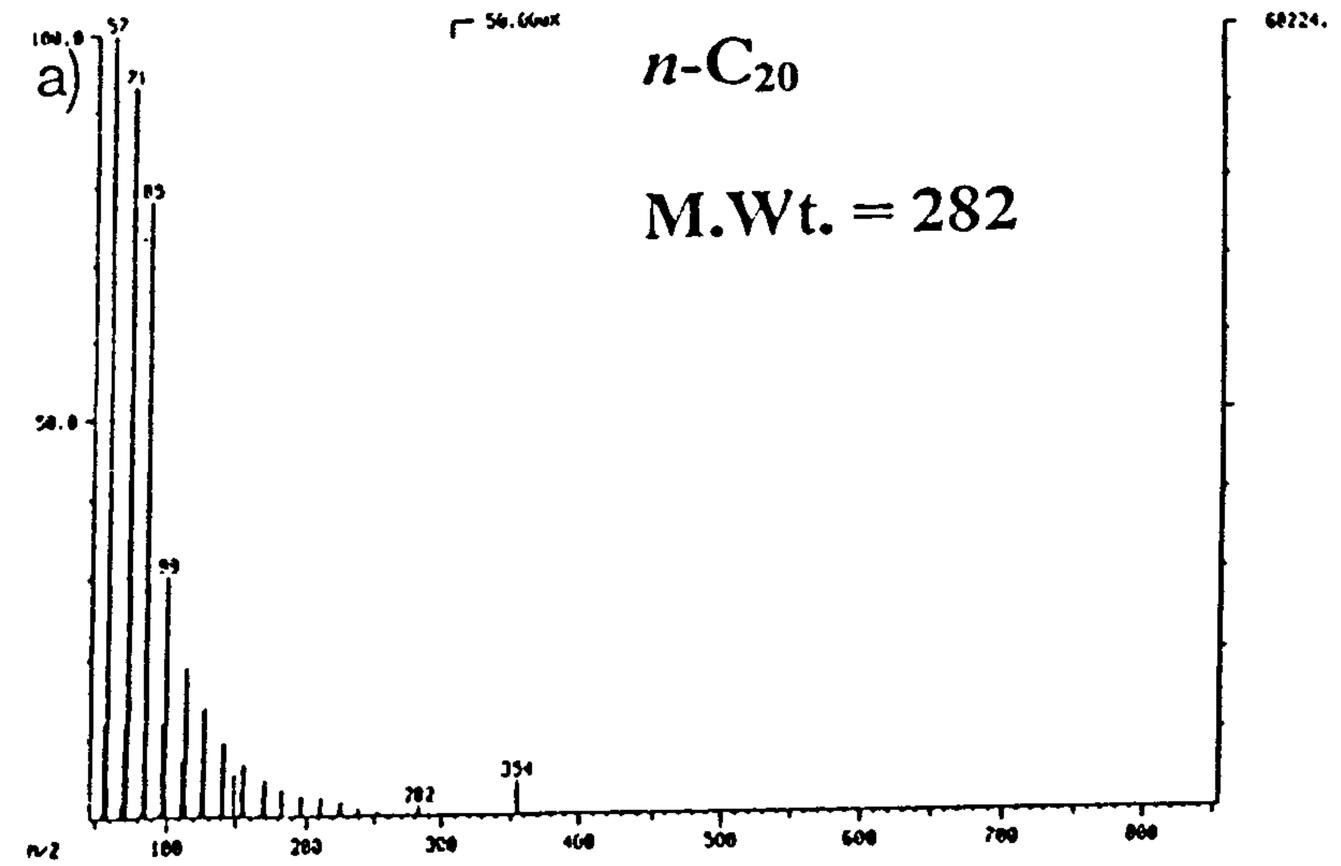

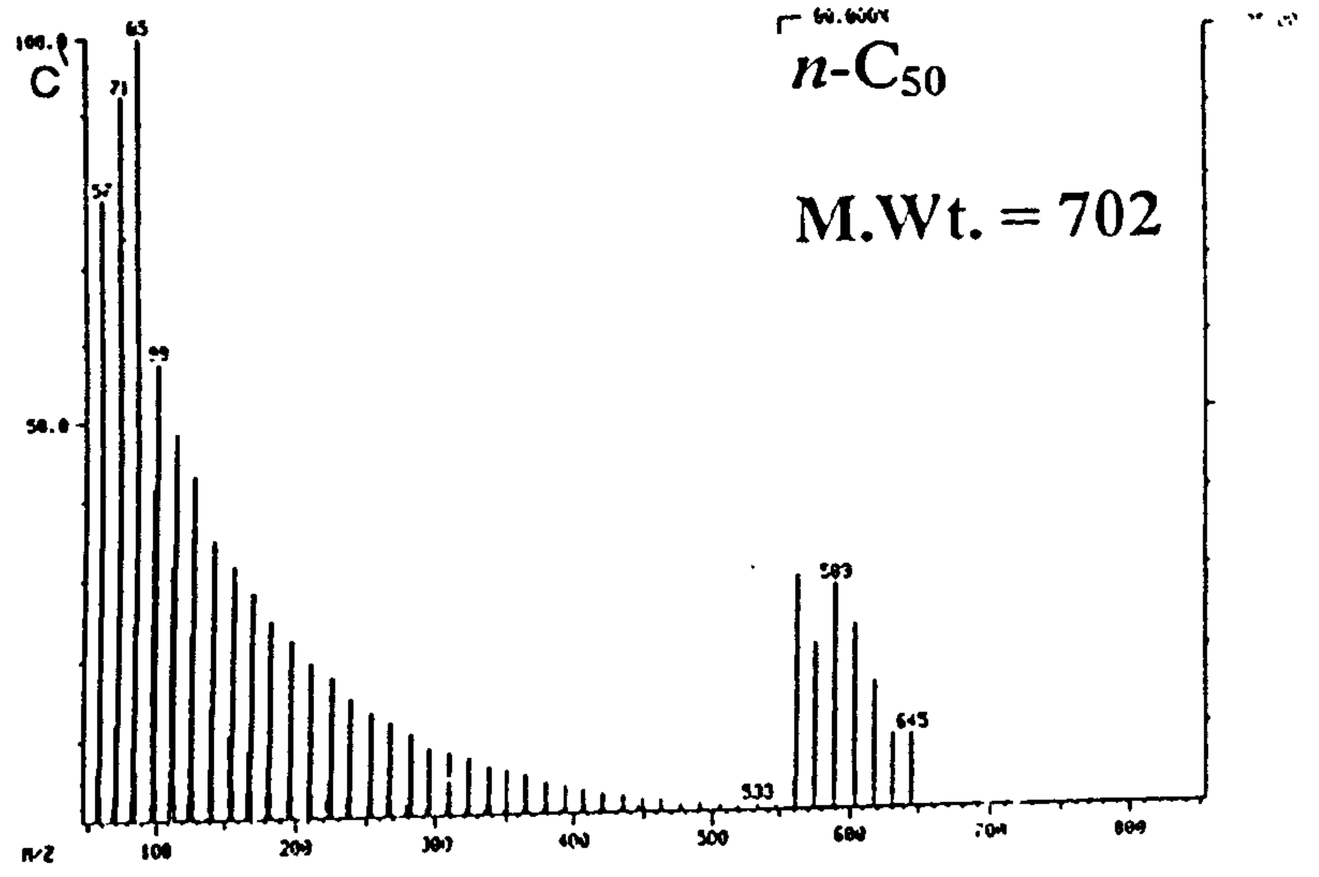

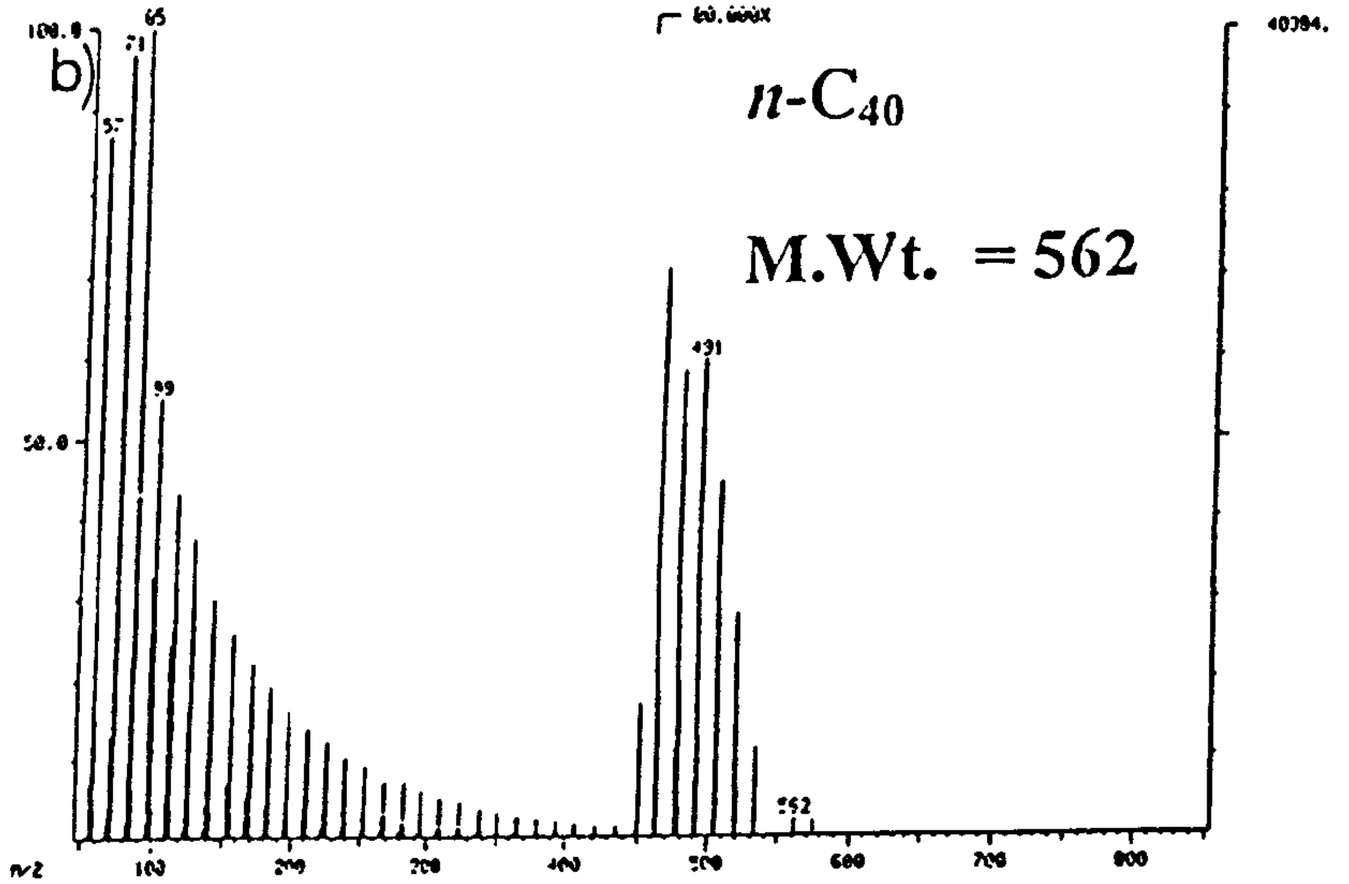

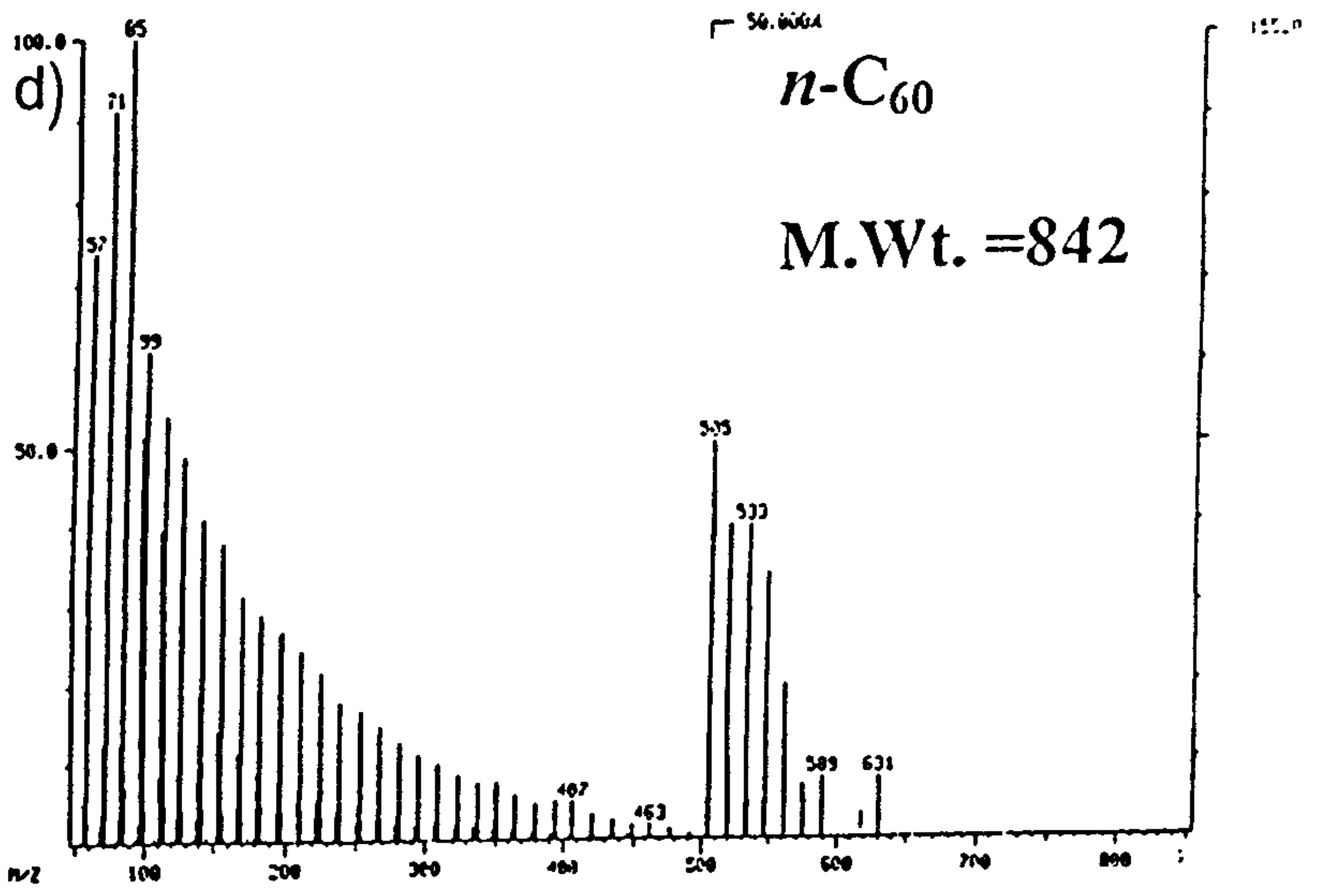

Figure 1-25 EI Mass spectra of a) n-C_{20} b) n-C_{40} C) n-C_{50} and n-C_{60}.

in intensity with increasing mass **(Rose and Johnstone, 1982).**

Figure 1-26 (A) shows the HTCGC-MS TIC of condensate U. Figure 1-26 (B) shows an expanded portion of the later part (scan time 500-600 scans) of the same chromatogram. The mass spectra of components producing peaks X and Y (Figure 1-27) appear not to contain molecular ions but show ions with enhanced abundances at *m/z* 294, *m/z* 435 for X and *m/z* 239 and *m/z* 290 for Y indicating possible branching points. It is clear that HTCGC-EI MS alone has limited use for rigorous identification of such HMW alkanes. HTCGC-MS of the centrifuged wax of condensate U resulted in the chromatogram shown in Figure 1-28 (A) and the mass spectrum of the compound labelled Z is given in Figure 1-28 (B). This compound was identified as *n*-$C_{42}H_{86}$ ($M^{+\bullet}$ *m/z* 590). Molecular ions for compounds with later retention times were not observed.

In an attempt to gain molecular weight information for the higher molecular weight ($>C_{40}$) compounds, chemical ionisation (CI) mass spectrometry with *iso*-butane as the reagent gas was used with HTCGC. CI is a much "softer" form of ionisation than EI because it relies on ionised gas to ionise the analyte **(Rose and Johnstone 1982).** Figure 1-29 (A) shows the HTCGC-CI MS TIC of centrifuged sample U. The mass spectrum of compound H (Figure 1-29, B) shows the characteristic *m/z* 701 $(M-H)^+$ ion of *n*-$C_{50}H_{102}$ formed by hydride abstraction. Other components were identified as *n*-alkanes from *n*-C_{38} to *n*-C_{57} (Figure 1-29, C). Beyond *n*-C_{57} the concentrations of the remaining components were low in the condensates and no molecular ions ($M-H^{+\bullet}$ or $M+H^{+\bullet}$) were observed. HTCGC-CI MS of Polywax 1000 (a mixture of even numbered *n*-alkanes formed via the Fischer-Tropsch process in which $>C_{57}$ compounds were more abundant), allowed the molecular ion of *n*-C_{60} to be detected (Figure 1-30 A). The CI mass spectrum of *n*-C_{60} (Figure 1-30 D) showed the molecular ion (*m/z* 842) rather than *m/z* 841 $(M-H)^+$ ion. This is most likely formed by charge transfer processes due to an increase in the proton affinity of *n*-C_{60} to that of *iso*-butane **(Rose and Johnstone, 1982)**, or may be due to a concentration effect which causes self ionisation to occur.

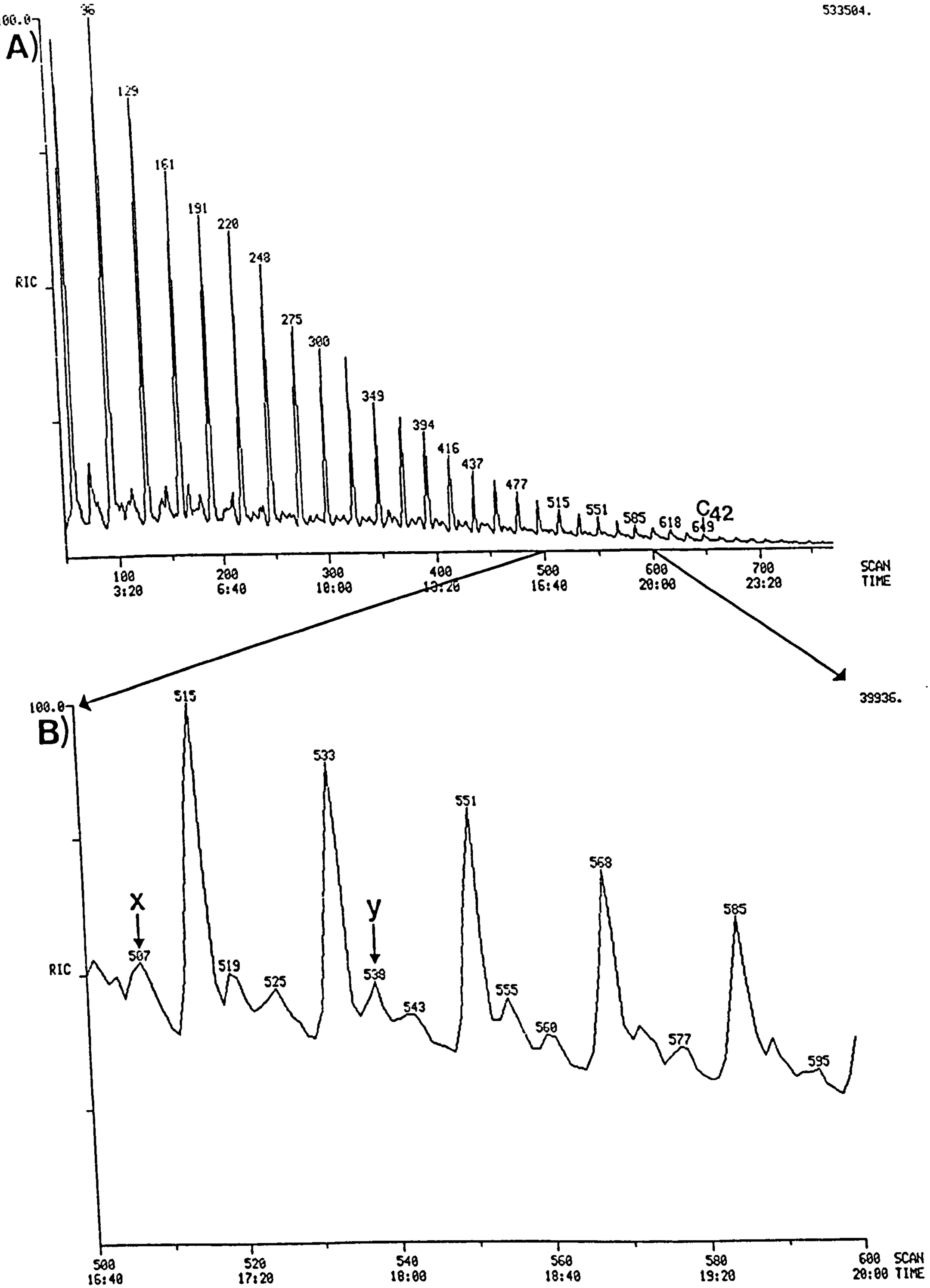

Figure 1-26 A) TIC of condensate U (EI) and B) expanded section of baseline (scan time 500-600).

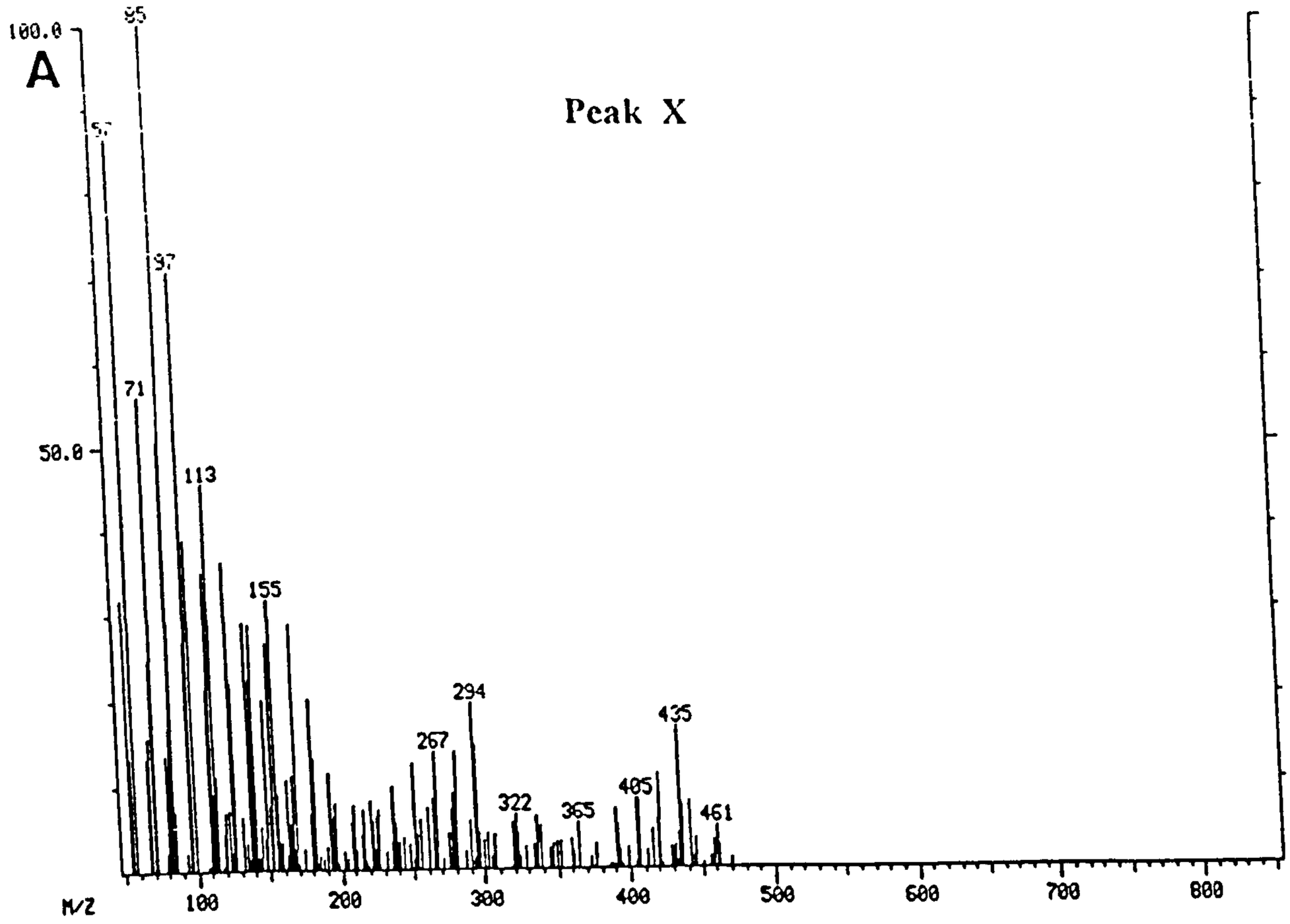

Figure 1-27 Mass spectra (EI) of components labelled X and Y.

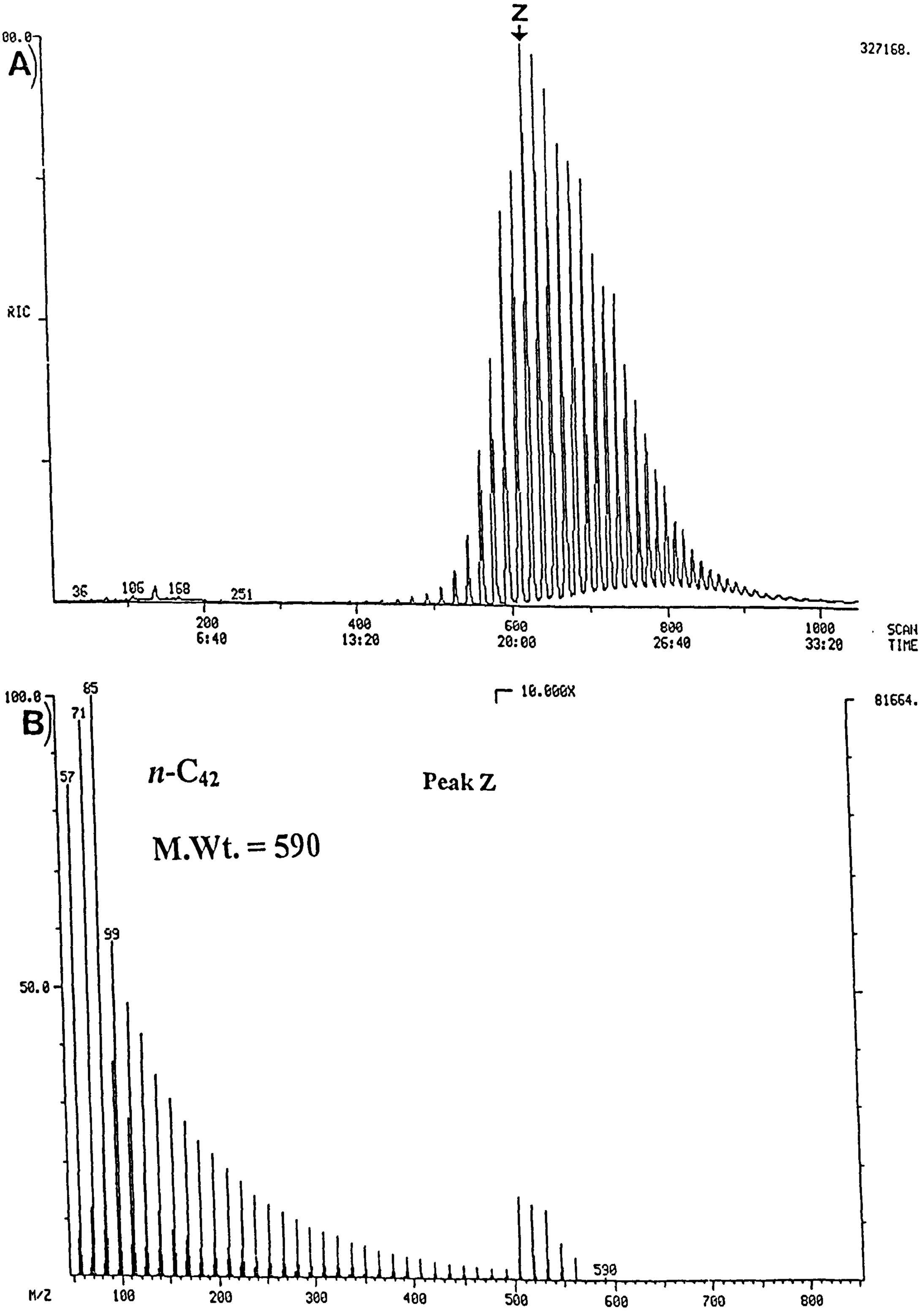

n-C_{42}

Peak Z

M.Wt. = 590

Figure 1-28 A) EI TIC of centrifuge residue of condensate U and B) mass spectrum of component Z (n-C_{42}).

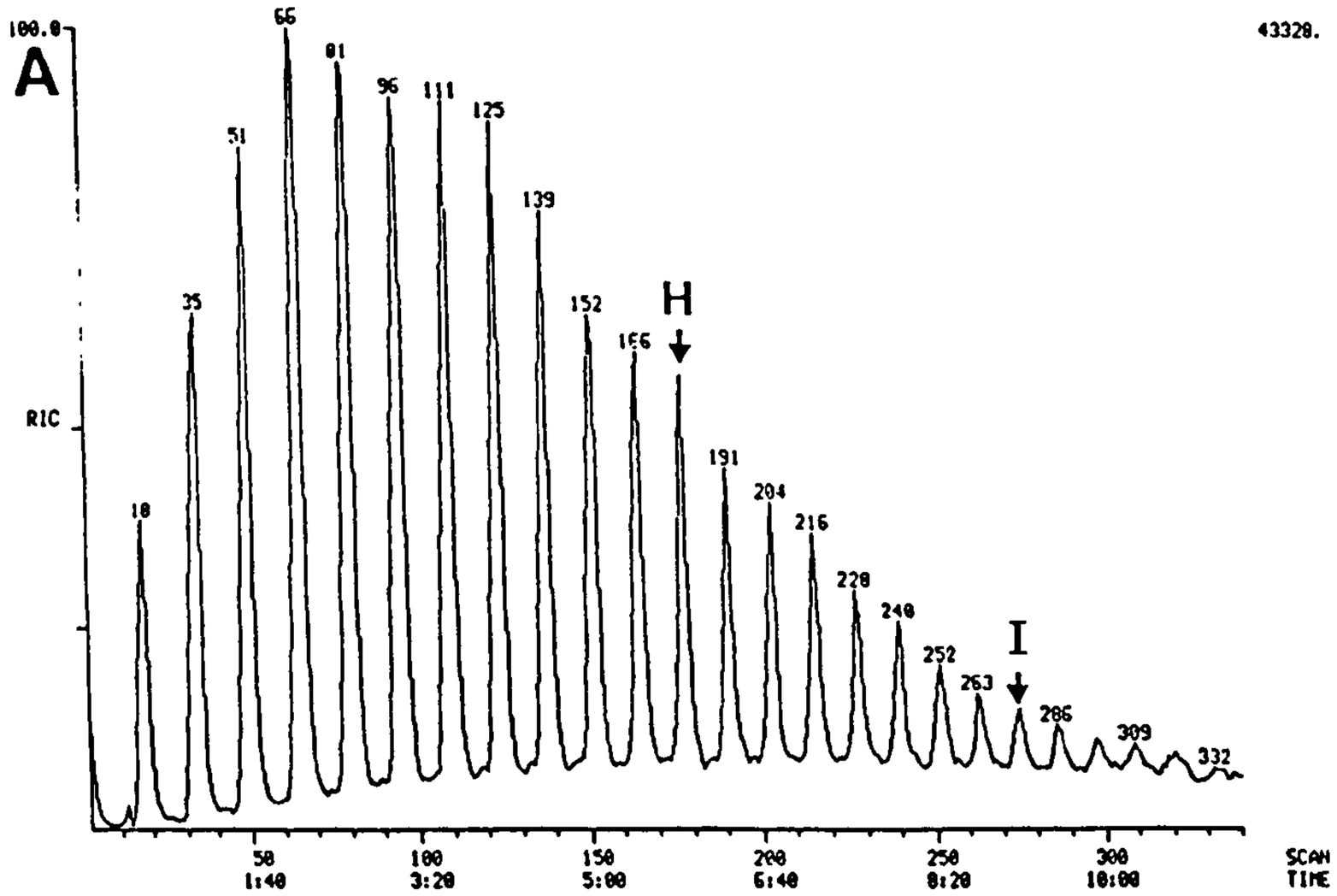

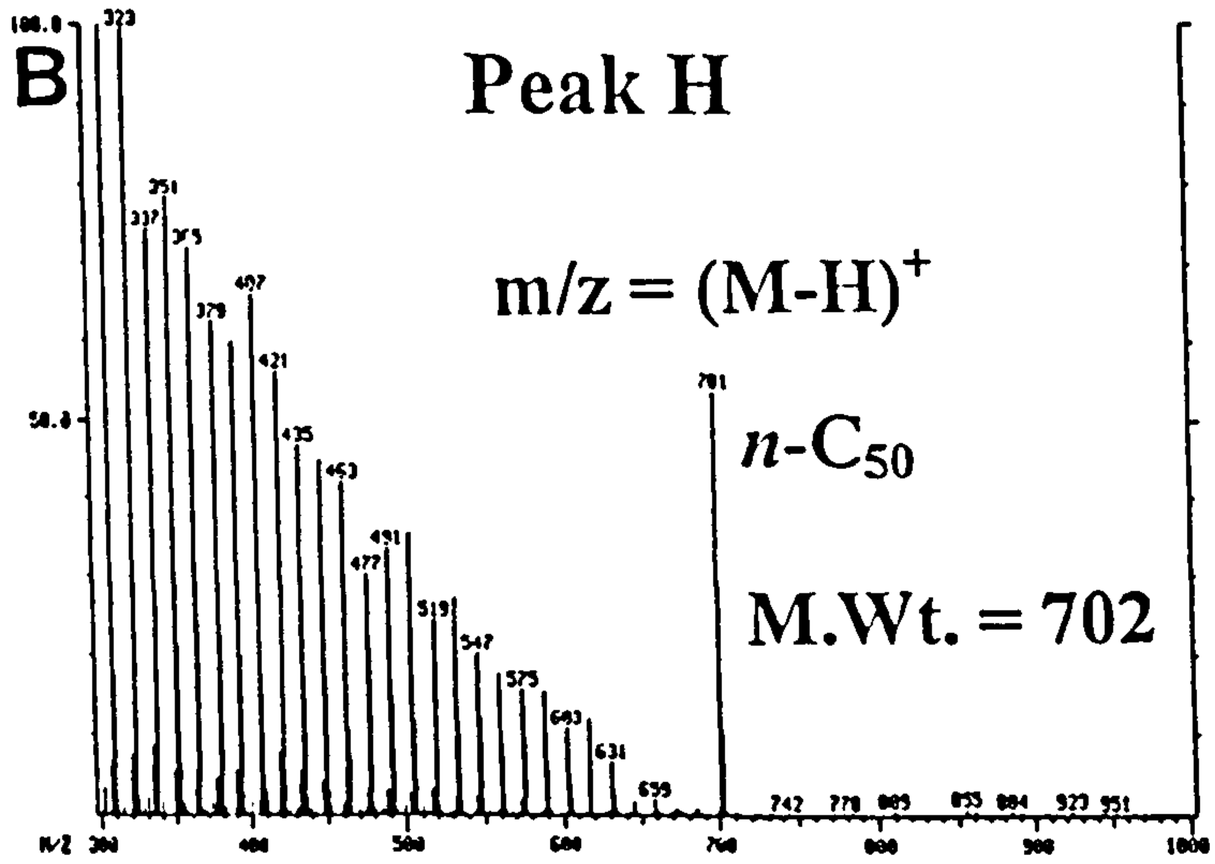

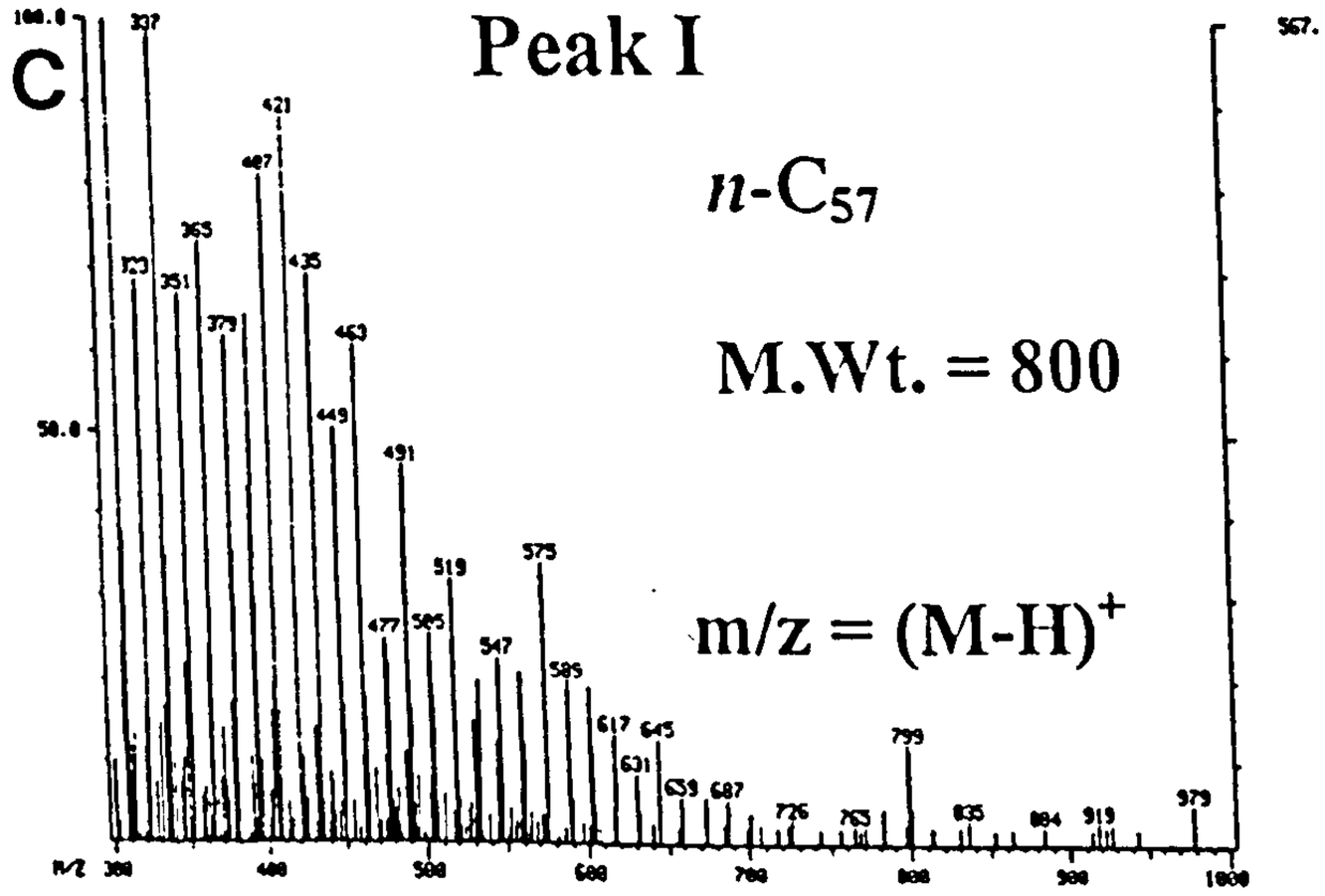

Figure 1-29 A) CI TIC for the centrifuged solid from condensate U, B) spectrum of compound H (n-C_{50}) and C) spectrum of compound I (n-C_{57}).

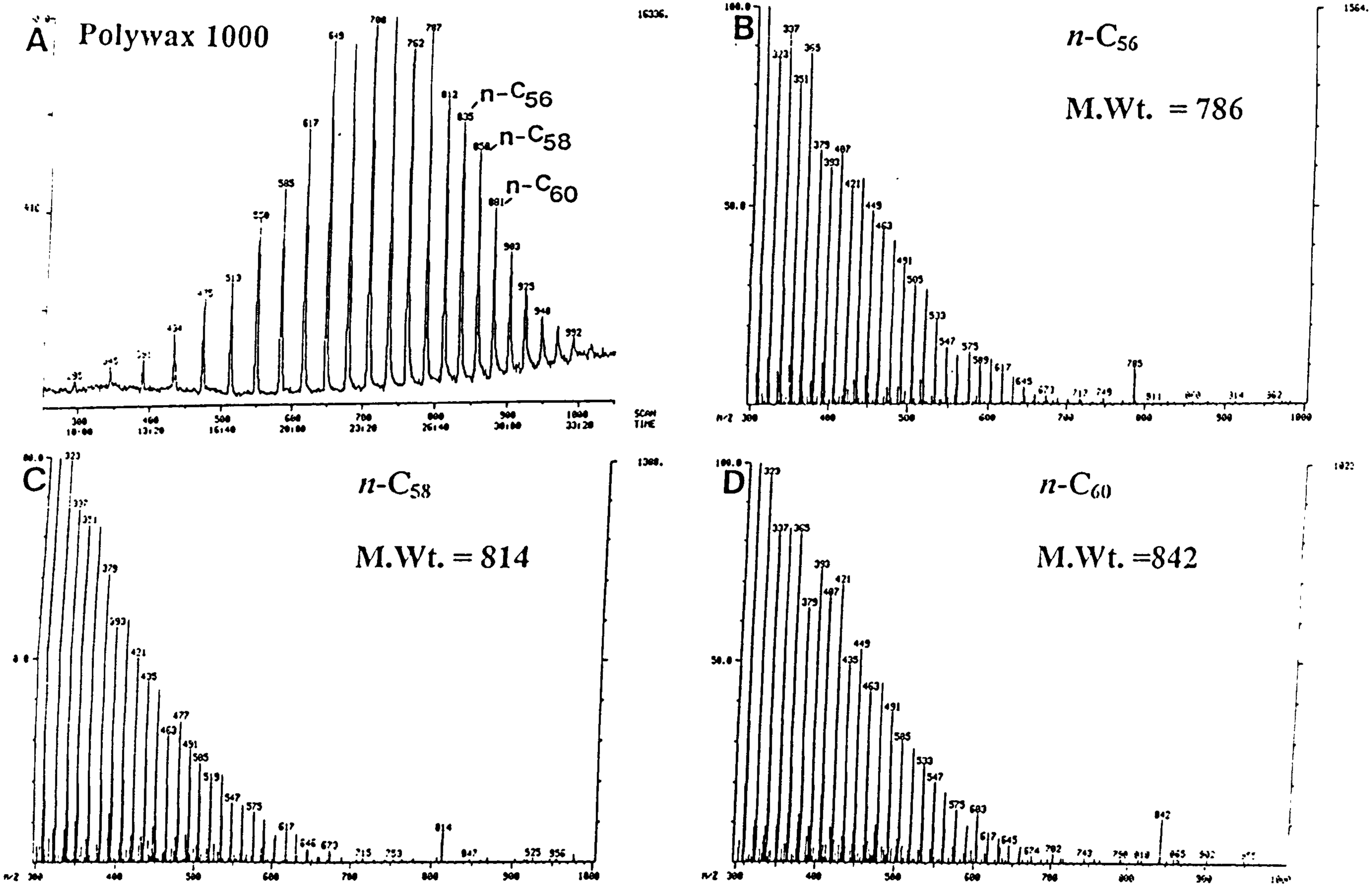

Figure 1-30 A) CI TIC of Polywax 1000, B) CI spectrum of n-C_{56}, C) CI spectrum of n-C_{58} and D) spectrum of n-C_{60}.

1.3.5 Summary

Good reproducibility and quantitative analysis of HMW *n*-alkanes by HTCGC is attainable. For the authentic *n*-alkanes the method developed herein gave C_{20} to C_{60} a RSD of under 5% for manual injection, a linear response factor, and a linear calibration over the concentration used (*ca.* 5 to 50). When applied to the analysis of two waxy North Sea gas condensates, *n*-alkanes with carbon numbers extending above C_{80} were observed. This is a surprising result because condensates are generally believed to be low molecular weight fluids similar to gasoline. Good quantitative agreement was observed between HTCGC and conventional gas chromatography for carbon fractions less than C_{30} but HTCGC was able to extend the analysis to carbon numbers of at least C_{65}.

HTCGC-EI MS of condensates produced molecular ions for n-alkanes up to *n*-C_{42}. Other HMW compounds showed fragment ions characteristic of branched compounds. HTCGC-CI MS produced molecular ion information for compounds as large *n*-C_{57} in a condensate sample and for *n*-C_{60} in a Polywax 1000 where such compounds were more abundant.

The following recommendations are made for future HTCGC analyses;

(1) Use of a dedicated high temperature instrument such as that used herein.

(2) Use of on-column injection.

(3) A heated auto-sampler would be desirable. However, good manual injection can be achieved if samples are carefully heated to above the cloud point of the analyte but not above the boiling point of the solvent. The temperature should be kept constant between samples. For *n*-hexacontane (C_{60}) 55°C was found to be adequate. Both a solvent plug and an air gap should be pulled into the syringe prior to the sample to wash any precipitated wax from the syringe onto the column. A fast injection speed should be used.

(4) A constant carrier gas flow rate (H_2 or He).

(5) For most applications involving HMW waxy hydrocarbons, cyclohexane is preferred.

(6) The triglyceride tristearin is proposed as a high temperature internal standard. Its response factor is close to that of HMW *n*-alkanes such as *n*-C_{60}, it had a linear FID response, and when co-injected with a waxy North Sea condensates was almost totally separated from the closest eluting *n*-alkanes between *n*-C_{59} and *n*-C_{60}.

CHAPTER TWO

CHARACTERISATION OF THE UNRESOLVED COMPLEX MIXTURE OF HYDROCARBONS IN A GAS-CONDENSATE BY CHEMICAL OXIDATION

When they are analysed by gas chromatography many hydrocarbons in fossil fuels appear as an unresolved complex mixture (UCM). Despite the quantitative significance of the UCM very little is known about the structures of hydrocarbons within the UCM. Knowledge of these structures may prove useful for improving phase behaviour models of petroleum reservoir fluids.

A series of UCMs isolated from distillation cuts of a waxy North Sea gas-condensate accounted for 21% of the whole condensate and 33-61% of each distillate cut. Oxidation of the UCMs with CrO_3/AcOH followed by GC-MS analysis of the oxidation products revealed a series of resolved compounds (27-81%) comprising mainly n-monocarboxylic acids (19-48%), with branched acids, ketones, ketoacids, n-dicarboxylic acids, lactones, isoprenoid acids, alkylcyclohexane carboxylic acids and toluic acids accounting for the remainder. The distillate UCMs showed variations in the relative amount of products but not in composition. The results show that the gas-condensate UCM is highly aliphatic with a high degree of alkyl substitution of average carbon length C_{12}.

2.1 Introduction

2.1.1 General

Insufficient knowledge of the identities and concentrations of hydrocarbons present in the heavier distillation fractions (C_{7+}) of oils and condensates may significantly reduce the accuracy of predicting their phase behaviour, thus leading to increased production costs (**Whitson, 1983**). This is particularly important for gas-condensates and volatile oils whose volumetric phase behaviour is significantly affected by the presence of the heavier components (**Newley and Merrill, 1989**). Detailed analysis of C_{7+} fractions by high resolution gas chromatographic techniques is carried out routinely but many hydrocarbons elute from the GC column so closely together that they produce a detector response which appears in the form of a "hump" or unresolved envelope underlying the resolved components (*e.g.* Figure 2-1 C). These so-called unresolved complex mixtures (UCMs) can account for up to 80% of the total hydrocarbons present in a fossil fuel (**Gough and Rowland, 1991; Revill, 1992; Rowland and Revill, 1995**) and may significantly affect phase behaviour. Ideally PVT models should take the composition of these fractions into account. Despite the quantitative importance and widespread (and probably ubiquitous) occurrence of hydrocarbon UCMs in fossil fuels, relatively little is known about their composition and there appear to have been no published studies at all of UCMs from gas-condensates. This important compositional data is thus not represented in existing gas-condensate reservoir fluid modelling.

3.1.2 Previous studies

Although there have been no studies of gas-condensate UCMs and it was not until the late 80's that a few studies attempted to unravel directly the UCM in crude (**Gough, 1989; Killops and Al-Juboori, 1990**) and refined oils (**Gough 1989; Gough and Rowland, 1990, 1991; Revill, 1992**), some information about UCM composition did appear in earlier studies of lubricating oils (**Rossini *et al.*, 1953; Clerc *et al.*, 1955; Melpolder *et al.*, 1956; Hood and O'Neal, 1959**). Lubricating oils are dominated by UCM hydrocarbons because the majority of resolved components are removed from lubes by dewaxing processes during refining (Figure 2-1 D). UCMs are also prominent in many other middle distillate refinery products including transmission fluids, hydraulic

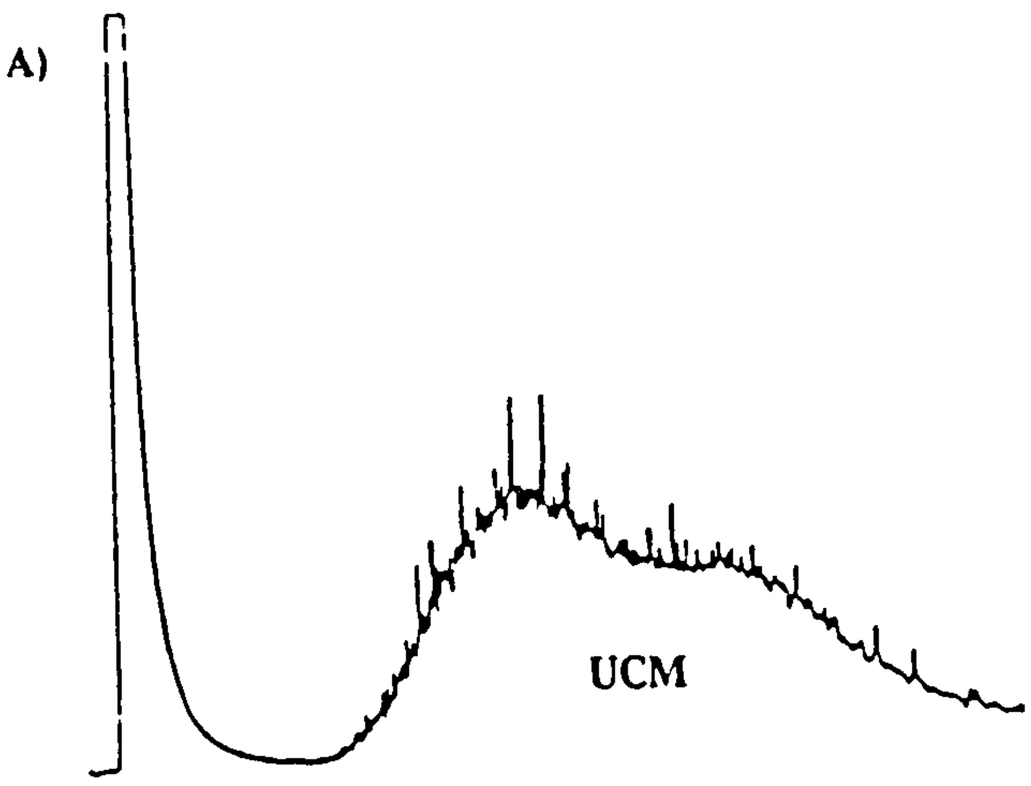

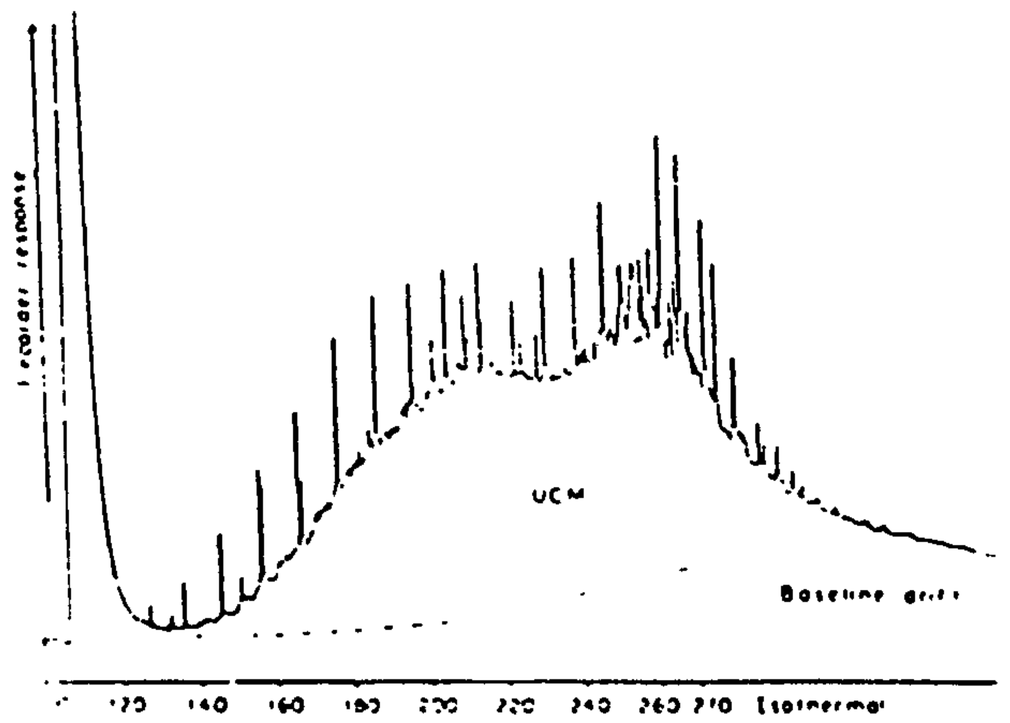

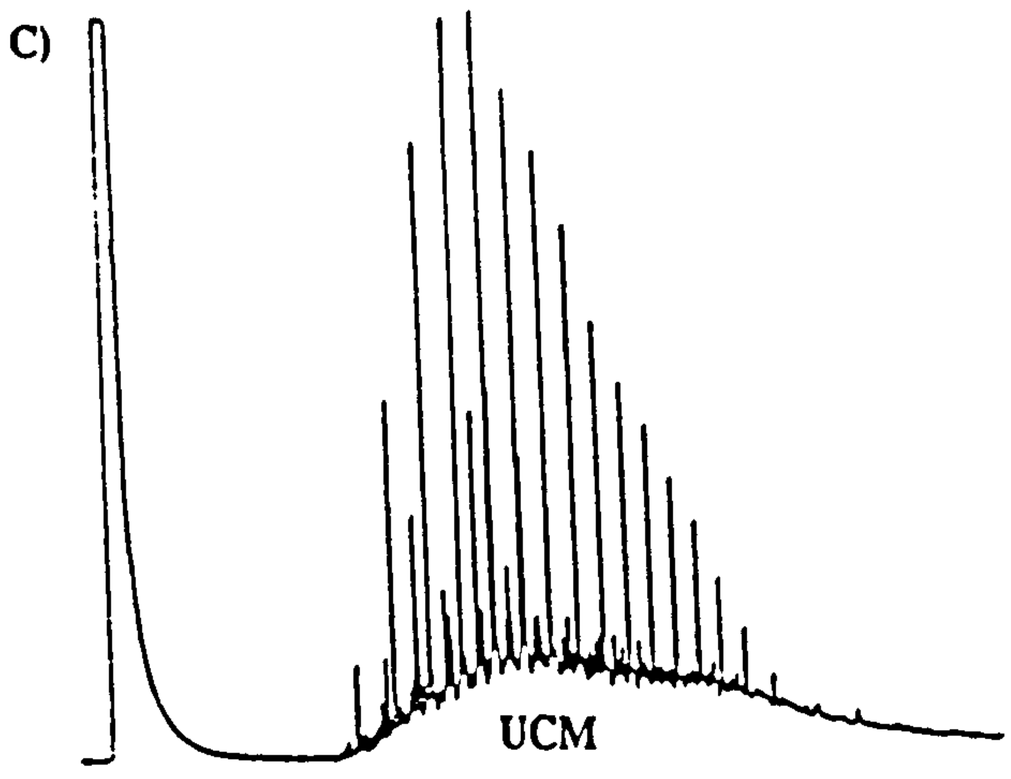

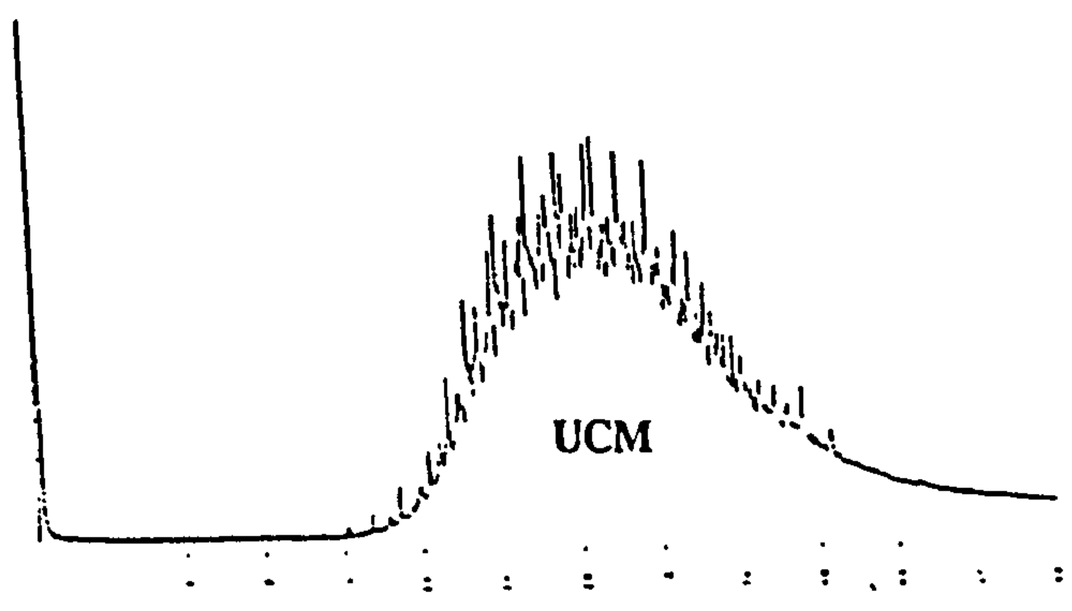

A) Keho crude oil, Western Canadian basin (from Leeheer 1984).
B) Polluted sediment extract (from Thompson and Eglinton 1978).
C) South Barrow No 19, Barrow-Prudhoe. (from Burwood *et al.* 1985).
D) Lubricating oil

Figure 2-1 Examples of capillary gas chromatograms of oils exhibiting UCMs.

oils, and gear oils. Therefore the study of lubricating oils in general can provide useful information about the types of structures contributing to the UCM. These studies have been extensively reviewed by **Gough (1989)**, and only a brief summary is given here.

Rossini *et al.*, (1953), in a study for the American Petroleum Institute (API) analysed a lubricant fraction UCM from Ponca City crude oil and determined the elemental compositions and physical properties. They concluded that one to three ringed aliphatic hydrocarbons (*e.g.* C_{25}-C_{40} alkycyclohexanes, Figure 2-2 III) and monocyclic aromatic hydrocarbons, dinaphthenonaphthalenes (VI), and naphthenophenanthrenes (VII) were the major of compounds present in the UCM. Later, **Clerc *et al.*, (1955)**, **Melpolder (1956)** and **Hood and O'Neal (1959)** used more sensitive and structurally informative instrumental methods including electron impact mass spectroscopy (EI-MS) to study the same samples. Their studies suggested that the major compounds were simple branched paraffinic hydrocarbons and monocyclo-alkanes with lesser amounts of 2 to 4-ringed cycloalkanes and aromatic hydrocarbons. **Hood (1959)** proposed that the cyclic alkanes consisted of mainly monocyclic or methyl-branched monocyclic compounds containing a long alkyl chain, which could either be unsubstituted or branched. The polycyclic alkanes were generally thought by **Hood (1959)** to comprise alkyldecalins (V). Generalised aromatic structures were similar to those proposed by **Rossini *et al.*, (1955)** comprising alkyl benzenes with long straight chains (VIII) and substituted alkyl chains (IX), and naphthalenes, with alkyl substituted octahydrochrysenes, tetrahydrochrysenes, and phenanthrenes.

Killops and Readman (1985) and **Jones (1986)** used several techniques (GPC, GC, GC-MS and HPLC) to characterise an aromatic UCM of a sediment extract sampled from an Alaskan biodegraded crude and a sediment from the Sullom Voe oil terminal (Shetland) respectively. The majority of unresolved components were found to be within the 1-2 aromatic ring fraction, and most were alkylated. **Jones (1986)** was able to show, using GC-FPD, that many sulphur-containing compounds, including alkylbenzothiophenes (XII) and alkyldibenzothiophenes (XIII) were also present.

More recent studies of UCMs (**Gough, 1989**; **Killops and AL-Juboori, 1990**; **Revill,**

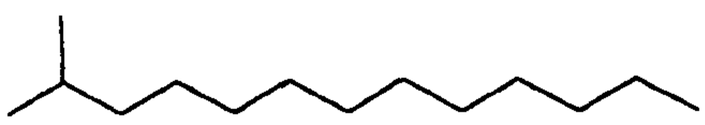

Methyl-branched

(I)

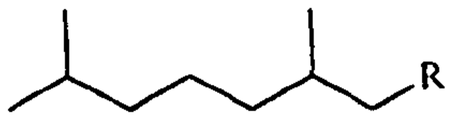

Isoprenoid

(II)

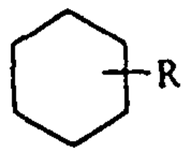

Alkyl-cyclohexane

(III)

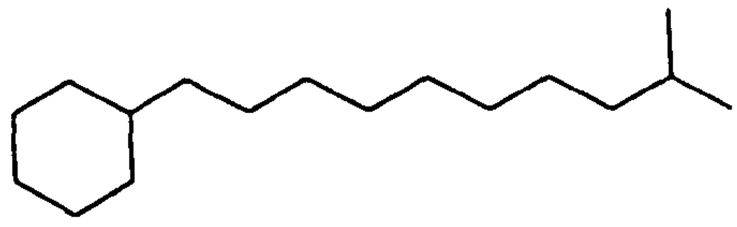

Branched alkyl-cyclohexane

(IV)

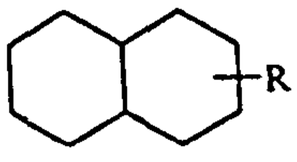

Alkyl-decalin

(V)

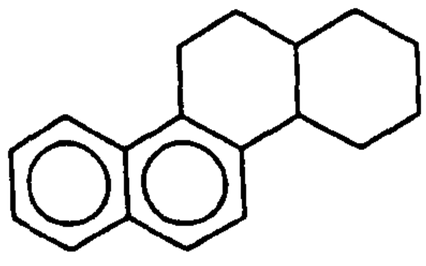

1,2,3,4,4a,11,12,12a-octahydrochrysene

(VI)

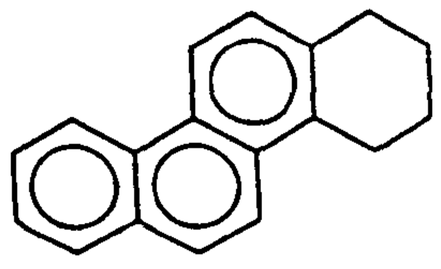

1,2,3,4-tetrahydrochrysene

(VII)

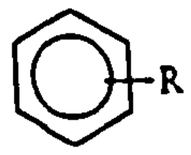

Alkyl-benzene

(VIII)

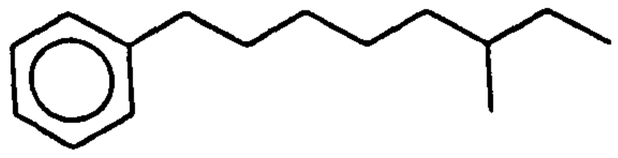

Branched alkyl-benzene

(IX)

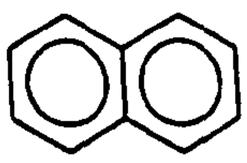

Naphthalene

(X)

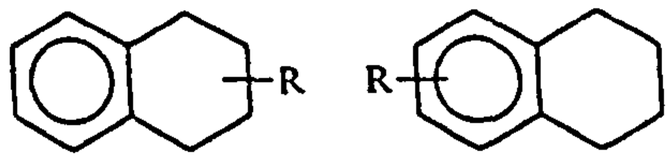

Alkyl-tetralin

(XI)

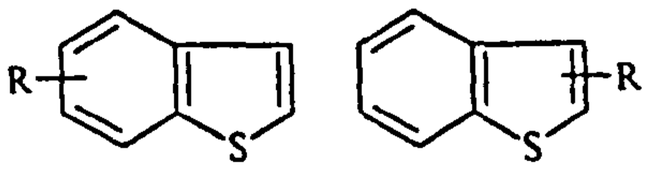

Alkyl-benzothiophene

(XII)

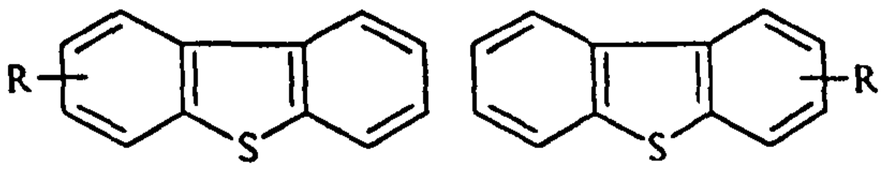

Alkyl-dibenzothiophene

(XIII)

Figure 2-2 General structures of compounds identified from the studies of lubricating oils (literature sources are given in text).

1992; **Revill *et al.*, 1992; Gough and Rowland, 1992, 1990**) have attempted not only to characterise the bulk properties of the UCM using modern spectrometric techniques, but also to analyze the UCM using classical chemical oxidative methods. Both **Gough (1989)** and **Killops and Al-Juboori (1990)** utilised chemical and pyrolytic degradative methods to elucidate the composition of UCMs from a variety of sources.

Spectroscopic methods (FT-IR and FT-^{1}H-NMR) produced spectra typical of aliphatic hydrocarbons, even for a biodegraded whole oil rich in aromatics (30%) (**Killops and Al-Juboori, 1990**). IR spectroscopy produced strong C-H stretching and bending signals but weak resonances in the aromatic region 675-900 cm^{-1} (out-of-plane C-H bending). NMR gave intense resonances for aliphatic protons (0-4 ppm compared with TMS) and only a low resonance signal ascribed to aromatic hydrogens (6-8 ppm relative to TMS) suggesting that most of the UCM carbon was aliphatic. Greater structural information was gained using mass spectrometry. Probe EI-MS produced predominant fragment ions at *m/z* 69 and 83, consistent with monocyclic alkane structures, and at *m/z* 81, 95, 109, 123, 137, consistent with bicyclic alkane structures. CI-MS with a NO/N_2 plasma gas was used to collect molecular ion data. Figure 2-3 shows the total number of carbon atoms associated with the different ring numbers of the acyclic and alicyclic compounds. The data for the biodegraded oil suggests that cyclic compounds with up to five rings were present (acyclic 40%, monocyclic 42%, bicyclic 15%, tricyclic 3%, tetra- and pentacyclic $<1\%$ each).

Gough (1989) used EI and CI mass spectrometry to analyze a lubricating oil UCM (Silkolene 150). This gave similar results to those reported by **Killops and Al-Juboori (1990)** for a whole biodegraded crude oil (*i.e.* a dominant proportion of acyclic and monocyclic alkanes with lower proportions of polycyclic alkanes).

Killops and Al-Juboori (1990), Gough (1989), and Revill (1992) used a modified existing CrO_3/acetic acid oxidation method (**Brooks *et al.*, 1977**) to oxidise UCMs. Several classes of identifiable resolved compounds were produced from the unresolved substrate (summarised in Table 2-1). Of these, *n*-acids and α,ω-diacids were the dominant classes of compounds formed. **Killops and Al-Juboori (1990)** found mono

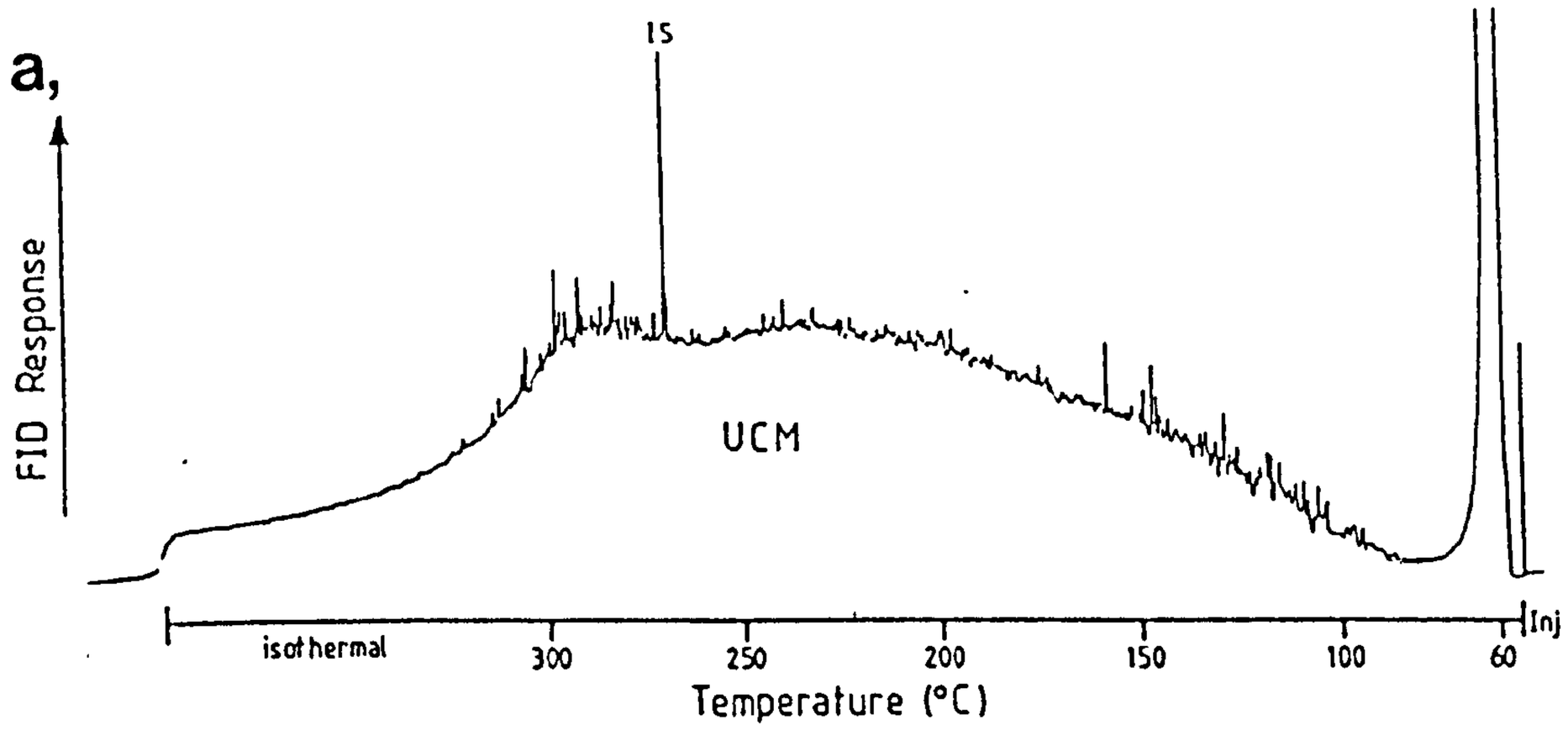

Figure 2-3 a) Capillary gas chromatogram of the total hydrocarbons fraction of a highly biodegraded petroleum and b) profiles of aliphatic hydrocarbon distributions obtained from NO/N_2 plasma CI-MS (after **Killops and Al-Juboori, 1990**)

Table 2-1 Summary of identified oxidation products of the aliphatic UCM of a lubricating oil (**Gough, 1989**) and a whole biodegraded oil (**Killops and Al-Juboori, 1990**).

	Lubricating oil		Biodegraded oil	
Compound	Carbon no. range	Maximum	Carbon no. range	Maximum
n-monocarboxylic acid	C6-C20	C9	C5-C18	C7-C8
α,ω-*n*-dicarboxylic acid	C6-C14	C9	C9-C17	-
Keto acid	C8, C10, C11	C10	C8	-
n-alkan-2-one	C8-C15	C12	C7	C7[c]
"iso"-methylbranched alkan-2-one	C8-C12	C8	C8	C8[c]
γ-methyl-γ-lactone	C6-C10	C8	-	-
methyl branched γ-methyl-γ-lactone	C11-C12	C11	-	-
ω-carboxy-γ-methyl γ-lactone	C8-C11	C8	-	-
methylbranched-ω-carboxy-γ-methyl-γ-lactone	C11-C13	C11	-	-
methylbranched mono-carboxylic acid	C6-C10	-	C6-C11	-
methyl branched α,ω-[a] diacid	C8, C9, C10	-	C5	C5[c]
Cyclohexyl carboxylic acid	C8	C8[c]	C7, C9-C11	-
methylcyclohexyl[b] carboxylic acid	-	-	C8	-
isoprenoid acid	C11-C16	-	C9-C11	-
isoprenoid ketone	C13	C13[c]	-	-

[a] In-chain methyl group position not definately known
[b] Varied positions for methyl group
[c] One compound identified only

carboxylic *n*-acids in the range C_5-C_{18}, (40.1%), and C_9-C_{17} α,ω-diacids (4.3%). C_{18} and C_{17} were the major *n*-acids and α,ω-diacids respectively, indicating a maximum bridging or chain length in the UCM of C_{19} for the biodegraded crude. The lubricating oil UCM studied by **Gough (1989)** also produced *n*-monocarboxylic acids (in the range C_6-C_{20}, maximising at C_9) thought to derive from the oxidation of terminal *n*-alkyl chains possibly linked on to cyclic/branched structures (Figure 1.2 A, I and II). Strong supporting evidence for this was acquired by **Gough and Rowland (1990)**, who also oxidised a series of synthetic hydrocarbons which produced oxidation products similar to those formed from the oxidation of the UCM. The *n*-diacids were probably formed from bridging alkyl chains, though further oxidation of monocarboxylic acids could not be ruled out.

Other components reported were branched acyclic alkanoic acids (including 2-methyl-alkanoic acids), cycloalkyl carboxylic acids (including cyclohexyl), *n*-alkan-2-ones (C_8-C_{15}), *iso*-methyl branched alkan-2-ones (C_8-C_{12}) and γ-methyl-γ-lactones, carboxylactones and methyl-branched carboxylactones **(Gough and Rowland, 1991).**

Killops and Al-Juboori (1990) reported only monocyclic aromatics among the oxidation products of a whole biodegraded oil and these were present in the form of benzenoid structures. However, the resolved oxidation components accounted for only 10% of the total products leaving 90% still unidentified. **Gough (1989)** separated an aromatic UCM from a lubricating oil (Silkolene 150) by column chromatography which accounted for only 8% of the total. This is not surprising because lubricating oils are usually dearomatised during processing and these results may not fully reflect the true composition of aromatic UCMs in unrefined oils. Nonetheless, using mass spectrometric techniques (EIMS, FIMS) **Gough (1989)** showed that the hydrocarbons present gave strong ion intensities indicative of phenyl alkanes (*m/z* 91/92), methylphenyl alkanes (*m/z* 105/106) and trimethylphenyl alkanes. Field ionisation mass spectrometry (FIMS), which is a useful technique for molecular weight determination because it produces virtually fragment-free mass spectra, suggested that the aromatic UCM was comprised in the main of alkyldinaphthenobenzenes > alkylnaphthalenes > alkylnaphthenonaphthalenes > alkyl tetralins > alkyl benzenes - results similar to the

earlier studies of **Rossini *et al.*, (1955)** for a crude oil.

Surprisingly, further investigation of the aromatic UCM using chemical oxidation with CrO_3/acetic acid produced compounds very similar to those obtained when the aliphatic fraction was oxidised (*i.e.* a major series of resolved compounds confirmed by GC-MS as *n*-alkanoic acids and diacids), although the proportion of additional resolved compounds compared with *n*-acids were fewer. **Gough (1989)** identified ketones and lactones, again similar to those identified in the aliphatic fraction. Certain aromatic acids and ketones were observed, including benzoic acids and a methyl substituted aromatic ketone.

In a later study, **Revill (1992)** carried out chromic acid and ruthenium tetroxide (RuO_4) oxidations of an aromatic UCM isolated from biodegraded Tia Juana Pesado crude oil (Venezuela). The results from chromic acid oxidation were similar to those reported by **Gough (1989)** and **Killops and Al-Juboori (1991)** for the lube and biodegraded oil, respectively. The relatively non-specific mechanism of the Cr(VI) oxidation led **Revill (1992)** to investigate the UCM using RuO_4, a reagent which oxidises the *ipso*-carbon of substituted aromatics. The results again showed that *n*-monocarboxylic acids were the dominant products, though overall RuO_4 produced fewer resolved compounds (5%) than CrO_3 oxidation (25%). Combining these findings with elemental and other analyses of the aromatic UCM, **Revill (1992)** proposed that the UCM comprised mainly naphthenoaromatic compounds with branched aliphatic side chains with or without a cyclic moiety (Figure 2-4 B, structures I, II, and III).

2.1.3 Structural isomers

Using a purpose-written computer program, **Gough and Rowland (1990)** calculated that for C_{20-30} so called "T-branched" alkanes (Figure 2-4 A [I]), which they proposed as constituents of the aliphatic UCM, there were 536 possible structures. **Revill (1992)**, using a similar program, calculated that for compounds with tetralin-type structures containing a monoalkyl branched side chain, terminating in 0-2 cyclohexyl rings, between C_{20} and C_{30}, (Figure 2-4 B) some 1,213 different structures were possible. If such high numbers of structural isomers of compounds are indeed present in UCMs,

A

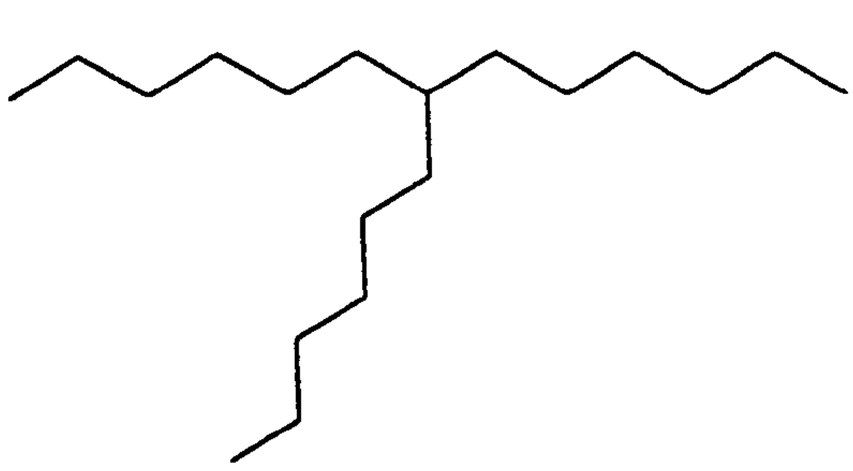

(I)

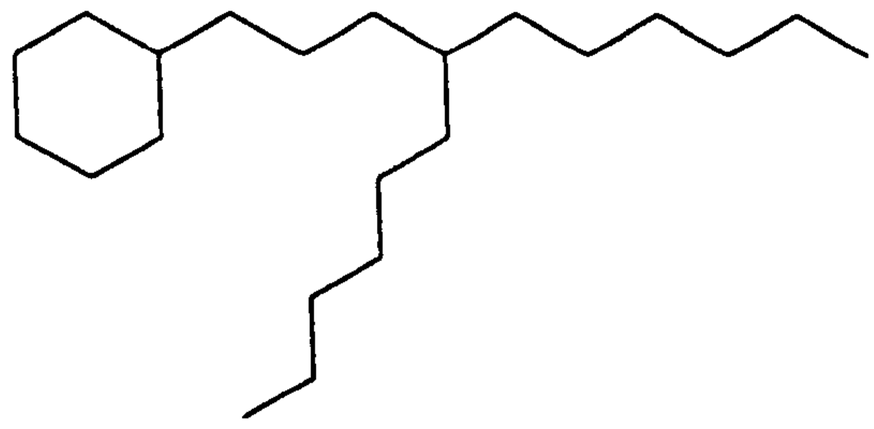

(II)

B

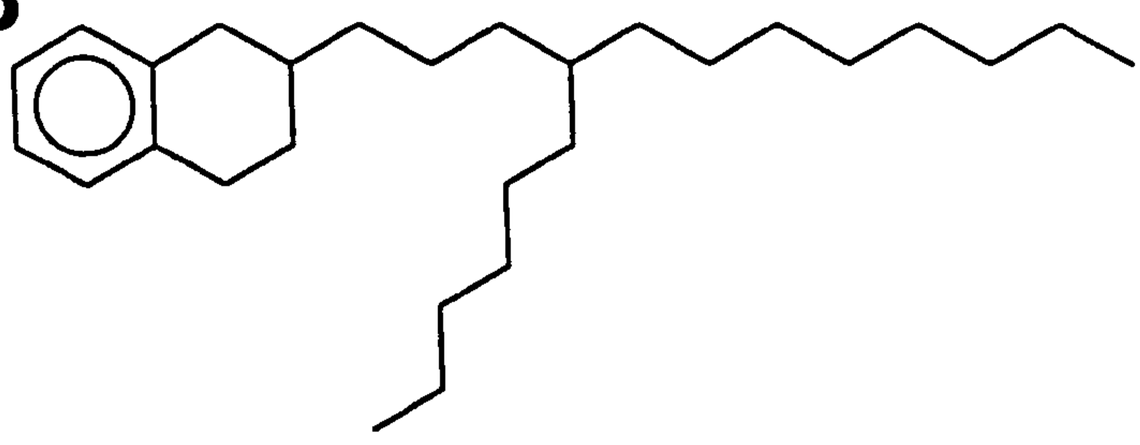

(I)

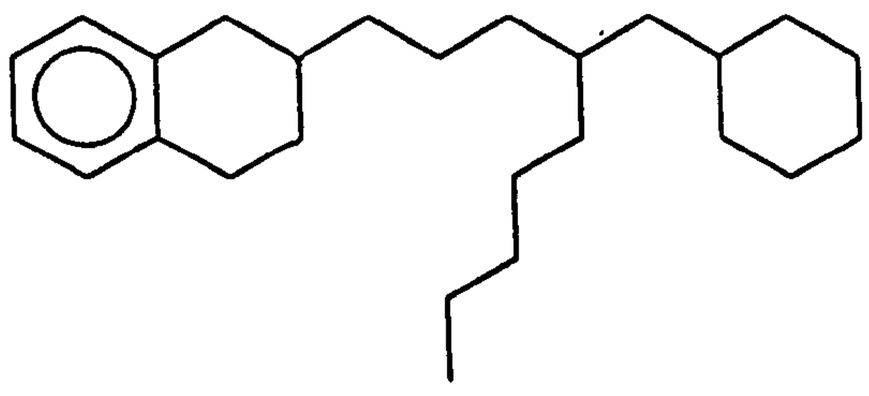

(II)

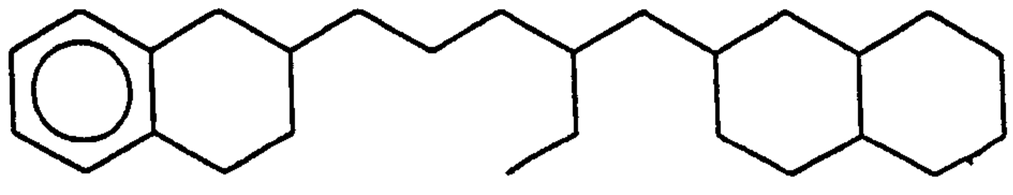

(III)

Figure 2-4 Proposed structures for the UCM by A) **Gough (1989)** and B) **Revill (1992)**.

then it is perhaps understandable that even the high resolution power of modern capillary gas chromatography does not resolve such complex mixtures.

2.1.4 Summary

Evidently UCMs are a result of the insufficient resolving power of the chromatographic technique. However, although theoretically the number of compounds comprising a UCM is very large, previous studies have shown that it is possible to start to unravel UCMs and to build models of the general types of hydrocarbons present. The UCMs studied so far originated from several lubricating oils, two biodegraded crude oils and a hydrocarbon-contaminated sediment extract. The results suggest that these UCMs all contain similar classes of hydrocarbons, comprising about 20% of simply branched acyclic compounds but also cyclic alkanes with up to five rings, of which the monocyclics are the most dominant. Aromatics are also present in the UCMs and are thought to be mainly alkyl (possibly branched) benzenoid type structure (*i.e.* with one aromatic ring). Larger aromatic compounds probably have alkyl-naphthalene and alkyl-tetralin type structures.

In practical terms studying the specific nature of UCMs provides valuable organic geochemical data. Their chemical compositions may serve not only to enhance the modelling of reservoir fluid properties but are also useful in the efficient refining of crude oils. However, knowledge of the different types and amounts of hydrocarbons present is far from complete. Clearly more research is required to broaden an understanding of the types and structures of those compounds that present themselves as UCMs.

2.2 Aims

All previous UCM studies have concentrated on biodegraded crude oils or refined lube oils. Clearly a study of the UCM of unrefined and non-biodegraded samples is needed. The simplest UCM-containing fossil fuel is likely to be a gas-condensate since the number of structural isomers possible for a low boiling fraction is necessarily lower. Thus the present study aimed to characterise, by oxidative degradation, the unresolved portion of an unrefined, non-biodegraded gas-condensate. Since even a low boiling UCM can be expected to contain many hundreds of compounds, the gas condensate was first fractionated by vacuum distillation to provide a series of simpler UCM fractions. The thirty four distillation cuts each covered a very narrow boiling point range (typically 10°C AET) between successive *n*-alkane homologues, within which was an UCM. This approach has not been taken previously. Structural information about the UCM should be valuable in further refining gas condensate PVT models.

2.3 Results and Discussion

2.3.1 Fractional distillation

From an initial condensate charge of nearly two kilograms, thirty-four separate distillate fractions, including a residue, were collected. The weights, volumes and the Atmospheric Equivalent Temperature (AET) of each fraction are presented in Table 2-2. From this data a true boiling point curve for the distillation can be drawn (Figure 2-5). The results show that at an AET of 344°C approximately 75% of the original condensate was distilled, leaving 20% remaining in the charge flask as a dark brown waxy residue. Overall recovery after fractionation was good (98.8%). The small loss of material is partly explained by the failure to recover a representative debutanised fraction. This is the gaseous part of the condensate which is usually collected prior to distillation. The amount of each distillate fraction as a percentage of the total gas-condensate is shown in Figure 2-6. Fraction 15 (AET 171°C) contained the largest amount of distillate (76.4g), equivalent to 4.4% of the total (debutanised).

Figure 2-7 shows representative conventional capillary gas chromatograms of the total gas condensate and of selected distillate cuts (Fractions 19, 23, 26, 27, 28, 29, 30 and the Residue). Table 2-3 lists the major components identified by gas chromatography in all the fractions and the average molecular weight of each fraction determined using the CRYETTE A cryoscope (see Experimental). C_5 to C_{34} components with molecular weights of 74 (Fraction 1) to 280 (Fraction 31) were detected. Figure 2-7 and the data in Table 2-3 show some overlap of components between consecutive distillate cuts. Table 2-4 (data represented as a histogram in Figure 2-8) shows the overall recombined concentrations (Wt/Wt%) of each component measured by GC and expressed as a percentage of the total. Component C_8 is dominant having a recombined concentration of 10 Wt/Wt%. Distillate Fraction 19 (AET 216°C, RI 1099-1278) accounted for 3.7% of the total condensate (Table 2-4) and GC analysis showed that it comprised mainly C_{12} (65.38%) with lesser amounts of C_{13} (31.61%) components, with C_{11} (3.01%, Table 2-3). Fraction 23 (AET 260°C, RI 1361-1599) accounted for 2.5% of the total condensate and comprised C_{13} (0.36%), C_{14} (40.94%) and C_{15} (58.7%). The alkanes *n*-C_{14} and *n*-C_{15} were the predominant resolved components. In Fraction 26 (AET 282°C, RI 1465-1698, 2.1%) C_{16} components accounted for $<80\%$ of the compounds present.

Table 2-2 True boiling point (TBP) distillation of a North Sea condensate.

Distillate Fraction	AET (°C)	Mass (g)	% of Total	Cumm % of Total	Volume cm3	Volume %	Cumm % of Total	Density
1	33.0	10.9	0.6	0.6	17.0	0.8	0.8	0.6423
2	54.0	26.4	1.5	2.1	39.3	1.8	2.5	0.6736
3	70.0	28.3	1.6	3.8	40.0	1.8	4.3	0.7068
4	80.0	22.0	1.3	5.0	30.6	1.4	5.7	0.7210
5	90.0	49.2	2.8	7.8	67.8	3.1	8.8	0.7256
6	100.0	61.3	3.5	11.3	82.2	3.7	12.5	0.7453
7	111.0	24.8	1.4	12.8	32.8	1.5	14.0	0.7541
8	108.0	36.7	2.1	14.9	48.4	2.2	16.2	0.7580
9	120.0	31.9	1.8	16.7	42.8	1.9	18.1	0.7460
10	130.0	69.6	4.0	20.7	91.4	4.1	22.3	0.7616
11	140.0	60.2	3.4	24.1	78.3	3.5	25.8	0.7682
12	146.0	19.3	1.1	25.2	24.7	1.1	26.9	0.7818
13	148.0	41.0	2.3	27.6	53.6	2.4	29.3	0.7658
14	158.0	36.7	2.1	29.7	47.2	2.1	31.5	0.7769
15	171.0	76.4	4.4	34.1	98.8	4.5	35.9	0.7730
16	182.0	40.6	2.3	36.4	52.2	2.4	38.3	0.7775
17	191.0	56.5	3.2	39.6	72.6	3.3	41.6	0.7789
18	204.0	44.4	2.5	42.2	56.4	2.6	44.1	0.7865
19	216.0	65.1	3.7	45.9	82.6	3.7	47.9	0.7873
20	226.0	40.5	2.3	48.2	50.7	2.3	50.2	0.7979
21	238.0	62.5	3.6	51.8	78.3	3.5	53.7	0.7977
22	249.0	56.5	3.2	55.0	70.4	3.2	56.9	0.8032
23	260.0	43.8	2.5	57.5	54.3	2.5	59.3	0.8073
24	269.0	48.5	2.8	60.3	60.0	2.7	62.1	0.8086
25	280.0	21.9	1.3	61.6	27.0	1.2	63.3	0.8116
26	282.0	37.5	2.1	63.7	45.9	2.1	65.3	0.8185
27	295.0	42.6	2.4	66.1	52.0	2.4	67.7	0.8180
28	307.0	44.8	2.6	68.7	54.8	2.5	70.2	0.8172
29	319.0	35.7	2.0	70.7	43.5	2.0	72.1	0.8194
30	337.0	50.0	2.9	73.6	60.2	2.7	74.9	0.8303
31	344.0	29.5	1.7	75.3	35.5	1.6	76.5	0.8313
Total		1314.9	75.3		1691.2	76.5		
Residue		360.05	20.6		431.2	19.5		
H2O		361	20.7		36	1.6		
Other		23.09	1.3		28	1.3		0.8194
Total Recovery		1734.09	99.8		2186.66	98.9		

Weight of original Charge = 1746.21
Volume of original Charge = 2211.512
Density of original charge = 0.78996

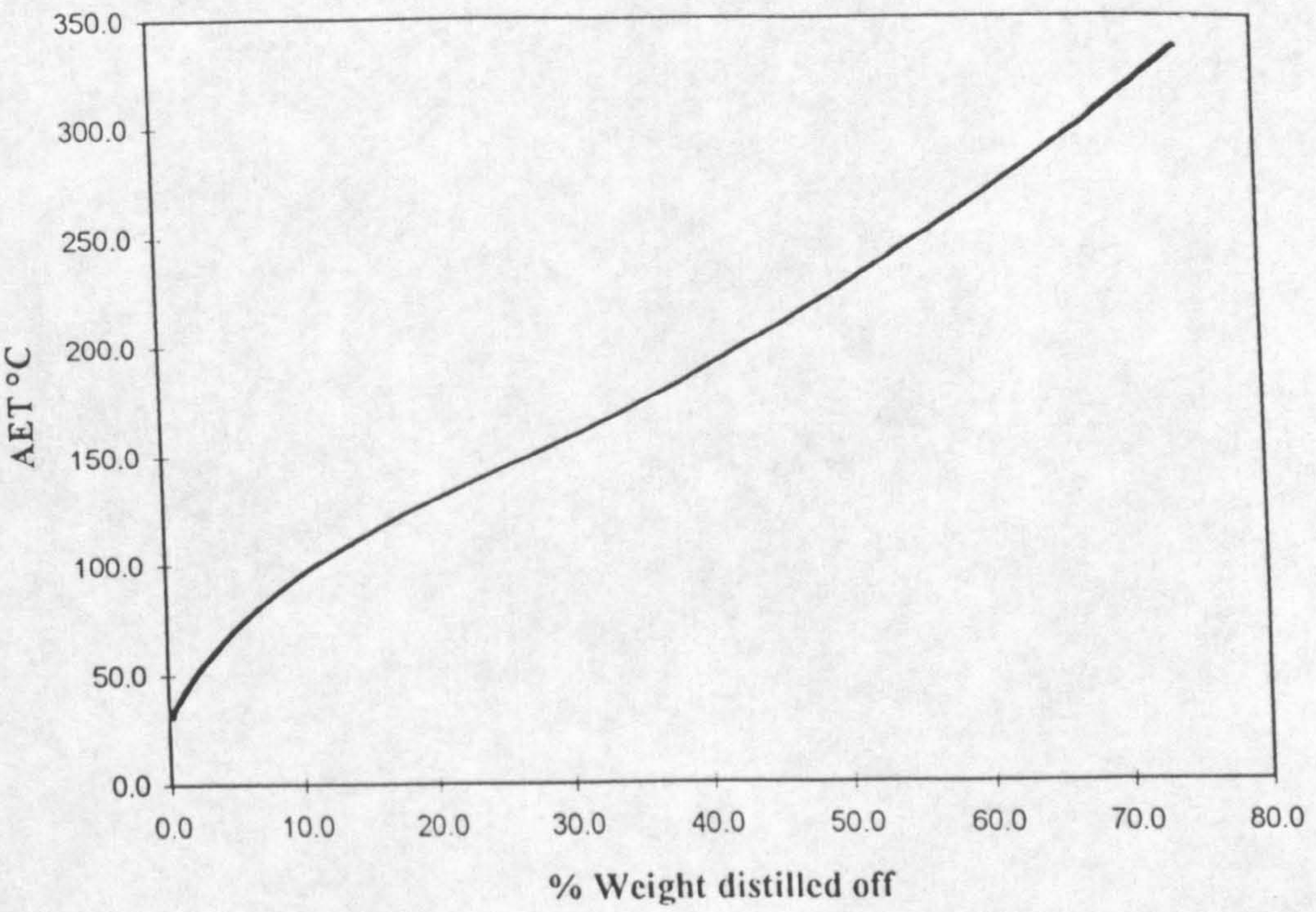

Figure 2-5 Distillation curve for a North Sea gas-condensate.

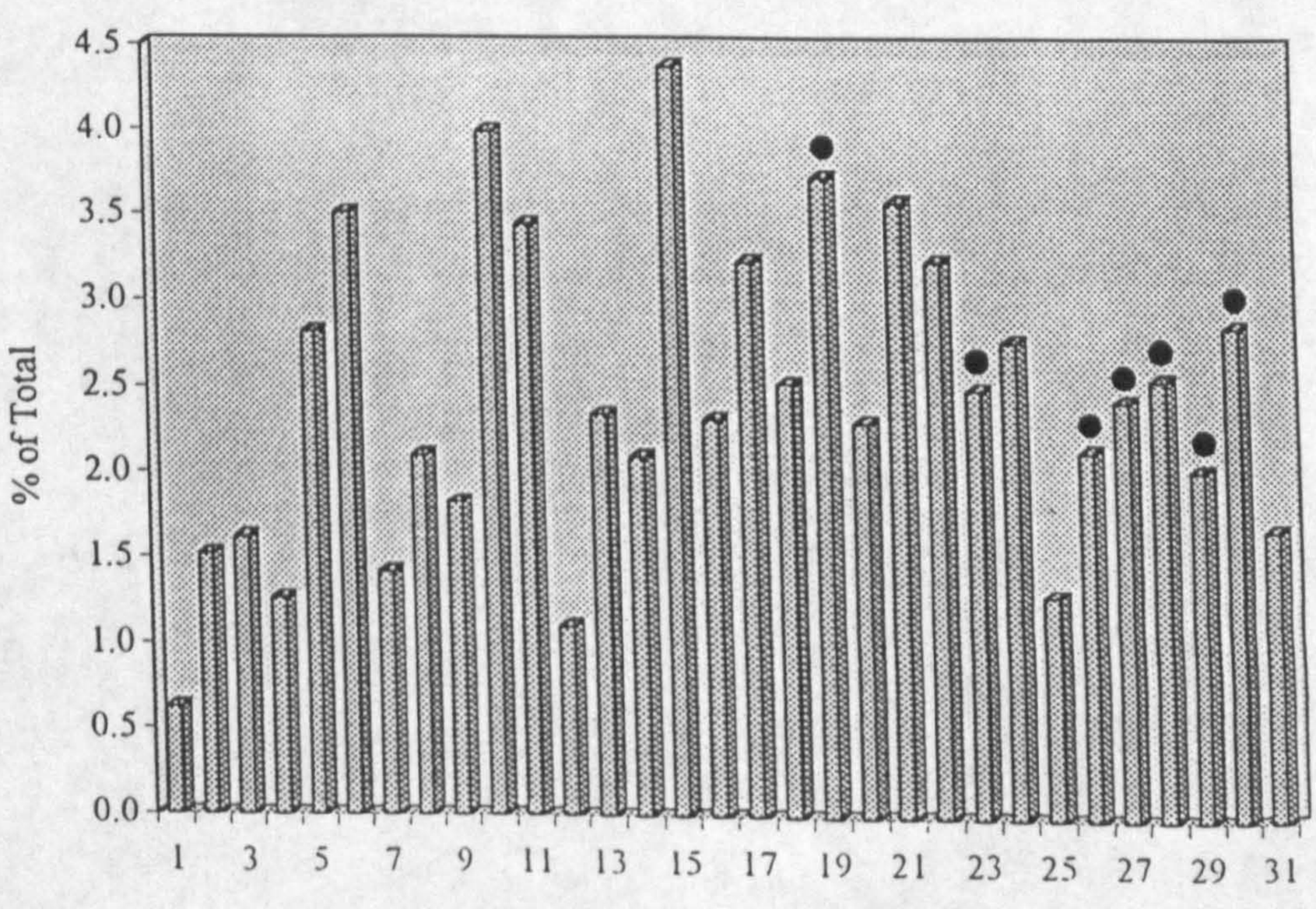

Figure 2-6 Histogram showing percentage of each distillate cut in the total condensate (● indicates distillate fractions examined by oxidation).

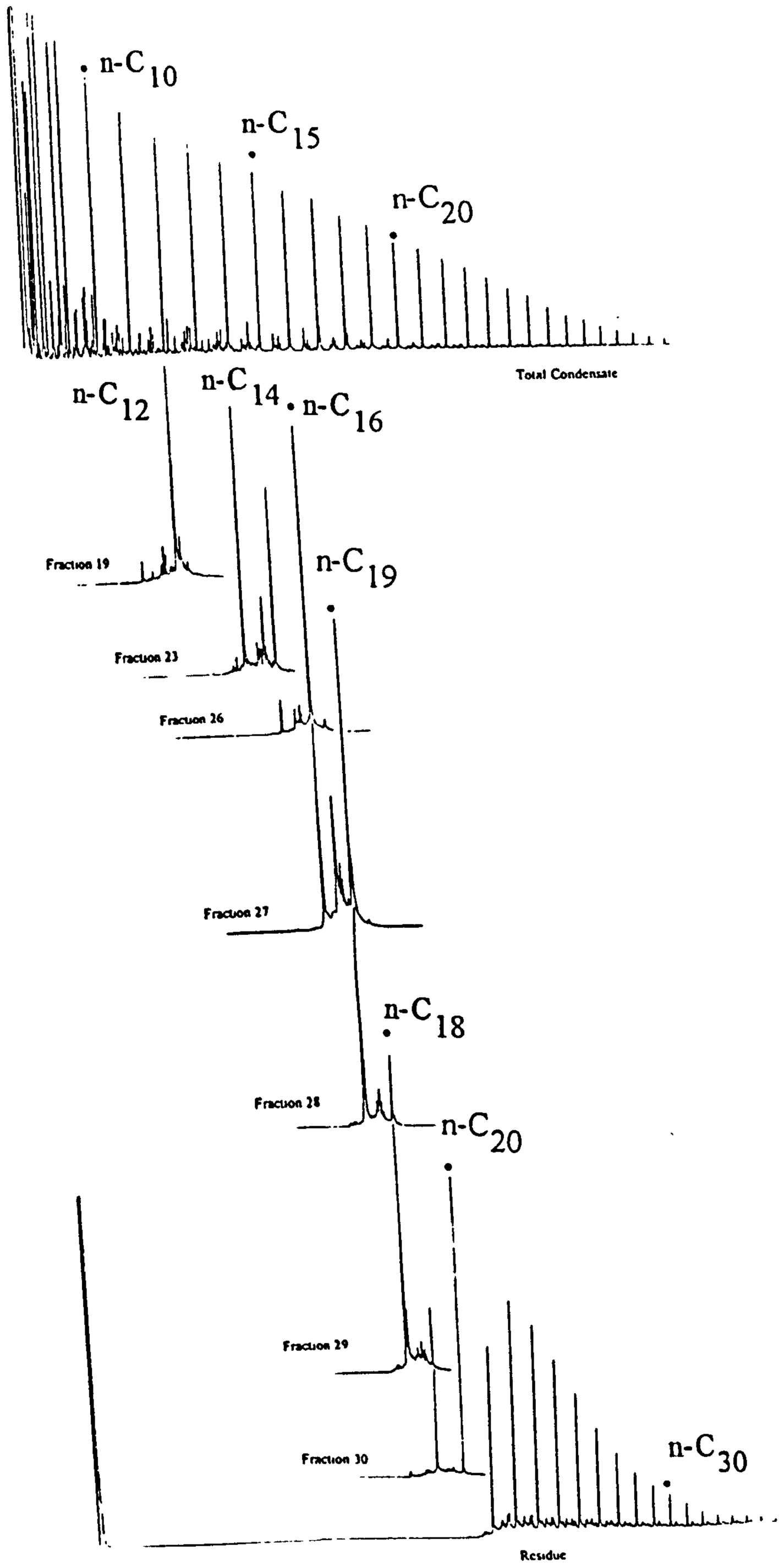

Figure 2-7 Gas chromatograms of the whole condensate, selected distillate cuts and the residue.

GC: J&W DB-5 (25m x 0.32 mm i.d.) Prog: 40°C to 300°C at 5°C/min 300°C (hold), H_2, FID.

Table 2-3 Component analysis and the calculated molecular weight of each distillate cuts.

Distillate Fraction	Component	Concentration (Wt/Wt%)	Calculated Molecular[1] Weight	Distillate Fraction	Component	Concentration (Wt/Wt%)	Calculated Molecular Weight
1	i-C5	26.23	74.02	6	C6	1.31	101.35
	n-C5	56.53			C7	45.52	
	C6	16.94			C8	53.17	
	C7	0.3					
				7	C7	16.01	105.35
2	i-C5	4.59	82.68		C8	81.67	
	n-C5	13.88			C9	2.32	
	C6	70.19					
	C7	11.34		8	C6	0.29	104.84
					C7	18.88	
3	n-C5	1.03	88.36		C8	79.29	
	C6	58.12			C9	1.54	
	C7	40.85					
				9	C7	2.26	108.36
4	C6	26.35	92.96		C8	84.64	
	C7	68.85			C9	13.1	
	C8	4.8					
				10	C7	0.54	113.8
5	C6	8.67	96.84		C8	47.29	
	C7	70.82			C9	52.17	
	C8	20.51					

Continued overleaf.....

Continued .....

Distillate Fraction	Component	Concentration (Wt/Wt%)	Calculated Molecular Weight	Distillate Fraction	Component	Concentration (Wt/Wt%)	Calculated Molecular Weight
11	C8	18.38	118.76	17	C10	3.13	149.04
	C9	76.28			C11	77.64	
	C10	5.34			C12	19.23	
12	C8	17.02	118.42	18	C11	28.31	157.12
	C9	82.38			C12	68.67	
	C10	0.6			C13	2.82	
13	C8	0.4	124.19	19	C11	3.01	164.69
	C9	72.62			C12	65.38	
	C10	26.98			C13	31.61	
14	C9	23.38	130.83	20	C12	19.49	172.61
	C10	75.59			C13	76.58	
	C11	1.03			C14	3.93	
15	C9	0.38	137.13	21	C12	0.6	180.08
	C10	73.37			C13	63	
	C11	26.25			C14	36.4	
16	C10	28.25	143.08	22	C13	10.26	189.4
	C11	71.75			C14	82.52	
					C15	7.22	

Continued overleaf.....

Continued.....

Distillate Fraction	Component	Concentration (Wt/Wt%)	Calculated Molecular Weight	Distillate Fraction	Component	Concentration (Wt/Wt%)	Calculated Molecular Weight
23	C13	0.36	199.01	28	C16	0.22	245.65
	C14	40.94			C17	39.2	
	C15	58.7			C18	56.95	
					C19	3.63	
24	C14	3.93	208.43				
	C15	75.29		29	C17	0.73	257.9
	C16	20.78			C18	44	
					C19	50.56	
25	C15	25.55	218.01		C20	4.71	
	C16	72					
	C17	2.45		30	C18	2.8	267.28
					C19	57.42	
26	C15	5.65	222.98		C20	39.78	
	C16	80.47					
	C17	13.88		31	C19	2.67	279.67
					C20	64.73	
27	C16	18.74	235.57		C21	32.6	
	C17	69.48					
	C18	11.78					

1 The molecular weight of each distillate fraction was determined uising a a CRYETTE A cryoscope.

Table 2-4 Concentrations (Wt/Wt%) of A) components measured in the whole condensate by gas chromatography and B) summation of analysis by gas chromatography of the separate distillate cuts.

Component	[A]Concentration Wt/Wt% Intial	[B]Concentration Wt/Wt% Recombined
C2	0.00	0.00
C3	0.06	0.00
i-C4	0.10	0.00
n-C4	0.31	0.00
i-C5	0.56	0.24
n-C5	0.79	0.60
C6	2.84	2.86
C7	6.24	6.24
C8	10.43	10.00
C9	9.34	8.49
C10	7.98	6.65
C11	6.88	6.45
C12	5.59	5.51
C13	6.37	5.86
C14	5.70	5.42
C15	4.71	4.42
C16	3.49	3.83
C17	3.84	3.17
C18	2.87	2.84
C19	3.16	2.93
C20	2.98	2.43
C21	2.35	2.41
C22	2.09	3.00
C23	1.88	2.66
C24	1.91	2.38
C25	1.57	1.82
C26	1.49	1.53
C27	1.09	1.25
C28	0.91	1.00
C29	0.81	0.95
C30	0.61	0.75
C31	0.44	0.66
C32	0.23	0.60
C33	0.24	0.47
C34	0.07	2.60
Total	100	100.018

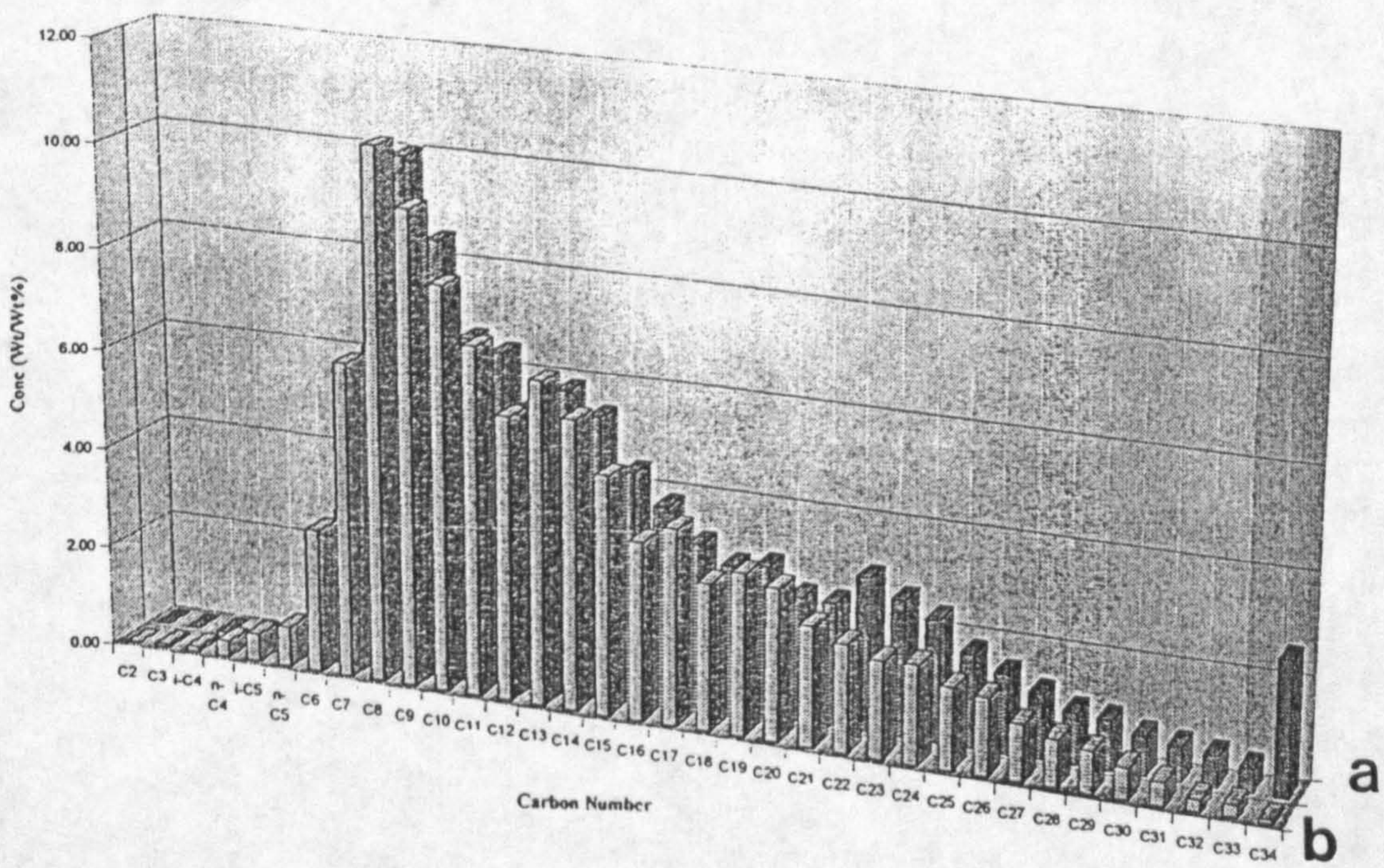

Figure 2-8 Histogram showing the percentages of each carbon number present measured by gas chromatography of a) total condensate and b) summation of results of GC analysis of the individual distillate cuts.

Fractions 27 (AET 295°C, RI 1562-1750), 28 (AET 307°C, RI 1649-1862), 29 (AET 319°C, RI 1745-1949) and 30 (AET 337°C, RI 1800-2010, 2.9) contained common components due to a high degree of co-elution, with high proportions of C_{17} (69.8%) and (39.2%) and C_{19} (50.56%) and (57.42%) respectively. Of the approximately 20% of condensate remaining in the residue (AET <344°C, RI 2025-3400) GC analysis showed the major peaks to be the *n*-alkanes *n*-C_{21-37}. Further characterisation of the high molecular weight components is discussed in Chapter 4.

2.3.2 Analysis of the unresolved complex mixture

When condensates and oils are analysed by GC the contribution of the UCM to the total response is often masked by the high proportions of a few resolved compounds. This is easily demonstrated by reducing the attenuation of the GC FID signal; the UCM then becomes more apparent (Figure 2-9). The total peak area of the chromatogram can be determined using a chromatographic time slice integration program. The resolved peaks can then be measured using normal valley-to-valley integration and the total integrated area minus the area of the resolved peaks gives an estimate of the proportion of the chromatogram that is unresolved (**Gough, 1989**). Of the total condensate 21% of the chromatogram was found to be unresolved under the experimental conditions (J & W, DB-5, 30 m x 0.32 mm i.d, prog: 50°C to 300°C at 5°C/min). This is a significant amount which perhaps would not be noted from initial visual inspection of the chromatogram of the whole gas-condensate. A test of the reproducibility of this method has not been published previously but was carried out herein by calculating the size of UCM in five repeat injections of a distillate fraction (Fraction 23). The results show an acceptable RSD of 3.4% (Table 2-5).

The proportions of UCM in the distillate fractions were calculated using the above method and are given in Table 2-6 and shown as a histogram in Figure 2-10 (A). The highest proportion of UCM occurred in Fraction 30 (61%). This is to be expected because Fraction 30 elutes where the UCM maximum is observed. The UCM in the remaining fractions ranged from 33% (Fraction 26) to 46% (Fraction 29) with an average of 38%.

For the further analysis of the UCM by degradative techniques, (*cf.* **Gough, 1989**;

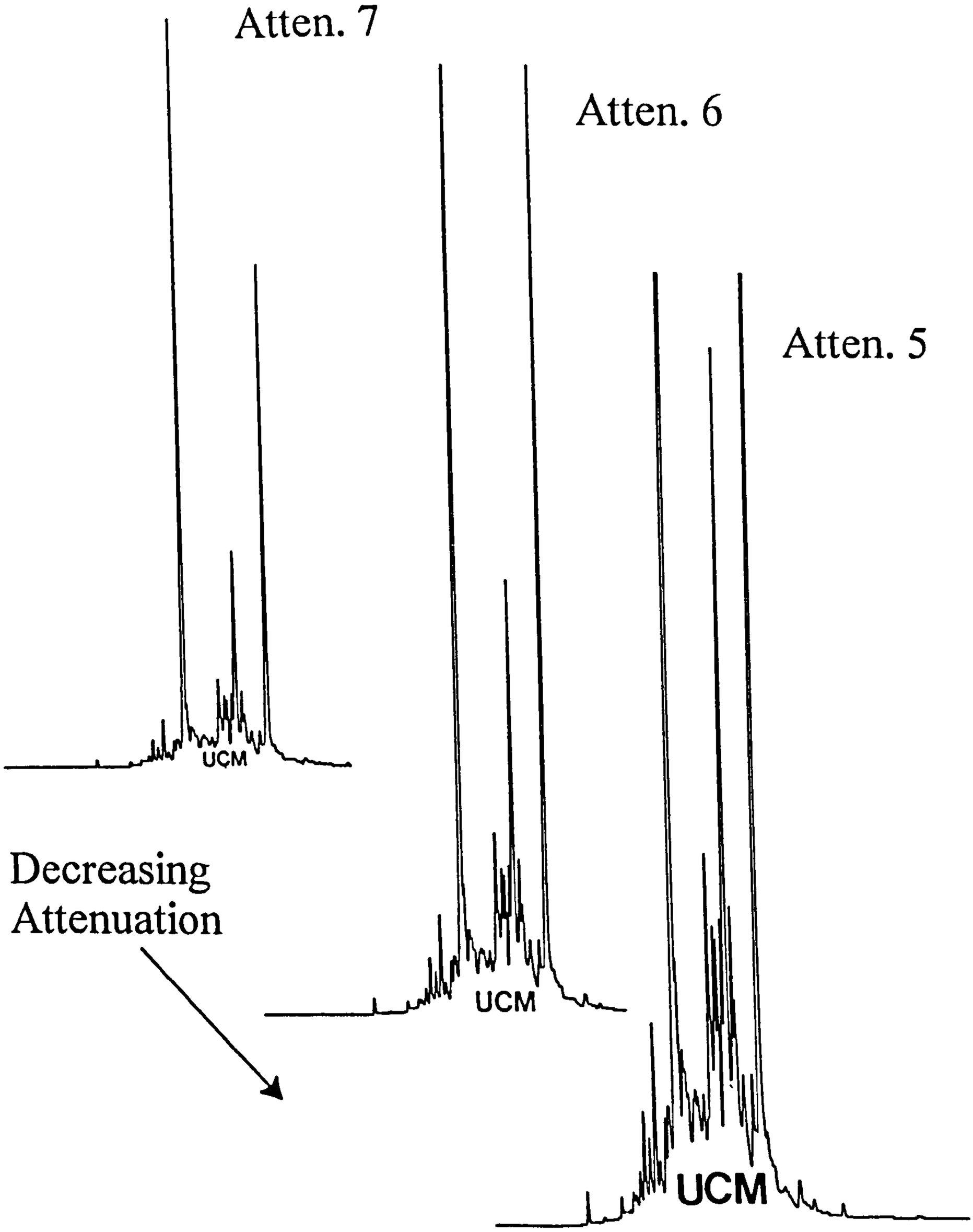

Figure 2-9 Gas chromatogram of distillate Fraction 23 showing easier observation of UCM with decreasing FID attenuation.

Table 2-5 Resolved and unresolved peak areas obtained from five injections of distillate Fraction 23 after clathration.

Total Area[1]	Resolved Peaks	%	Unresolved Hump	%
4187160	1441129	34	2746031	66
3631160	1320595	36	2310565	64
6006900	2165062	36	3841838	64
3746470	1351733	36	2394737	64
3407410	1361101	40	2046309	60
Mean		36.4		63.6
Std.Dev.		2.19		2.19
%RSD		3.4		3.4

1 Integration was performed using the SHIMADZU CR 9 integrator.

Table 2-6 Percentage UCM in the whole condensate, distillate fractions and the residue.

Distillation Fraction	Retention Indices (RI)	Original Distillate Fraction				Clathrated Distillate Fraction[1]			
		Resolved Peaks		UCM		Resolved Peaks		UCM	
		Area	%	Area	%	Area	%	Area	%
19	1099-1278	793864	66	273279	34	424490	30	1003460	70
23	1361-1599	937061	56	224599	44	1441129	34	2746031	66
26	1465-1698	632113	77	304798	33	205526	17	996594	83
27	1562-1750	1659723	54	1386297	46	405394	10	3832376	90
28	1649-1862	3302806	66	1674074	34	512386	29	1276804	71
29	1745-1949	3552309	65	1913651	35	1527924	36	2667896	64
30	1800-2010	5727393	39	8817307	61	6599	3	262798	97
Residue	2025-3400	1566000	64	1005441	36	156600	16	848841	84
Total Condensate	1099-3400	926143	79	1175352	21	3810035	44	6765450	66

1 The non-sieved and non-urea adduct of the distillate fractions.

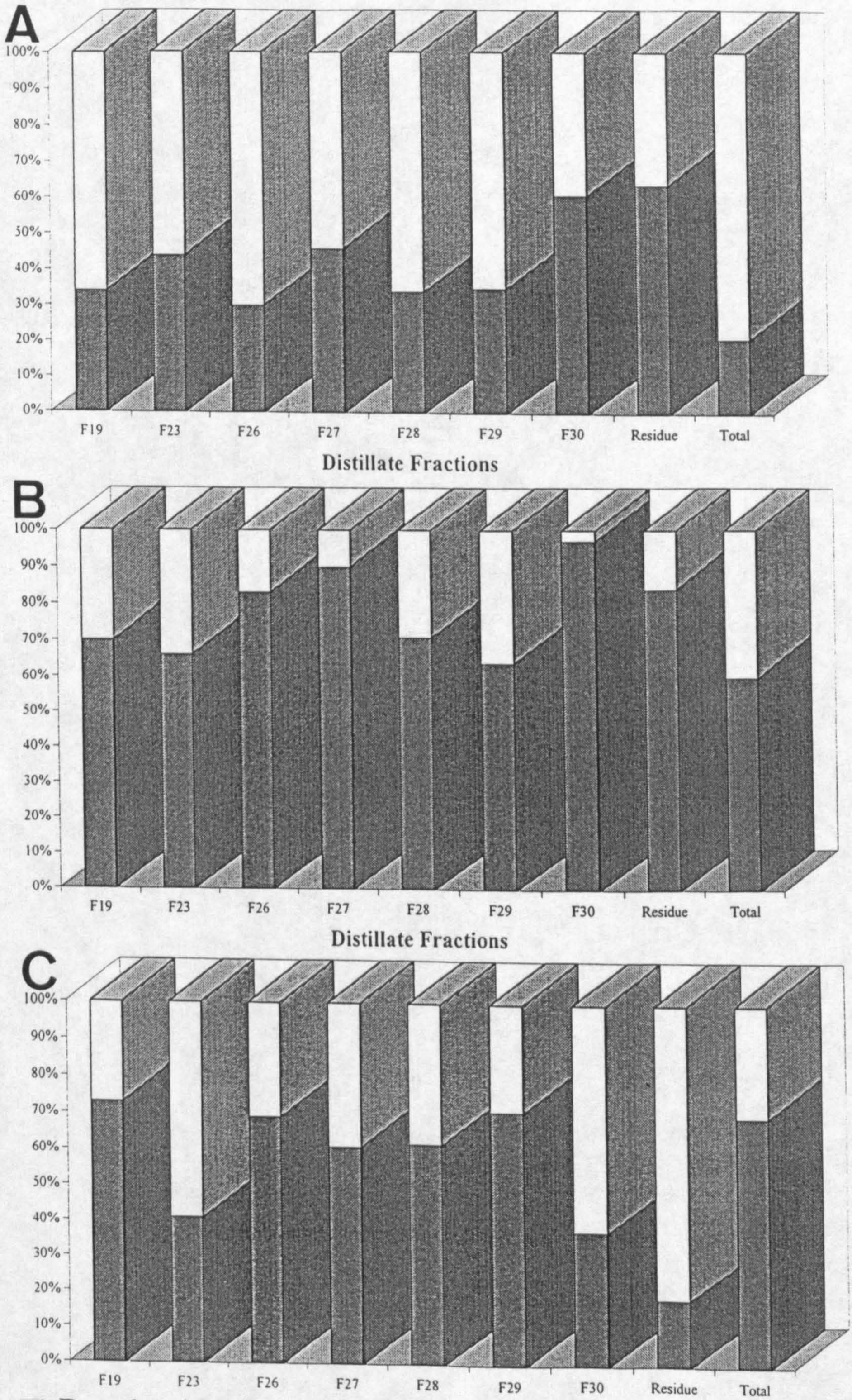

Figure 2-10 Percentage of the UCM present in A) original distillate cuts, b) material remaining after molecular sieving (5A) and urea adduction and C) the total products recovered after oxidation.

Killops and Al-Juboori, 1991), it is necessary to remove the majority of the resolved compounds (*i.e.* mainly *n*-alkanes) so that compounds resulting from oxidation can be assigned to precursor compounds from within the UCM. The most common methods for removing straight chain aliphatic compounds are molecular sieving and urea adduction.

2.3.3 Clathration by 5A molecular sieve and urea adduction

Clathration is effectively a way of separating certain classes of compounds according to molecular radius. 5A molecular sieves are most useful for clathrating normal alkanes (**Murphy, 1969; Dimmler and Strausz, 1983**). The sieve works because the diameter of the microscopic pores in the clay structure are the correct width to trap *n*-alkanes. Compounds with larger radii are not able to enter the pores of the sieve and smaller compounds will pass freely in and out of the sieve. For the latter reason the compounds of interest are refluxed in a solvent whose molecular diameter is larger than the sieve. Urea adduction works in a similar way, but in this method a saturated solution of urea in methanol is added drop-wise into a non-polar solvent (hexane) containing the *n*-alkanes. As the crystals of the urea form they encapsulate the *n*-alkanes (and *iso*-alkanes) removing them from solution (**Meinschein and Kenny, 1957**).

The present study found that while the major resolved compounds were readily removed by urea adduction from the residue fraction, this was not the case for the distillate fractions, and several repeat adductions were needed. This led to a poor recovery of sample and increased the risk of contamination due to extra manipulation. The method was found to be time consuming and only effective for quantities of < 50 mg. Therefore, each fraction was initially sieved using a 5A molecular sieve (BDH). This enabled a large sample to be sieved (> 200mg) and because the majority of the *n*-alkanes were removed, subsequent urea adductions were more efficient. Each fraction was further adducted with urea to remove the remainder of the adductable compounds. Figure 2-11 shows chromatograms of the total condensate and the distillate cuts after clathration. In each fraction, the proportion of material remaining after 5A molecular sieving (Table 2-7) ranged from 49% (Fraction 19) to 62% (Fraction 27). The clathrated material was not recovered from the sieve and so the percentage recovery

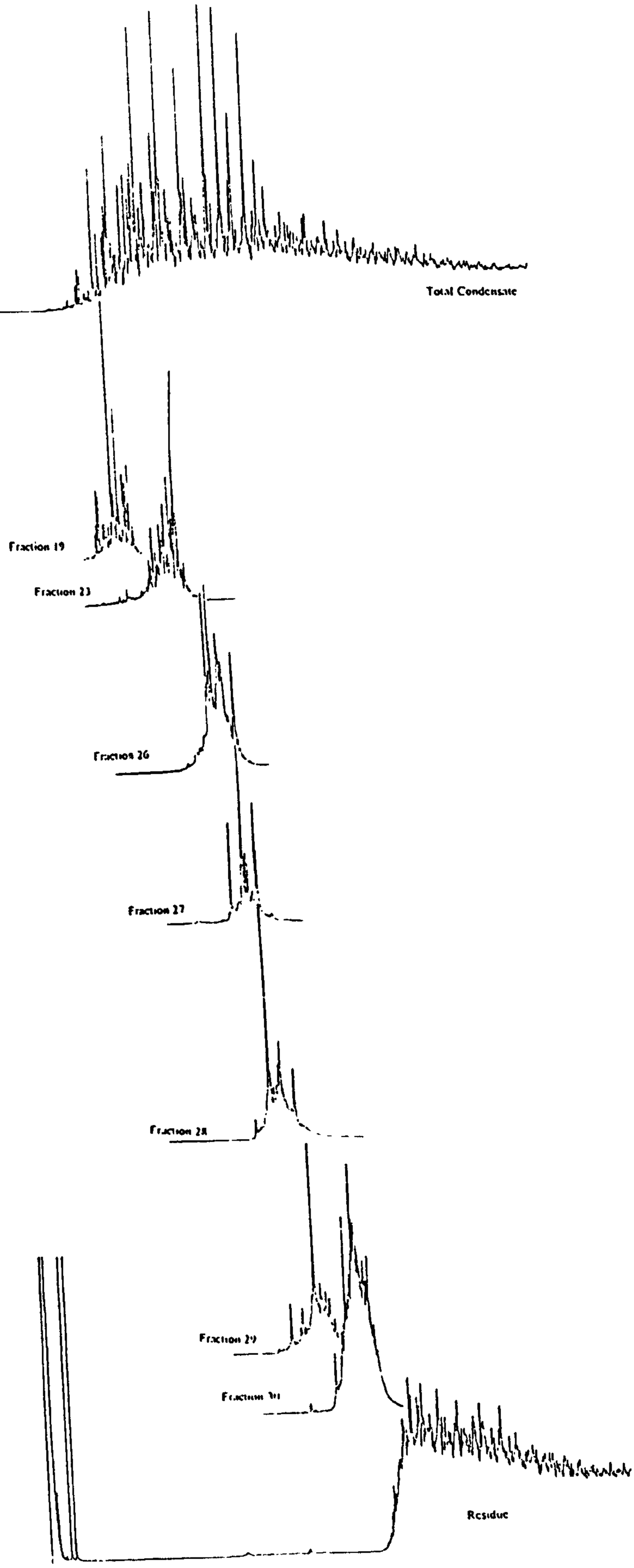

Figure 2-11 Gas chromatograms of the remaining nonclathratable hydrocarbons.

GC: J&W DB-5 (25m x 0.32 mm i.d.) Prog: 40°C to 300°C at 5°C/min 300°C (hold), H_2, FID.

Table 2-7 Percentage of material remaining after molceular sieving and urea adduction of the whole condensate, distillate fractions and the residue.

5A Molecular Sieve				Urea Adduction of Sieved Fractions					
Distillation Fraction	Original Amount (mg)	Non Sieved (mg)	Recovery %	Original Amount (mg)	None Adduct (mg)	Urea Adduct (mg)	Total (mg)	Recovery %	Total %
19	171.8	83.5	49	44.3	37.2	5.5	42.7	96	41
23	212.7	130.1	61	94.8	75.3	6.7	82.0	86	49
26	177.0	97.1	55	94.9	70.4	7.4	77.8	82	41
27	231.4	144.3	62	102.1	66.5	12.9	79.4	78	41
28	217.5	120.0	55	87.4	61.3	8.7	70.0	80	39
29	187.7	101.0	54	80.6	57.7	10.0	67.7	84	39
30	267.1	130.9	49	96.5	63.3	15.3	78.6	81	32
Residue	/	/	/	126.1	82.5	42.6	125.1	99	65
Total Condensate	208.0	118.5	57	100.4	56.0	16.8	72.8	73	32

values are calculated using the non-clathrated material only. The recoveries of the urea adduct (UA) and urea non-adduct fractions (UNA) are also given in Table 2-7.

For Fraction 30, 51% of material was found to be removed after molecular sieving and a further 66% was removed by urea adduction. The remainder accounted for 32% of the total distillate fraction and 0.54% of the original condensate (Table 2-7). The results were calculated for all the fractions and the total recoveries after urea adduction ranged from 73% to 96% with an average recovery of 84%. The amounts of non-clathrated material as a percentage of the total fractions were 32% to 65% (Table 2-7).

With the removal of the dominant resolved peaks from each fraction the contribution of the UCM to the total fraction increased, as expected. For non-clathrated distillate, the percentage UCM when analysed by capillary gas chromatography (Table 2-6), ranged from 64% (Fraction 29) to 97% (Fraction 30) with an average of 77%. Table 2-6 and Figure 2-10 shows the percentage of UCM in each fraction as a total of each whole fraction calculated before and after clathration. The percentage of UCM calculated in the original fractions is slightly lower then the percentage of UCM calculated from the clathrated fractions, but overall the data are in very good agreement, with an average difference of only 6%.

2.3.4 GC-MS Analysis of the clathrated distillate fractions

After molecular sieving and urea adduction, GC showed that the gas condensate distillates comprised mainly UCM. Indeed, UCM accounts for between 64% (Fraction 29) to 97% (Fraction 30), with the residue fraction being the most unresolved. Identification of the few major resolved components still present by GC-MS was made difficult because of co-elution, but the identities of those compounds which could be assigned are listed in Table 2-8 (peak numbers refer to Figure 2-12). GC-MS revealed that the majority of resolved components in the distillates had branched and/or isoprenoid acyclic structures the major spectral characteristic of which was the increased abundance of fragment ions originating from cleavage around tertiary carbon centres. In Fraction 19 the most abundant resolved component was identified by comparison with library spectra (NBS54k, Hewlett Packard) and that of published spectra (**Philp, 1985**) as the isoprenoid 2,6-dimethyldecane (K.R.I. 1211, 25.1%, Figure 2-13). The

Table 2-8 Identification of the remaining resolved peaks present in the distillate Fractions.

Distillate Fraction	Identified Compound	Peak Number	K.R.I.	Major Ions (m/z)	Wt/Wt% of Resolved Peaks	Identification
19	Pentylcyclohexane	19.1	1120	55, 83[1], *154*[2]	3.8	L.M.
	Methyl-3-Pentylcyclohexane	19.2	1136	55, 97, *168*	n.d.	L.M.
	2,6-Dimethyldecane	19.3	1151	57, 85 , 113	4.0	L.M.
	4-Methylundecane	19.4	1154	43, 71, 126, *170*	4.0	L.M.
	2-Methylundecane	19.5	1159	43, 155, *170*	10.0	L.M.
	3-Methylundecane	19.6	1166	57, 141, *170*	7.2	L.M.
	Methyl 2-pentylcyclohexane	19.7	1173	55, 97, *168*	4.1	L.M.
	Methyl 3-pentylcyclohexane	19.8	1179	55, 97, *168*	2.4	L.M.
	Methyl 2-pentylcyclohexane	19.9	1183	55, 97, *168*	1.7	L.M.
	2, 6-Dimethylundecane	19.10	1211	43, 57, 141, 169, 18	25.1	L.M.
	Hexylcyclohexane	19.11	1225	55, 83, *168*	11.3	L.M.
	1,2,3,4-Tetrahydro-5-methyl naphthalene	19.12	1231	105, 118, 128, 131, *146*	3.4	L.M.
	6-Methyldodecane	19.13	1248	57, 98, 112, 184	1.6	L.M.
	Methylnaphthalene	19.14	1253	71, 115, *142* , 143	6.3	L.M., Karcher (1983)
	2,6-Dimethylundecane	19.15	1259	43, 57, 141, 169, *184*	3.7	L.M.
	Isoprenoid	19.16	1264	57, 155, *184*	2.9	L.M
	7-Methyltridecane	19.17	1269	57, 71, 113, 112, *198*	3.3	L.M.
	Methyl-hexylcylohexane	19.18	1277	55, 97, *182*	n.d.	L.M
23	Heptylcyclohexane	23.1	1327	55, 83, *182*	n.d.	L.M.
	2,6,10-Trimethyldodecane	23.2	1372	57, 113, 127, 197, *212*	8.3	L.M.
	Methyl-heptylcyclohexane	23.3	1378	55, 97, *196*	2.2	L.M.
	Methyl-heptylcyclohexane	23.4	1385	55, 97, *196*	2.2	L.M.
	Methyl-heptylcyclohexane	23.5	1389	55, 97, *196*	2.0	L.M.
	Octylcyclohexane	23.6	1432	55, 83, *196*	12.2	L.M.
	Methylbiphenyl	23.7	1439	83, 152, 153, 168, *169*	5.1	L.M., Karcher (1983)
	4-Methyltetradecane	23.8	1453	43, 57, 71, 169, *212*	9.1	L.M.
	2,6,10-Trimethytridecane	23.9	1459	57, 155, 183, *212*	28.7	L.M., Philp (1985)
	3-Methyltetradecane	23.10	1465	57, 183, *212*	7.7	L.M.
	Methyl-octylcyclohexane	23.11	1482	55, 97, *210*	n.d.	L.M.

Continued overleaf.....

Continued.....

Distillate Fraction	Identified Compound	Peak Number	K.R.I.	Major Ions (m/z)	Wt/Wt% of Resolved Peaks	Identification
26	Nonylcyclohexane	26.1	1534	55, 83, *210*	12.9	L.M.
	2,6,10-Trimethyltetradecane	26.2	1551	57, 85, 155, 211, *22*	19.2	L.M.
	2-Methylpentadecane	26.3	1558	43, 57, 183, *226*	12.7	L.M.
	3-Methylpentadecane	26.4	1564	57, 197, *226*	8.5	L.M.
	Methyl-nonylcyclohexane	26.5	1592	55, 97, *224*	2.7	L.M.
	Decylcyclohexane	26.6	1638	55, 83, *224*	10.8	L.M.
	8-Hexylpentadecane	26.7	1655	43, 196, 197, 210	1.6	L.M.
27	Decylcyclohexane	27.1	1640	55, 83, *224*	24.8	
	4-Methylhexadecane	27.2	1652	43, 197, *240*	15.7	L.M.
	2-Methylhexadecane	27.3	1658	57, 197, *240*	13.4	L.M., Philp (1985)
	3-Methylhexadecane	27.4	1664	57, 211, *240*	17.6	L.M., Philp (1985)
	2,6,10,14-Tetramethyl-pentadecane (Pristane)	27.5	1701	57, 183, *268*	20.7	L.M., Philp (1985)
	Phenanthrene/Anthracene	27.6	1708	89, 152, 174, *178*	14.0	L.M.
	Phenanthrenol	27.7	1750	82, 139, 163, 165, 193, *194*	2.0	L.M., Karcher (1983)
28	Methyl-decylcyclohexane	28.1	1687	55, 97, *238*	n.d.	
	2,6,10,14-Tetramethyl-pentadecane (Pristane)	28.2	1703	57, 183, *268*	58.9	L.M., Philp (1985)
	Phenathrene/Anthracene	28.5	1706	152, 174, *178*	n.d.	L.M.
	Undecylcyclohexane	28.3	1708	55, 83, *238*	14.9	L.M.
	2,6,10,14-Tetramethyl-hexadcane (Phytane)	28.4	1803	57, 183, 197, *282*	21.4	L.M., Philp (1985)
	Methyl-Anthracene	28.5	1828	165, 176, *192*	n.d.	L.M., Karcher (1983)
29	2-Methylhexadecane	29.1	1655	57, 197, *240*	n.d.	L.M.
	Methyl-undecylcyclohexane	29.2	1686	55, 97, *238*	n.d.	
	2,6,10,14-Tetramethyl-pentadecane (Pristane)	29.3	1702	57, 183, *268*	11.6	L.M., Philp (1985)
	Phenathrene/Anthracene	29.4	1706	152, 174, *178*	n.d.	L.M., Karcher (1983)
	Undecylcyclohexane	29.5	1742	55, 83, *238*	n.d.	L.M.
	2-Methylheptadecane	29.6	1755	43, 211, 254	3.9	L.M.
	3-Methylheptadecane	29.7	1763	57, 225, 254	2.5	L.M.
	Methyl-undecylcyclohexane	29.8	1793	55, 97, *252*	9.3	
	2,6,10,14-Tetramethyl-hexadcane (Phytane)	29.9	1803	57, 183, 197, *282*	47.3	L.M., Philp (1985)
	Methylphenathrene	29.10	1830	165, 188, *192*	6.9	L.M., Karcher (1983)
	Dodecylcyclohexane	29.11	1847	55, 83, *252*	10.3	L.M., Philp (1985)

Continued overleaf.....

Continued.....

Distillate Fraction	Identified Compound	Peak Number	K.R.I	Major Ions (m/z)	Wt/Wt% of Resolved Peaks	Identification
30	2,6,10,14-Tetramethyl-hexadecane (Phytane)	30.1	1802	57, 183, 197, *282*	4.5	L.M., Philp (1985)
	Dodecylcyclohexane	30.2	1846	55, 83, *252*	11.2	L.M., Philp (1985)
	4-Methyloctadecane	30.3	1857	57, 225, *254*	13.2	Philp (1985)
	3-Methyloctadecane	30.4	1864	57, 239, *254*	9.9	L.M.
	Methyl-dodecylcyclohexane	30.5	1896	55, 97, *266*	11.0	L.M.
	Tridecylcyclohexane	30.6	1950	55, 83, *266*	14.4	L.M.
	2-Methylnonadecane	30.7	1956	43, 239, *282*	6.5	L.M., Philp (1985)
	3-Methylnonadecane	30.8	1963	57, 254, *282*	5.2	L.M.

[1]**Base Peak**

[2]*Molecular Ion*

n.d. = Not determinable

L.M. = Comparison with library spectrum

K.R.I. = Linear Retention Indicies

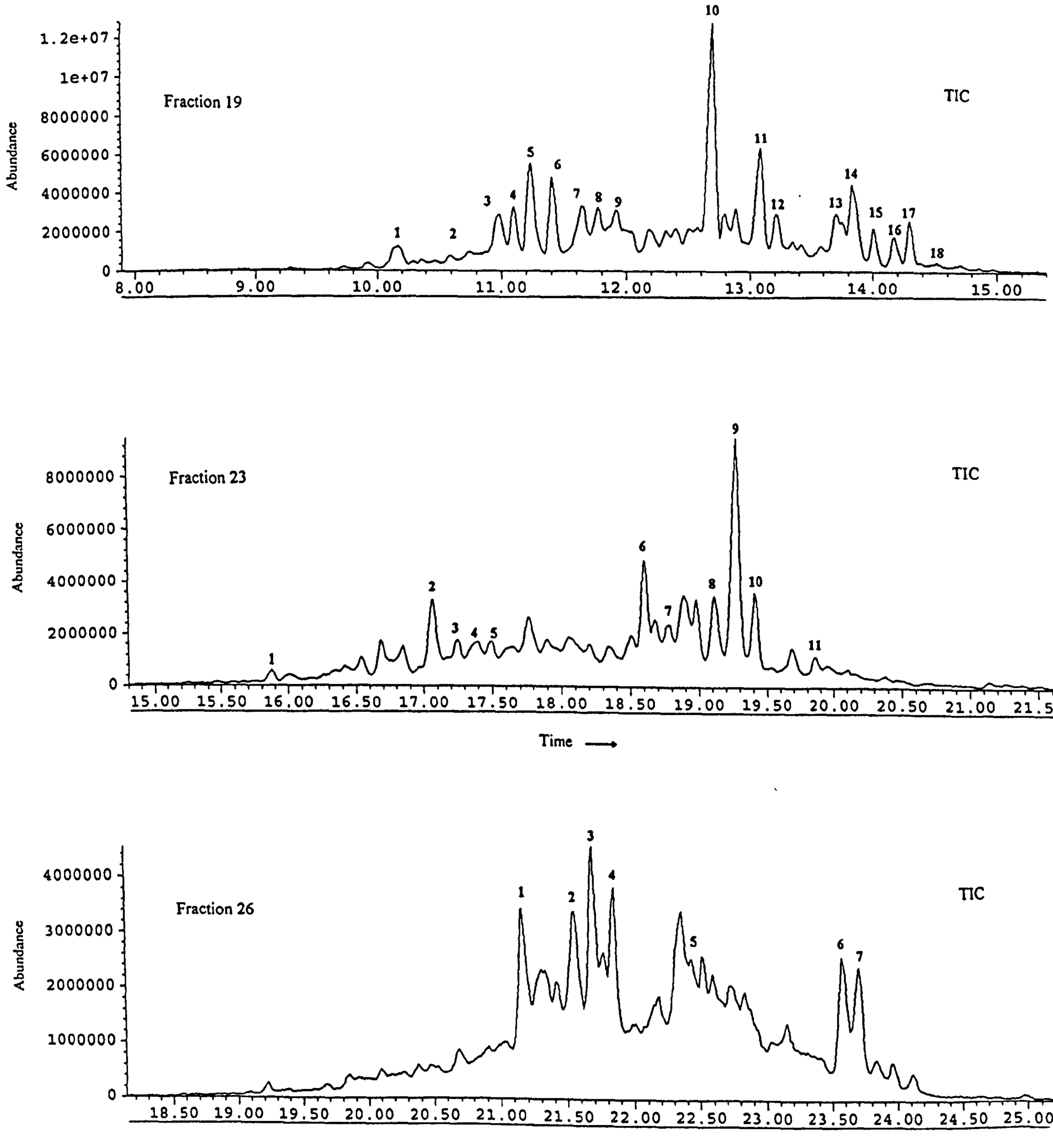

Continued overleaf.....

Figure 2-12 Total ion chromatograms of the non-clathrated distillate fractions.

Continued .....

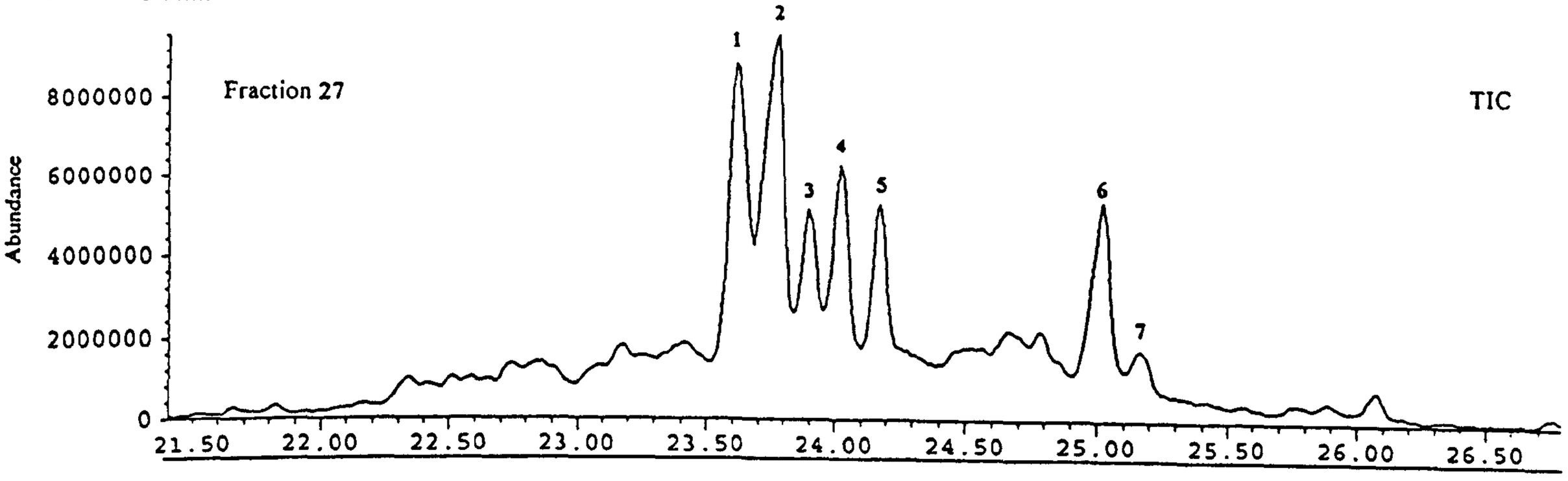
Fraction 27
TIC
Abundance
8000000
6000000
4000000
2000000
0
1
2
3
4
5
6
7
21.50
22.00
22.50
23.00
23.50
24.00
24.50
25.00
25.50
26.00
26.50

Fraction 28
TIC
Abundance
1e+07
8000000
6000000
4000000
2000000
0
1
2
3
4
5
23.00
23.50
24.00
24.50
25.00
25.50
26.00
26.50
27.00
27.50
28.00
28.50
29.00
29.50
Time

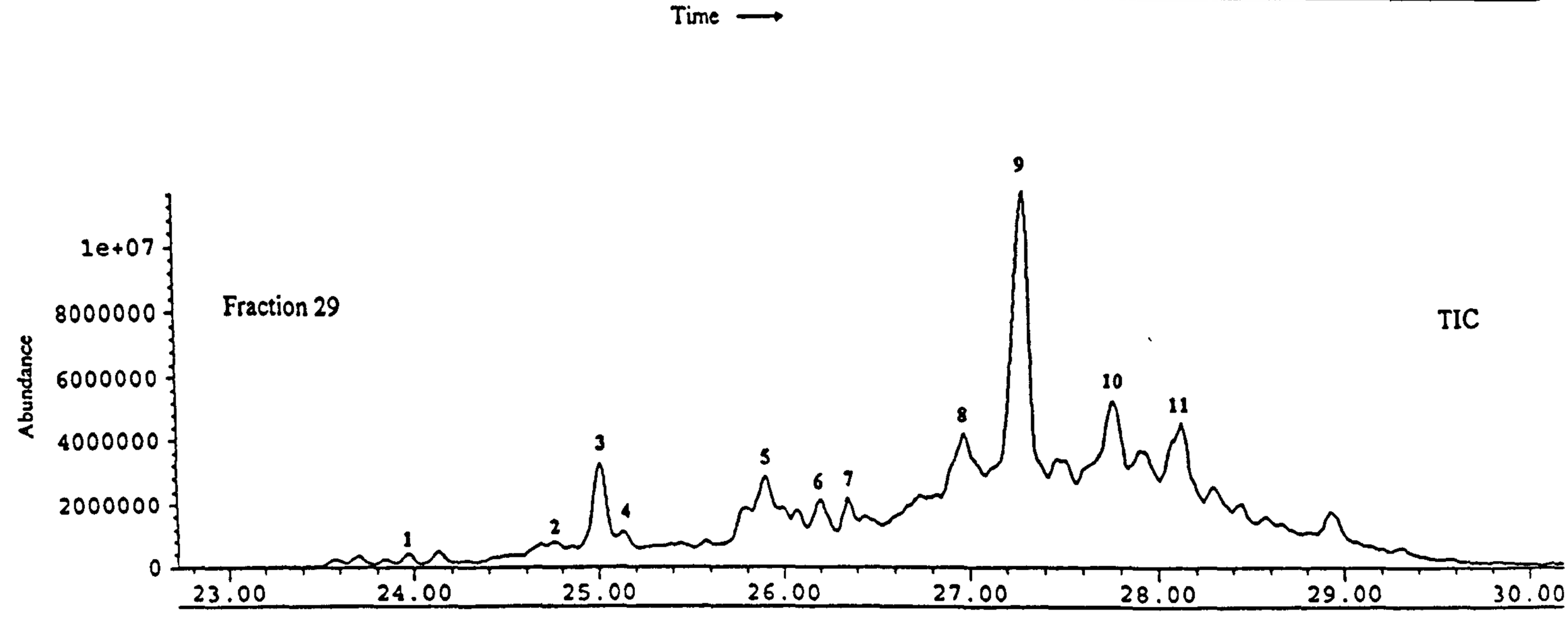
Fraction 29
TIC
Abundance
1e+07
8000000
6000000
4000000
2000000
0
1
2
3
4
5
6
7
8
9
10
11
23.00
24.00
25.00
26.00
27.00
28.00
29.00
30.00

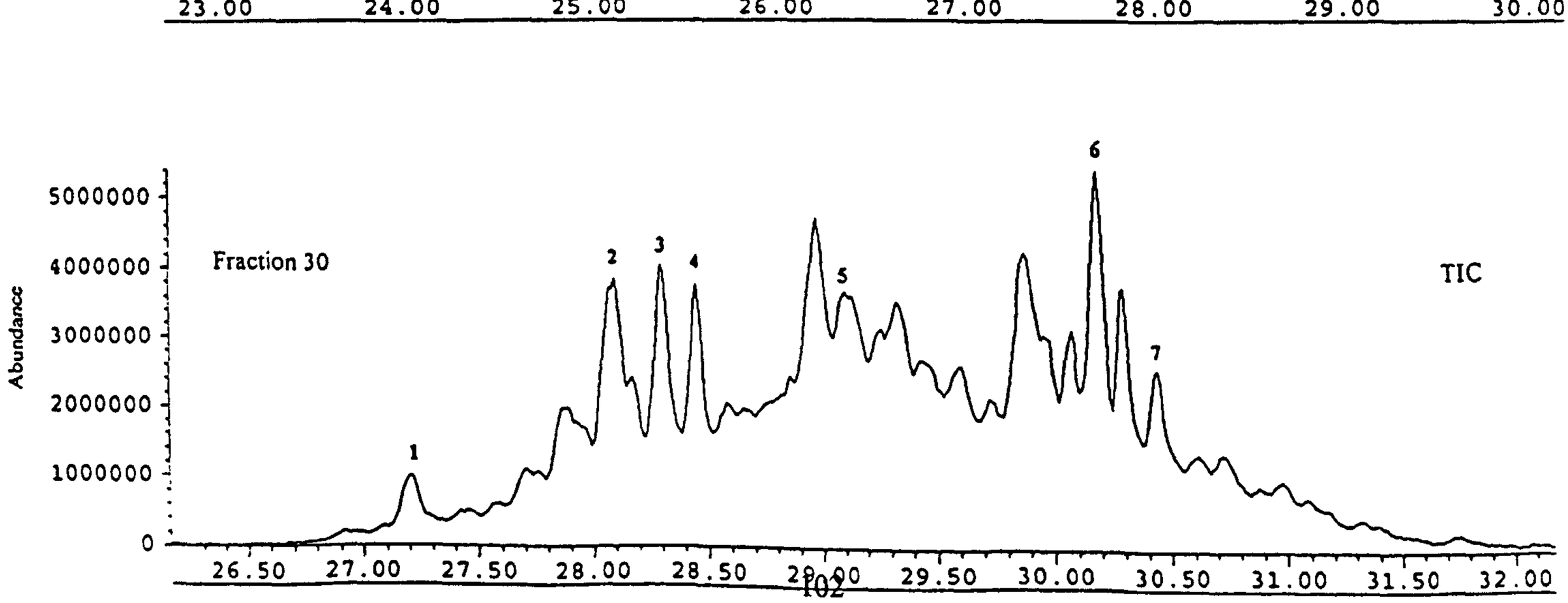
Fraction 30
TIC
Abundance
5000000
4000000
3000000
2000000
1000000
0
1
2
3
4
5
6
7
26.50
27.00
27.50
28.00
28.50
29.00
29.50
30.00
30.50
31.00
31.50
32.00

mono methyl branched alkanes 4-methyl- (19.4, K.R.I 1154, 4%), 2-methyl- (19.5, K.R.I 1159, 10%), and 3-methylundecane (19.6, K.R.I. 1167, 7.2%) were also identified, with the elution order matching that reported by **Kissin (1990)**. In Fraction 23, the isoprenoid 2,6,10-trimethyldodecane (23.9, K.R.I 1459, 28.7%) was the single most abundant component and in Fractions 26 the major resolved component was assigned as 2,6,10-trimethyltetradecane (26.2, K.R.I 1551, 19.2%). A compound eluting at K.R.I 1655 was tentatively identified as the "T" branched 8-hexylpentadecane (Figure 2-14) the identification of which perhaps confirms the importance of such structures deduced from the oxidation studies of synthetic and UCM "T" branched compounds by **Gough and Rowland (1991)**. The resolved compounds in both Fractions 28 and 29 were dominated by the two isoprenoids, pristane (K.R.I 1701) and phytane (K.R.I 1803), which accounted for over 50% of the total resolved compounds in each fraction.

Both *n*-alkylcyclohexanes and *n*-alkylmethylcyclohexanes were also present in the distillate fractions and were identified by comparing their individual spectra with published spectra (**Fowler *et al.*, 1986**; **Hoffmann *et al.*, 1987**; **Yangming and Zhongyi, 1991**). The *n*-alkylcyclohexanes produce a characteristic base peak of *m/z* 83, due to the cyclohexyl ion resulting from loss of the alkyl chain (Figure 2-15 a). The methyl-*n*-alkylcyclohexanes have the corresponding diagnostic base peak ion, *m/z* 97 (Figure 2-15 b), resulting from the removal of the alkyl chain to leave the methylcyclohexyl ion. In Fractions 19 and 23, four and three *n*-alkylmethylcyclohexanes respectively of a possible six isomers (*cis*- and *trans*- 2-, 3-,and 4-methyl-*n*-alkylcyclohexanes), are observed. However, the position of the methyl group could not be established positively from the spectra.

Aromatic compounds were also identified in several of the distillate fractions. These included methylnaphthalene (K.R.I. 1253) identified in Fraction 19 and a methylbiphenyl (K.R.I. 1439) in Fraction 23. The spectrum of each compound gave a good match to a library spectrum and to literature data (**Karcher, 1983**). In Fraction 27 both phenanthrene/anthracene (K.R.I 1708) and phenanthrene-9-one were present. Phenanthrene (or possibly anthracene) was identified in Fraction 28 (K.R.I. 1703) and

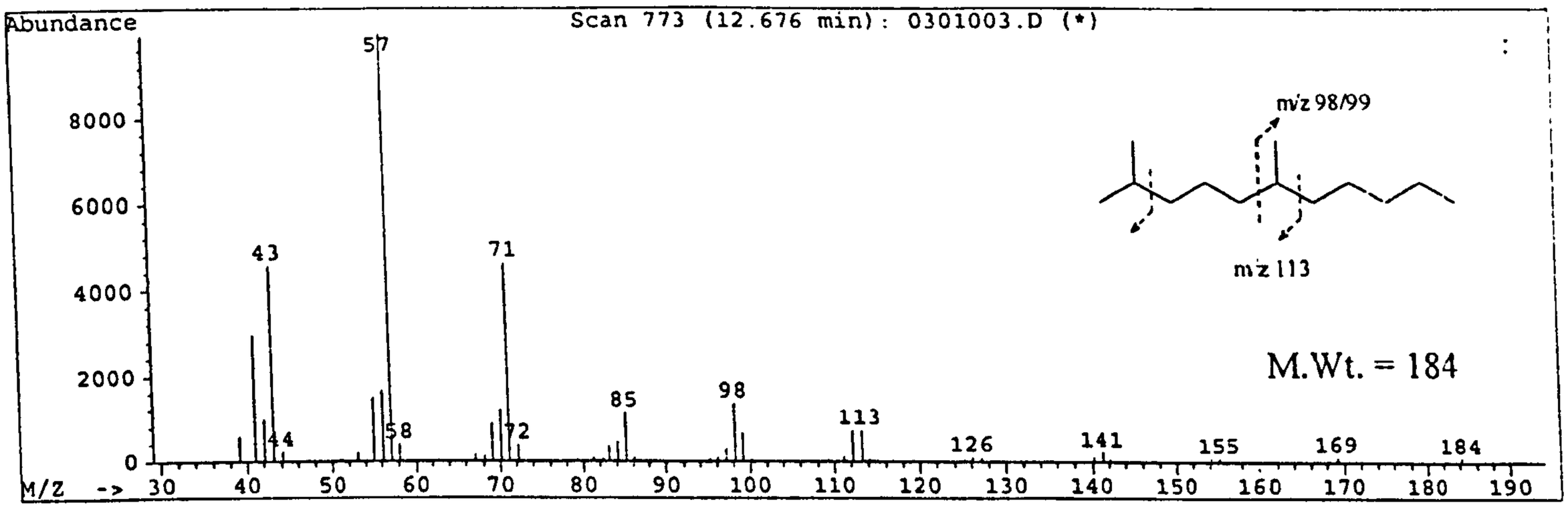

Figure 2-13 Mass spectrum of 2,6-dimethyldecane.

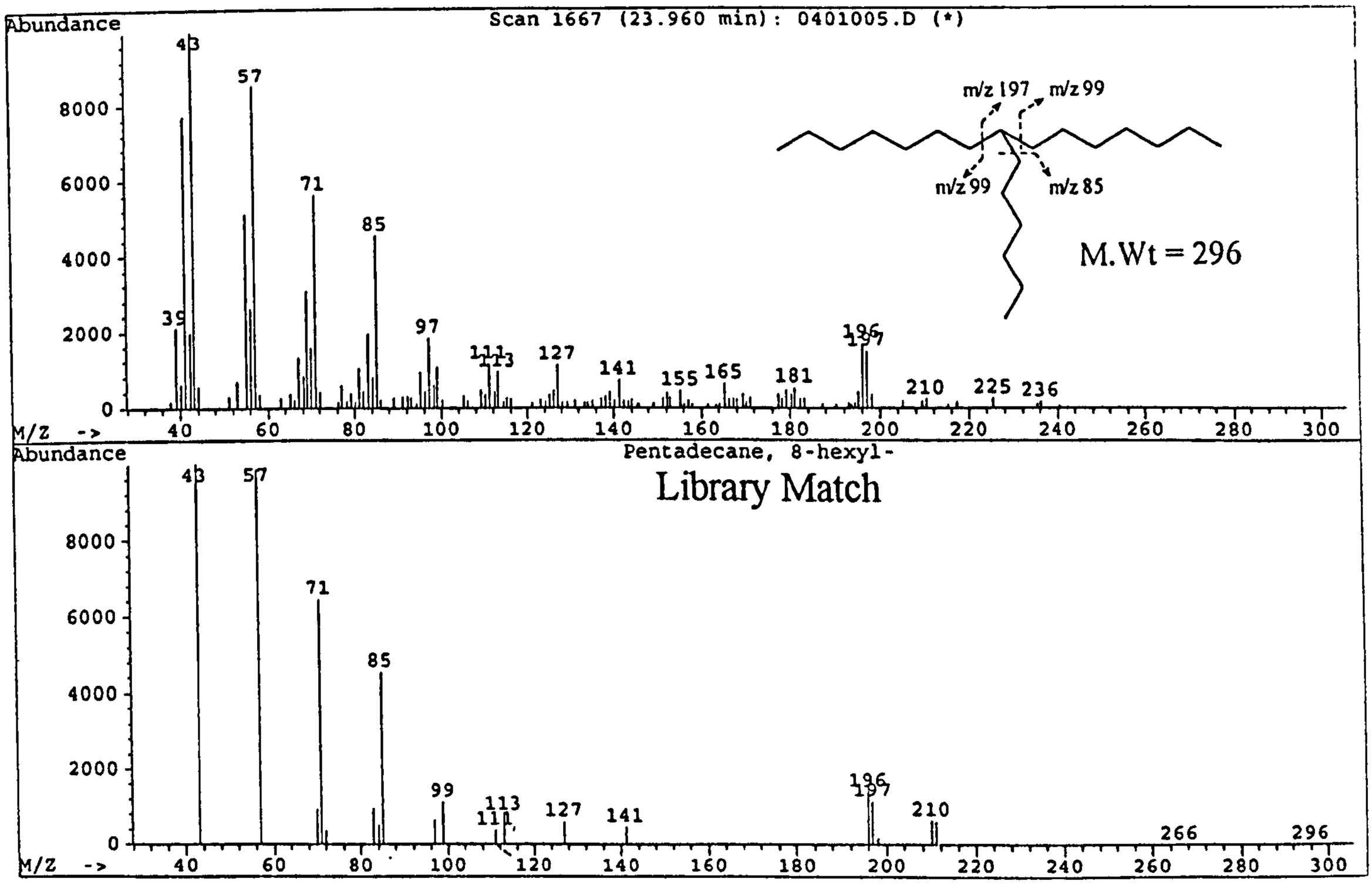

Figure 2-14 Identification of a possible "T" branched compound (8-hexylpentadecane).

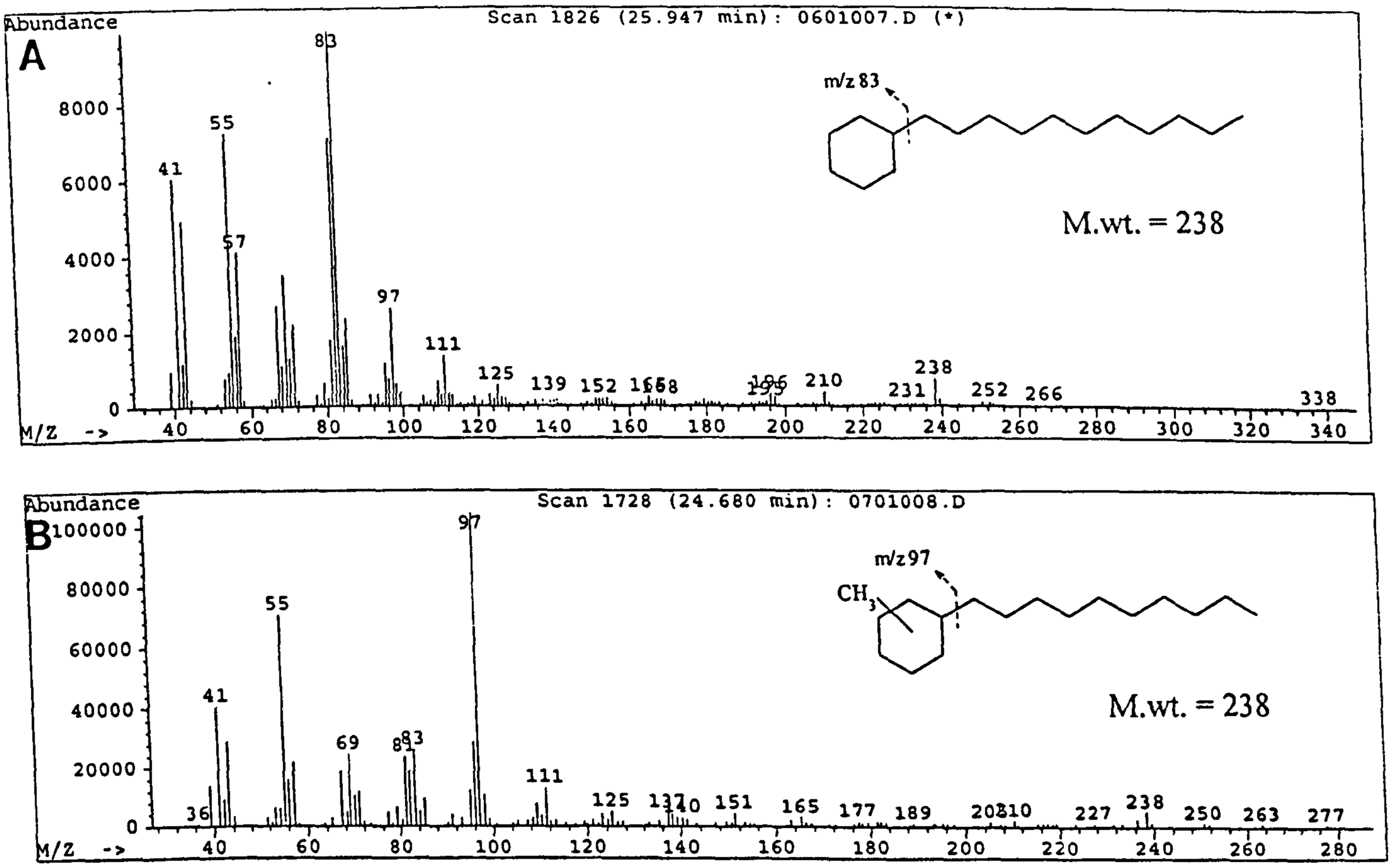

Figure 2-15 Mass spectra of A) undecylcyclohexane, B) Methyl-decylcyclohexane, and C) methyl-decylcyclohexane reported by **Fowler (1985)**.

in Fraction 29 a methyl substituted phenanthrene (K.R.I. 1830) was detected, although the position of the methyl group again could not be assigned positively.

2.3.5 Oxidation the UCMs in the distillate fractions

After clathration the remaining UCMs were oxidised with $Cr(VI)O_3$/acetic acid and the DCM extractable products refluxed with BF_3/MeOH to form methyl esters of carboxylic acid functionalities (see Experimental). The amounts of total recovered products are given in Table 2-9. The percentage recoveries varied between fractions, Fraction 27 producing the lowest yield (55%) and the residue giving the highest (83%), with an average percentage recovery of 73%. This compares with values obtained by **Gough (1989)** (44% to 84%), **Revill (1992)** (83%) and **Killops and Al-Juboori (1990)** (33%) for their oil UCMs. Chromatograms of the total oxidised fractions are shown in Figure 2-16.

In a refinement of the previous oxidative studies of UCMs (**Gough, 1989; Killops and Al-Juboori, 1990; Revill, 1992**), which determined only the DCM soluble oxidation products of UCMs, the present study incorporated a semi mass balance of the oxidation products by additionally measuring the amount of CO_2 liberated during oxidation (see Experimental) using a method developed by **Standen (1992)** and later modified by **Thomas (1994).** The results are given in Table 2-10 and show values ranging between 5% (total condensate) and 12% (Fraction 27) of CO_2 liberated when corrected for both blank and CO_2 trapping efficiency (73%). Thus between 65% and 94% of the oxidation products were accounted for as CO_2 plus DCM soluble products. The remaining products are assumed to be water soluble acids ($<C_6$) which could not be detected because of the excess acetic acid used as a reactant. The amount of resolved compounds had also increased after oxidation. The percentages of resolved compounds in the distillate fractions after oxidation were 27% to 81% (Table 2-11) compared with 3% to 44% (Table 2-6) before oxidation. Fraction 19, however showed a smaller percentage of resolved compounds after oxidation (27%) than before (30%). This is thought to be because the loss of volatile compounds would be greater in Fraction 19, which was the lowest boiling fraction.

Column chromatography (see Experimental) of the total recoverable products (Table

Table 2-9 Total amount of recovered products from the oxidation of the whole condensate, distillate fractions and the residue by CrO_3/AcOH.

Distillation Fraction	Original Amount (mg)	Recovered Products (mg)	Recovery %	CO_2 %	Total Recovery %
19	22.6	13.2	58	7	65
23	9.7	8.0	82	10	92
26	46.3	36.3	78	6	84
27	50.7	28.1	55	12	67
28	29.7	23.5	79	10	89
29	44.8	34.0	75	7	82
30	36.6	25.6	70	7	77
Residue	35.6	29.4	83	11	94
Total Condensate	19.8	15.3	77	5	82

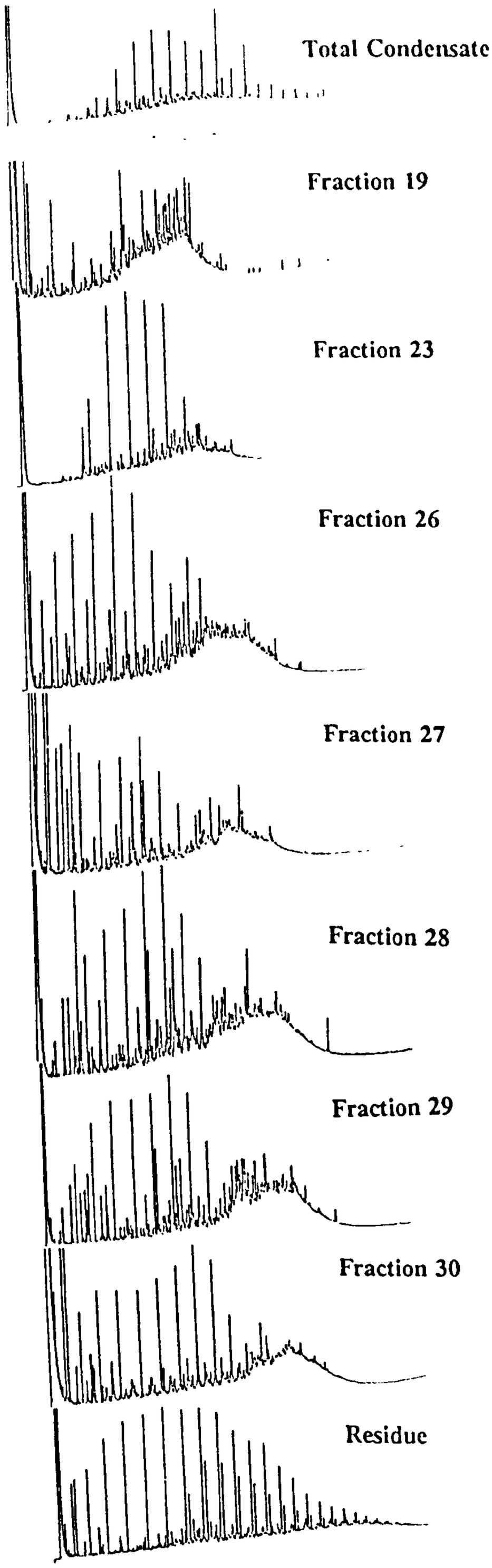

Figure 2-16 Gas chromatograms of the total products after oxidation.

GC: J&W DB5 PROG: 40-300°C at 5°C/min, 300°C (HOLD), H_2 Carrier, FID.

Table 2-10 Percentage of fractions converted to CO_2 during oxidation.

Distillation Fraction	Original Amount (mg)	Titrations (cm^3)		CO_2 (mg)	Efficiency[1] Corrected (mg)	Blank Corrected (mg)	CO_2 %
		Phenolphthalein	Methyl Orange				
19	22.6	24.5	25.6	2.4	3.3	1.5	7
23	9.7	24.8	25.7	2.0	2.7	0.9	10
26	46.3	23.9	25.5	3.5	4.8	3.0	6
27	50.7	23.4	26.0	5.7	7.7	6.0	12
28	29.7	23.8	25.4	3.5	4.8	3.0	10
29	44.8	24.0	25.7	3.7	5.1	3.3	7
30	36.6	24.1	25.6	3.3	4.5	2.7	7
Residue	35.6	23.5	25.4	4.2	5.7	3.9	11
Total Condensate	19.8	24.7	25.6	2.0	2.7	0.9	5
Blank	0	24.6	25.2	1.3	1.8	/	/

1 = Method efficiency 73% (see experimental).

Table 2-11 Percentage of UCM in the products after oxidation.

Distillation Fraction	Retention Indices (RI)	Total Oxidised Products			
		Resolved Peaks		UCM	
		Area	%	Area	%
19	1090-1950	293043	27	796367	73
23	1300-2150	2071469	59	1393821	41
26	1290-2380	4278478	31	9361322	69
27	1250-2410	1691630	39	2693440	61
28	1250-2610	3058674	38	7.8E+07	62
29	1300-2650	3950136	29	9654364	71
30	1245-2710	1640544	62	984436	38
Residue	1350-3500	455657	81	106883	19
Total Condensate	1300-3500	736069	33	2133281	77

2-12) showed that on average 7% of the total condensate eluted with hexane and was therefore attributed to non-oxidised UCM hydrocarbons. Only Fractions 19 (15%), 27 (6%), 29 (7%), and the residue (10%) produced weighable quantities of oxidation products eluting with DCM. The majority of material was only eluted from the column by methanol (average 67%) Fraction 29 gave the highest value of products in the DCM/MeOH fraction (95%). The average overall recovery of the combined DCM and MeOH fractions was 77%.

The chromatograms showed that quite large proportions (27% to 81%) of resolved compounds were formed by oxidation (Figure 2-17). By oxidising the small distillate UCM sub-fractions for the first time it becomes obvious that there is both an increase in retention range of the original distillate UCMs after oxidation as well as a decrease for some products (*i.e.* earlier and later eluting products are formed). For example the initial UCM in Fraction 30 (Figure 2-17 A) originally eluted (GC) over 4 minutes whereas, after oxidation the elution time of the oxidised fraction had increased to 24 minutes (under the same GC conditions).

Differences between the DCM fraction and the methanol fractions can also be seen (Figures 2-17 B2 and B3). The majority of the oxidised UCM components with the increased retention times are found in the methanol fraction which is also the fraction that contained the highest proportion of products (>60%). This suggests that the majority of the UCM has undergone considerable oxidation with several functionalities being introduced into the molecules, resulting in increased polarity and later GC retention times.

2.3.6 Analysis of the oxidation products by GC-MS

After oxidation (see Experimental) the most obvious class of resolved components identified in the oxidation products of the distillate UCMs was a homologous series of methyl esters of straight chain mono carboxylic acids (the methyl ester being formed via the methylation of a carboxylic group using BF_3/MeOH derivatising agent, Figure 2-18). These were identified via the *m/z* 74 fragment ion which is formed by a characteristic mass spectral cleavage called the **McLafferty Rearrangement (McLafferty and Tureček, 1993)**. In this rearrangement, a hydrogen atom is

Table 2-12 Column chromatography of the total products after oxidation.

Distillation Fraction	Total Products mg	Hexane mg	Hexane %	DCM mg	DCM %	Methanol mg	Methanol %	Total (mg)	Recovered %
19	8.6	0.4	5	1.3	15	5.1	59	6.8	79
23	3.3	n/d	n/d	n/d	n/d	2.4	73	2.4	73
26	16.8	0.7	4	n/d	n/d	11.9	71	12.6	75
27	8.8	0.4	5	0.5	6	5.5	63	6.4	73
28	8.4	0.2	2	n/d	n/d	5.8	69	6.0	72
29	17.8	0.8	5	1.2	7	15.7	88	17.7	99
30	10	1.5	15	n/d	n/d	6.5	65	8.0	80
Residue	9.4	1.1	12	0.9	10	5.6	60	7.6	81
Total Condensate	7.9	0.6	8	n/d	n/d	4.5	57	5.1	65

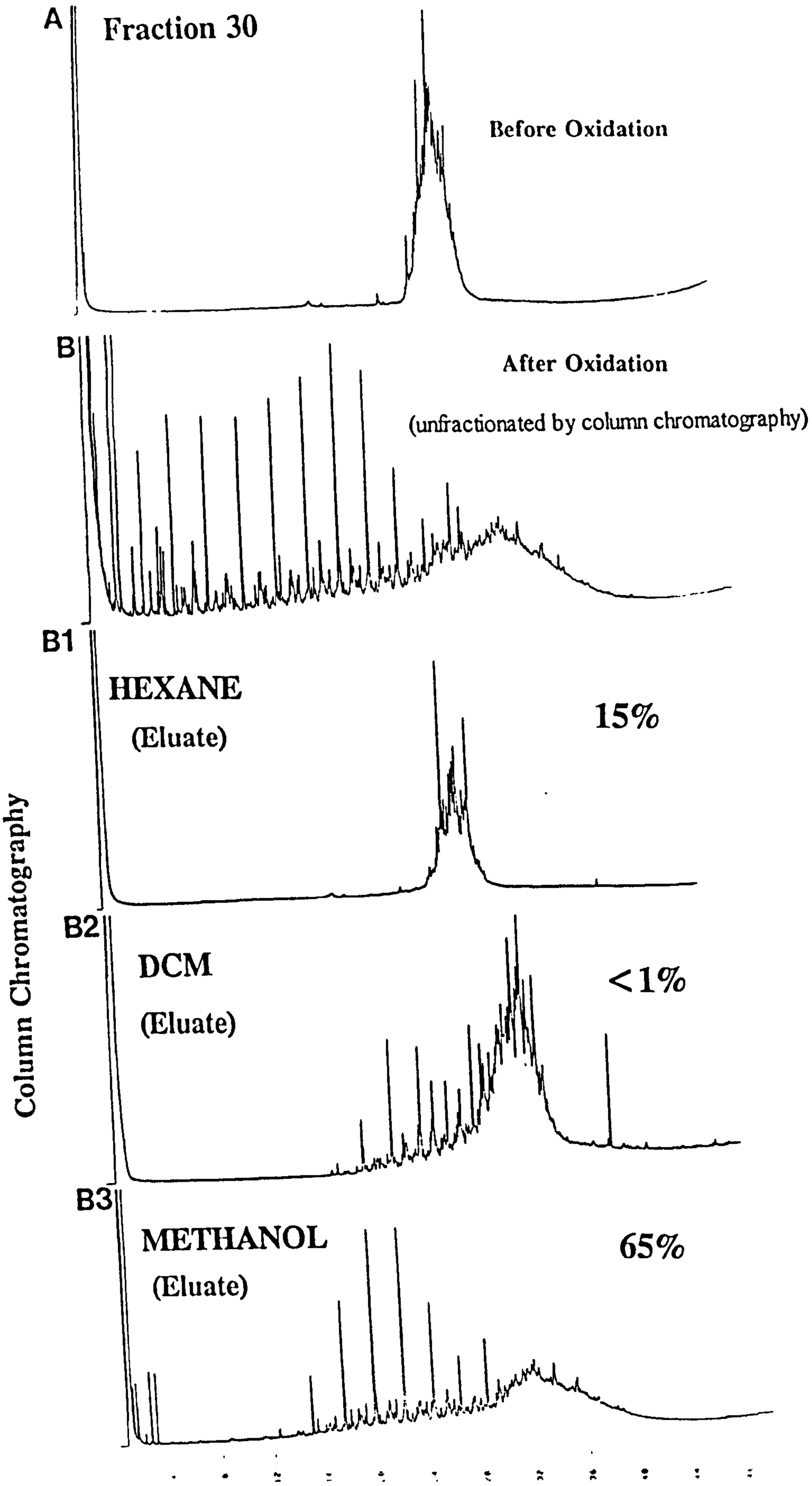

Figure 2-17 Gas chromatograms of A) an un-oxidised distillate (Fraction 30), B) the total products after oxidation, B1) the hexane eluate collected after column chromatography, B2) DCM eluate and B3) Methanol eluate.

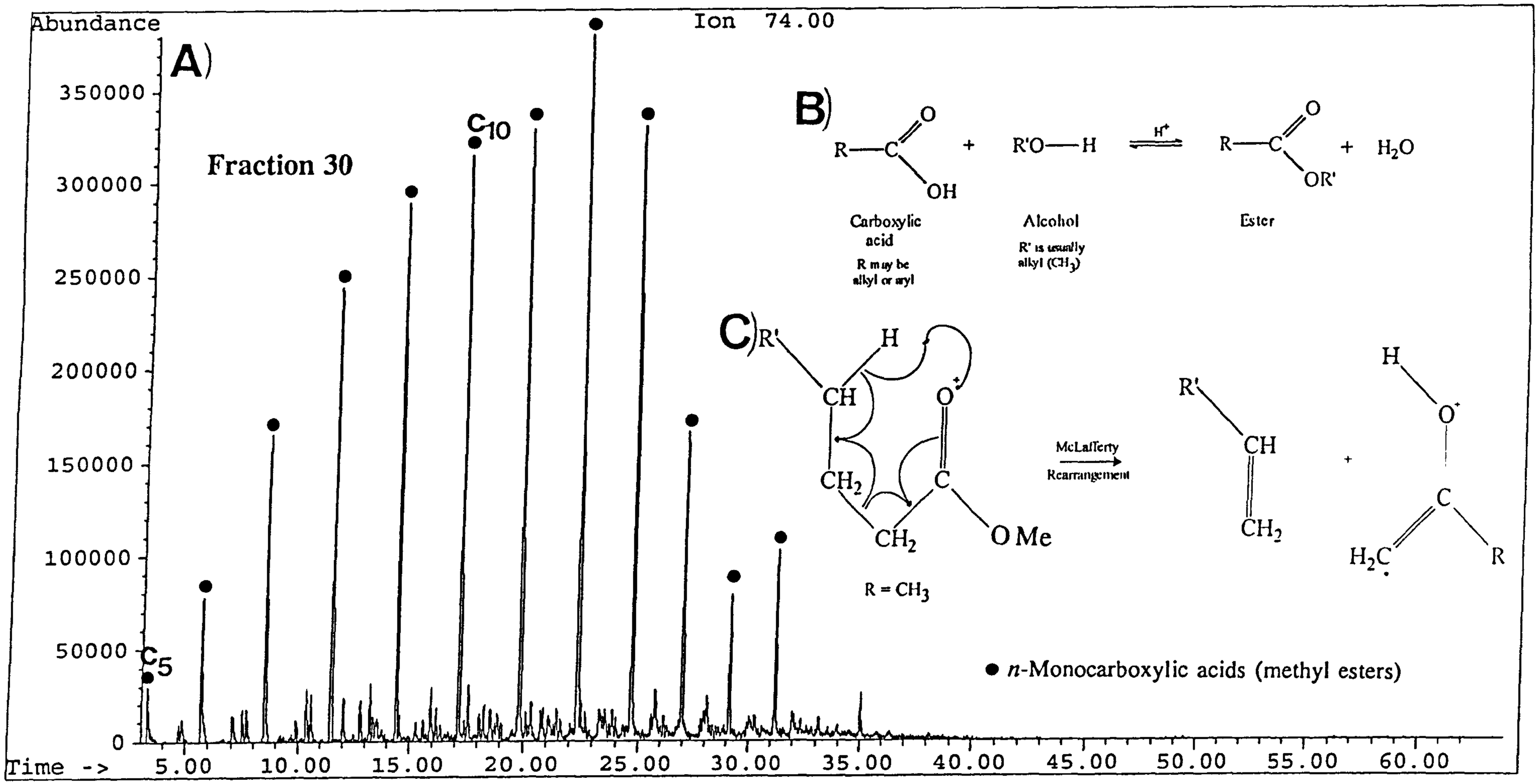

Figure 2-18 A) GC-MS fragmentogram (m/z 74) showing the distribution of *n*-acids in the total oxidation products of distillate Fraction 30, B) the derivatisation of the carboxylic acid to a methyl ester, and C) the McLafferty rearrangement.

transferred from the γ carbon to the carbonyl-group oxygen, the bond between the alpha and beta carbons is broken and a neutral alkene fragment is produced. The charge remains with the oxygen-containing fragment (Figure 2-18 C). The mass spectra of the *n*-monocarboxylic acids (Figure 2-19 A, B, and C) matched closely those of the library (quality > 90%) and published spectra (*e.g.* **Eglinton and Murphy, 1969**).

The distribution of the *n*-monocarboxylic acids and the percentage of the total resolved compounds they represented are shown in Table 2-13 and Figure 2-20. In the whole condensate the *n*-acids accounted for 24% of the total resolved products compared with 40% observed by **Killops and Al-Juboori (1989)** for a biodegraded crude oil. The amount of *n*-acids observed in the distillate UCMs varied. Fractions 23 and 26 produced the highest amount of *n*-acids (44% and 48%) and Fraction 19 the lowest 19%. Overall the average amount of *n*-acids in the resolved products was 30%. The carbon number distribution of *n*-acids in the whole gas condensate was from $C_{5\text{-}26}$ with an average of C_{12}. The maximum carbon number of the *n*-acids identified from the oxidation products of the distillate cuts increased with increasing boiling point from Fraction 19, the lightest, to the residue, by *ca.* 12 carbons yet the average chain length only increased by four carbons (C_8 to C_{12}).

Straight chain *n*-monocarboxylic acids may be formed during oxidation in several ways; by the terminal oxidation of *n*-alkanes; by oxidation at branched positions on branched acyclic structures, or the oxidation of n-alkylcyclic compounds. The formation of the *n*-monocarboxylic acids from the oxidation of *n*-alkanes in this study is unlikely since *n*-alkanes were removed by extensive molecular sieving and urea adduction and a small amount of residual alkane would not account for the quantity of *n*-monocarboxylic acids produced. The more likely precursors to the *n*-monocarboxylic acids are simply branched and alkyl-cyclic compounds. Such compounds readily oxidise at tertiary carbons branch points by a known mechanism **(Gough, 1989)**. This is summarised in Figure 2-21.

Distillate Fraction 23 (K.R.I. 1361-1509) included those compounds which eluted (GC) between *n*-C_{14} and *n*-C_{15}. Of the few resolved compounds identified by GC-MS

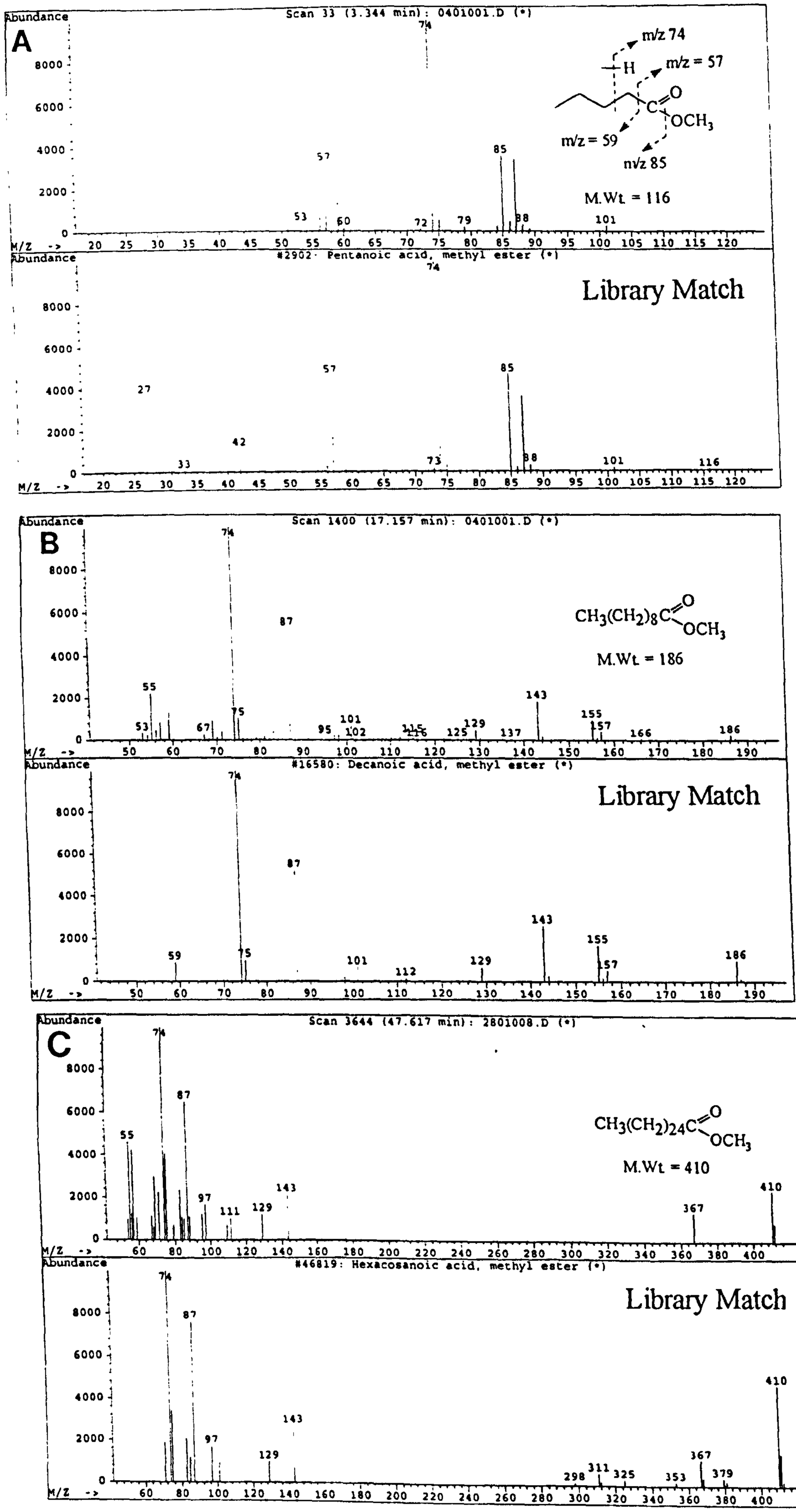

Figure 2-19 Mass spectra and library spectra of A) Pentanoic acid methylester, B) Decanoic acid methylester and C) Hexacosanoic acid methylester.

Table 2-13 The distribution and amount of *n*-acids in the total resolved oxidation products.

Distillate Fraction	*n* -Acids		
	% Total	Range	Maximum
19	19	C_5-C_{12}	9
23	44	C_5-C_{13}	8
26	48	C_5-C_{14}	9
27	26	C_5-C_{15}	10
28	21	C_5-C_{17}	11
29	29	C_5-C_{17}	11
30	36	C_5-C_{19}	12
Residue	27	C_5-C_{28}	12
Total	24	C_9-C_{28}	12

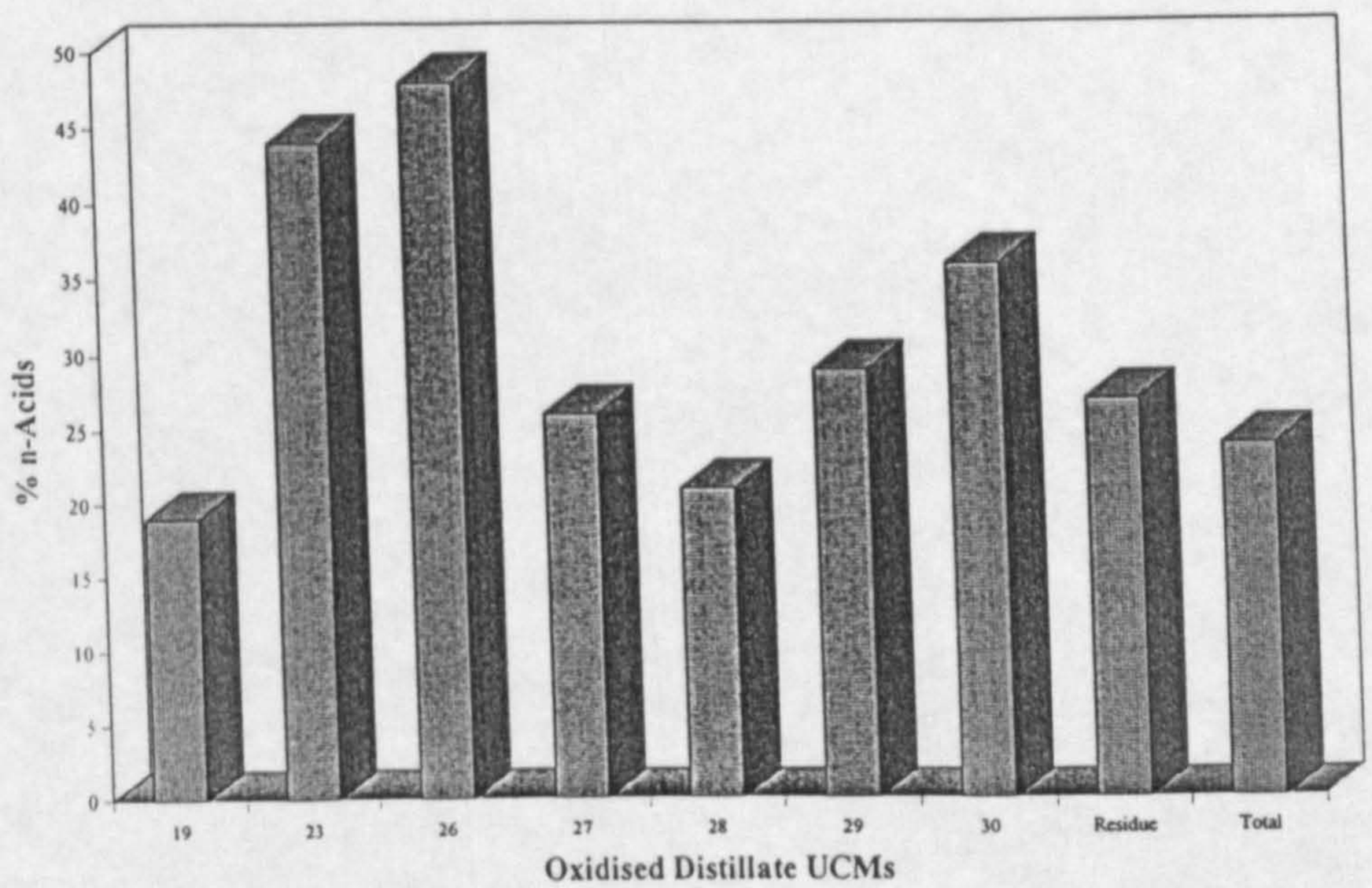

Figure 2-20 Histogram showing the amount of *n*-acids formed during oxidation of the UCMs.

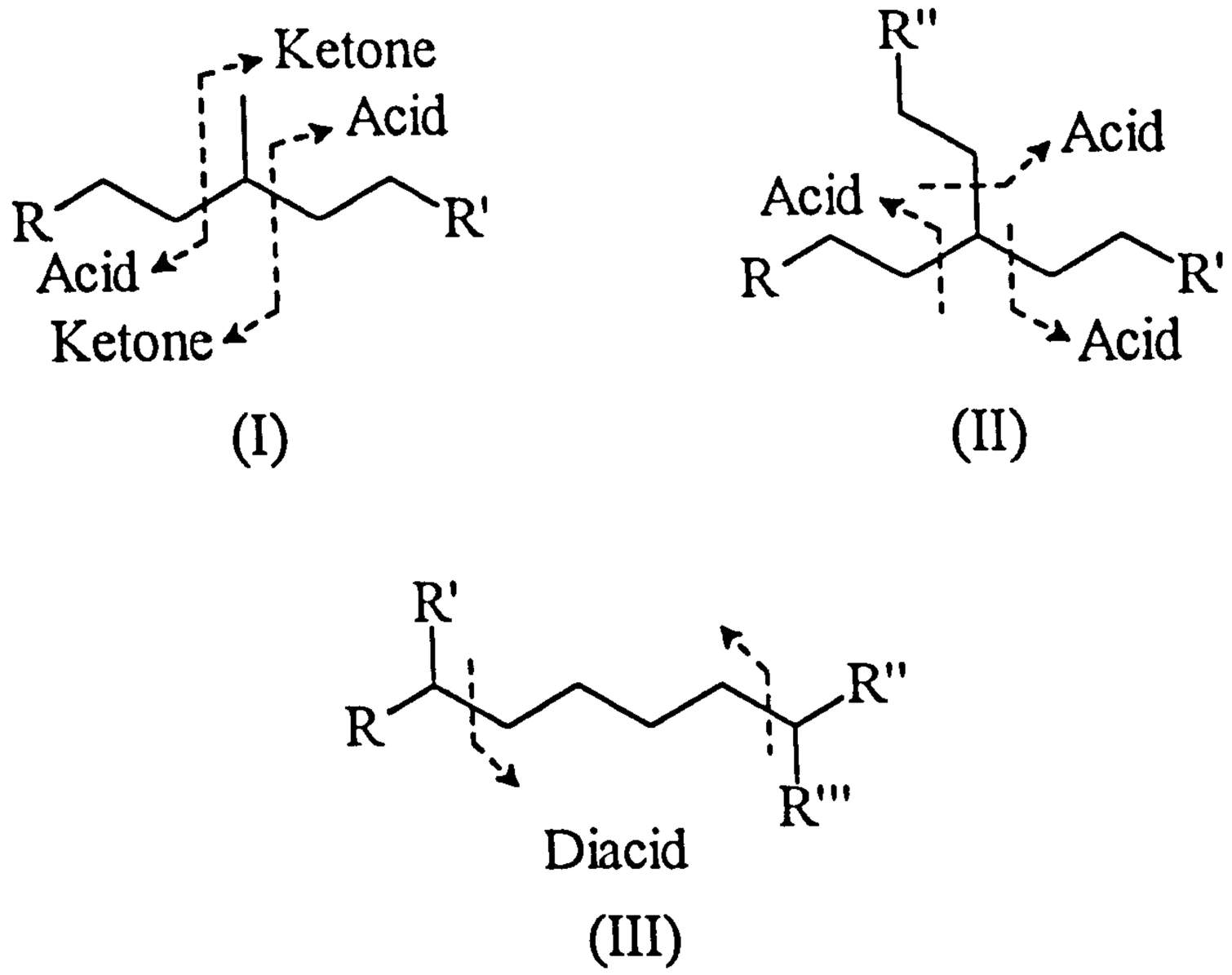

Figure 2-21 The formation of *n*-acids from simple branched structures.

before oxidation the major components were 4-methyl (K.R.I. 1453) and 3-methyltetradecane (K.R.I 1465), and a dominant isoprenoid compound (K.R.I. 1459). After oxidation of this fraction *n*-monocarboxylic acids ranged from C_5 to C_{13}, although C_{13} was found in only trace amounts and there was a sharp concentration cut off after C_{12}. The 4-methyl C_{14} and 3-methyl C_{14} hydrocarbons would be expected to oxidise to C_{10} and C_{11} *n*-monocarboxylic acids respectively. The C_{12} acid could be derived from oxidation of 2-methyltetradecane. This compound was not observed in the resolved components of the UCM but related compounds were identified in Fraction 19 (2-methylundecane, K.R.I. 1159) and Fraction 26 (2-methylpentadecane; K.R.I. 1558). It may be assumed that 2-methyltetradecane was removed by urea adduction or was present within the UCM but was probably masked by other compounds. The most abundant *n*-monocarboxylic acids produced in Fraction 23 were octanoic acid and nonanoic acid, which suggests an average *n*-alkyl chain length of 8 and 9 carbons. Obvious precursors for these compounds would be 6-methyl and 5-methyltetradecanes respectively. These were not identified as resolved components but again may have been present in the UCM. 7-methyl and 6-methylpentadecanes would produce the equivalent *n*-monocarboxylic acids, though it is unlikely that these compounds would elute within Fraction 23. If the 6-methyl and 5-methyl branched alkanes were present in Fraction 23, the concentration of these compounds would be expected to be greater than that of the other similar components i.e. in a concentration greater than the 4-methyl and 3-methyl C_{14} compounds in order to produce an overall greater amount of the C_8 and C_9 *n*-acid.

The amount of resolved compounds present before oxidation containing mono methyl branched structures could account for some, but not all, of the *n*-acids observed in the distillate fractions. For example, in Fraction 30 simple mono methyl branched alkanes accounted for less than 2% of the unoxidised UCM yet after oxidation 22% of the UCM was identified as *n*-acids. The difference must have come from oxidation of alkyl chains on compounds present in the UCM.

The precursor compounds for these large *n*-acids present in Fraction 30 must have boiling points between 320°C and 344°C and elute between KRI 1800 to 2010, though

carry over of compounds, particularly aromatic compounds into different boiling fractions can occur **(Rønningsen and Skjevrak, 1990)**.

Since the modal *n*-carboxylic acid carbon chain length is between C_{12} and C_{13}, likely precursors for the longer chain acids are *n*-alkylbenzenes. Oxidation of such compounds to form toluic acid and an *n*-acid has also been shown by **Gough (1990)** and **Revill (1992)**. The amount of mono-aromatics in the condensate was unfortunately not determined and whether these compounds could account for the amount of $C_{12\text{-}13}$ *n*-acids observed is uncertain. The same reasoning can also be applied to the other fractions and the total condensate UCM.

Another possible source of these straight chain *n*-acids is oxidation of "T" branched mono-alkyl branched acyclic (R = alkyl) or mono-cyclic compounds (R = cyclohexane) shown in Figure 2-22 (II) **(Gough, 1989)**. These types of structures could conceivably occur within the UCM and in the case of an acyclic "T" branched compound oxidation around the branch position would result in the formation of three possible *n*-monocarboxylic acids. A compound tentatively identified as 8-hexylpentadecane (*viz*: a "T" branched compound) was observed in the unoxidised hump of Fraction 26 (Figure 2-13).

In several of the distillate samples C_{16} and C_{18} *n*-monocarboxylic acids occurred in high abundance. These acids would not be expected products of oxidation, certainly in the case of the lighter fractions eg Fraction 19. Even though these compounds were not detected in the procedural blank, their likely origin is thought to be contamination **(Middleditch, 1989)**.

The formation of *n*-dioic acids by oxidation has also been reported by **Gough (1989)**; **Killops and Al-Juboori (1990)** and **Revill (1992)**. In the present study *n*-diacids were only found in small amounts in the oxidised distillates, with the exception of the residue where they were much more abundant (Figure 2-23). The mass spectrum of a compound eluting at K.R.I 1588 (Figure 2-23 X) produced characteristic fragment ions of (*m/z* 74, 97, 111, 129, 138, 171) and matched the library spectrum of,

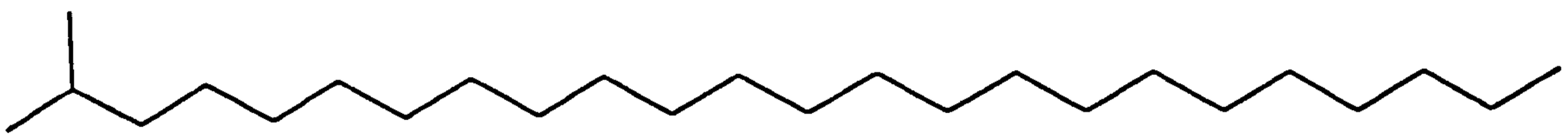

2-methyltetracosane

(I)

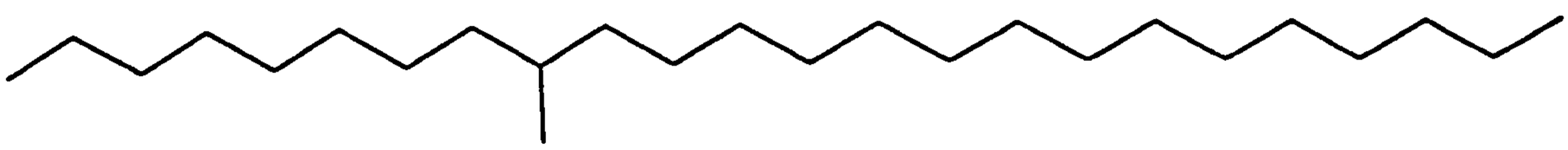

9-methyltetracosane

(II)

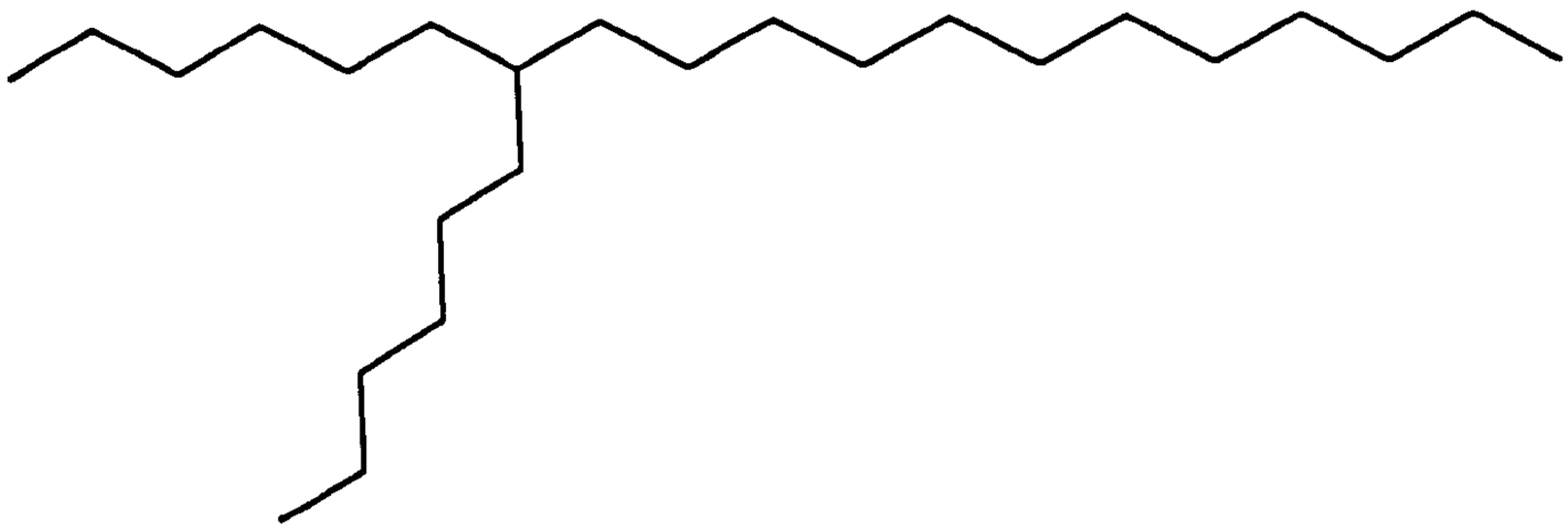

7-n-Hexylnonadecane

(III)

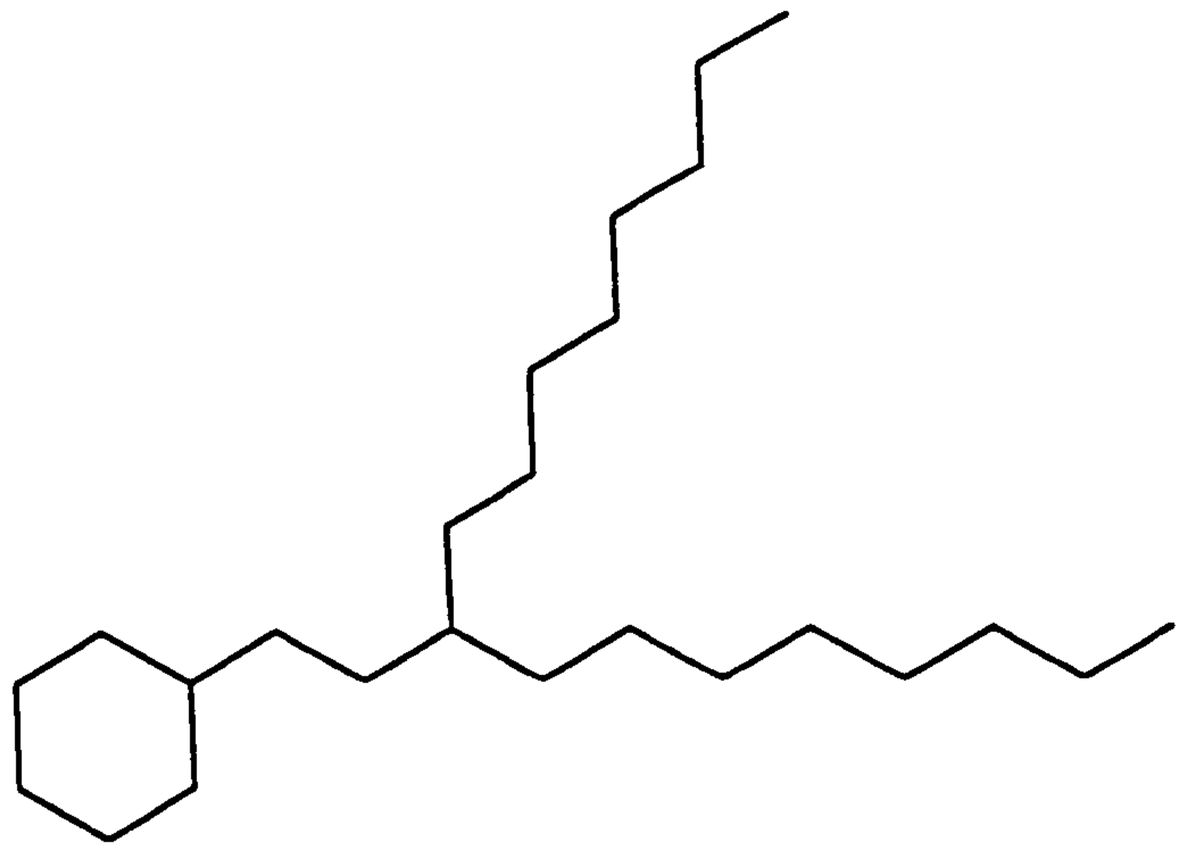

9-(2-cyclohexylethyl)-heptadecane

(IV)

2,6,10,14-Tetramethylpentadecane (Pristane)

(V)

Figure 2-22 Compounds oxidised by **Gough and Rowland (1990).**

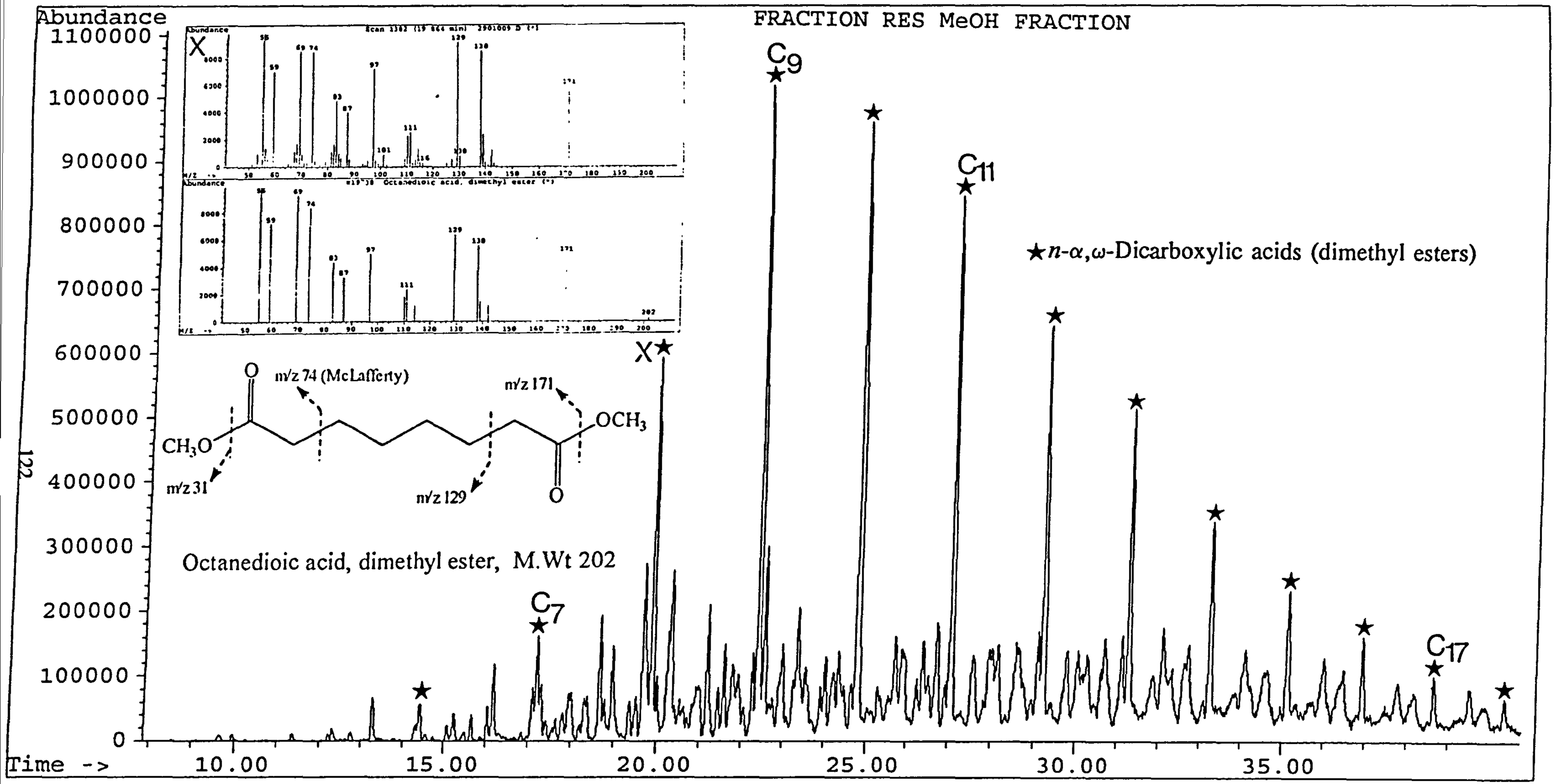

Figure 2-23 Total ion current chromatogram showing diacids present in the residue.

dimethylnonandioate. The spectrum of a second compound (K.R.I. 1435) did not match published or library spectra, but the major fragment ions suggested a possible branched di-carboxylic acid. Methyl branched dicarboxylic acids were identified **Gough (1989)** in the oxidation products of a lube oil aliphatic UCM and the oxidation products of a series of mixed standards (Figure 2-22). The *n*-dioic acids produced during the oxidation of the residue ranged from C_8 to C_{18} and maximised at C_9 and accounted for 15% of the total resolved compounds (*cf.* 27% *n*-monocarboxylic acids). All their spectra matched closely those of published spectra and library spectra (**Gough, 1989**).

Diacids are thought to arise from oxidation of alkyl chain bridging links (Figure 2-21 III) between other alkyl chains or cyclic structures (**Killops and Al-Juboori, 1990; Gough and Rowland, 1991**). **Killops and Al-Juboori (1990)** also suggested that they may also be formed by further oxidation of terminal *n*-alkyl chains. Evidence for this is provided in both of the previous studies. Thus, oxidation of icosane *n*-C_{20} and pentacosane *n*-C_{25} produced not only *n*-acids but also dioic acids in similar relative amounts to those found in UCM oxidations.

Why a homologous series of dioic acids should be formed in high concentrations in the residue (Figure 2-24), but, with few exceptions, not in the other distillate fractions, is unclear but may be a reflection of the structures of the higher molecular weight portion of the UCM found in the residue. One reason may be that the residue fraction is made up of more compounds with alkyl bridges. When oxidised the residue fraction also produced the highest proportion of resolved compounds of all the samples oxidised (81%). Further oxidation of mono carboxylic acids is perhaps the most likely explanation, especially because the stoichiometry of the oxidant substrate was only estimated for the residue but accurately measured for the other fractions using the cryoscope molecular weight data. Excess oxidant may have resulted in secondary oxidation of *n*-acids as well as increasing the highest proportion of resolved compounds.

A range of compounds with mass spectra characteristic of mono-methyl branched acids was identified in the oxidation products, though in much lower quantities than the *n*-monocarboxylic acids. The majority of these compounds were found to be substituted

Table 2-14 The distribution and amount of diacids in the resolved oxidation products.

Distillate Fraction	n-Diacids		
	% Total	Range	Maximum
19	n.d.	n.d.	n.d.
23	<0.01	C_9	C_9
26	n.d.	n.d.	n.d.
27	n.d.	n.d.	n.d.
28	n.d.	n.d	n.d.
29	n.d.	n.d.	n.d.
30	n.d.	n.d.	n.d.
Residue	15	C_7-C_{18}	C_9
Total	n.d.	n.d.	n.d.

n/d = non-determinable

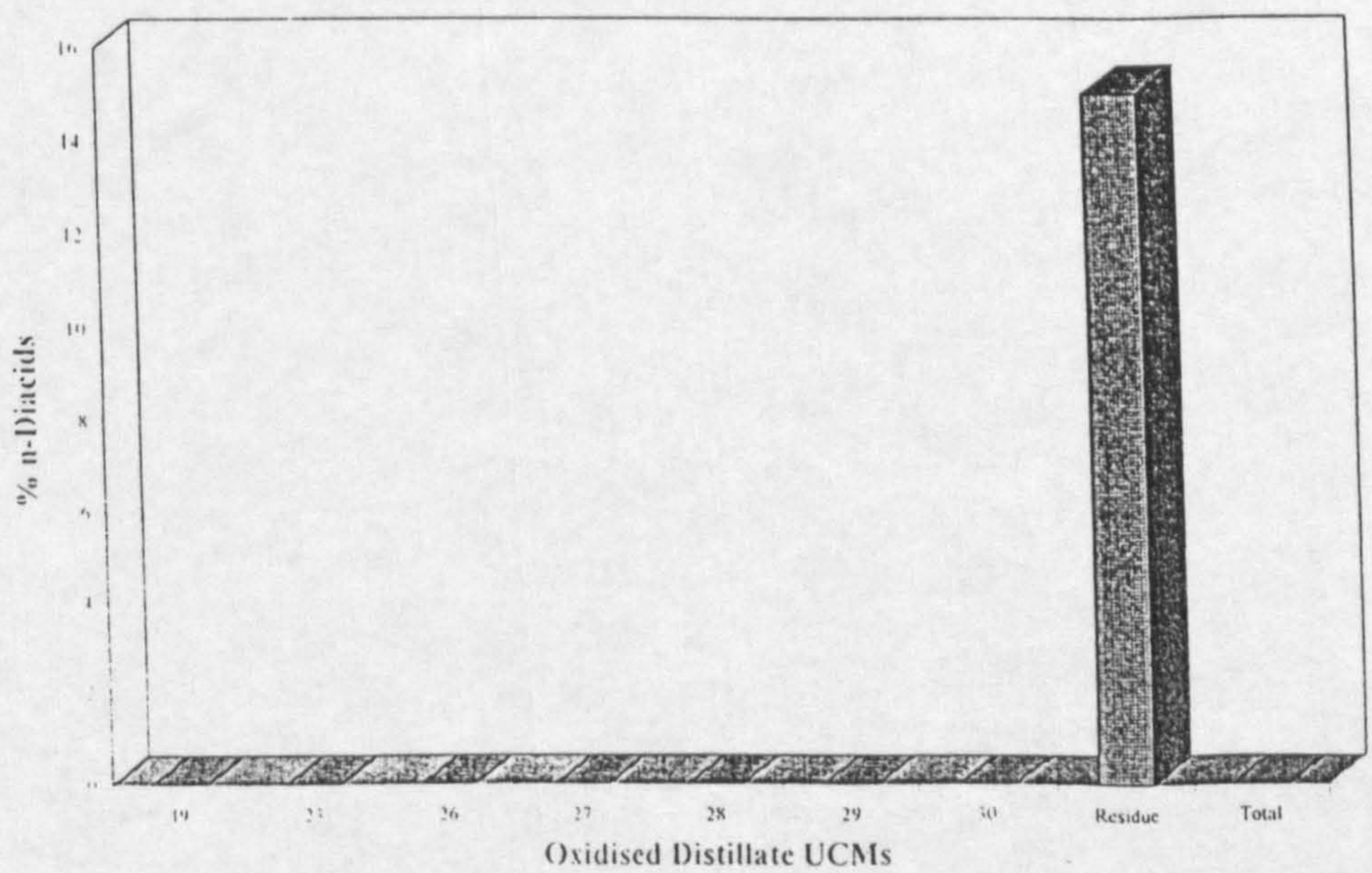

Figure 2-24 Histogram showing percentage of diacids in the oxidised samples.

at the *iso*-position with a large *m/z* 87 ion, with carbon numbers from C_8 to C_{17} (Figure 2-25 A). Other mono-methyl branched acids were present but they could not be further positively identified. Compounds with spectra characteristic of isoprenoid acids were also detected in the oxidation products of the distillate fractions. Of the few isoprenoid acids whose structures could be determined by comparison with published and library spectra, both 2,6-dimethylundecanoic acid (K.R.I. 1563) and 2,6,10-trimethylundecanoic acid (K.R.1. 1624) are shown in Figure 2-25 C. Both compounds showed a base peak *m/z* 88 (indicating a methyl branch on the beta carbon) and large ions at *m/z* 101, 129, 157, **(Douglas *et al.*, 1970)**. In Fraction 27 a compound (K.R.I. 1850) with a base peak ion at *m/z* 87 was present indicating a cleavage at the 3,4 bond position. A fragment *m/z* 74 ion was the second most abundant ion with fragment ions at *m/z* 115 > 101, 157 and 156 >171, 227. A close match to the library spectrum of 4,8,12-trimethyltridecanoic acid was obtained. Isoprenoids shown to be present in the original fraction are known precursors of such compounds, proved by the oxidation of pristane **(Gough and Rowland, 1991 and references therein)**. The spectra of several other compounds contained fragment ions similar to those expected from isoprenoid acids but interpretation was made difficult because they were present in only low abundances and suffered from interference from co-eluting components.

Many of the branched compounds might be expected to come from the isoprenoids identified in the original fractions, particularly pristane and phytane. As with the *n*-acids, although the amount of pristane and phytane in the original distillates may as much as 50% of the resolved compounds (Fraction 29) this could still not have accounted for all the oxidation products. The products of CrO_3/AcOH of pristane and phytane are well documented **(Cox *et al*, 1972; Brooks *et al.*, 1977; Patience *et al.*, 1978; Gough, 1989; Yon *et al.*, 1982)**. It is also known that the yields of pristane and phytane oxidation with CrO_3/AcOH products are very poor (*op cit.*) Indeed **Gough (1989)** showed that regular acyclic isoprenoids (Figure 2-22 V) were much more readily oxidised to undetectable low molecular weight products than six other branched and cyclic C_{25} alkanes (Figure 2-22) presumably because of the generally larger number of tertiary carbon centres. Therefore it is considered that the majority of the functionalised and methyl branched oxidation products detected herein from oxidation of fraction 29

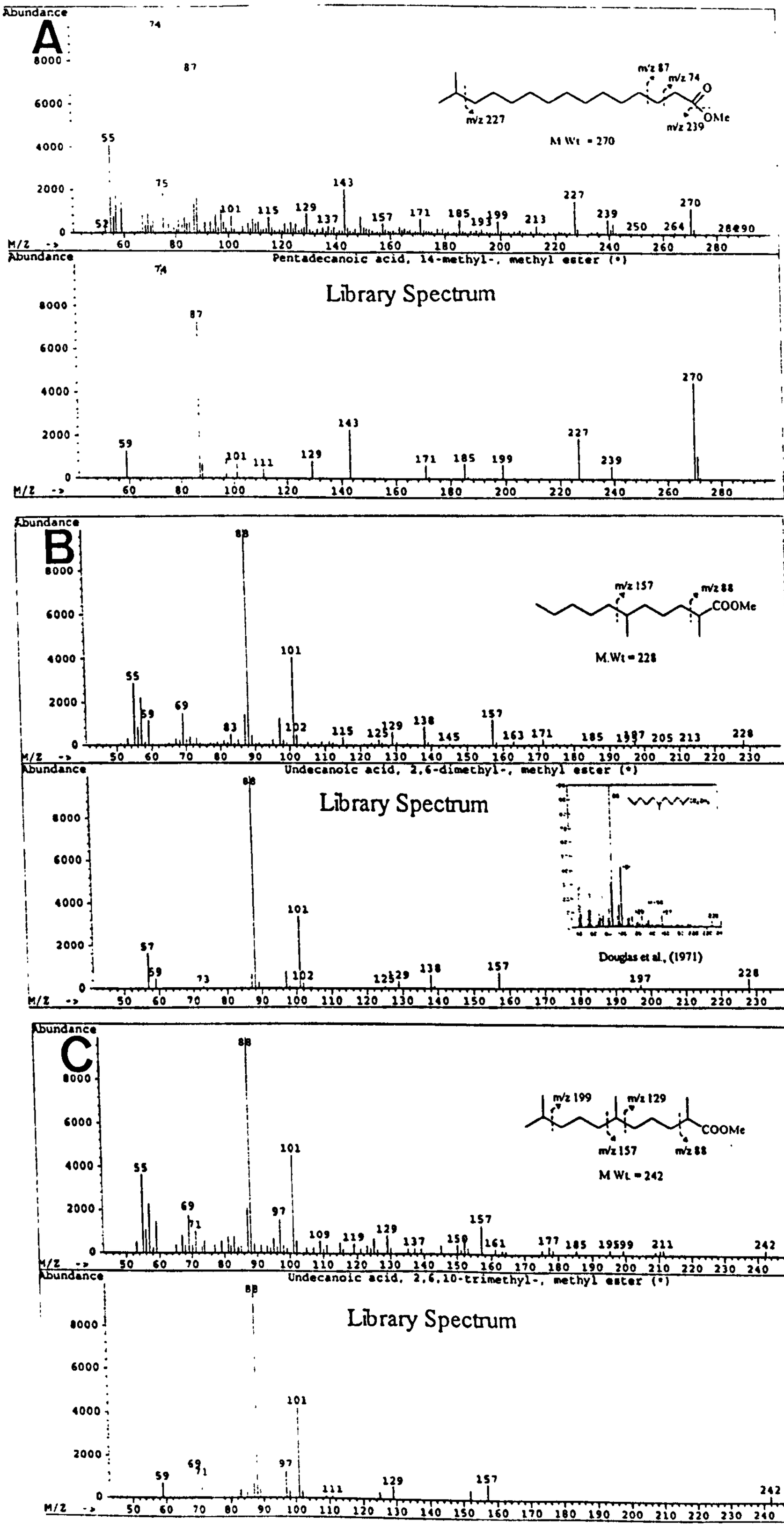

Figure 2-25 Mass spectra and library spectra of A) 14-methylpentadecanoic acid, methyl ester, B) 2,6-dimethylundecanoic acid, methyl ester and C) 2,6,10-trimethylundecanoic acid, methyl ester.

are likely to have come from structures present within the UCM.

Ketones are normally absent, or are present in only small amounts in non-weathered fossil fuels (**Tissot and Welte, 1984**). After oxidation of the condensate with CrO_3/AcOH, an homologous series of methyl ketones, ranging from C_7 to C_{19} was detected (Figure 2-26). Like carboxylic acids, ketones which have hydrogen atoms on carbon atoms γ to the carbonyl carbon can undergo a McLafferty rearrangement (Figure 2-26 B). In ketones this produces a characteristic diagnostic m/z 58 ion (**McLafferty and Tureček, 1993**). The absence of any M^+ -18 ion indicates that these compounds had straight chain rather than isoprenoid structures (**Hertz *et al.*, 1994**). The distributions of ketones in the oxidised samples are shown in Table 2-15 and as a histogram in Figure 2-27. The levels of ketones present in the oxidation products were lower than those of the *n*-acids even though CrO_3/AcOH oxidation of simple branched compounds produces acids and ketones (**Gough and Rowland, 1990**), *e.g.*

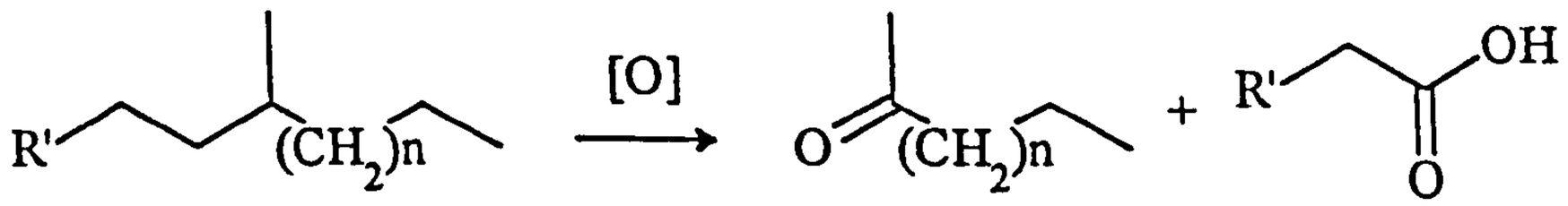

Ketone Acid

Gough (1989)

Surprisingly, very few ketones were identified in the oxidation products of the Residue. Ketones are known to be to be degraded quite rapidly by CrO_3 to acids via C-C bond cleavage adjacent to the carbonyl (**Gough and Rowland, 1991**) and this might explain their relatively low abundance compared to the *n*-acids. The average carbon chain length of the ketones (C_{13}) was one carbon number higher than the *n*-acid chain length, as expected from the oxidation of simple branched compounds. Oxidative cleavage at either side of the methyl branch position (Figure 2-21) could result in the formation of a carboxylic acid and a ketone (**Gough, 1989**). When authentic 9-methyltetracosane was oxidised the resultant ketones were one carbon greater in chain length than the largest acid (**Gough, 1989**) similar to the above results. The largest concentration of ketones was observed in the distillate Fraction 29 (11%).

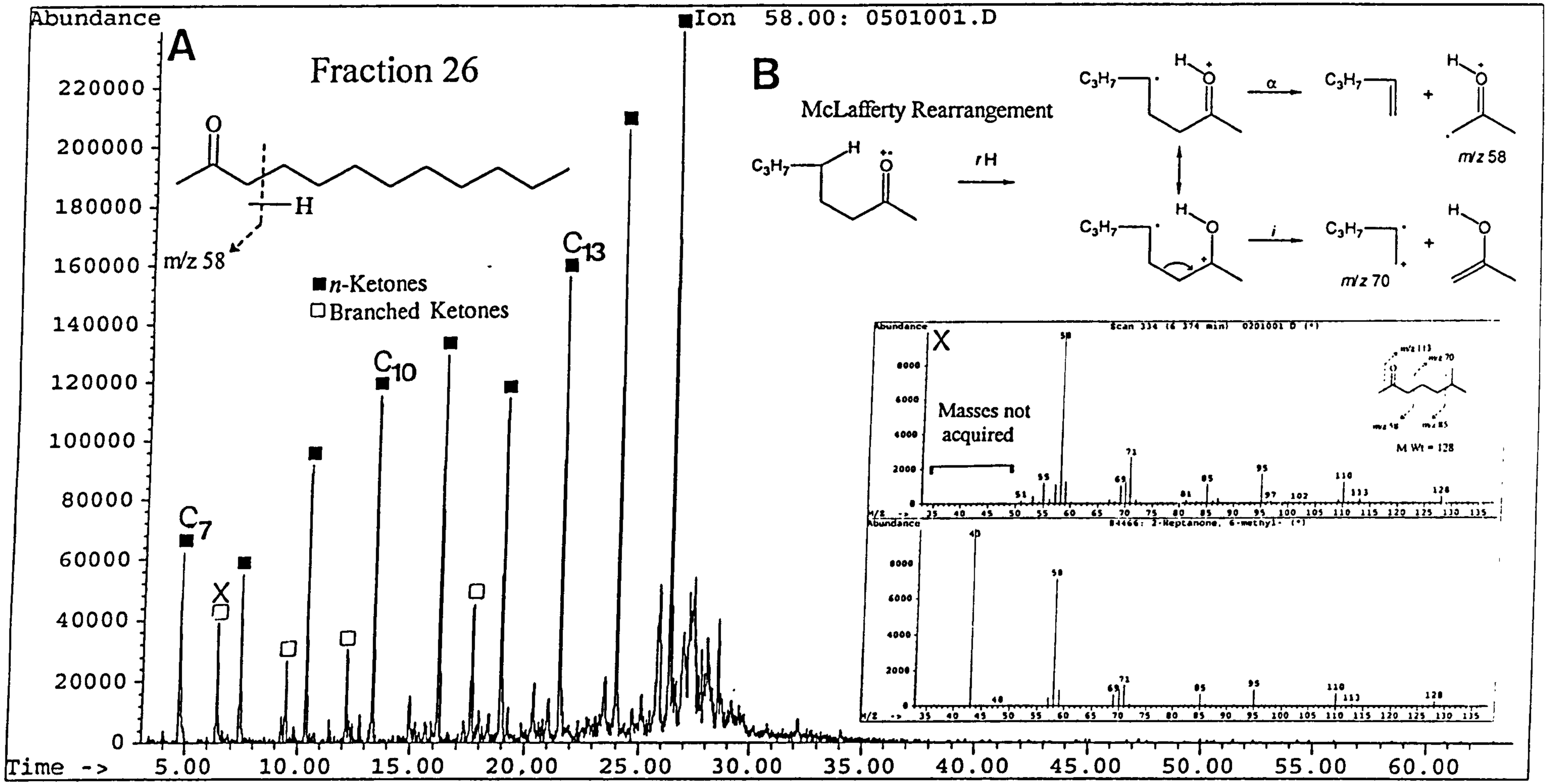

Figure 2-26 A) GC-MS fragmentogram (m/z 58) showing the distribution of ketones in the total oxidation products of Fraction 26, and B) the Mclafferty rearrangement showing the formation of the m/z 58 ion.

Table 2-15 The distribution and amount of ketones in the resolved oxidation products.

Distillate Fraction	Ketones		
	% Total	Range	Maximum
19	1	C_8-C_{12}	C_8
23	0.4	C_7-C_{14}	C_{13}
26	3	C_7-C_{16}	C_{15}
27	0.1	C_7-C_{19}	C_{11}
28	3.1	C_7-C_{16}	C_{11}
29	11	C_7-C_{17}	C_{13}
30	0.2	C_7-C_{19}	C_{13}
Residue	n/d	n/d	n/d
Total C.	1	C_7-C_{17}	C_{13}

n/d = non-determinable

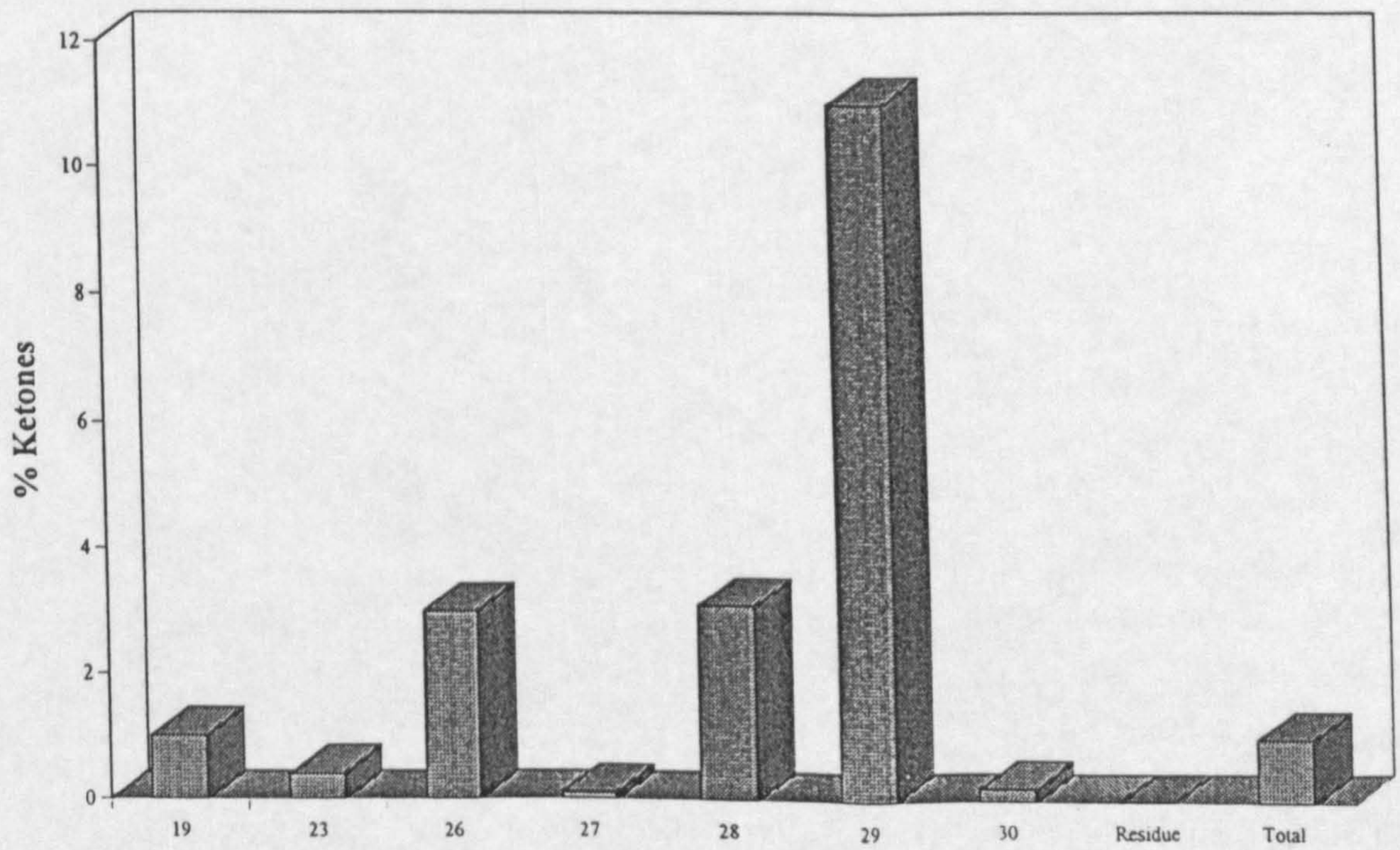

Figure 2-27 Histogram showing the percentage of ketones in the resolved products after oxidation.

Other oxo-compounds (keto acids), containing both a carboxylic group and a keto group (Figure 2-28) were also identified among the oxidation products of the whole condensate UCM and distillate fraction UCMs. Likely precursors are isoprenoid hydrocarbons from which the keto acids are formed by oxidation at two positions. The exact structures could only be inferred because of their low concentrations, lack of molecular ions in the spectra, and interference from ions of co-eluting compounds.

Another series of cyclic compounds present in the oxidation products of the distillate fractions were those identified by a dominant *m/z* 99 ion (Figure 2-29). **Gough and Rowland (1991)**, identified these compounds as dialkyl γ-lactones (Figure 2-29), which are formed from the internal esterification of hydroxy acids in acid (*i.e.* compounds that contain both a hydroxyl and a carboxylic acid group within the same molecule, **Carey, 1992**). For formation of a γ-methyl-γ-lactone, a 4-hydroxy-4-methyl carboxylic acid precursor is required **(Gough, 1989)**. Such a precursor compound is itself likely to be formed from the oxidation of isoprenoid structures (Figure 2-30).

Lactone distributions (Table 2-16) varied dramatically between the fractions (Figure 2-31). Only one lactone (C_6) was identified in Fraction 19. Present in Fractions 26, 27, 28, 29 and Residue were a series of C_6-C_{10} γ-methyl-γ-lactones. The formation of these compounds requires precursors which contain a dialkyl substituted alkyl chain *e.g.*

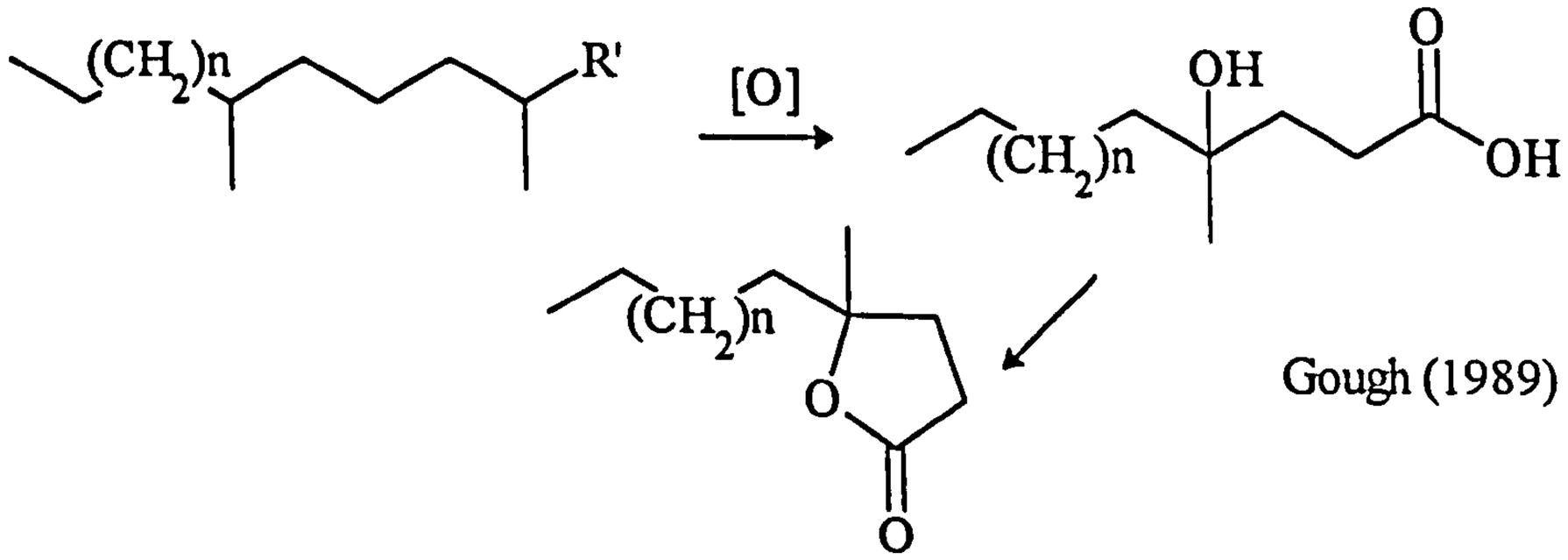

Gough (1989)

In the case of the $C_{6\text{-}10}$ γ-lactones the two methyl groups would need to be positioned at C-2 and C-6 and the carbon chain length comprising 7 carbons (C_6) to 11 carbons (C_{10}) *e.g.*

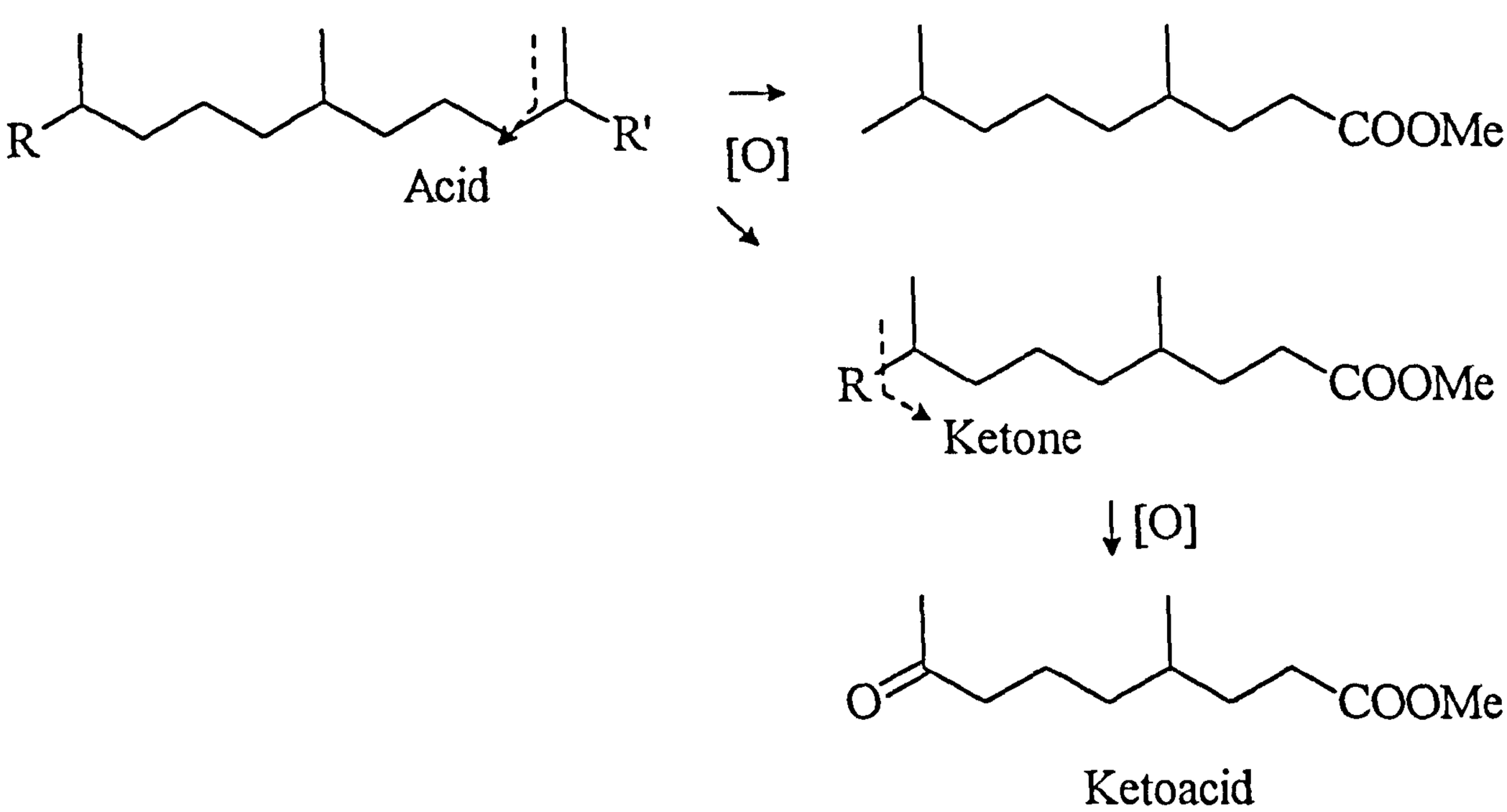

Figure 2-28 Formation of a keto acid (adapted from **Gough 1989**).

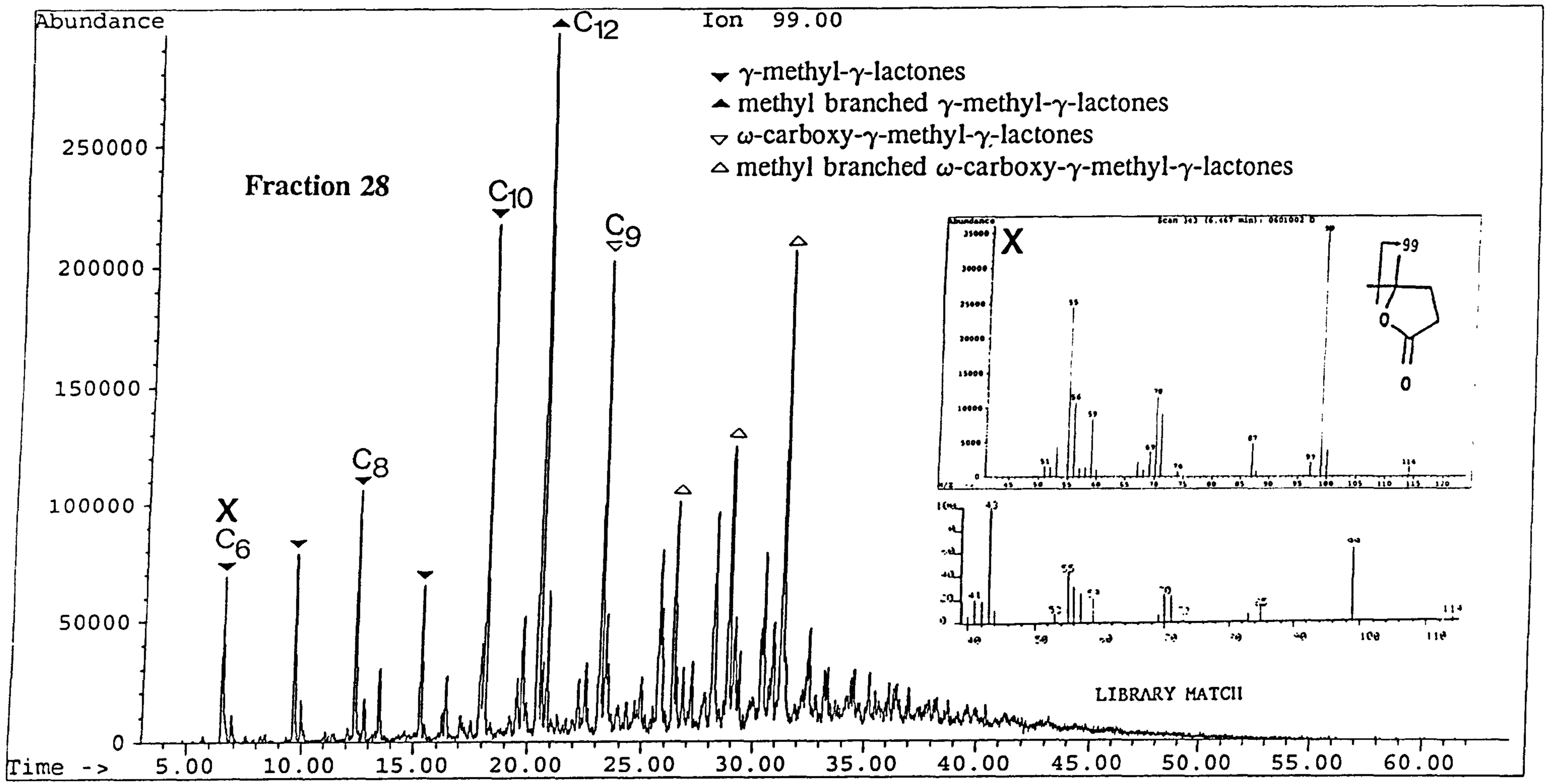

Figure 2-29 GC-MS fragmentogram (m/z 99) showing the distribution of γ-lactones in Fraction 28.

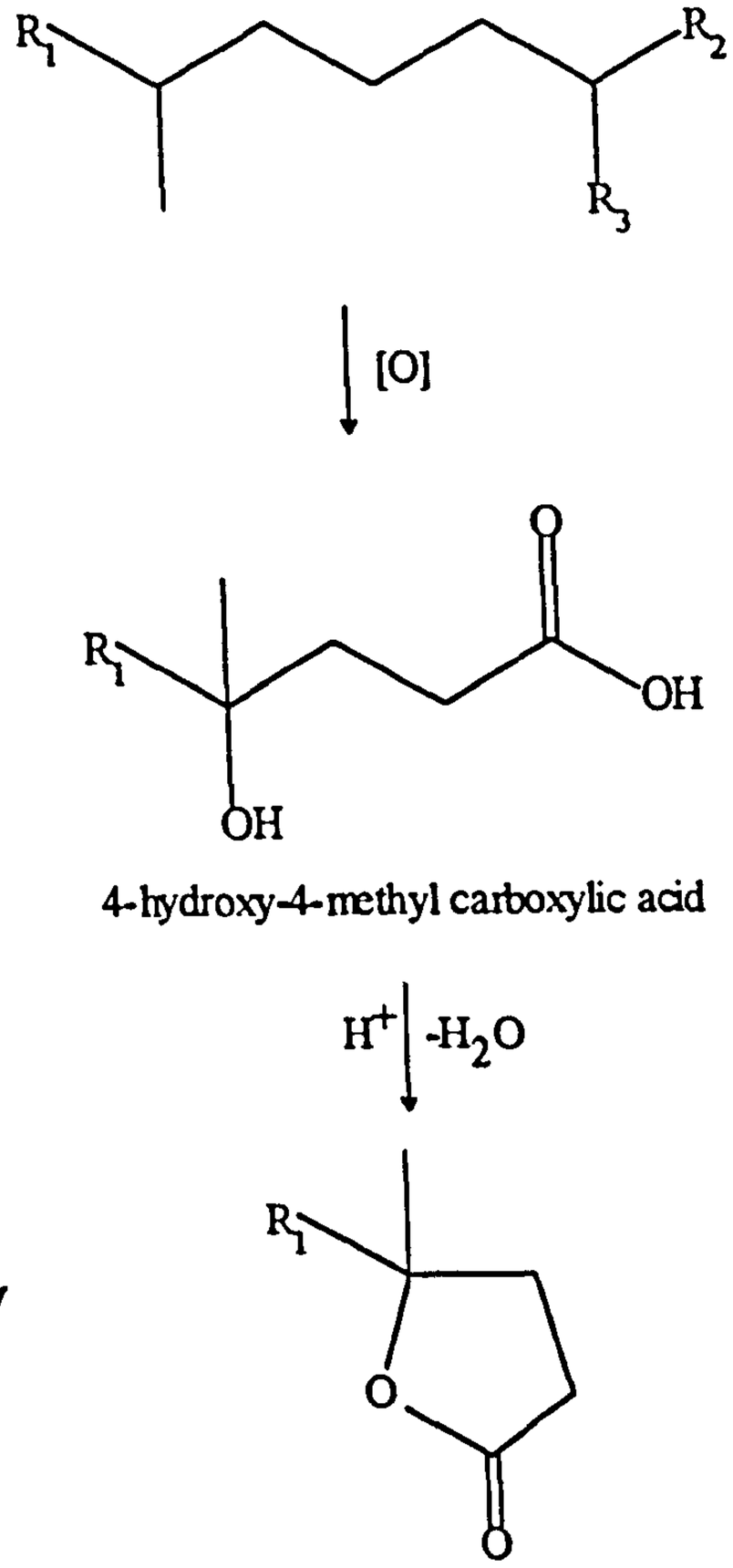

Figure 2-30 Formation of a γ-methyl-γ-lactone.

Table 2-16 The distribution and amount of γ-lactones in the resolved oxidation products.

Distillate Fraction	Lactones		
	% Total	Range	Maximum
19	< 0.1	C_6-C_{12}	C_6
23	0.4	C_6, C_{12}	C_{12}
26	1	C_6-C_{16}	C_6
27	< 0.1	C_6, C_7, C_{12}	C6
28	0.8	C_6-C_{16}	C_{12}
29	< 0.1	C_6-C_{14}	C_{12}
30	0.2	C_6-C_{19}	C_{12}
Residue	< 0.1	C_6-C_{17}	C_{12}
Total	< 0.1	C_6-C_{17}	C_{12}

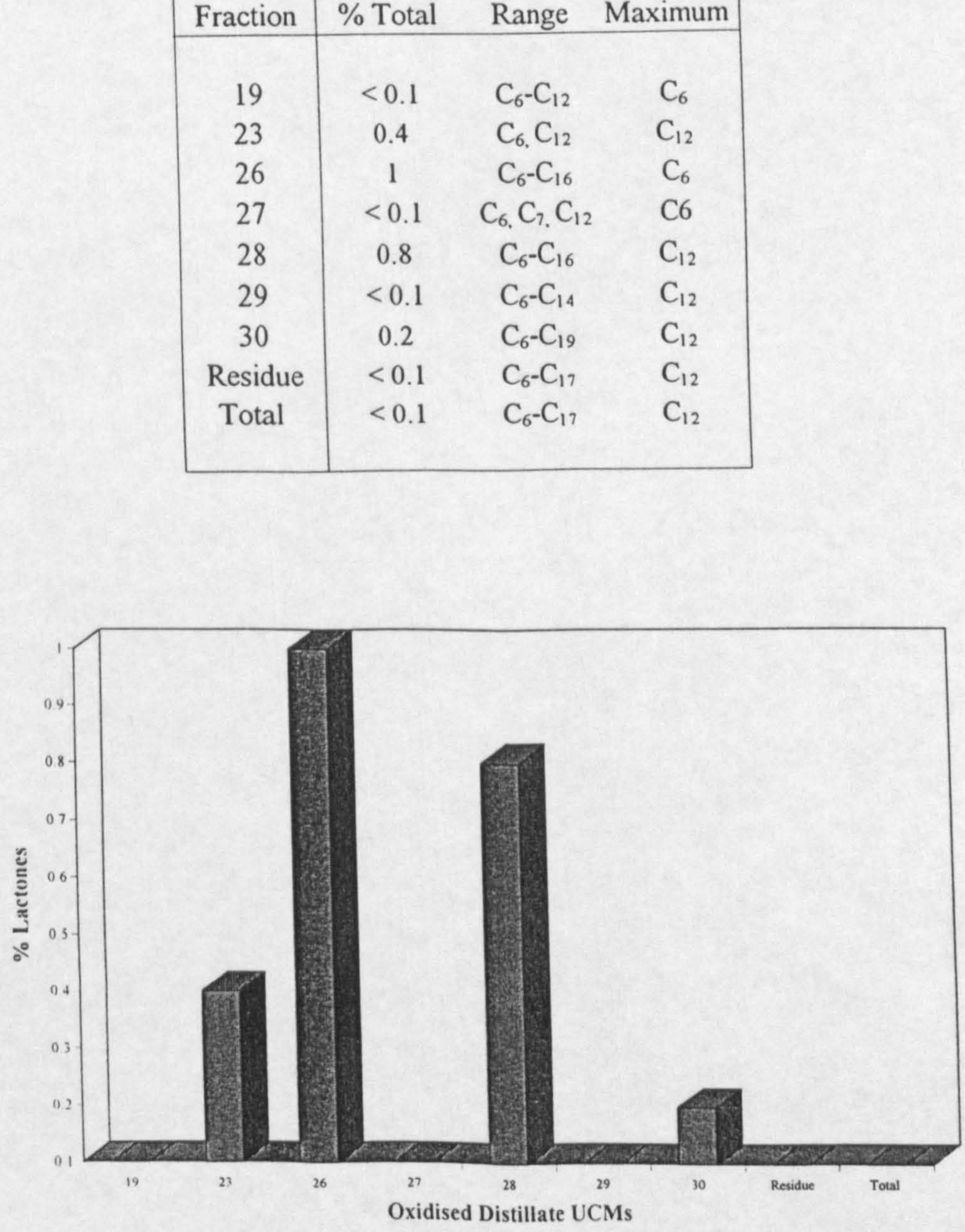

Figure 2-31 Histogram showing percentage of γ-lactones in the resolved oxidation

e.g.

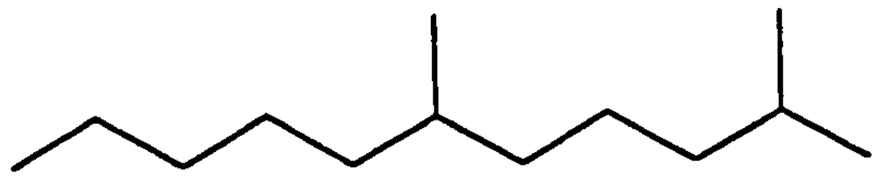

2,6-methylundecane

Fractions 23, 26, 27, 28, 29 and the Residue were dominated by a compound with a K.R.I. 1502 which could not be identified but may be a carboxy-γ-methyl-γ-lactone or a branched γ-methyl-γ-lactone. Both were reported as products of oxidation of pristane by **Gough (1989)**. Fractions 29 and the Residue produced much greater numbers of compounds with the *m/z* 99 fragment than the other fractions with the Residue containing the highest amounts. Fraction 30 was unusual because no lactones were detected.

Trace amounts of a cyclohexane carboxylic acid was identified in the oxidation products of the condensate distillate fractions (2-32 A). These were also observed in the oxidation products of a lube oil (**Gough and Rowland, 1990**) and a biodegraded crude oil (**Killops and Al-Juboori, 1990**). The expected products of oxidation of a substituted alkylcyclohexane (Figure 2-32 B) would be *n*-acids and an alkyl cyclic acid as confirmed by **Gough and Rowland (1991)** who oxidised synthetic 9-(2-cyclohexylethyl)-heptadecane. The low proportion of aliphatic cyclic compounds observed in the oxidised UCMs compared to the high amount of *n*-alkyl cyclohexane compounds originally in the unoxidised UCMs may be caused by opening of the cyclic group to form both an acid and a ketone (Figure 2-32 C).

Several classes of aromatic compounds were also identified in the oxidation products of the distillate fractions. The four main types of compounds were benzoic acids, methyl substituted benzoic acids (toluic acids), benzene dicarboxylic acids and methyl substituted benzenedicarboxylic acids.

Methyl esters of benzoic acid (*m/z* 51, 77, 105, 136 and 137) and methyl substituted benzoic acids (two isomers) were common to all the distillate fractions after oxidation and esterification (Figure 2-33 A). The two isomers (K.R.I. 1233 and 1243) are thought to be 4- and 3-methylbenzoic acid *i.e. meta* and *para* toluic acids (Figure 2-33 B). The

A

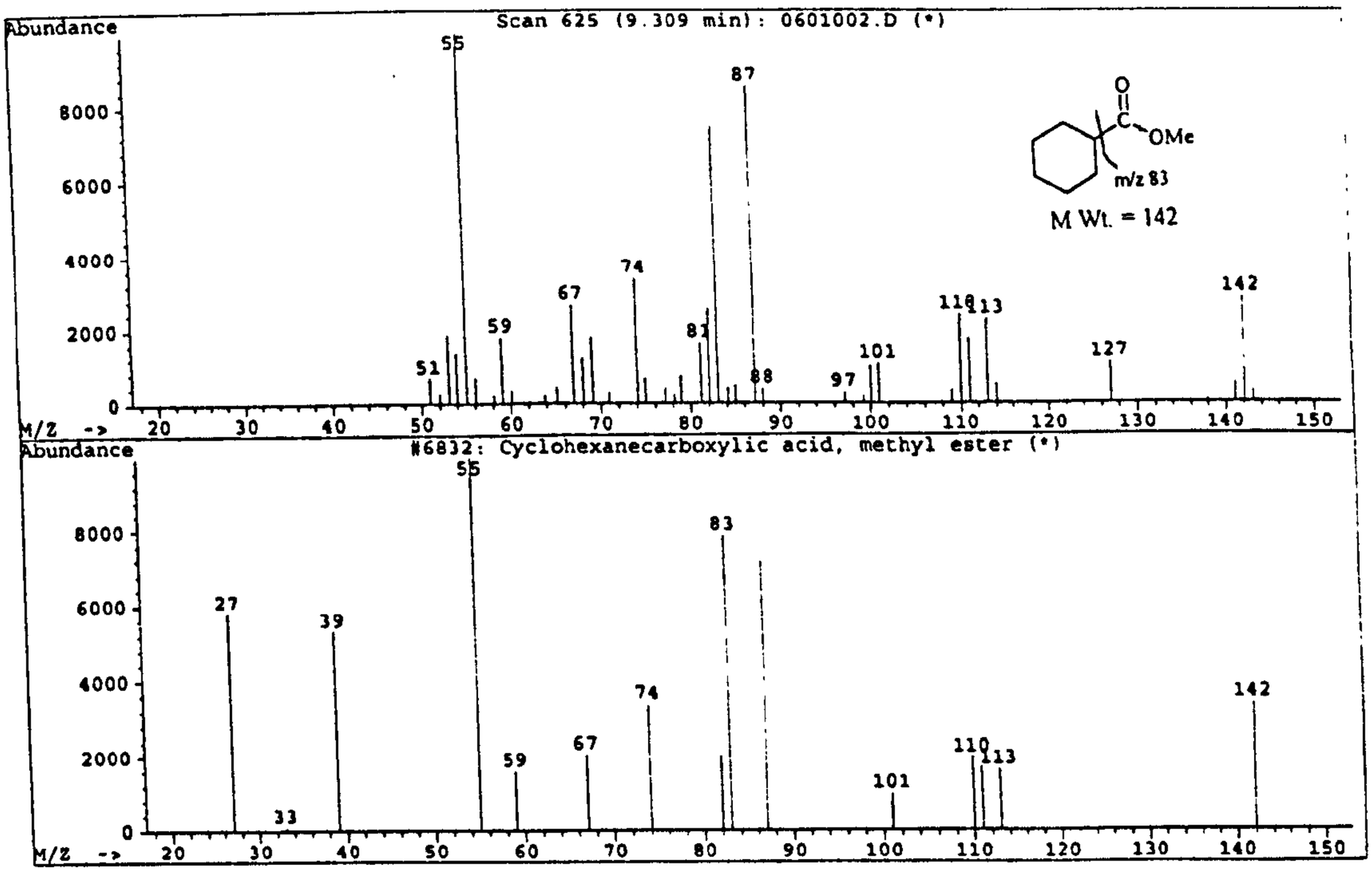

B

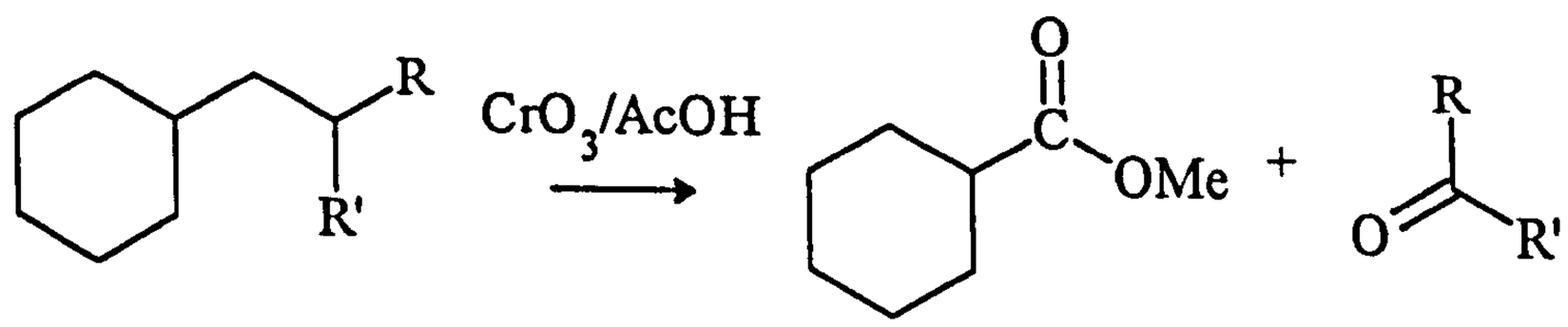

C

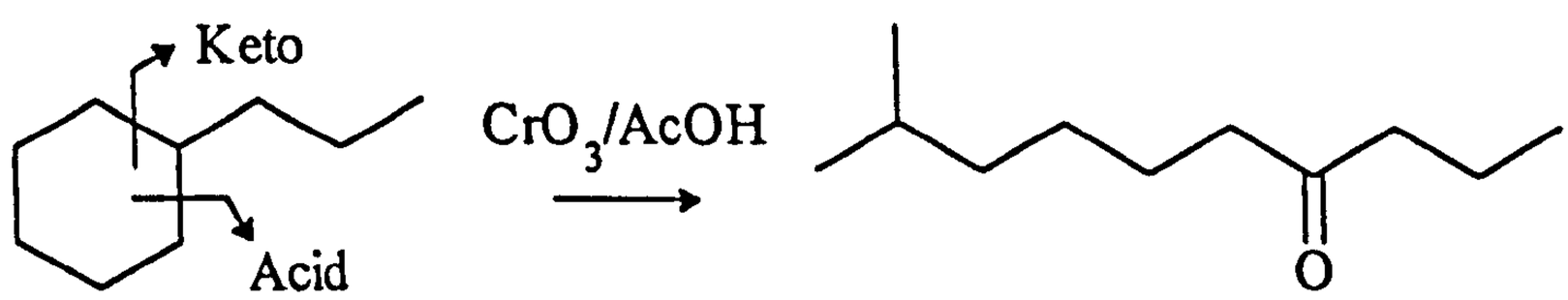

Figure 2-32 A) Mass spectra and library spectra of a cyclohexanecarboxylic acid, methyl ester and B) Oxidation of at a tertiary centre to form a cyclohexanecarboxylic acid, and C) oxidation of the ring (adapted from **Gough, 1989**).

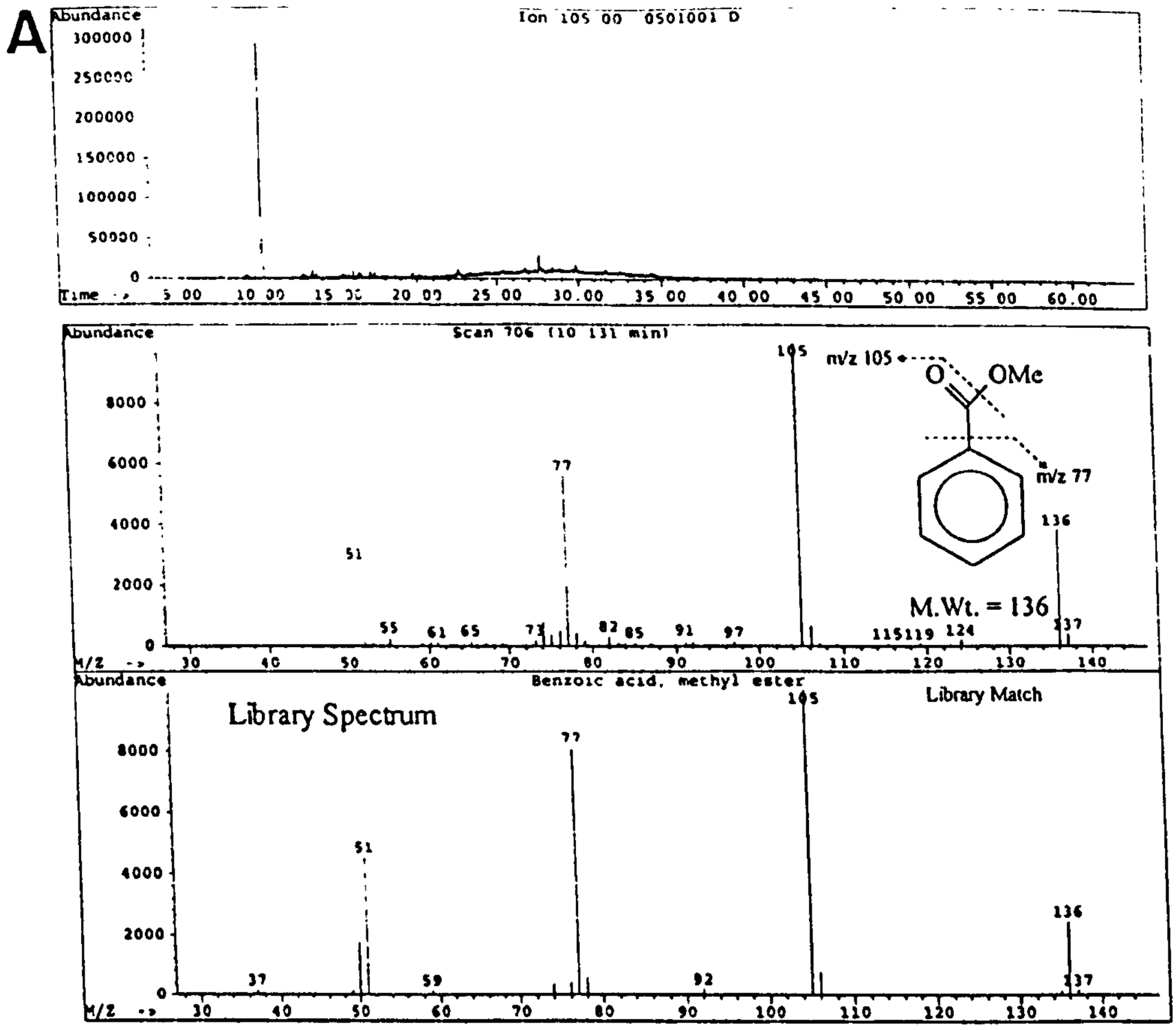

Figure 2-33 Mass spectra and library spectra of A) benzoic acid methyl ester and B) methyl substituted benzoic acid methyl ester.

2-methyl isomer was not identified. Compounds with spectra similar to those of dimethylbenzoic acids were also tentatively identified (abundant fragment ions at *m/z* 105, 133 (base peak) and at 164).

Chromic acid oxidation of alkyl-substituted aromatic compounds takes place almost exclusively at the benzylic position rather than at a tertiary C-H centre with oxidation occurring between the α and β carbon atoms **(Brandenberger and Dvoretzky, 1961)**, *e.g.*

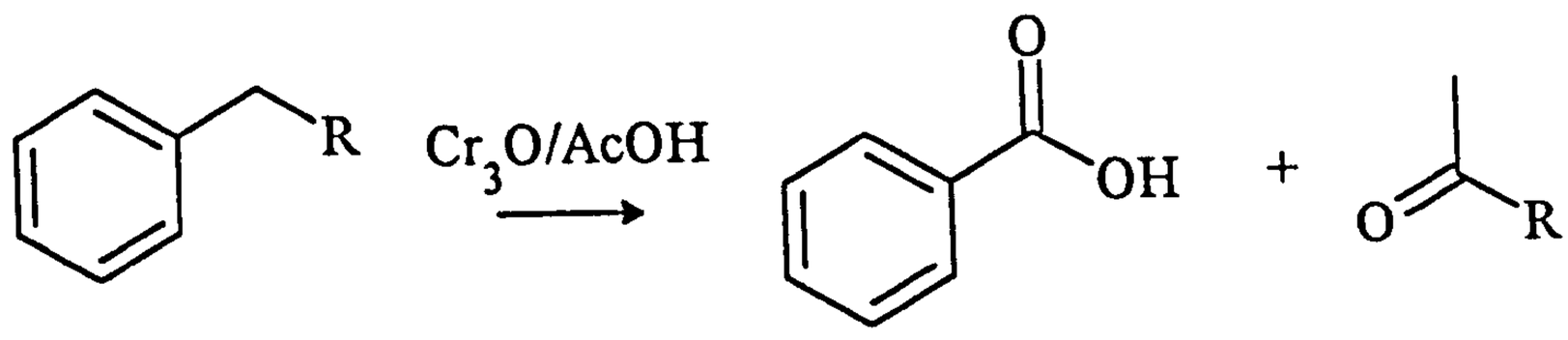

The benzoic acids and methyl substituted benzoic acids may arise from the oxidation of alkylbenzoic and alkyl polymethylbenzoic structures, with either straight or branched alkyl chain. As previously mentioned, such compounds have been fractionated from a gas condensate by **Rønningsen and Skjevrak (1990)**. The mono aromatic fraction was shown to be predominantly unresolved, probably from possible multiple branching positions on the aromatic ring and the alkyl chain.

Spectra of two other components present in the oxidised distillate fractions were characterised by base peak ions of *m/z* 177. The spectrum of the later eluting compound (K.R.I 1597) matched the published and library spectrum of the dimethyl ester of a methyl substituted 1,2-benzenedicarboxylic acid, giving fragment ions at *m/z* 91, 177 and 208 (Figure 2-34 A). The earlier eluting (K.R.I. 1563) compound also contained a base peak ion of *m/z* 177 with other abundant fragment ions at *m/z* 118 and 178. The compound was not identified.

A compound (K.R.I. 1478) with a spectrum matching that of dimethylphthalate **(Middleditch, 1989)** was also observed in several fractions. Although not present in the blank, this compound is a common plasticizer and is found in some solvents and water

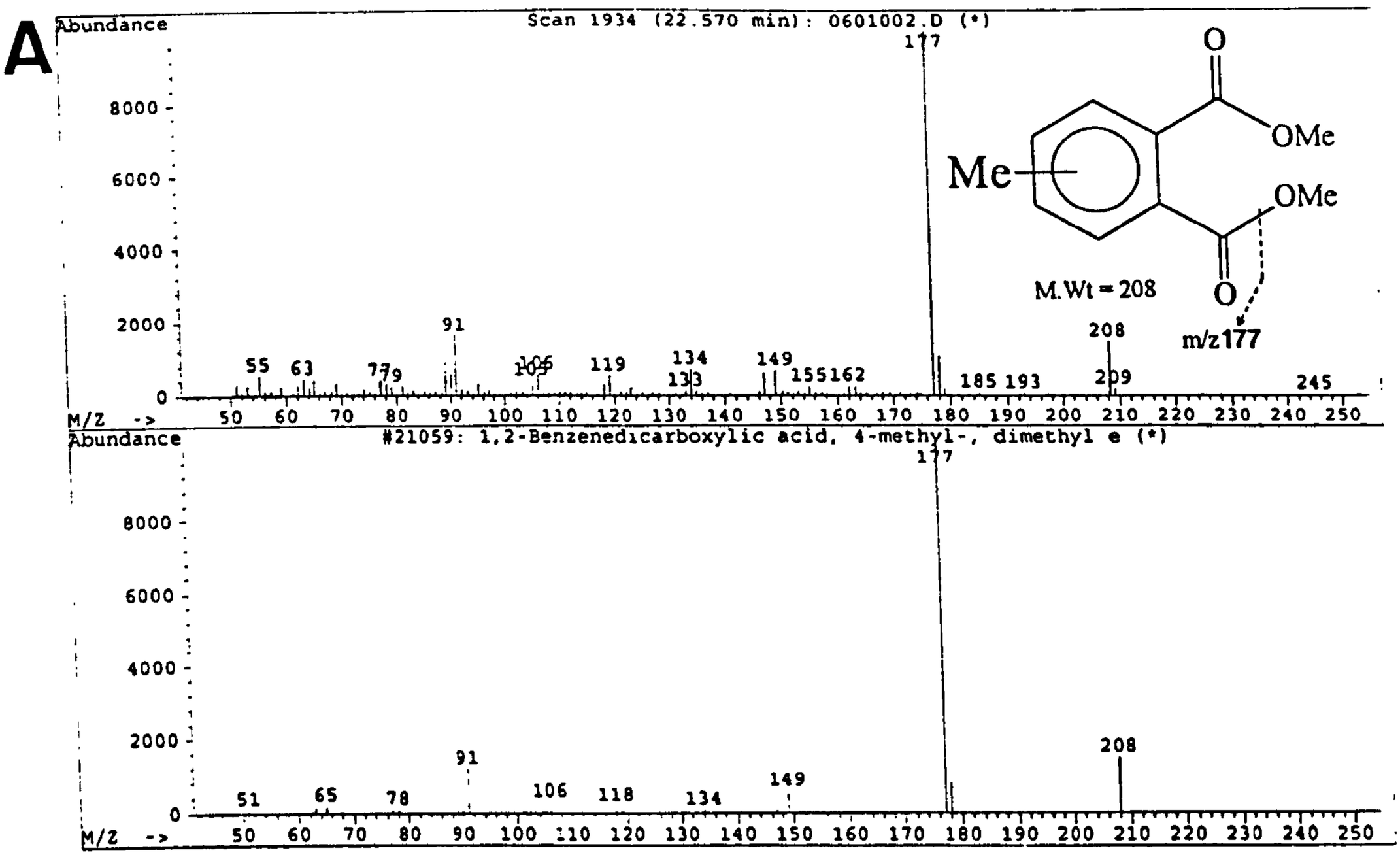

Figure 2-34 Mass spectra and library spectra of A) methyl-benzenedicarboxylic acid, dimethyl ester and B) dimethyl phthalate.

that has passed through rubber and plastic tubing. Its spectrum is unlike other many other phthalate esters and has a base peak at *m/z* 163 rather than the *m/z* 149 ion (Figure 2-34 B). A non-contamination source of this compound was suggested by **Revill (1992)** to be from the oxidation of naphthenobenzene type structures in TJP oil UCM and a similar tentative interpretation is made here for the condensate UCM.

A summary of the compounds identified from the oxidation of the condensate is given in Table 2-17 and is compared with the findings from previous studies by **Gough (1989)** and **Killops and Al-Juboori (1990)**. Overall the compounds identified from the oxidation of the condensate UCM were similar to the oxidation products of lubricating oil and the biodegraded oil. The majority of the resolved oxidation products were aliphatic. The condensate UCM did show a greater carbon number range (C_5-C_{28}) for the *n*-acids than the other two UCMs and an average carbon chain length which was greater by 3 carbon atoms.

Retro-structural analysis is the process of relating the structures formed (in this case from oxidation) to compounds originally present in the UCM (**Thomas, 1995**). This is difficult because the number of compounds present is large. Using a specially developed program (**Lewis, 1992**) the number of simple mono branched alkanes, excluding stereoisomers, in the total condensate was calculated ($C_{11\text{-}34}$). The number of isomers calculated for the distillate fractions increased with boiling point from 200 (Fraction 19) to 595 (Fraction 30). The data for all the fractions are given in Table 2-18 and is shown graphically Figure 2-35. These values were calculated using the carbon number range of the n-alkanes eluting in the original distillate fractions. The actual number of isomers will be different. For example in Fraction 30 the number of compounds which elute between *n*-$C_{19\text{-}20}$ will be greater than the number of isomers calculated for *n*-$C_{19\text{-}20}$ because increasing the amount and size of side chains on simple alkanes reduces the boiling point. For example a C_{21} methyl branched alkane will elute between *n*-C_{19} and *n*-C_{20} and a C_{21} "T" branch compound (8-hexylpentadecane) is known to elute between *n*-C_{16} and *n*-C_{17}. These figures are only for simple branched alkanes and do not include compounds with multiple branches, aromatic compounds and so forth which will add even more to the number of compounds present in the fraction. With so many

Compound	Lubricating Oil Carbon no.	Maximum	Biodegraded Oil Carbon no.	Maximum	Gas-Condensate Carbon no.	Maximum
n-monocarboxylic acid.	C_6-C_{20}	C_9	C_5-C_{18}	C_7-C_8	C_5-C_{28}	C_{12}
α-ω-*n*-dicarboxylic acid	C_6-C_{14}	C_9	C_9-C_{17}	-	C_9-C_{18}	C_9
keto acid	C_8,C_{10},C_{11}	C_{10}	C_8	-		
n-alkan-2-one	C_8-C_{15}	C_{12}	C_7	C_7	C_7-C_{17}	C_{13}
"iso"-methyl branched alkan-2-one	C_8-C_{12} C_8		C_8	C_8	C_8-C_{14}	-
γ-methyl-γ-lactone	C_6-C_{10}	C_8	-	-	C_6-C_{10}	C_{10}
methyl branched γ-methyl-γ-lactone	C_{11}-C_{12}	C_{11}	-	-	C_{11}-C_{12}	C_{12}
ω-carboxy-γ-methyl-γ-lactone	C_8-C_{11}	C_8	-	-	C_8-C_{10}	C_8

Continued overleaf ....

Table 2-17 Summary of compounds identified in the resolved oxidation products of a gas condensate UCM. The results are compared with previous studies of a lubricating oil UCM (Gough, 1989) and a biodegraded oil UCM (Killops and Al-Juboori, 1990).

Continued .....

Compound	Lubricating Oil		Biodegraded Oil		Gas-Condensate	
	Carbon no.	Maximum	Carbon no.	Maximum	Carbon no.	Maximum
methyl branched-ω-carboxy-γ-methyl-γ-lactone	C_{11}-C_{13}	C_{11}	-	-	C_{11}-C_{13}	C_{13}
methyl branched mono-carboxylic acid	C_6-C_{10}	-	C_6-C_{11}	-	C_6-C_{15}	-
methyl branched α,ω-diacid	C_8,C_9,C_{10}	-	C_5	C_5	-	-
cyclohexyl carboxylic acid	C_8	C_8	C_7,C_9-C_{11}	-	C_8	C_8
methylcyclohexyl carboxylic acid	-	-	C_8	-	-	-
isoprenoid acid	C_{11}-C_{16}	-	C_9-C_{11}	-	C_{11}-C_{16}	-
isoprenoid ketone	C_{13}	C_{13}	-	-	C_{13}	-

Table 2-18 The number of isomers of simple branched alkanes (excluding stereoisomers).

Distillate Fraction	Carbon Number Range	Sum of Isomers
	C_7-C_8	83
	C_8-C_9	105
	C_9-C_{10}	135
	C_{10}-C_{11}	164
19	C_{11}-C_{12}	200
	C_{12}-C_{13}	236
	C_{13}-C_{14}	277
23	C_{14}-C_{15}	321
26	C_{15}-C_{16}	369
27	C_{16}-C_{17}	422
28	C_{17}-C_{18}	476
29	C_{18}-C_{19}	532
30	C_{19}-C_{20}	595
	C_{20}-C_{21}	659
	C_{21}-C_{22}	723
Residue	C_{20}-C_{34}	8890
Total	C_{11}-C_{34}	15045

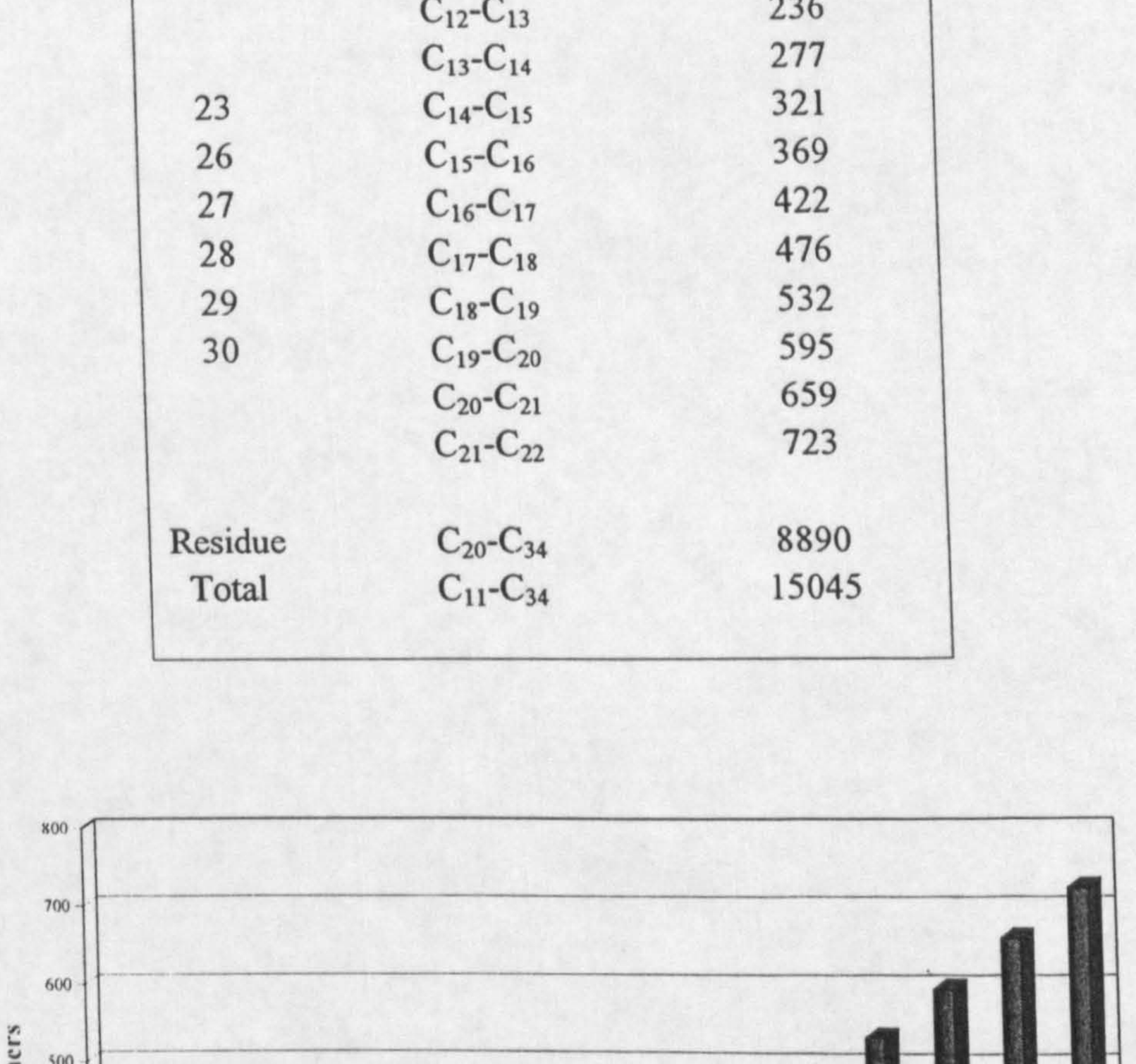

Figure 2-35 Histogram showing the increasing number of isomers with carbon number.

compounds and isomers the identification a single compound structure is difficult, if not impossible.

Even if oxidation does not give structural information for discrete molecules, it does provide information about the general structures present. Figure 2-36 E, represents a general overview. Components I to VIII represent structures identified herein the resolved oxidation products of condensate fractions. The diagram is not meant to represent a single compound but shows the structures that could be attached to one that is unknown. The point of attachment of the structure I to VIII to the unknown is the position at which the acid group or functionality was observed after oxidation indicating the cleavage position of the whole molecule. The central unknown part of the molecule to some extent remains unidentified but may consist of a structure similar to I to VIII or another compound such as a polycyclic. For example, if the unknown is a benzene ring then it could have been joined to either (I) to produce an *n*-alkyl benzene molecule (such compounds having been reported by **Rønningsen and Skjevrak 1990**) or be attached to an isoprenoid structure (VII), simple branched structure (V) (and all the isomers thereof) or even structure (II) to give benzylic "T" branch compounds as proposed by **Gough (1989)**. If the unknown is a tetralin it could be attached to a cyclic structure (VIII) and (III) to give compounds similar to those proposed by **Revill (1992)**.

For PVT analysis it is important to determine the relative amounts of different structural types. Figure 2-36 shows the quantitative importance of the compounds identified by oxidation as a percentage of the total condensate. Using Fraction 30 as an example, the resolved oxidised products accounted for *ca.* 0.43% of the total condensate. About 0.15% comprises *n*-alkyl chains. The same assumptions can be applied to the other fractions. For the total condensate UCM structural information of approximately 9% is deduced (≈43% of the UCM).

This means that a significant proportion (≈57% of the UCM) is still unidentified. This accounts for about 7% of the total condensate which represents a fraction greater than that of the C_{30+} fraction for many condensates and oils discussed in Chapter 1.

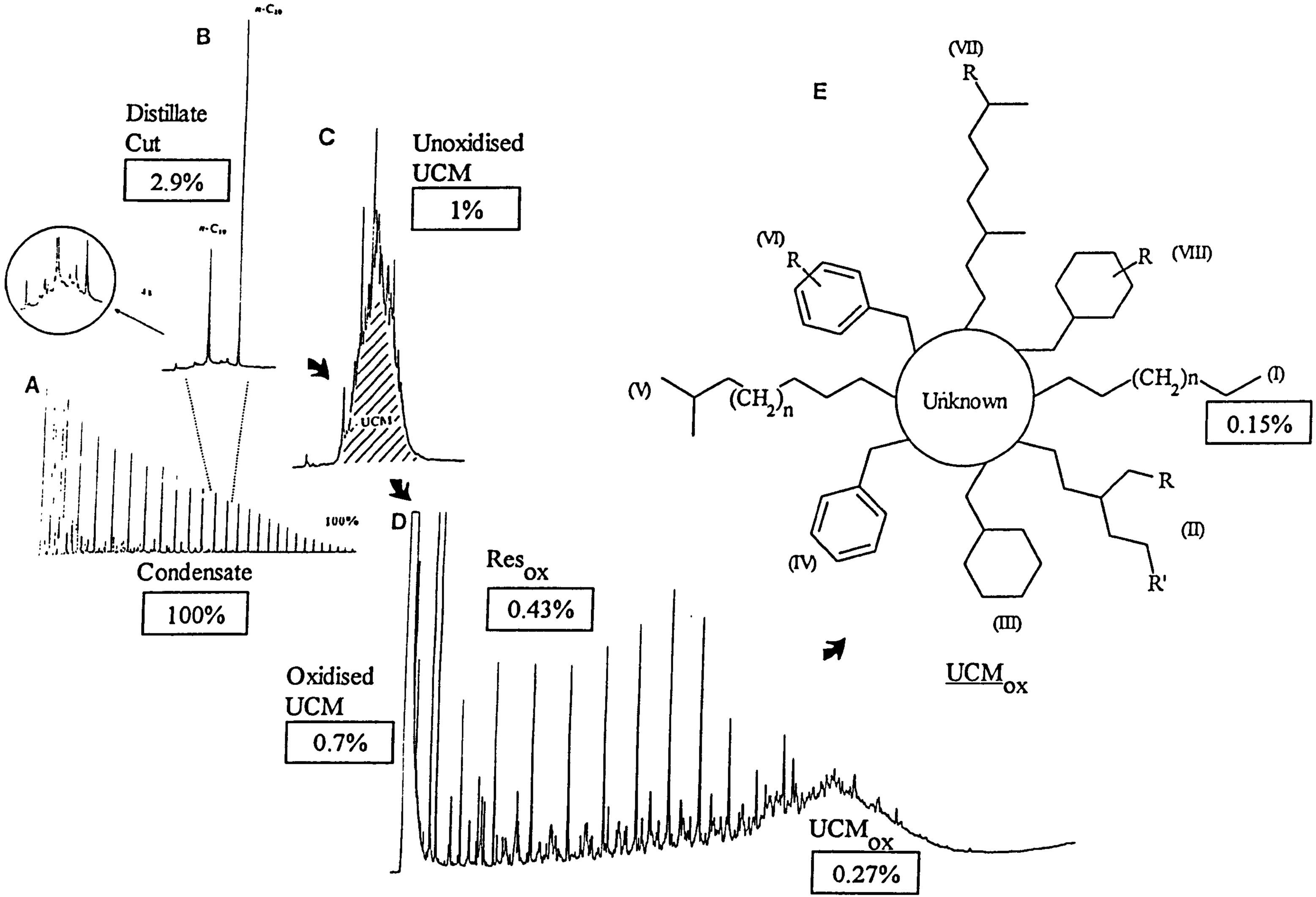

Figure 2-36 Overall view illustrating *retro*-structural analysis.

2.3.7 Summary

When analysed by gas chromatography the UCM of a waxy North Sea gas condensate accounted for 21% of the total hydrocarbons eluted by GC. The whole condensate was fractionated by distillation and the UCM measured in the distillate fractions. The UCM was found to account for 34 to 61% of each fraction.

These UCMs were isolated using molecular sieves (5A) and urea adduction leaving relatively few resolved compounds (3-36%). These were identified by GC-MS as a series of isoprenoids, simple mono methylalkanes, and substituted and non-substituted cyclohexanes. The UCM fractions were between 64 and 97% unresolved.

A semi mass balance of the oxidation of the UCMs with CrO_3/AcOH showed for the first time that an average of 8% was converted to CO_2 while 63% was recovered with DCM. The total recovery accounted for 65% to 94%. The losses were probably low molecular weight water soluble acids ($<C_6$). Of the recovered products, column chromatography showed that only 2 to 15% remained unoxidised. The majority of the oxidised products eluted from silica column chromatography with MeOH.

GC revealed that in most cases over half of the oxidised products were resolved; 81% in the case of the distillation residue. The majority of these were identified by GC-MS as *n*-acids, ketones, isoprenoid acids, and cyclic acids including mono aliphatic and cyclic aromatic acids suggesting that the condensate UCM is mainly aliphatic, in agreement with previous studies of fossil fuels. *Retro*-structural analysis of the resolved products gives a general picture of the structures present in about half of the condensate UCM. With further quantification an estimate of the overall percentages of the many types of compounds present could be made and this may be adequate to significantly improve PVT models of phase behaviour.

The number of possible isomers of simple branched alkanes was large. For the distillate UCMs between 200 - 600 compounds were possible and for the total condensate over 15,000. Adding to this the other compounds present (*i.e.* with a cyclic or polycyclic moieties), it is clear that even with the most efficient column currently available the number of compounds will remain beyond the scope of capillary gas

chromatography.

A significant proportion of UCM remains unresolved and the structures in it unidentified. For the total condensate this accounts for 10% which is greater than that of the C_{30+} fraction in many condensates. Clearly further studies need to be undertaken.

CHAPTER THREE

THE USE OF HIGH TEMPERATURE CAPILLARY GAS CHROMATOGRAPHY TO STUDY THE BIODEGRADABILITY OF HIGH MOLECULAR WEIGHT HYDROCARBONS

A consequence of the weathering of petroleum in the environment is that lower molecular weight compounds are removed preferentially to the higher molecular weight compounds ($>C_{30}$). The extent to which the latter compounds are biodegraded has rarely been studied. One reason for this is the technical difficulty associated with carrying out biodegradability tests with solid, water-insoluble substances.

A HTCGC method was developed to monitor quantitatively the biodegradability of the aliphatic fraction of a waxy Indonesian oil by Pseudomonas fluorescens. Recoveries of over 90% were obtained for n-alkanes up to C_{60} using liquid-liquid continuous extraction. After only 14 days 80% of the aliphatic hydrocarbons had been degraded. At the end of the study 14% of the original fraction remained which comprised mainly C_{40+} compounds. No decrease in the concentrations of compounds above C_{45} was observed. However, the use of a rapid screening biodegradation method proved conclusively that Pseudomonas fluorescens was capable of utilising n-alkanes up to C_{60} once the bacteria had acclimated to HMW alkanes.

3.1 Introduction

3.1.1 General

The role of microbial degradation in the alteration and removal of petroleum hydrocarbons from the environment has long been realised (*e.g.* **Dennis, 1959**; reviewed by **Kallio, 1982; Connan, 1984**) but this area of knowledge is enjoying the renewed interest of scientists because of its importance in bioremediation of polluted environments (**Aldous, 1991**; **Atlas, 1991**; **Venosa *et al.*, 1992**). The study of microbial degradation (biodegradation or biotransformation) is also of continuing interest in petroleum geochemistry, particularly due to its importance in the formation of heavy crude (**Connan, 1984, Kallio 1982**).

Biodegradation is one of the major processes involved in the modification or "weathering" of spilled crude oil (**Atlas and Bartha, 1992**). Indeed, along with dissolution, evaporation and photopolymerisation, the alteration of crude oil residues by microbes is a major process in the formation of tar balls, the long-term visible products of the aftermath of oil spills. Nonetheless, despite the common occurrence of tar balls on beaches worldwide (**Golik, 1992**), few studies have reported a detailed compositional analysis, due partly to the relatively high molecular weight of the residues which are not amenable to chromatographic analysis (*i.e.* conventional capillary gas chromatography). Similarly, laboratory studies of the involvement of microbes in tar ball formation have rarely included examination of the quantitatively important HMW residues, again due to the absence or relative incapacity of suitable analytical techniques. The analysis of hydrocarbons with boiling points greater than *n*-C_{35} has recently been made easier with the introduction of high temperature capillary columns (as described in Chapter One).

3.1.2 Tar ball formation and fate

The beaching of tar balls along the shorelines of the world is a common occurrence and has been the subject of active research since at least the late 1950's. Most studies have focused on tar found on western beaches, including those of Florida (**Dennis, 1959, Curtis and Saner, 1974**), Bermuda (**Butler *et al.*, 1973**), Barbados (**Corbin *et***

al., 1993) and Texas (Ray *et al.*, (1974). Other studies have also been undertaken in the Mediterranean (UNEP, 1980), Israel (Golik, 1982; Golik and Rosenberg, 1987), Saudi Arabia (Fayad, 1986) and Africa (Okera, 1974; Shannon and Chapman, 1983).

Tar balls found on beaches result from the weathering of oil originally spilled into the sea. The amount of petroleum hydrocarbons entering the marine environment is difficult to calculate but is estimated to be around 2.5 m t yr^{-1} (Clark, 1992). The main inputs of petroleum hydrocarbons are by accidental or deliberate spillage or natural seepage. The major sources are shown in Figure 3-1.

Deliberate or accidental inputs usually occur during oil transportation. Clark (1992) calculated the world production of crude oil to be about 3 b t yr^{-1} of which half is transported by sea. The major shipping routes are shown in Figure 3-2 A. The main input of oil to the marine environment is from bilge and fuel oils. When travelling unladen or during poor weather conditions it is necessary for ships to take on ballast. Ballast tanks are usually small to allow for maximum cargo capacity so additional ballast is often carried in the empty fuel tanks and this may become contaminated. Also, shipping needs to pump out bilge water that has collected, which is usually contaminated with fuel oil from the engines. Although as a point source for pollution, contamination of this kind is small, since all shipping contributes, the total amount of oil entering the sea is considerable *e.g.* 0.252 m t yr^{-1} in 1989 (Clark, 1992, Figure 3-1) Other tanker operations including the cleaning of the contaminated ballast water and residual oil from the sides of the oil storage compartments, account for approximately 0.16 m t yr^{-1} (Figure 3-1).

Accidental spillage is also an important route by which oil enters the marine environment. Single tanker accidents can release large amounts of oil. For example, the *Exxon Valdez* released 35 000 t of oil into Prince William Sound, Alaska, in March 1989 (Kvenvolden, 1993) and more recently the *Braer*, which ran aground at Garth Ness in Shetlands, released 85 000 t of crude (Wolff *et al.*, 1993). Non-tanker shipping accidents also release oil into the environment. Some cargo ships, particularly bulk

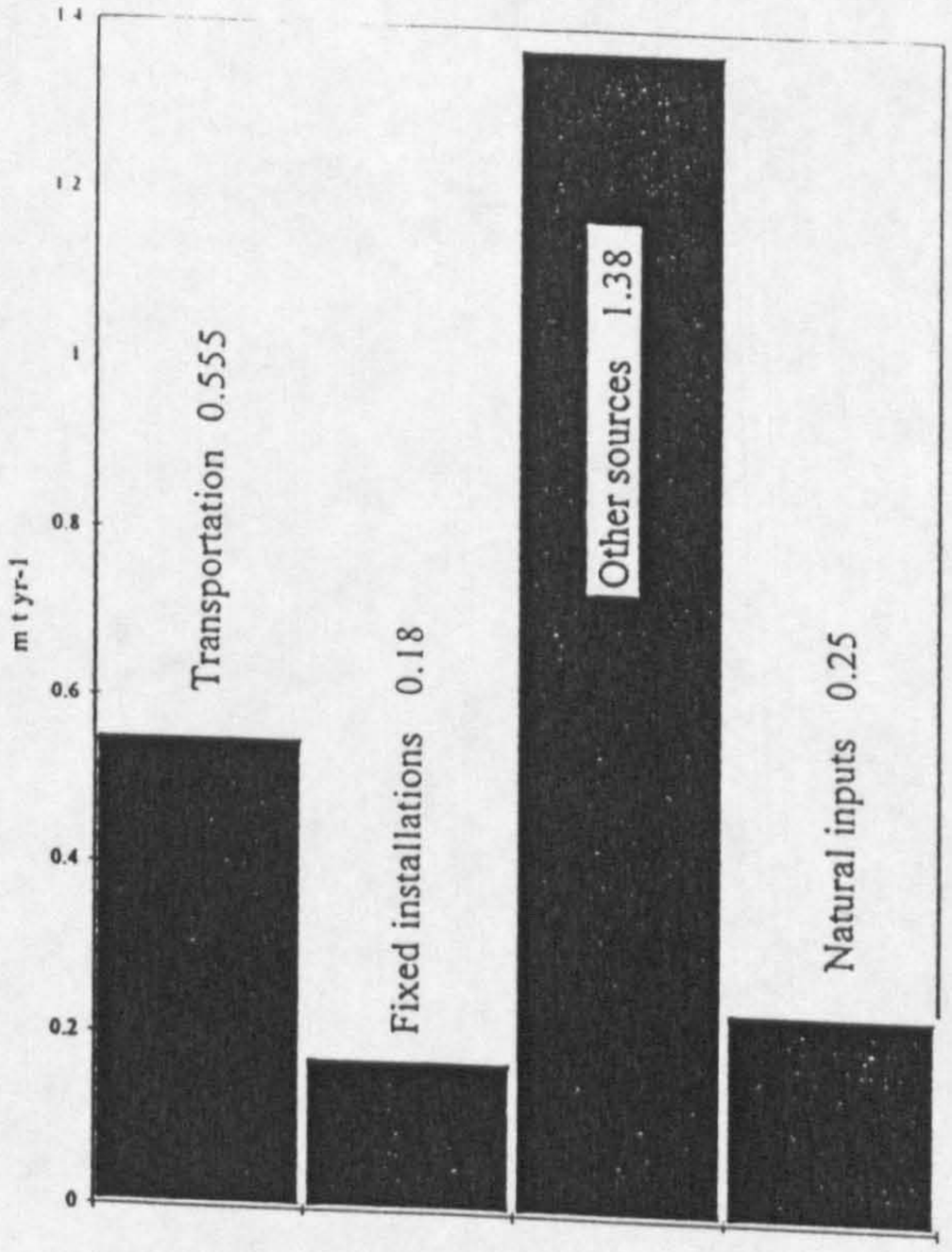

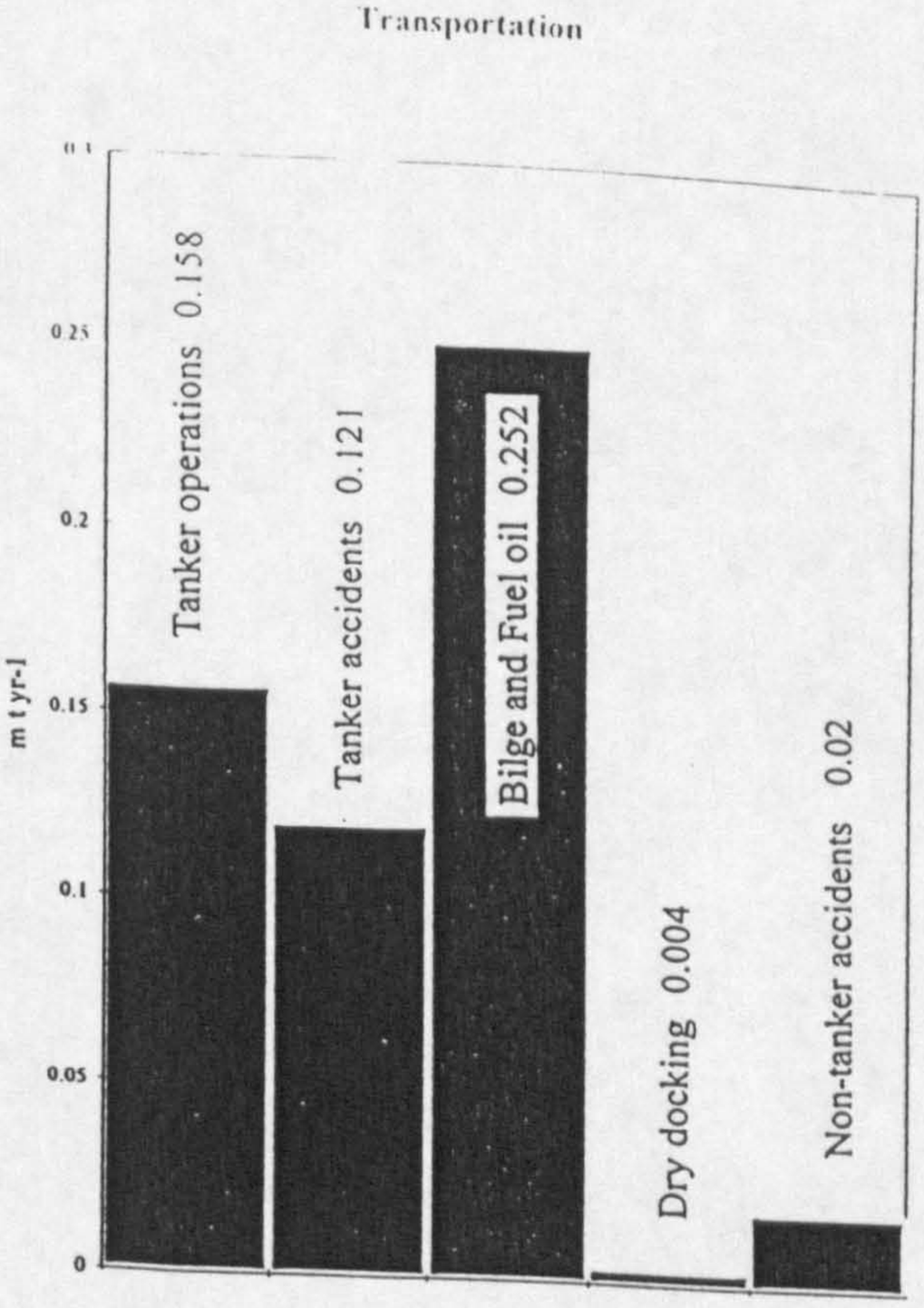

Fixed Installations

Other Sources

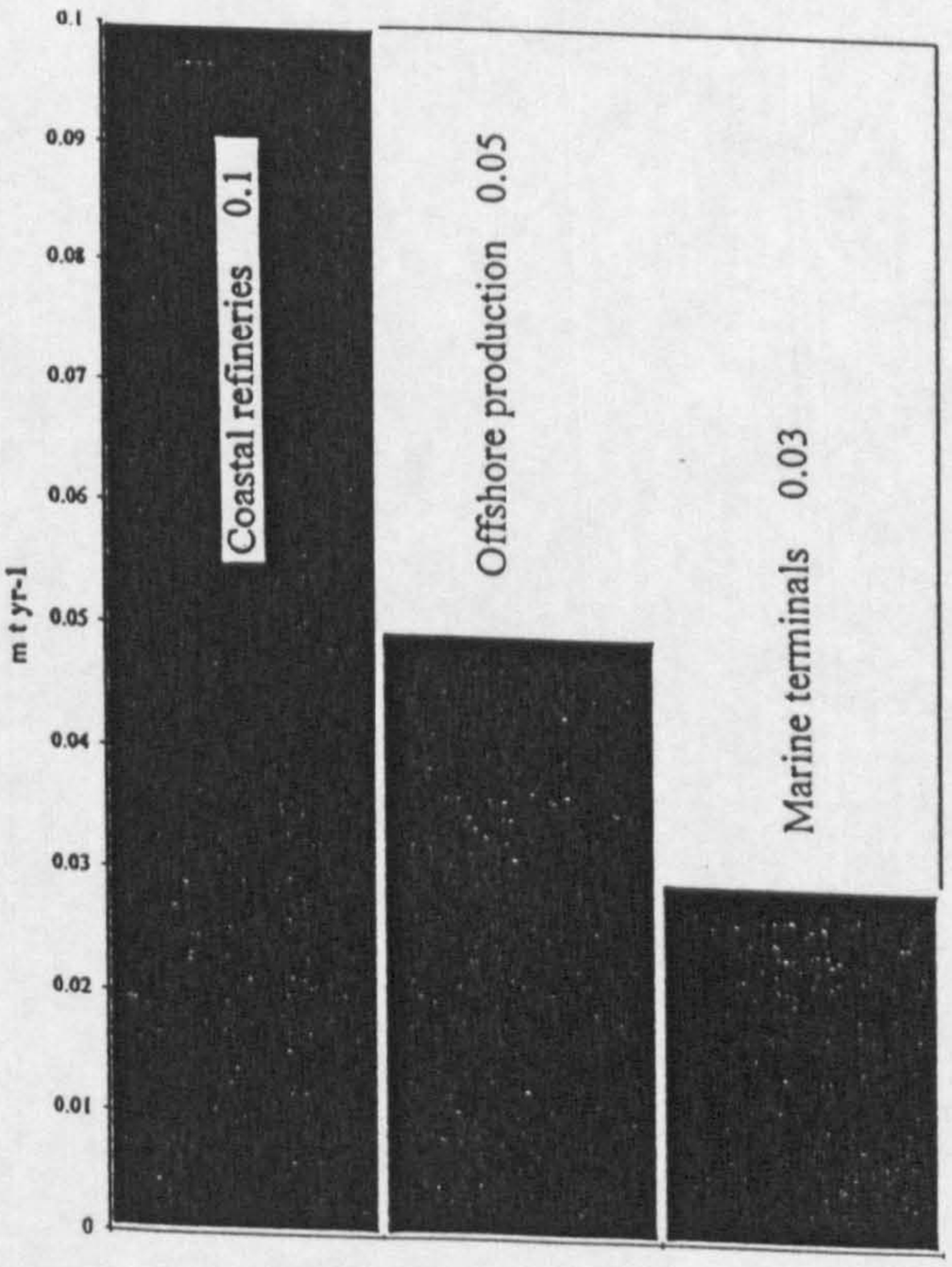

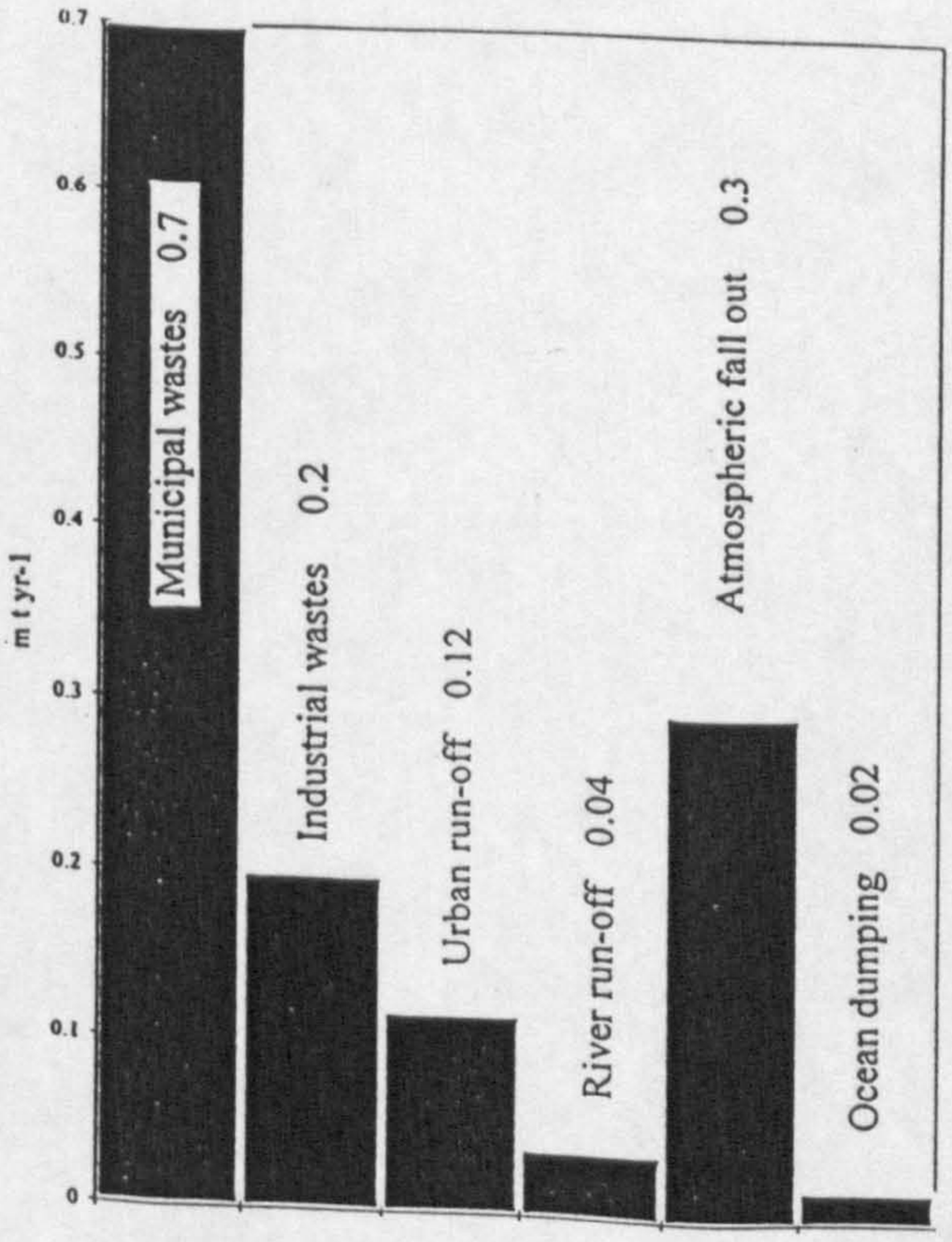

Figure 3-1 Major sources of oil entering the marine environment (adapted from **Clark, 1992**).

A

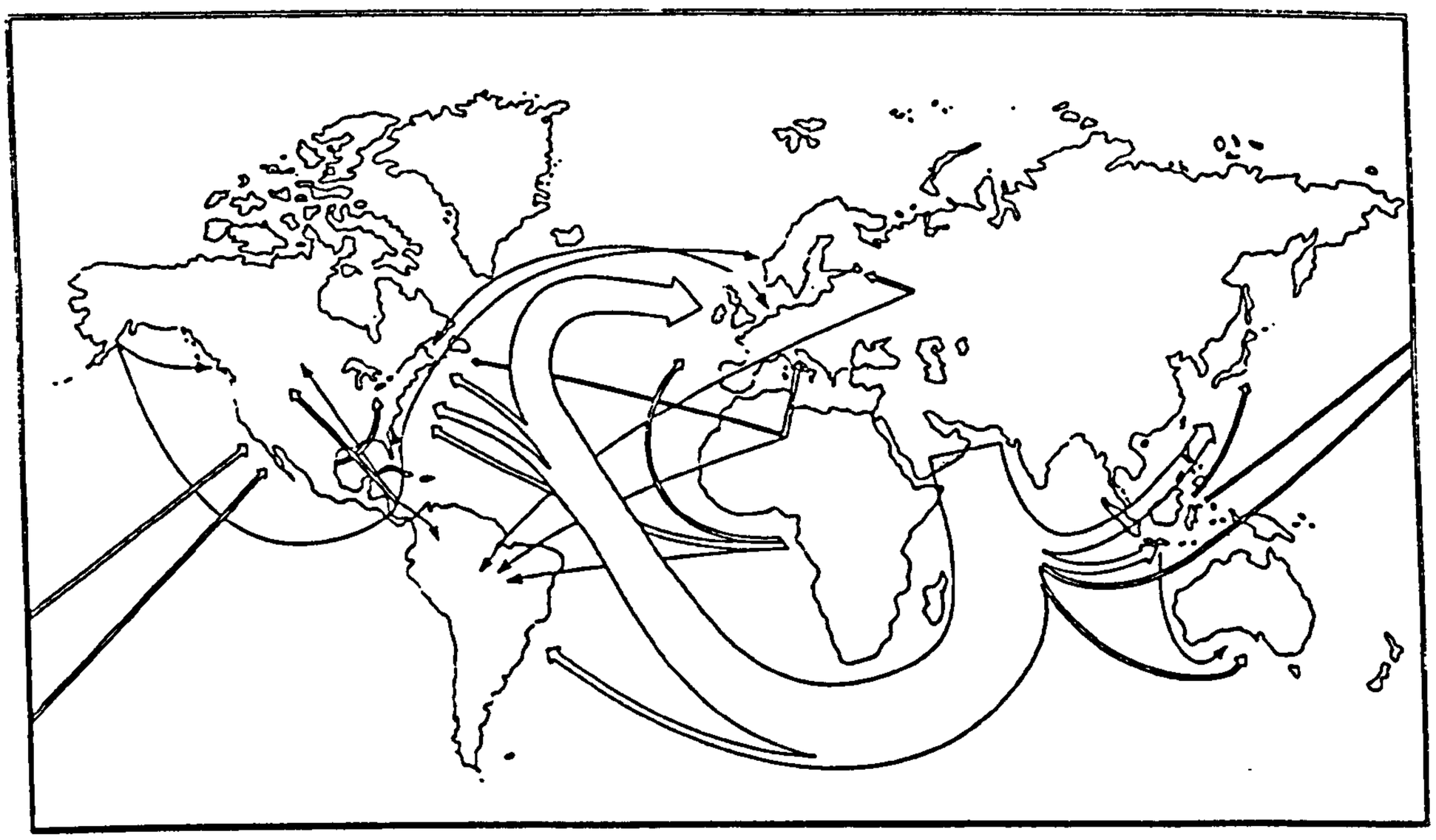

B

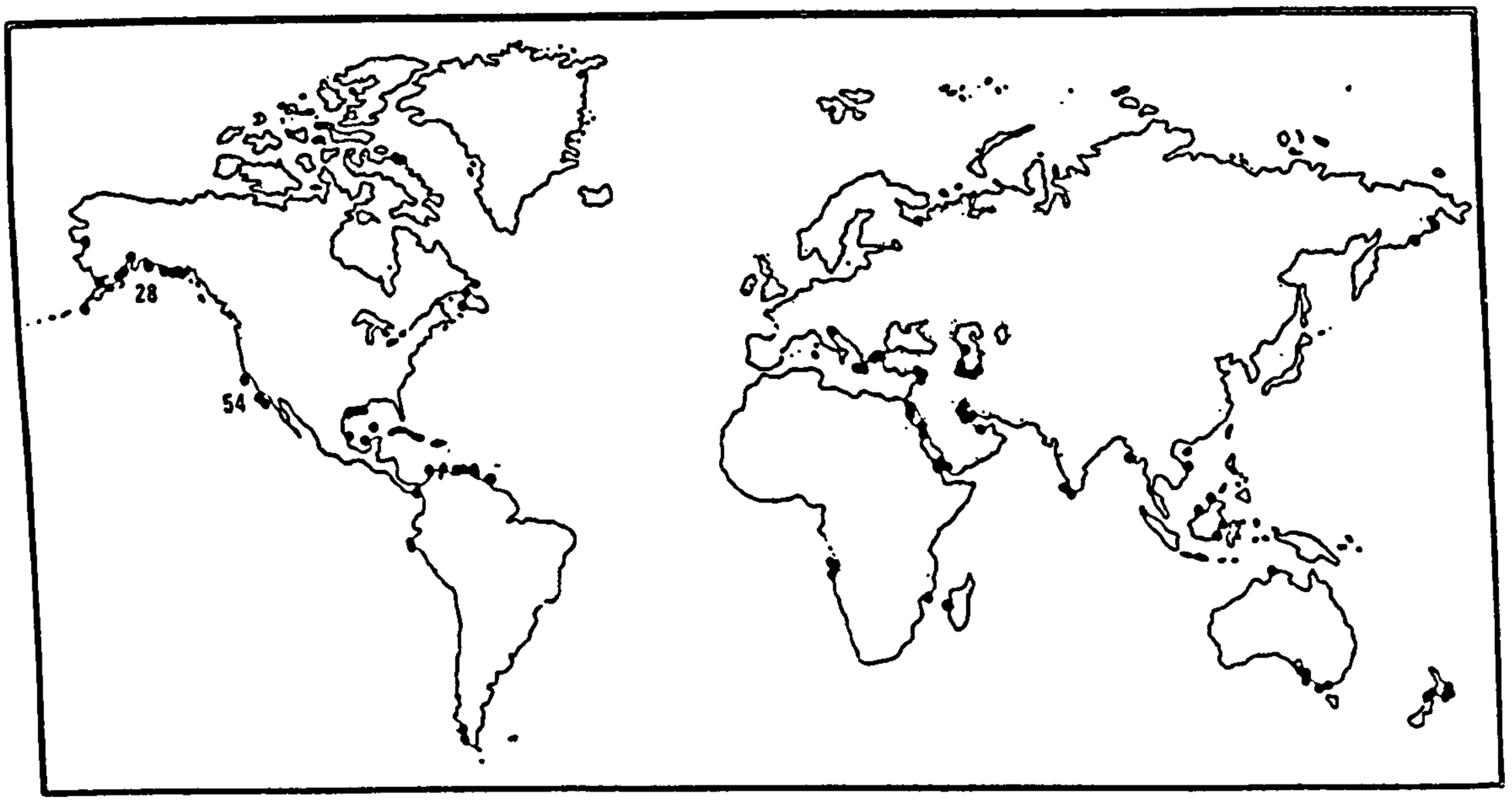

Figure 3-2 A) Major oil shipping routes and B) major natural oil seeps (adapted from **Clark, 1992**).

carriers, are now very large and releases from these should also be taken into account **(Clark, 1992)**.

Natural oil seeps are a significant input of oil into the world's oceans. Oil deposits close to the earth's surface have been seeping oil for many thousands of years. They occur in many parts of the world. The most important known seeps are shown in Figure 3-2, B.

Whatever the route of entry of oil into the marine environment it will immediately undergo changes caused by physical, chemical and macro/micro biological processes acting upon it (summarised in Figure 3-3). These processes occur on different timescales ranging from minutes to years (Figure 3-4). Evaporation, and some dissolution, occurs within hours of a spill, while biodegradation may take months or even years. As the lighter fractions of these oils are dissipated by dissolution, evaporation, and photo-oxidation, the viscosity of the residue is increased and the more viscous "oil" may eventually break up to form particulates which can range in size from 1 mm to greater than 10 cm. These petroleum particulate residues are called "tar balls". It has been estimated that 10-30% of all oil discharged to the sea remains in this form **(Hoult, 1985)**. The shape of the tar balls results in a reduction of their surface area and the outer surface photopolymerises rapidly to form a hard skin. This may slow significantly the processes of further weathering such that tar balls remain in the environment for many years. Even so, if these tar balls have been in the environment for a considerable time then they are likely to have undergone significant microbial degradation.

Tar balls in the ocean are carried by the winds, currents and waves and may eventually be washed ashore. **Golik (1981)**, in a study of tar balls washed up on the coast of Israel, found that they were eventually moved inland with rising tides, and each successive higher tide, wave or storm caused an increased landwards movement. Finally many were buried and remained as fossil deposits. Rivers valleys or other topographical depressions also serve as final traps for stranded tar. Once stranded, tar balls may continue to weather, shrink and become increasingly fissured. Eventually they may disintegrate into small fragments and be further dispersed by winds.

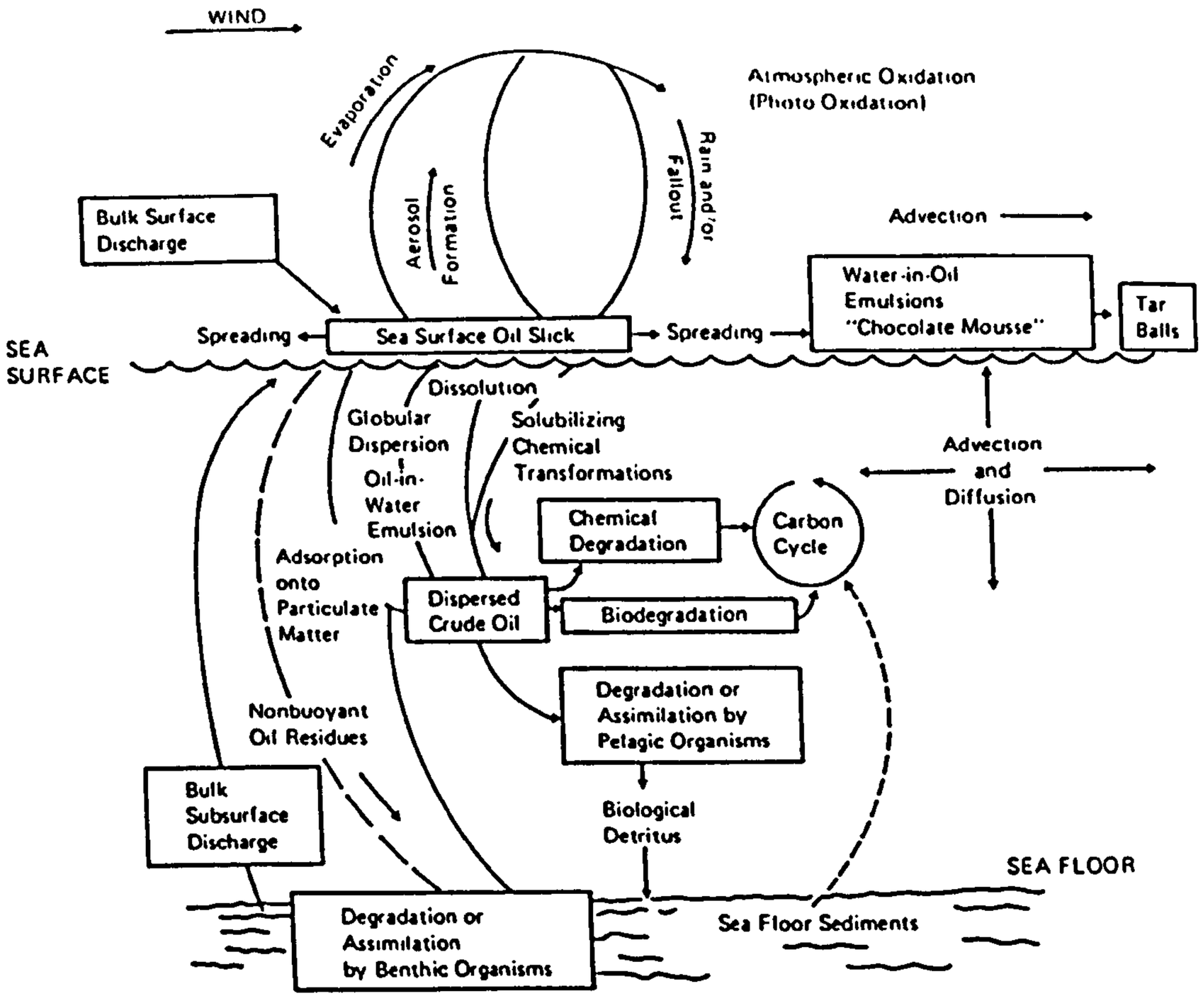

Figure 3-3 Overview of physical, chemical, and biological processes (adapted from **Burwood and Speers, 1974**).

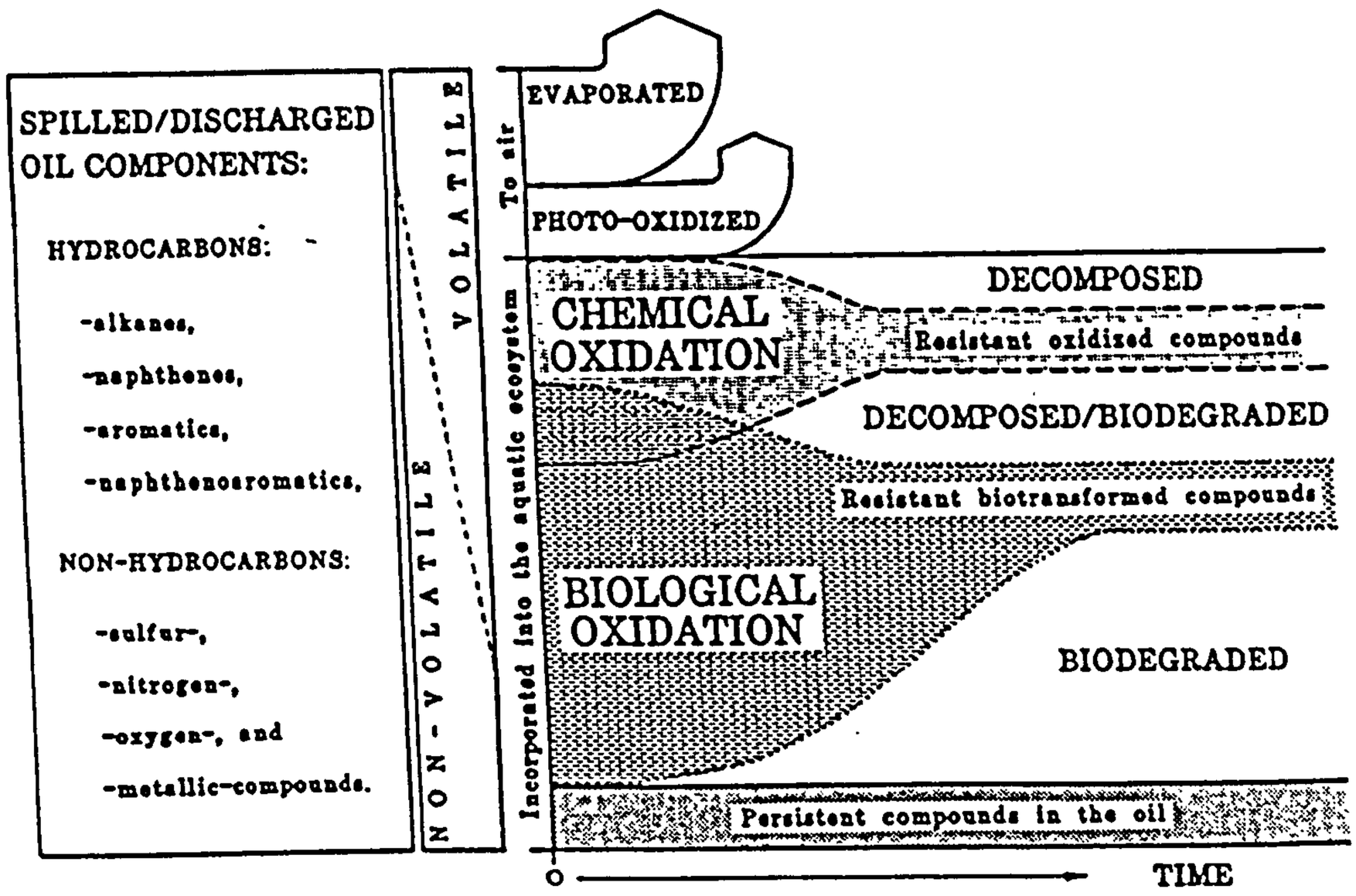

Figure 3-4 Changes in oil composition during environmental weathering with time of spilled/discharged oil as a result of physical, chemical and biological weathering process (**Literathy *et al.*, 1989**).

One recent study (**McKirdy 1994**), aimed to discover the origin of tar ball deposits along the coastlines of South Australia and Western Victoria (Figure 3-5). The tar deposits consisted of lumps of weathered waxy crude oil and black asphaltic material found mainly at the high water mark of sandy beaches. Fossil tars were also discovered within blowouts in Holocene dune deposits. The initial hypothesis put forward was that these tar deposits originated from nearby offshore oil and gas seeps (Otway and Duntroon basins), because the amount of tar washed ashore seemed to correlate with increases in local earthquake activity. It was later proposed that the tar deposits and other coastal bitumens found on the south coast of Western Australia and the north coast of the Northern Territory arose from the long distance marine transport of waxy crude oils from Indonesia and related areas (Figure 3-6).

McKirdy, (1994) pointed out that in order to understand the origin of these tar balls, it is essential to document their physical properties and chemical compositions. It is also important to understand the changes that have occurred to these tar deposits due to weathering processes. In particular, microbial degradation, which can significantly alter the composition of the original oil from when it first enters the marine environment, should be considered.

3.1.3 Microbial degradation of petroleum hydrocarbons

When hydrocarbons in a complex mixture such as petroleum are made available to a microbial community, biodegradation of most petroleum components occurs simultaneously, but at widely differing rates. Biodegradation of *n*-alkanes is most rapid, followed closely by alteration of simple aromatic components. Branched alkanes, cyclo-alkanes, isoprenoids and condensed aromatic compounds are degraded more slowly **(Ratledge 1979; Singer and Finnerty, 1984)**. Hydrocarbons also influence the degradation of other components indirectly through co-metabolism. Co-metabolism is defined by **Foster (1962)** as those conditions pertaining where "non-growth hydrocarbons are oxidised when present as a co-substrate in a medium in which one or more different hydrocarbons are furnished for growth".

Physical properties have an important influence on the biotransformation rates of hydrocarbons. For example, short chain *n*-alkanes, those with fewer than nine carbons

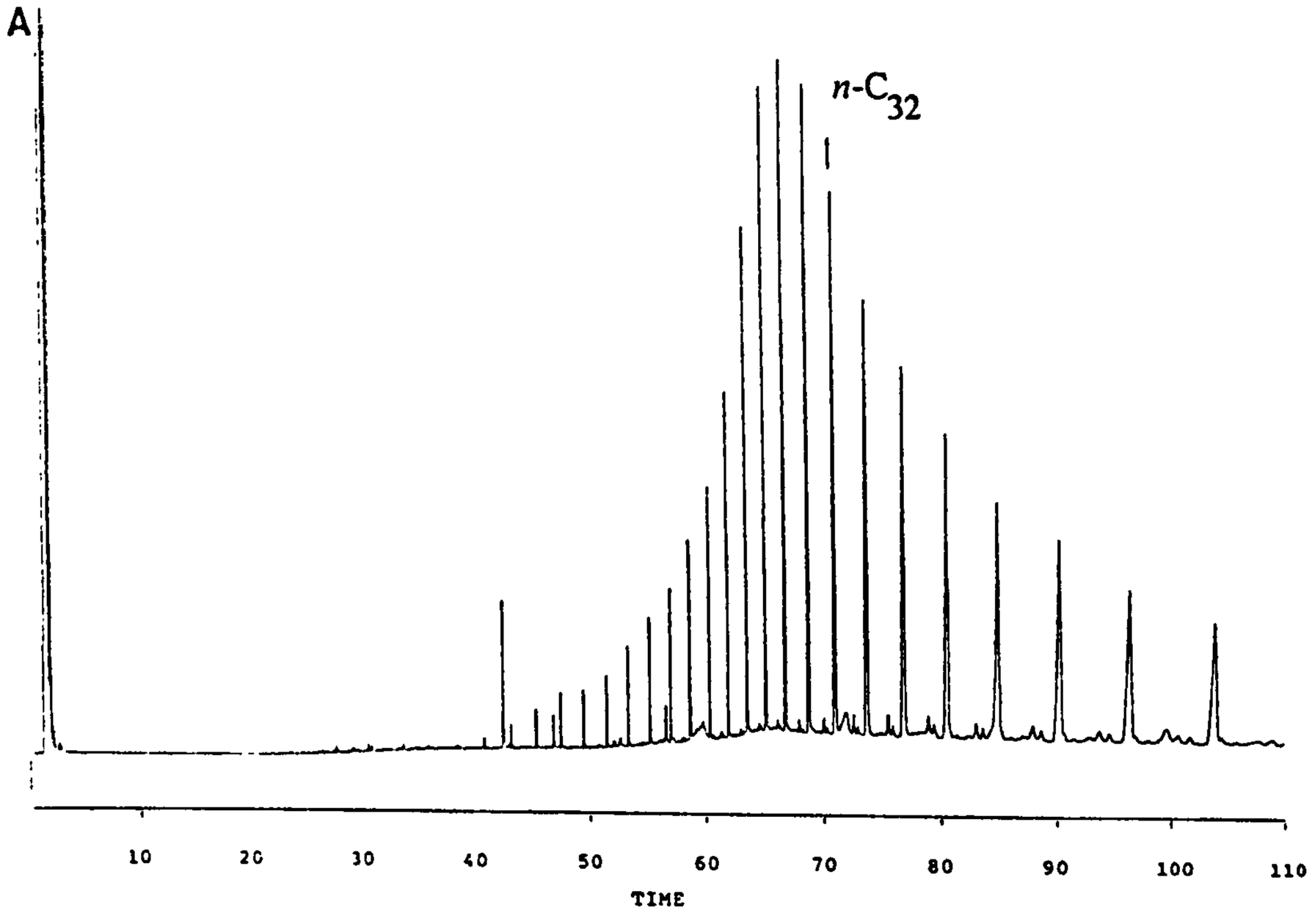

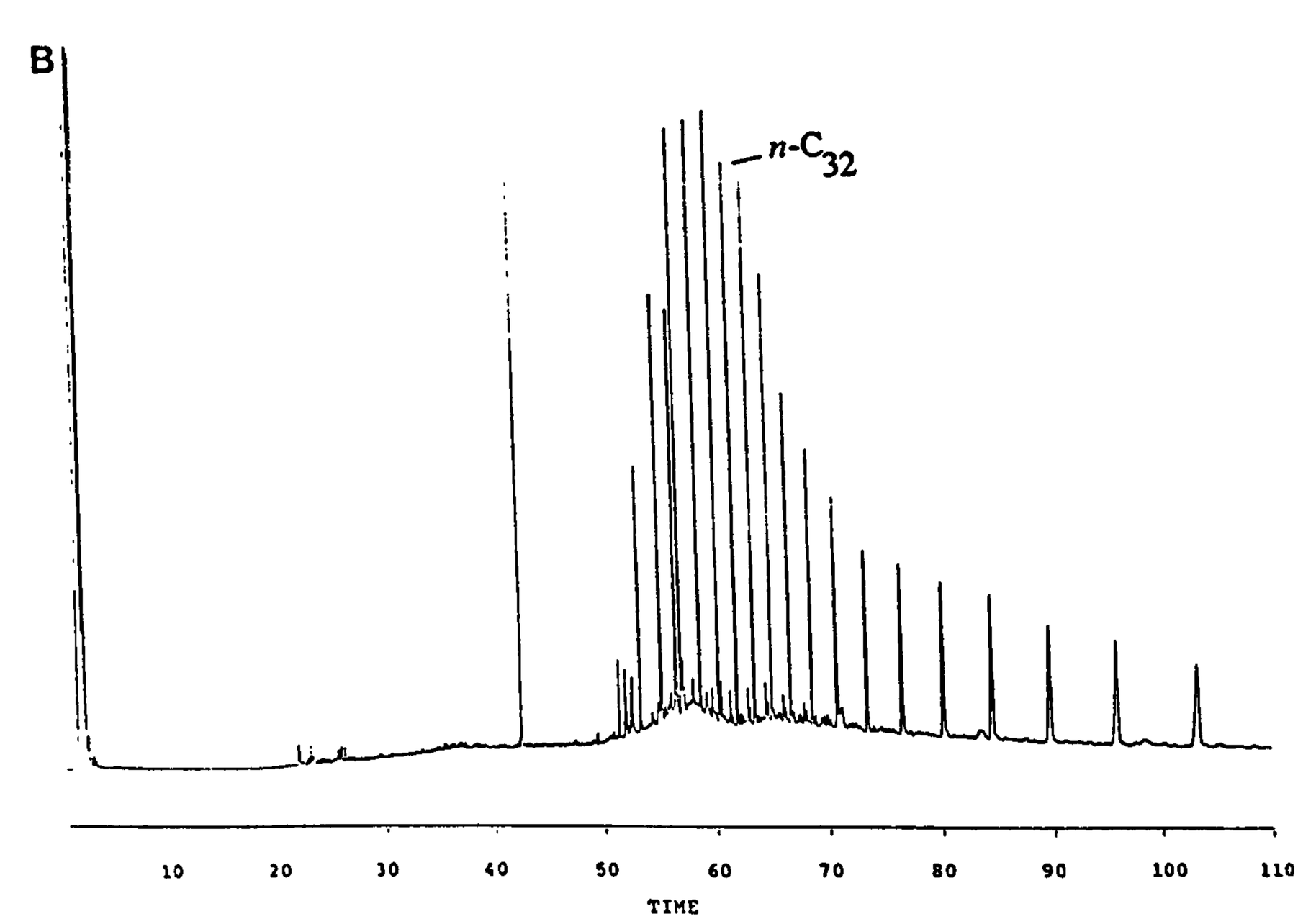

Figure 3-5 Gas chromatograms of tar balls collected from the coastline of South Australia (**Padley *et al.*, 1991**).

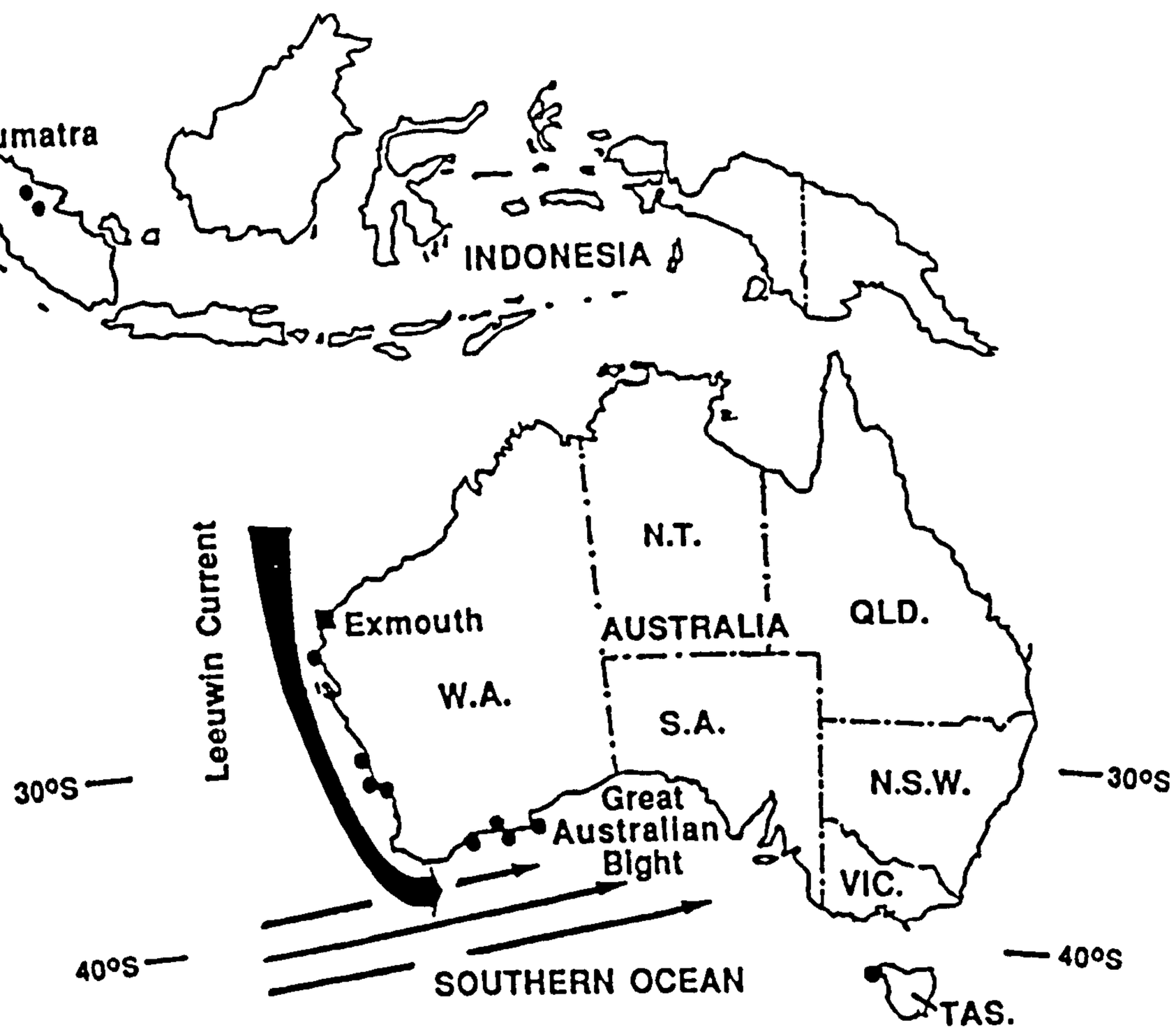

Figure 3-6 Map showing locations of stranded tar and the path of the Leeuwin Current (adapted from **Currie *et al.*, 1992**).

which are mainly liquids at common environmental pressure and temperature, are toxic to most bacteria and are only utilised by a few organisms **(Ratledge, 1979; Swaranjit *et al.*, 1990)**. This toxicity is linked to their greater solubility in water. A high concentration is thought to cause disorganisation of the cytoplasmic cell membrane resulting mainly from non-specific effects on proteins, including those associated with transport and oxidation. When *n*-alkanes with chain lengths greater than nine carbons are present, the toxicity of the shorter chain alkanes is decreased because either their solubility is reduced by partitioning between the larger hydrocarbons and the aqueous phase or they may be co-oxidised or co-metabolised. Such synergistic effects partly explain how microorganisms are able to grow on the complex hydrocarbon mixtures that are crude oils.

As the chain length increases beyond that of nonane (n-C_9) the rate of bacterial growth usually increases. **Setti *et al.*, (1993)** proposed two different degradation patterns, one for liquid *n*-alkanes (n-C_{13} to n-C_{16}), *n*-hexadecane being the highest molecular weight *n*-alkane that is still liquid at room temperature, and another for those *n*-alkanes with greater than 17 carbon atoms. The authors then further subdivided biodegradation within the solid *n*-alkanes. The first *n*-alkane sub-group included those between n-$C_{17\text{-}27}$ which showed a constant degradation rate over the entire range of compounds, while for the second group comprising n-$C_{28\text{-}35}$ alkanes, the biodegradation rate was found to decrease with increasing hydrocarbon chain length.

Setti *et al.*, (1993) explained these observations by stating that the microbial degradation of aliphatic hydrocarbons was not only a function of their chemical and physical properties but also of biological factors. The latter included enzyme activity (substrate reactivity and affinity). Physical and chemical effects include water solubility, emulsification and the surface tension of the substrate. As previously mentioned, lower chain *n*-alkanes are more soluble in aqueous phases and the solubility decreases with increasing molecular weight. **Setti *et al.*, (1993)** reported that the biodegradation of low molecular weight solid *n*-alkanes is correlated with the carrier effect of the liquid *n*-alkanes. The much slower microbial degradation of so called "high" solid *n*-alkanes ($>n$-C_{28}) is thought to be a function of the steric hindrance of the large paraffinic

molecules to the bacterial enzymes.

3.1.4 Degradation pathways of aliphatic hydrocarbons

Of the studies that have investigated the microbial degradation of solid *n*-alkanes, there is still some argument as to whether bound bacterial cells (*i.e.* cells that are attached to the substrate) and/or free cells are more metabolically active. **Chakravarty et al., (1972)** noted that cells of a *Pseudomonas* species did not usually adhere to solid paraffin particles and suggested that growth and substrate uptake resulted primarily from the utilisation of solubilized substrate in the aqueous phase. This was also a view supported by **Cameotra, (1983)** and **Reddy *et al.*, (1982)**. **Zilber *et al.*, (1980)** showed, using microscopy, that cultures of a Pseudomonad UP-2 growing on *n*-tetracosane (*n*-C_{24}) contained both free cells and cells actually bound to the surface of solid hydrocarbon particulates. During the early exponential growth phase, over 80% of the cells were bound to large pieces of the *n*-alkane substrate. Experiments also showed that growth occurred both on the surface of the solid substrate and in the aqueous medium. The use of electron microscopy has also shown paraffinic inclusions within bacterial cells **(Scott and Finnerty, 1976)**. The physical size of the substrate may also be a limiting factor and micro-micelles formation may play an important role in substrate uptake. The authors suggest that the hydrocarbons are absorbed directly into the lipophilic areas of the cell membrane. Whatever the mechanism of assimilation of *n*-alkanes by microorganisms this is only the first step in their metabolism. The microbiological degradation pathways of petroleum hydrocarbons have been extensively studied (see reviews by **Atlas, 1984** and **Ratledge, 1979**).

3.1.5 Microbial degradation of solid long chain *n*-alkanes greater than *n*-C_{35}

In tar balls that have been in the environment for a considerable time most of the lighter material will have been removed by weathering including biodegradation, so knowledge about the heavier hydrocarbons may be the only useful source of information concerning their origins. It is therefore clear that the effects of microbial action on these HMW compounds ($>n$-C_{35}) must be better understood. However, the microbiological

Table 3-1 Results of biodegradability of waxes and wax blends (Taken from **Hanstveit, 1992**).

Sample	% degradation (mean values)				
	28 days			84 days	
	I	II	III	II	III
paraffin wax 50/52	80	78	84	85	89
paraffin wax 58/60	79				
paraffin wax 58/60 + antioxidant (0.01% BHT)	82				
paraffin wax 58/60 + ethyl-vinyl-acetate + antioxidant (0.075% BHT)	83 (92)[a]				
paraffin wax 58/60 + poly-ethylene	75 (83)[a]				
paraffin wax 58/60 + C-5 resin + antioxidant (0.2% Irganox 1076)	75 (84)[a]				
intermediate wax 66/68		66		77	
microcrystalline wax		21		25	
microcrystalline wax + C-5 resin		18 (20)[a]	21 (23)[a]	22 (25)[a]	30 (34)[a]
beeswax		67		79	

a) *corrected for the amount of synthetic polymer.*

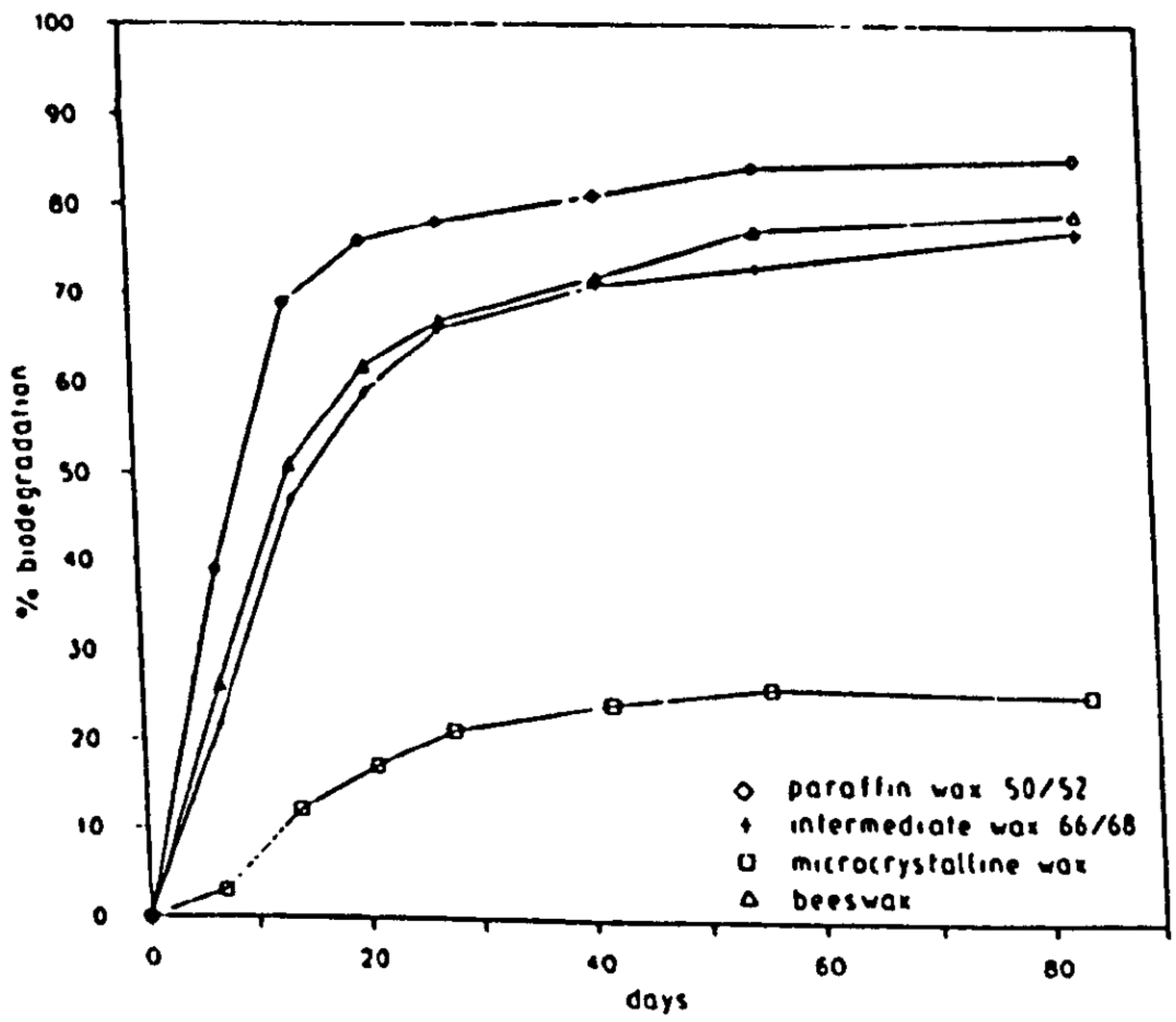

Figure 3-7 Biodegradation of intermediate wax, microcrystalline wax, beeswax and paraffin wax 50/52 in a CO_2 evolution test (taken from **Hanstveit, 1992**).

degradation of *n*-alkanes and other hydrocarbons with boiling points above that of *n*-C_{35} has rarely been reported. One reason for this is the technical difficulty associated with the analysis of solid and insoluble substances (See Chapter 4). In one of the few studies that appear to have been made **Hanstveit (1992),** investigated the potential degradability of petroleum (C_{18-50}), intermediate (C_{22}-C_{60}) and microcrystalline (C_{23}-C_{85}) waxes to discover if they might be environmentally more acceptable alternatives to the persistent polymers currently in use as packaging materials. This appears to be the only study which has examined the effect of microbial degradation of *n*-alkanes greater than *n*-C_{44}. Hanstveit monitored the amount of *n*-alkane degradation by measuring CO_2 evolution with time and analysing the residues by high temperature capillary gas chromatography (HTCGC). The experiment was carried out in shake flasks equipped with CO_2 traps, mineral media and inoculated with a bacterial culture that had been isolated from contaminated soil from a land farm treatment project. The wax samples were adsorbed to glass fibre filters to create a large surface area:volume ratio to enhance the degradation. The cultures were incubated for periods of 28 and 84 days.

Results (Table 3-1 in graphical form Figure 3-7) showed that >60% of the paraffin (C_{24}-C_{60}), and intermediate (C_{23}-C_{85}) waxes were degraded within 28 days incubation. The microcrystalline wax (C_{23}-C_{85}) was degraded more slowly; 21% within 28 days and only a further 4% within 84 days. The rapid degradation phase (Figure 3-7), when microbial growth is presumably also fastest, had ended by two weeks for the microcrystalline wax substrate, but extended for four weeks in the case of intermediate and paraffin substrate. This can be explained by the higher proportion of lower molecular weight hydrocarbons which can sustain an increasing bacterial population in the petroleum wax.

Chromatograms from HTCGC (Figure 3-8) analysis showed that a large proportion of the hydrocarbons up to *n*-C_{40} had been removed. Unfortunately no quantitative data were reported, and the author stated simply that *n*-alkanes up to *n*-C_{50} were completely or partially degradable in petroleum wax. In the microcrystalline wax only *n*-alkanes < *n*-C_{43} were degraded. Although this was an interesting and provocative study which raised important new questions about the degradability of HMW *n*-alkanes, the lack of

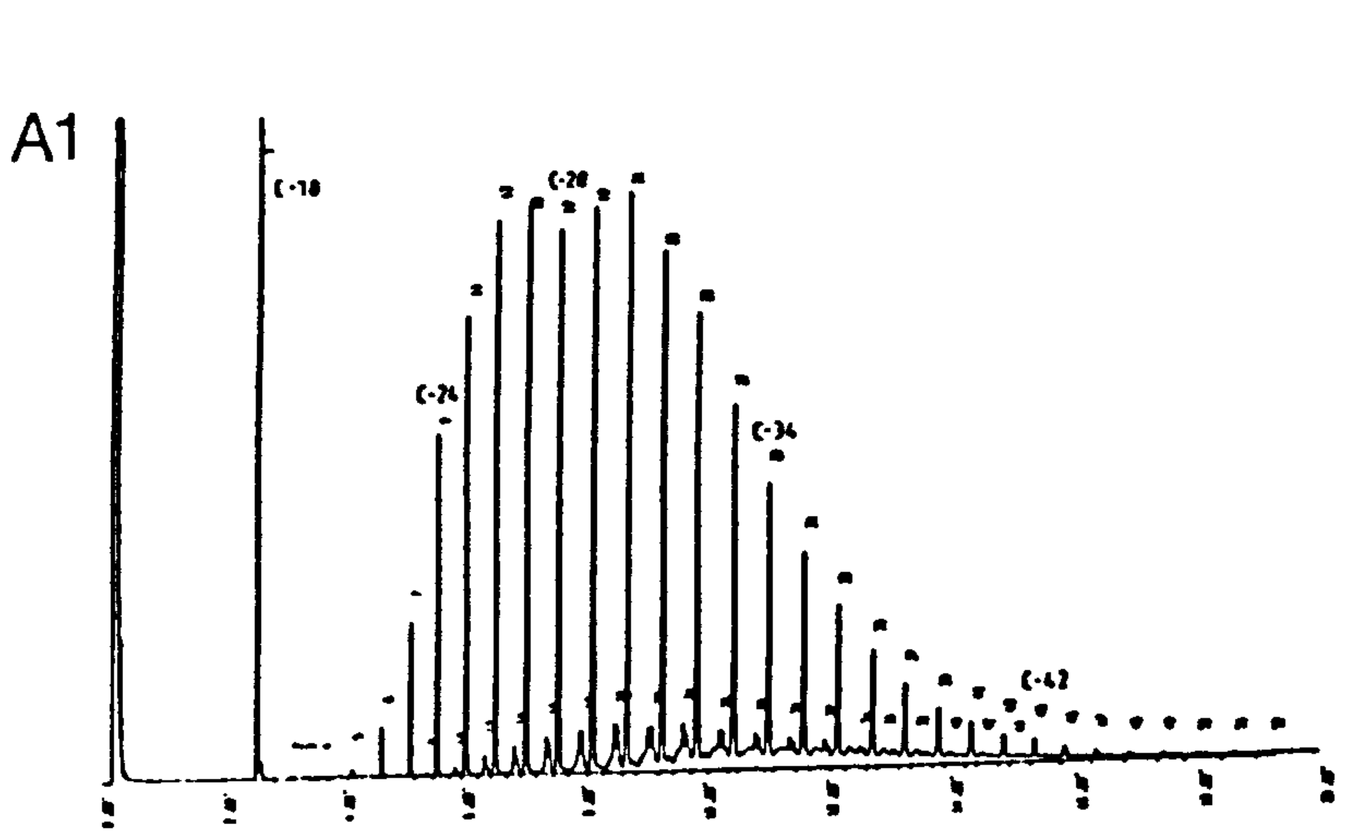

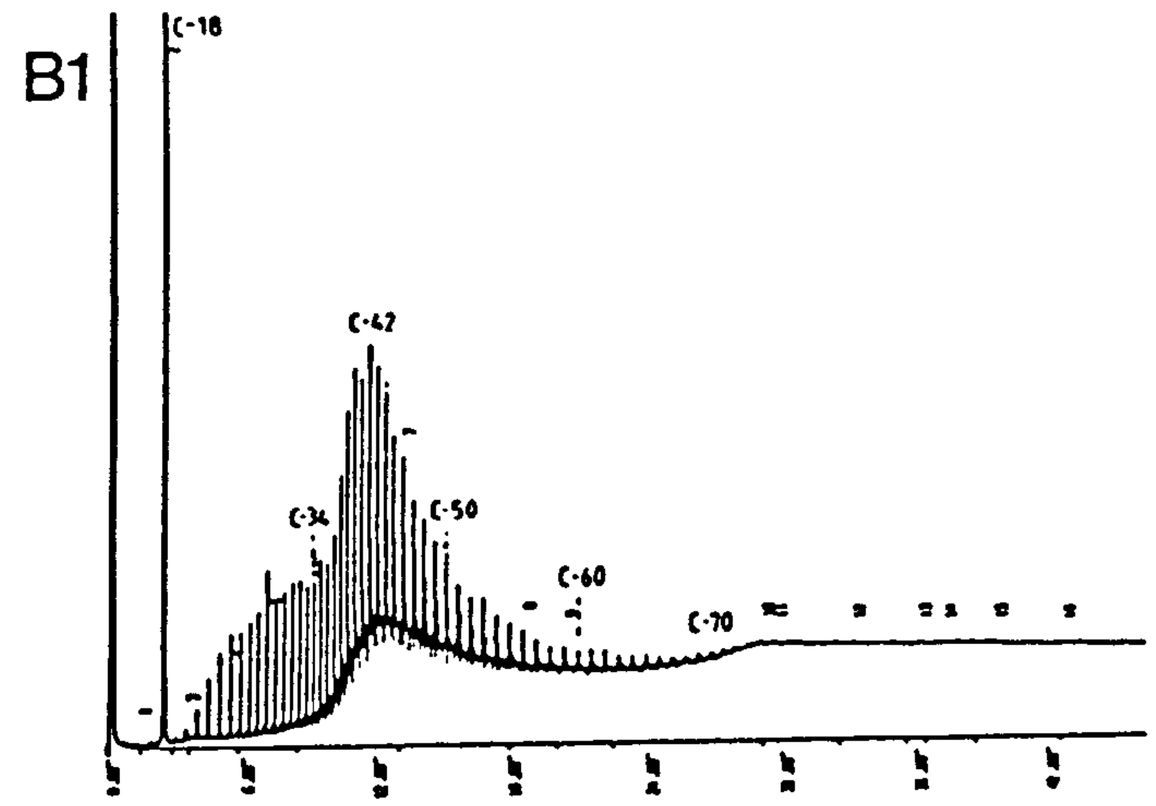

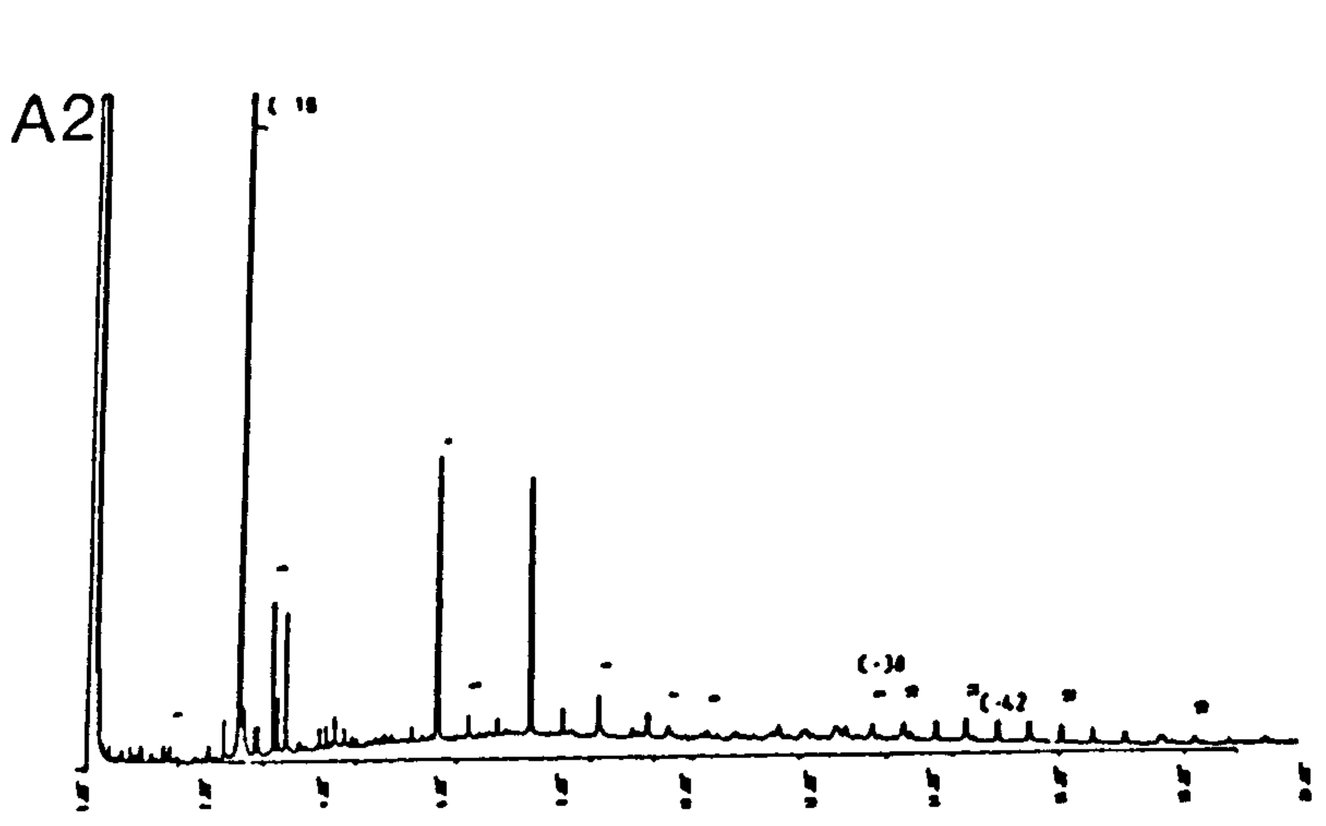

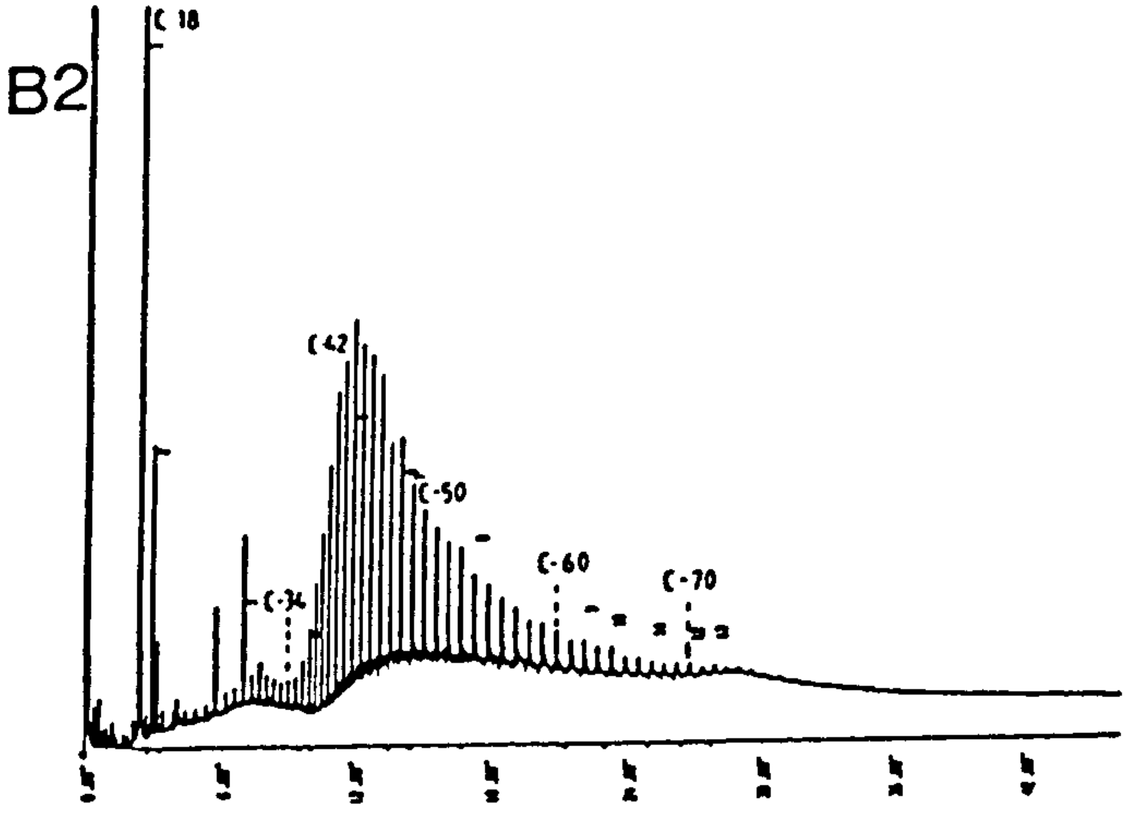

Figure 3-8 HTCGC of paraffin wax at the start (A1), and the end of the 28 day biodegradation test (A2) and microcrystalline wax at the start (B1) and after 84 days of incubation (B2) **(Hanstveit, 1992).**

quantitative data, the probable errors in HTCGC analysis (estimated herein in Chapter One) and the absence of reproducibility data, all suggest that the experiment would bear repetition with careful attention to the analytical detail. The errors in the reproducibility of GC injections for *n*-alkanes above *n*-C_{40} (see Chapter One) may be high and the response factors between heavy analytes ($>$*n*-C_{40}) and light *n*-alkanes such as *n*-C_{18} can be less than one. The low solubility of *n*-alkanes greater than *n*-C_{40}, even in organic solvents, casts doubt as to whether these compounds were effectively removed from the filters used by **Hanstveit (1992)**. Furthermore, losses occurring during work up may be large since LMW *n*-alkanes such as *n*-C_{18} may be more easily extracted into organic solvents than the HMW analytes.

3.2 Aims

The aims of the present study, were therefore, to isolate the aliphatic hydrocarbons of a waxy crude oil from Indonesia and to study the rate of biodegradation of the *n*-alkanes up to *n*-hexacontane using the quantitative HTCGC techniques developed earlier (Chapter One) in order to investigate the theory (**McKirdy, 1994**, and references therein) that Indonesian oils are the source of the tar balls and palaeo-tar balls found on the coasts of North, West and South Australia.

Particular emphasis was placed on validation of the techniques for reproducible recovery and analysis of high molecular weight (C_{35}-C_{60}) *n*-alkanes from the biodegradation media. Such studies have not been possible prior to the advent of HTCGC.

3.3 Results and Discussion

3.3.1 HTCGC Analysis of *n*-C_{20} to *n*-C_{60} alkanes

Quantitative analysis of the biodegradation of HMW *n*-alkanes requires prior validation of the HTCGC analytical methods. Thus the response factors of a series of authentic *n*-alkanes (*n*-C_{20} to *n*-C_{60}; Figure 3-9) were measured (each five times) relative to squalane (internal standard) after manual on-column injection of solutions in cyclohexane at 55°C (see also Chapter One). The results are given in Table 3-2 along with standard deviations of the replicate measurements.

Response factors (RF) were very close to unity for all the *n*-alkanes except *n*-C_{30} (RF 1.13). As expected, *n*-hexacontane showed the greatest variation between analyses with a standard deviation of 5%. This is probably due to the relatively low solubility of *n*-hexacontane in cyclohexane. Although the temperature of the solution was kept above the cloud point of *n*-hexacontane in cyclohexane (53°C) and the solution mixed thoroughly prior to injection, once the sample is drawn into the syringe barrel from the needle the temperature of the solution decreases. Indeed, a close examination of the sample within the syringe showed the formation of a waxy precipitate only a few seconds after the sample had been drawn up. It is thought that the solvent plug drawn into the syringe prior to the sample might have been insufficient to flush adequately all of the waxy material onto the column. This might be overcome with a heated auto-injector but with manual injection it was not practical to heat the syringe needle. Nonetheless the RF and reproducibility data were deemed adequate for the purpose of monitoring biodegradation and gave confidence in the data compared with the only previous study where no reproducibility data were reported **(Hanstveit, 1992)**.

3.3.2 Culture methodology

Designing a perfect microbiological degradation experiment is difficult. Use of a single bacterial species with a single substrate in surroundings ideal for growth rarely reflects conditions in the "real" environment and where studies often involve so many unknown variables that definitive interpretation of data is impossible. Whatever the scale of the experiment, it should be designed so that a good estimation of the errors

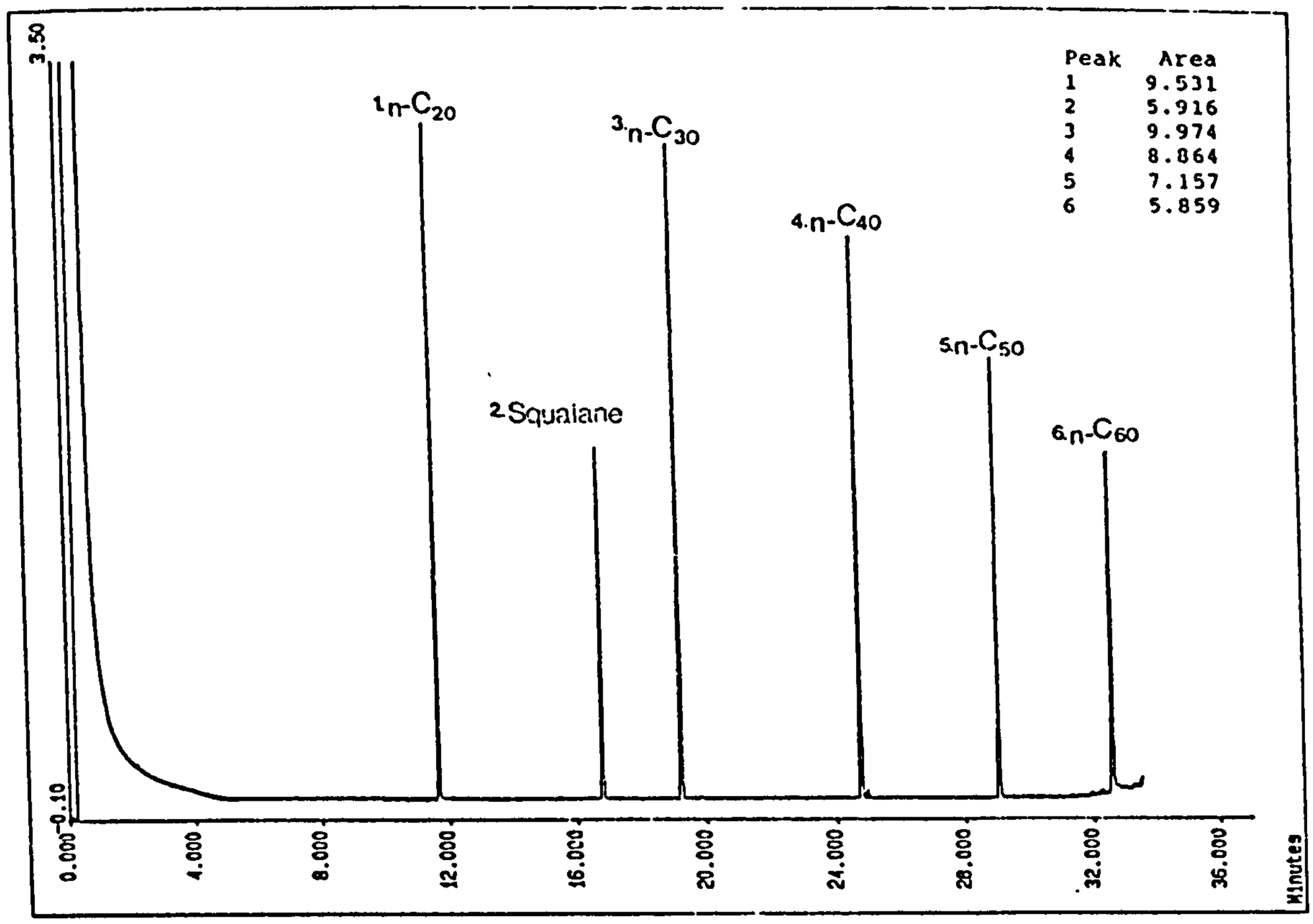

Figure 3-9 HTCGC of squalane co-injected with a mixture of *n*-alkane standards.

Table 3-2 Response factors for a series of *n*-alkanes relative to squalane (32 ng on-column) using manual on-column injection.

n-Alkane	n-C_{20}	n-C_{30}	n-C_{40}	n-C_{50}	n-C_{60}
Actual amount (ng)	50.7	53.7	49.2	38.8	32.0
Measured amount (ng)	51.5	53.6	48.0	38.7	31.6
	52.7	52.0	48.0	37.0	31.9
	51.2	54.0	47.5	36.5	32.3
	50.2	53.1	47.2	37.4	28.5
	51.6	52.9	48.0	37.4	31.1
mean	51.4	53.1	47.7	37.4	31.1
%	101.5	98.9	97.0	96.4	97.1
SD(n-1)	0.896	0.760	0.371	0.815	1.507
[1]RF	1.01	1.13	0.98	0.99	0.99

can be placed on the results. The time factor in an experiment of this kind is an important consideration, *n*-alkanes with fewer than twenty eight carbons are rapidly metabolised within a matter of days while *n*-alkanes with greater chain lengths are either partially or non-degraded over a period of two months (**Setti *et al.*, 1993**). The duration of the experiment must either allow time for the bacteria to degrade the HMW compounds, or the rate of microbial degradation must be accelerated.

Only two studies of high molecular weight ($>C_{35}$) *n*-alkane biodegradation have been published previously (**Setti *et al.*, 1993; Hanstveit, 1992**). Both noted that an important requirement for the utilisation of such insoluble compounds was a high surface:volume ratio of substrate. **Hanstveit, (1992)** achieved this by adsorbing samples of wax onto glass fibre filter papers; thus effectively increasing the surface area of the substrate while providing a solid support on which the bacteria could grow.

An experiment similar to that of **Hanstveit (1992)** was carried out herein using a series of glass fibre filters (Whatman) impregnated with a *n*-C_{20} to *n*-C_{60} alkane mixture (Figure 3-9). The filter papers were left in sealed flasks containing Milli-Q water for seven days. The flask contents were then extracted with warm hexane and dried using anhydrous Na_2SO_4. The extraction efficiency was then measured using squalane as an internal standard (see Experimental) and the results are given in Table 3-3. The extraction efficiency for the *n*-alkanes, *n*-C_{20} (82%) and *n*-C_{30} (78%) was poor but acceptable; however, extraction of the wax back from the filter papers proved discriminative against alkanes *n*-$C_{40\text{-}60}$ when compared with the non-adsorbed alkane mixture (Table 3-3). The efficiency for these HMW alkanes were less than 50% and as low as 18% percent for *n*-hexacontane (C_{60}). One reason for this discrimination was that during the seven day incubation period the filter papers became very soft and started to break up. This made the percolation of the solvent through them during extraction difficult and inefficient, and small pieces of filter paper caused the neck of the separating funnels to become blocked. Losses were also thought to occur by adsorption onto (or absorption into) the Na_2SO_4.

Therefore an alternative method to increase the surface:volume ratio was sought. The

Table 3-3 Comparison of the extraction efficiency of a mixture of an *n*-alkanes adsorbed on to glass fibre filter papers and non-adsorbed.

n-Alkane	Filter method recovery			
	Non-adsorbed wax		[a]Adsorbed wax	
	%	[c]RSD(%)	%	RSD(%)
C_{20}	87	±14	82	±17
C_{30}	90	±4	78	±17
C_{40}	89	±10	33	±21
C_{50}	68	±27	18	±52
C_{60}	51	±40	18	±28

a. Waxes adsorbed to Whatman glass fiber filter papers

Recovery of waxes with hot hexane using a separating funnel

c. n = 5

inner glass surface of the flasks could be coated with a very thin film of the wax (see Experimental). This was achieved by dissolving a known amount of the sample in cyclohexane and transferring it to the bottom of an sterile Erlenmeyer flask, followed by slowly rolling the wax around the inside of the flask with gentle warming, producing a very thin wax coat over the bottom third of the flask. This had the effect of increasing the surface area and prevented the wax from floating on the surface of the aqueous culture medium. In the majority of the abiotic control flasks the wax remained adhered to the surface of the glass even after continual swirling for 136 days. It was calculated that this would still not increase the surface:volume ratio as much as the filter paper method of **Hanstveit (1992)** so the incubation period of the experiment was increased to 136 days, almost a third longer than in previous studies (*i.e.* 80 days) (**Setti *et al.*, 1993; Hanstveit, 1992**), to compensate.

3.3.3 Extraction of *n*-alkanes by continuous liquid-liquid extraction

Having established an adequate analytical measurement technique (*viz* HTCGC) and a method of supplying the waxes to the bacteria by coating the flasks, it was equally important that the efficient recovery of the wax from the culture medium also be obtained.

The extraction efficiency of simple shaking with solvent was measured by adding the standard *n*-C_{20-60} mixture to five Erlenmeyer flasks (250 ml) each containing 100 ml of water. These were shaken and left for 24 hr before being extracted in a separating funnel using cyclohexane. The samples were dried with anhydrous sodium sulphate (see Experimental), the squalane internal standard was added and the concentration of *n*-alkanes measured by HTCGC. The percentage recovery for each of the *n*-alkanes is listed in Table 3-4.

For *n*-C_{20}, *n*-C_{30}, and *n*-C_{40} the percentage recovery was approximately 90%, although the standard deviation was high (averaging, approximately RSD 10%). Most reproducible results were obtained for *n*-C_{30} with a RSD of only 4%. The percentage recovery and the reproducibility of *n*-C_{50} (68%) and *n*-C_{60} (50%) were much lower. This is a serious problem because such a potentially large error in determination of the

HMW compounds would not be accounted for when measurements were made relative to an internal standard with a boiling point lower than *n*-tetracontane (*e.g.* squalane). One solution to this problem would be to use internal standards with boiling points spanning the range of analytes but suitable HMW internal standards are difficult to find (see discussion in Chapter One). For example, the higher solubility of putative internal standards such as triglycerides relative to the *n*-alkanes in cyclohexane would introduce inaccuracies. An alternative was to find a more efficient extraction technique.

Liquid-liquid continuous extractors have been used for many years (**Vogel, 1981**) but to the author's knowledge, the efficiency of liquid-liquid extraction for extracting *n*-alkanes > *n*-C_{40} has not been reported. A typical apparatus is shown in Figure 3-10. Solvent distils from the flask and condenses in a reflux condenser, passes through the funnel down a narrow tube to the lower end of the aqueous solution and out through a sintered glass aspirator in small droplets. The droplets rise to the surface and the solvent returns to the flask via an overflow, having extracted some portion of the *n*-alkanes from the aqueous mixture. Thus pure solvent is continually introduced to the sample by refluxing. A significant advantage of the liquid-liquid extraction over cold cyclohexane extraction is that extraction takes place at the boiling point of cyclohexane (79.7-81.7°C; **CRC, 1993**). Thus the temperature of the apparatus, including both the aqueous and organic phases, is above the cloud point of hexacontane in cyclohexane (53°C) when refluxing. A further advantage of liquid-liquid extraction, unlike simple extraction with the separating funnel, is that no carry-over of water into the sample occurs. This means that it is not necessary to dry the sample with anhydrous sodium sulphate, further reducing losses of the HMW alkanes due to adsorption onto the solid salt.

The results of repetition of the *n*-alkane recovery experiment using liquid-liquid extraction are shown in Table 3-4 and a histogram of the results comparing both extraction methods is shown in Figure 3-11. The percentage recoveries of the *n*-alkanes using the liquid-liquid extractor were greatly improved and all were above 90%. Both *n*-C_{50} and *n*-C_{60}, which were only poorly recovered using the previous method, had a much greater recovery (95% and 93%, respectively). The reproducibility of extraction

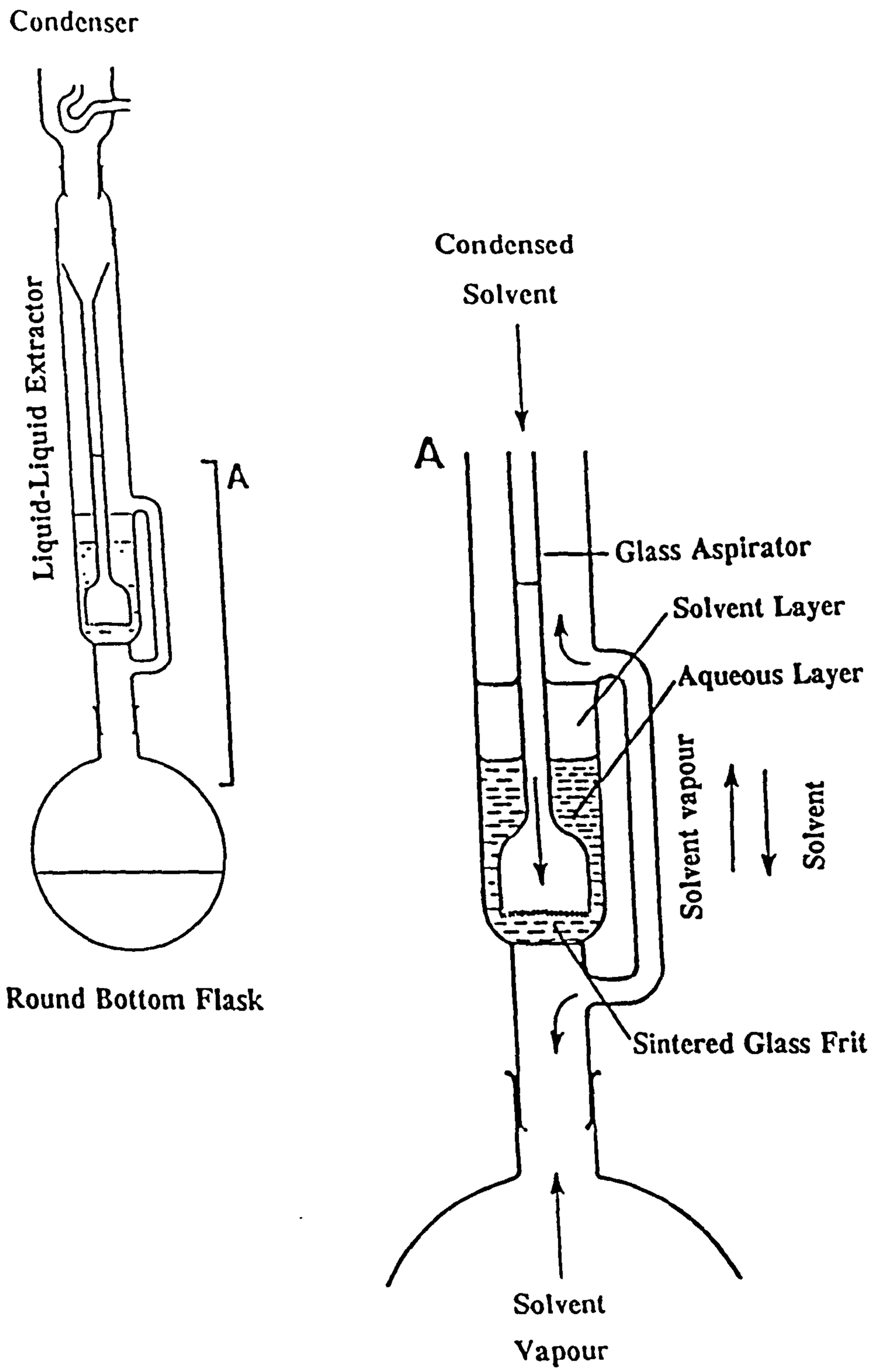

Figure 3-10 Liquid-Liquid extraction apparatus.

Table 3-4 Comparison of the extraction efficiency using a separating funnel and a continuous liquid-liquid extraction method.

n-Alkane	Comparison of Extraction Methods			
	Liquid-Liquid Extractor		Separating Funnel	
	[a]%	[b]RSD (%)	%	RSD(%)
C_{20}	93.7	±2.2	87.3	±15
C_{30}	98.0	±3.8	89.6	±3.4
C_{40}	97.5	±4.0	89.2	±9.6
C_{50}	94.7	±7.0	68.3	±18.6
C_{60}	93.1	±4.8	50.8	±20.6

a. Percentage recovery calculated relative to the Internal Standard squalane (16.1ng /µl).

b n=5

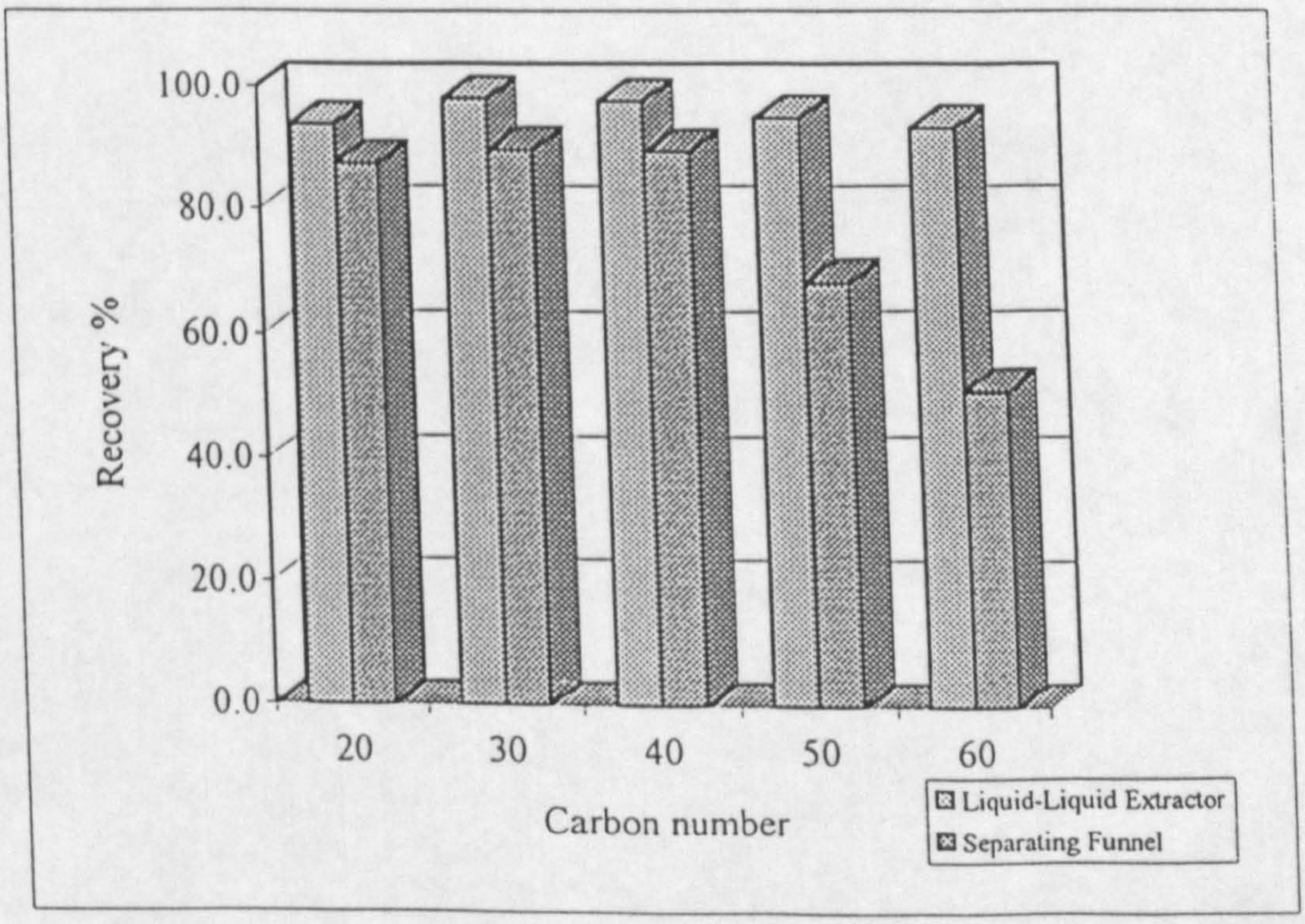

Figure 3-11 Histogram comparing the recoveries of *n*-alkanes using a separating funnel and a continuous liquid-liquid extractor.

was also greatly improved with an average RSD of under 5% compared with 17% for simple extraction with cold cyclohexane in the separating funnel.

3.3.4 Isolation of the aliphatic fraction

The substrate chosen for the biodegradation experiments was the aliphatic hydrocarbon fraction of a waxy Indonesian crude oil. The oil is typical of that from which the tar deposits that have been washed up on the shores of South Australia are thought to have originated (**McKirdy, 1994**) and is rich in HMW hydrocarbons.

Traditional methods of obtaining aliphatic hydrocarbons from whole crude oil are thin layer chromatography (TLC) or column chromatography (reviewed by **Peters and Moldowan, 1993**). Whole oil and aliphatic fractions obtained herein by TLC and CC on silica were analyzed by HTCGC and the results are shown in Figure 3-12. Figure 3-12 A shows the HMW portion of the aliphatic fraction obtained using TLC while figure 3-12 B shows the same fraction obtained by CC. The chromatograms show that a large proportion of the *n*-alkanes eluting after *n*-C_{38} have not been recovered by TLC or CC. This problem has not been reported previously, perhaps because losses of these HMW components would not be noticed by conventional capillary column gas chromatography and because most HTCGC studies have involved investigation of whole oil samples.

The reasons for poor recovery of these HMW compounds from silica adsorbent are not clear, although solubility may play an important role. In Chapter One it was demonstrated that the solubility of the HMW *n*-alkanes ($>n$-C_{40}) is low, even in organic solvents such as warm cyclohexane. The higher molecular weight compounds could precipitate from cold cyclohexane eluent and remain on the silica column or be sufficiently retarded on the TLC adsorbent so that they are not efficiently re-extracted by simple elution with cold cyclohexane. Addition of warm solvent to the chromatography column was unsuccessful in improving recovery; solvent soon cooled and warming the column was found to produce vapour pockets within the silica and consequently to disturb the packing. Repeat analysis using greater volumes of solvent eluent did not improve the recovery.

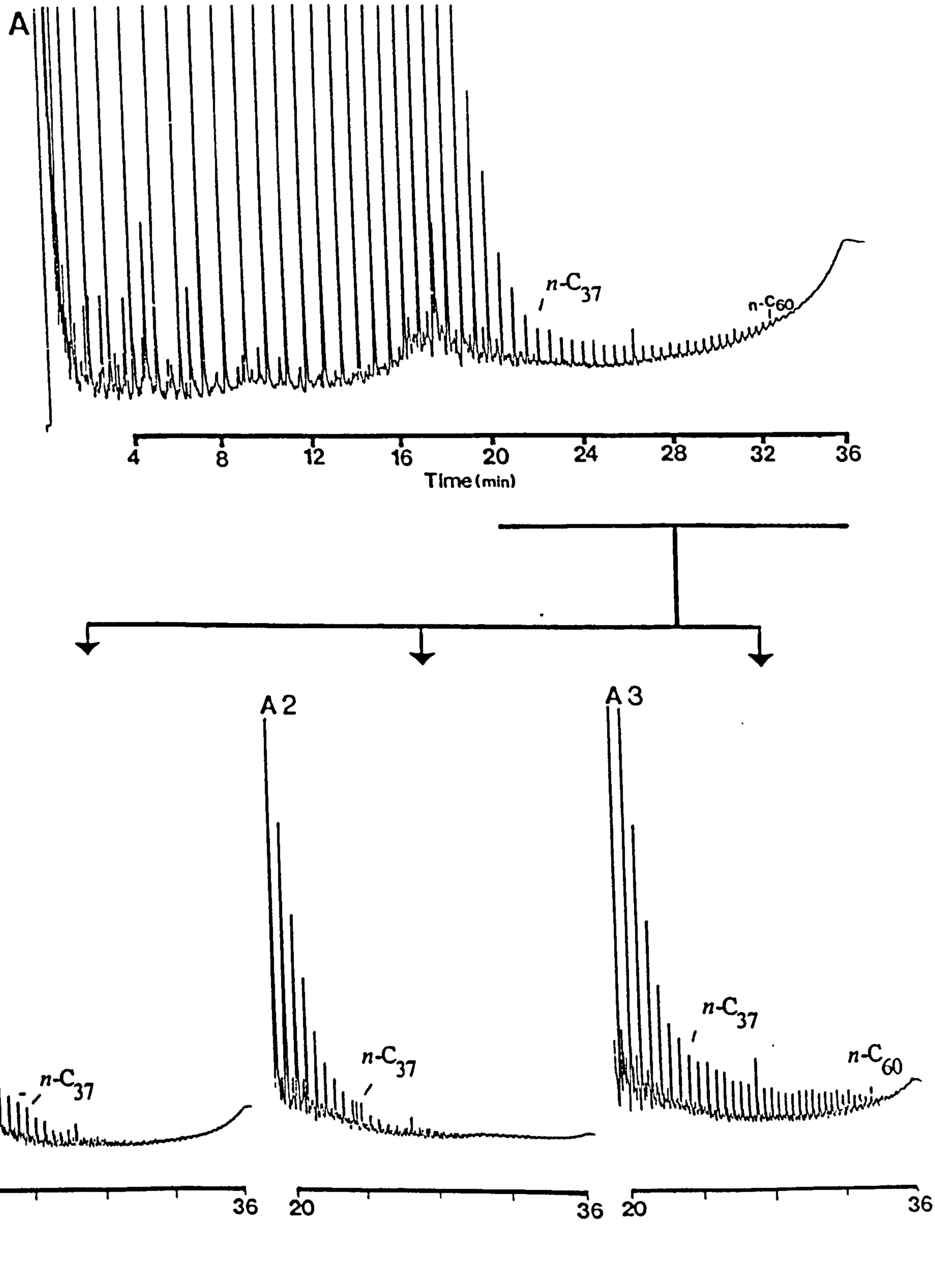

Figure 3-12 A) HTCGC of a whole Indonesian oil, and three partial chromatograms of the aliphatic compounds from the same oil fractionated by: A1) thin layer chromatography, A2) column chromatography, and A3) adsorption on to activated alumina.

An alternative method for isolation of the aliphatic components of the whole oil was sought. This involved adsorption of oil onto activated alumina (Al_2O_3), which is a more polar adsorbent than silica (SiO_2) **(Hamilton and Hamilton, 1987)**. Dissolution of the oil in cyclohexane into which was added the activated alumina (see Experimental), followed by thorough shaking and removal of solvent by rotary evaporation produced a mixture with a sticky consistency which clung to the sides of the flask. After addition of more solvent and adsorbent, followed by solvent removal the remaining mixture had the consistency of a dry powder. Addition of fresh solvent and gentle heating (50°C), aspiration and filtration of the solvent a number of times produced washings which were combined and the solvent removed to leave a soft, white waxy residue similar in appearance to the aliphatic fractions collected by both TLC and CC. When this fraction was analyzed by HTCGC *n*-alkanes up to *n*-C_{60} were observed (Figure 3-12 C).

Since this fraction had not been subjected to elution chromatography it was considered possible that the non-adsorbed fraction may still contain significant amounts of non-aliphatic material for example aromatic compounds. However, UV spectroscopy indicated this was not the case. Aromatic compounds are strongly absorbing chromophores in the 200 to 400 nm region of the e.m. spectrum **(Kemp, 1991)** and any aromatic components present, even in small amounts will thus be readily revealed by UV spectroscopy. Figure 3-13 A shows the UV spectrum of *n*-hexane, while Figure 3-13 B (see Experimental) shows the spectrum of the non-alumina adsorbed ("aliphatic") compounds. Neither spectrum showed any absorption in the 200 to 400 nm region. This can be compared with the original oil (Figure 3-13 C) which shows a strong absorption in this range even though the concentration of the non-adsorbed compounds in hexane was approximately ten times higher than that of the whole oil solution. This indicates that preferential adsorption of the aromatic and more polar compounds onto activated alumina is an efficient means of fractionating waxy oils.

3.3.5 Bacteria

The species of bacterium known as *Pseudomonas fluorescens* (Texaco), a gram negative rod bacterium, was chosen as the degrading culture. *Pseudomonas fluorescens* was originally isolated from a metal working fluid waste (an emulsion of oil and water)

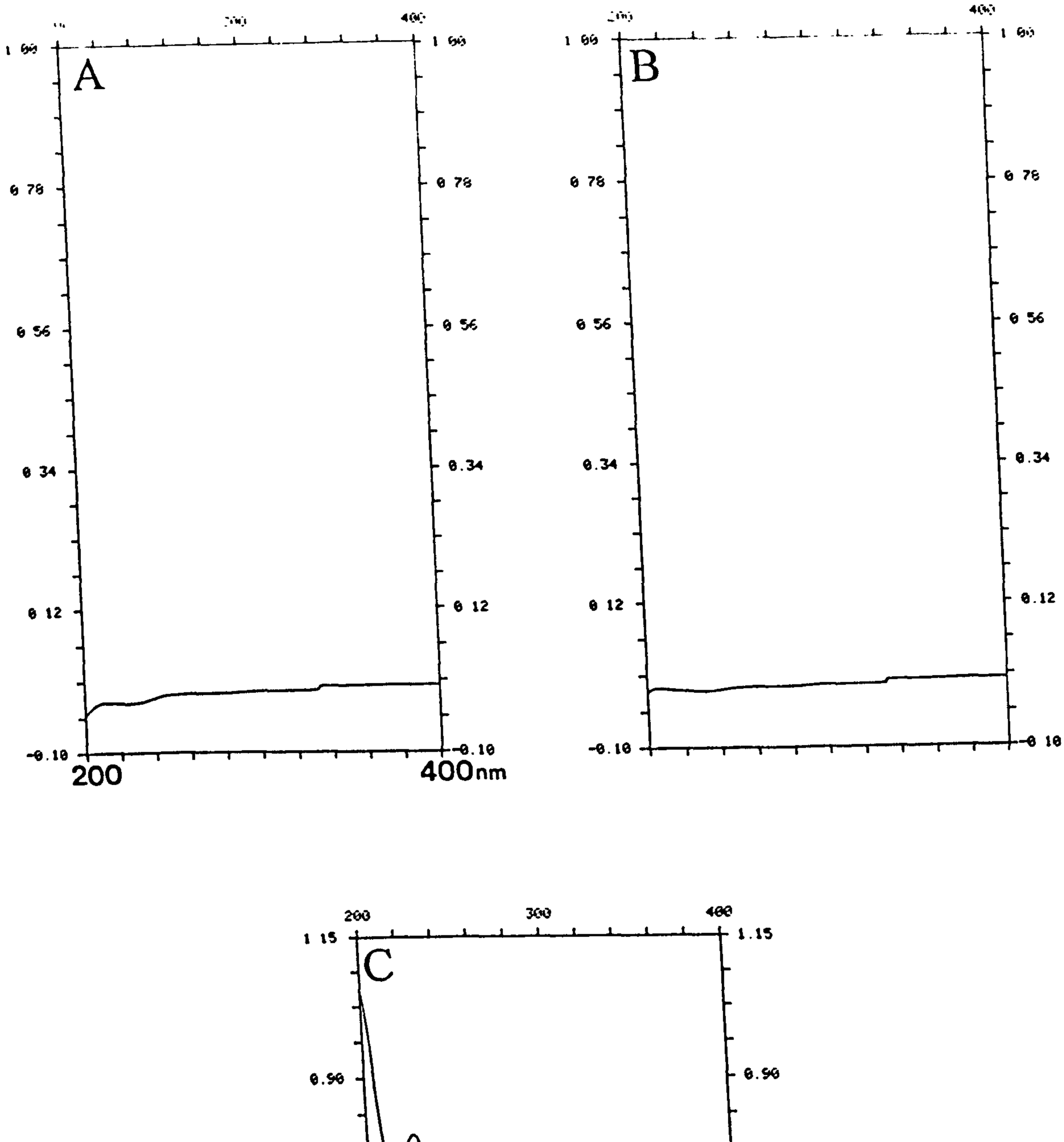

Figure 3-13 UV absorbance spectra (200 to 400 nm) for A) pure hexane, B) non-adsorbed fraction and C) whole oil. Both sample spectra recorded in hexane.

by **Beech and Gaylarde, (1989)**. Since then it has been used in a number of hydrocarbon degradation experiments and has been shown to be an efficient oil degrading organism (see **Robson and Rowland, 1990; Gough and Rowland, 1990; Šepič *et al.*, 1994**). Preparation of the bacterial culture is illustrated in Figure 3-14 and described fully in the Experimental. So that none of the agar broth was carried over into the cultures, the bacteria were separated from the broth by repeated centrifuging and washing with phosphate buffer solution. Mineral medium was used to provide the essential nutrients for the bacteria so that substrate concentration would be the only limiting factor for growth. Each batch culture was gently swirled and incubated at room temperature in the dark to prevent any photo-oxidation. Each batch consisted of two biotic samples, two abiotic controls, and a reagent blank.

It was important that only the test organism was present in the biotic samples and that controls remained sterile, particularly if abiotic losses only were to be measured. The glassware and mineral media solution were easily made sterile in an autoclave, though using the autoclave for the aliphatic substrate was obviously not possible. Therefore the sample was introduced into the culture flasks in a solution of cyclohexane so that the toxic effect of the solvent would sterilise the sample. Very few organisms can withstand high concentrations of solvents (**Ratledge, 1979**). The cyclohexane was allowed to evaporate before inoculation. Contamination of the controls during incubation is often curtailed by the use of growth inhibitors such as mercuric chloride (**Gough, 1989**). It was decided not to add a growth inhibitor, because mercuric chloride is a grade one poison, and because the addition of a growth inhibitor may interfere with the substrate. Instead careful aseptic treatment of the apparatus and mineral media was adopted. At each sampling both the biotic and abiotic cultures were checked for contamination by streaking a loop of culture onto a nutrient agar plate. After incubation the plates were visually examined for growth of organisms. All the abiotic samples tested negative and the biotic samples showed only the presence of *Pseudomonas fluorescens* (Texaco) during the entire 136 days of incubation, indicating that no contamination of the samples had taken place.

Several methods exist for the estimation of bacterial populations including methods

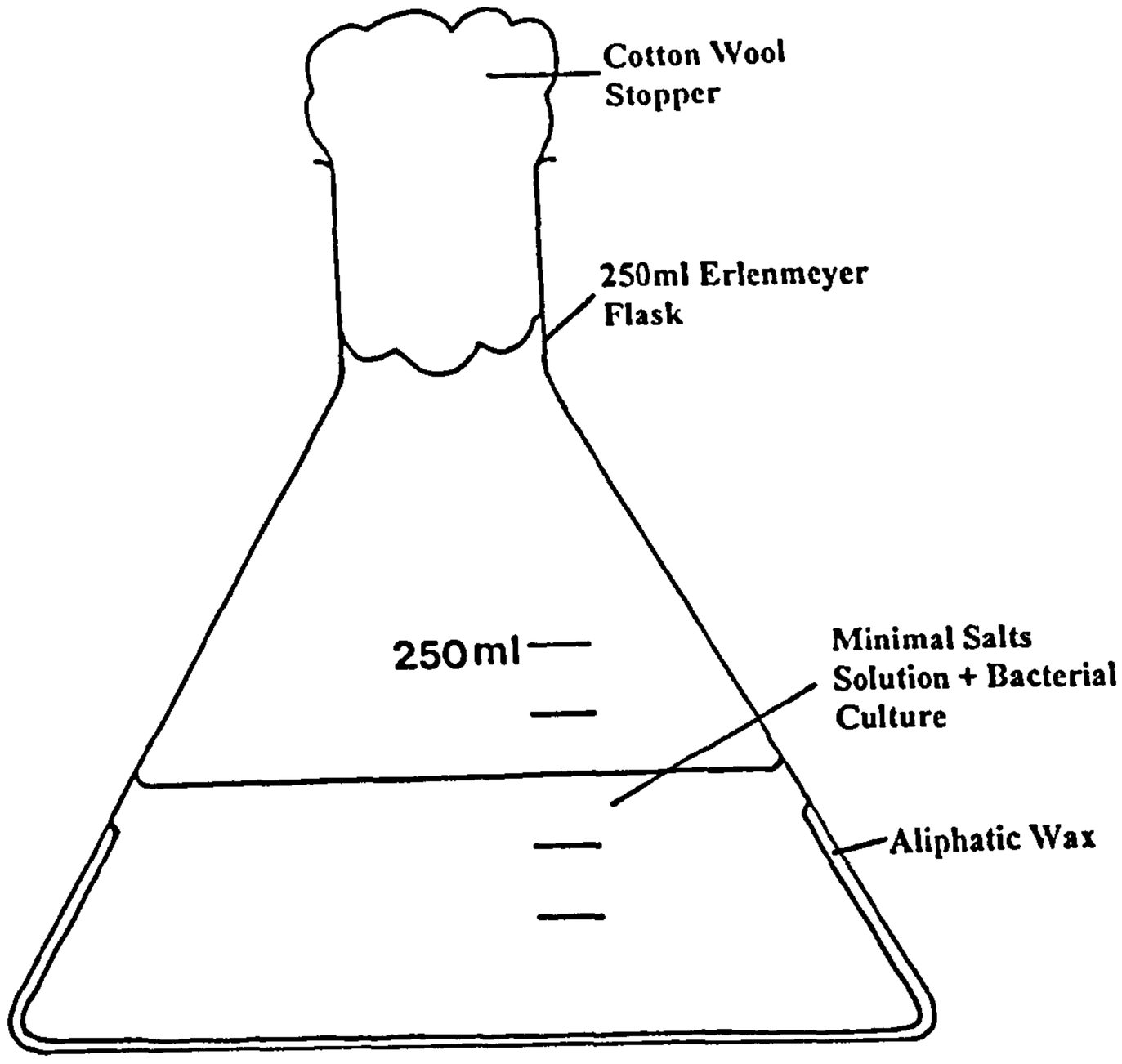

Figure 3-14 Bacterial culture.

Incubation time (days)	[a]Viable count ([b]C.F.U./ml x10^8)
0	14.9
24hr	3.5
3	9.0
7	25.9
14	13.4
21	8.4
28	7.3
45	6.0
136	5.8

a. Cell count determined by the Miles Misra drop method.

b. C.F.U. = Colony forming unit

Table 3-5 Bacterial growth expressed as the number of colony forming units (CFU) measured using the Miles Misra drop count method.

that measure the number of bacterial cells directly and those that measure growth indirectly. The former include monitoring the turbidity of the solution; measurement of N_2, O_2 consumption, or of CO_2 evolution. Methods which involve direct counting of cells are those which measure both living (viable) and dead cells and those which just measure the viable cells. The technique used in this study is known the Miles Misra drop count method (**Miles and Misra, 1938**). This method and the more common spread plate count method (**Collins and Patricia, 1984**) are very similar and both involve making a series of serial dilutions, except in the Miles Misra method only a small amount of solution (25 μl) in the form of a single drop or lens is placed onto the agar plate. Unlike the plate spreading this drop is left to dry rather than being spread over the entire plate surface. The plate is then incubated for 24 hr and the number of colonies counted using a microscope. It was found that if the plates were incubated for too long the colonies grew too large and merged together; if the plates were examined too early then the colonies were too small to be seen with a binocular microscope and thus not accounted for. It was found that the best time to observe the plates was after 24 hr incubation at 37°C and then again after a further six hours. This method was much quicker than the spread plate method and used a fraction of the consumable materials.

3.3.6 Bacterial growth

Table 3-5, shows the number of colony forming units (CFU) counted during incubation. The data is also shown graphically in Figure 3-15. The number of bacteria decreased dramatically from a concentration of 15×10^8 to 3.5×10^8 per ml within 24 hr. This period of adjustment is known as the lag phase (**Monod, 1949**) where the growth rate is nil. Usually an initial decrease in the number of bacterial cells is due to non-viable cells present in the original inoculum. In this study the inoculum was added to the culture flask, thoroughly mixed and then the number of viable cells measured. Thus measured cell population in the flask is a measure of the initial viable cell concentration. In this case the decrease in bacterial numbers is probably an effect of "flash lysis" which occurs when an organism is exposed to sudden changes in composition of the growth media (in this experiment the transition from an nutrient rich agar cultural broth to a nutrient-limited minimal media). The rate of sampling was too

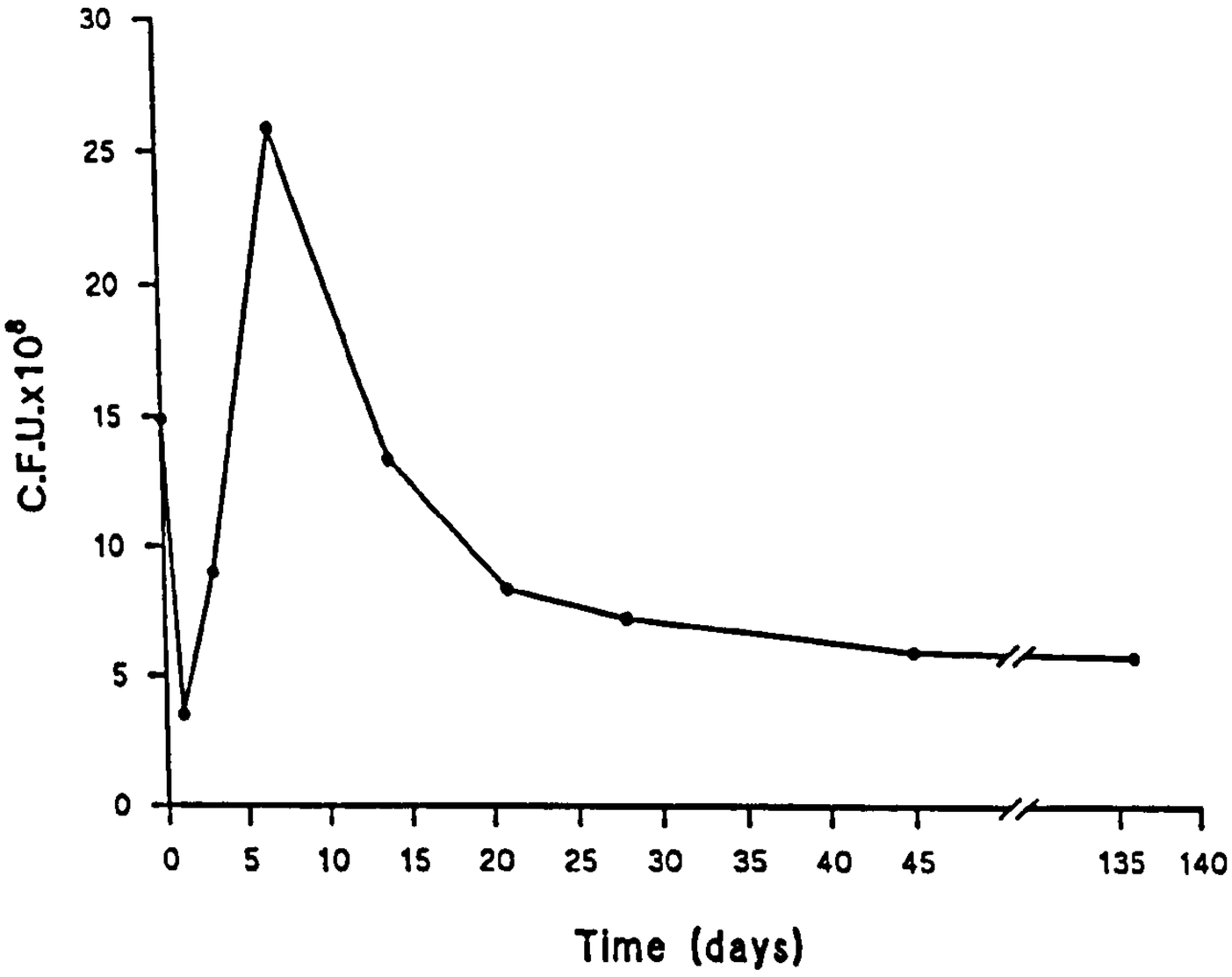

Figure 3-15 Graph of bacterial population against incubation time.

Table 3-6. Concentration of the total aliphatic compounds measured during the 136 day incubation period.

Incubation time (days)	[a]Total Aliphatic (µg/ml)			
	Biotic	[b]Err.	Abiotic	Err.
0	1466	±26	1466	±26
24hr	1287	±40		
3	773	±71	1454	±82
7	546	±47		
14	302	±24		
21	316	±21	1485	±76
28	283	±5		
45	299	±15		
136	209	±7	1577	±77

a. Concentration expressed as total aliphatic compounds extracted and dissolved in 1 ml of Cyclohexane.

b. Error expressed as the range.

low to give a good description of the lag phase period which is a common feature of bacterial growth and is caused by enzymatic adaptation and is defined by **Monod (1949)** as the "formation of a specific enzyme under the influence of its substrate". In this study the bacterial inoculum was transferred from a medium where the substrate for growth (glucose) is very different to that of the aliphatic compounds that are the sole source of carbon in the experiment. Growth will therefore occur when the enzyme system of the bacteria has developed to utilise the new substrate, in this instance probably within hours.

The low sampling rate also meant that the acceleration phase (the initial stage of exponential growth) was not well defined but it is apparent (Figure 3-15) that the lag and acceleration phase must have occurred within the first three days of incubation. The greatest amount of bacterial growth is seen between day 3 and day 7. This period of growth is known as the exponential phase, where the growth rate remains constant and a steady state situation is established. Here the substrate is not limited and the rate determining step is likely to be the complex enzymatic reactions taking place within the bacteria.

After seven days of incubation the growth of the bacterium can be seen to enter the so called "phase of decline" where the growth rate is negative. This decline is sharp until day 21 when the rate of decline decreased. After 45 days of incubation the bacterial population remained almost constant (6×10^8 cells ml^{-1}). The decline phase was probably associated with the decrease of the more soluble and degradable *n*-alkanes in solution.

Estimating cell growth in this experiment failed to take account of those bacteria fixed to the solid wax particles, since sampling of a small amount of solution with a wire loop, even from a flask which had been thoroughly shaken, would not sample this fraction of bacteria. Subsequent serial dilutions may also have separated the solid particles out so the actual numbers of bacteria present in the culture may have been higher than Figure 3-15 indicates.

Once all the slightly soluble *n*-alkanes have been used up the concentration of *n*-

alkanes in the solution would be expected to decrease causing a decline in the number of free cells. The concentration of the HMW *n*-alkanes in the media will be practically zero. The solubility of *n*-alkanes in water is shown in Table 3-7 and Figure 3-16. The only carbon source therefore would be actually on or very close to the wax solids. These solid wax particles probably act both as substrate reservoirs and a support for the majority of the bacteria in the cultures.

3.3.7 *n*-Alkane degradation

Replicate measurements of the microbial degradation of the aliphatic fraction of the Indonesian oil extracted by liquid-liquid extraction and analysed by HTCGC using squalane as the internal standard resulted in the data given in Table 3-6 and plotted in Figure 3-17 and plotted as substrate percentage removed against time in Figure 3-18. The rate of degradation of the substrate correlated closely to the growth curve of the *Pseudomonas fluorescens* (Texaco) in Figure 3-15. The rate of removal of substrate was greatest between day 3 and day 7 of incubation which correlated with the exponential growth phase of the bacteria. The amount of material being degraded decreased between 7 and 14 days incubation. By day 14, 80% of the original wax had been degraded whereas from day 14 to the end of the incubation period (136 days) only a further 6% of substrate was metabolised by the bacteria.

Chromatograms obtained by examination of the substrate residues by HTCGC are shown in Figure 3-19. The differences in the chromatograms are most noticeable between the 1 day and 3 day samples when the majority of the *n*-alkanes below *n*-C_{27} had been degraded. Between day 7 and day 21 total removal of the LMW *n*-alkanes (C_{14}-C_{26}) from the chromatograms is apparent. Between day 28 and day 136 of incubation the amount of degradation of the HMW compounds greater than *n*-C_{34} was too small to be observed from the chromatograms.

The variations in concentrations of selected *n*-alkanes through the experiment are shown in Table 3-8 and plotted against time in Figure 3-20. All the *n*-icosane (*n*-C_{20}) had disappeared within 3 days; *n*-pentacosane (*n*-C_{25}) decreased rapidly within 3 days (88%) and was totally degraded within 14 days of incubation. A similar trend can be

Table 3-7 Solubility (ppm) of hydrocarbons in water.

Compound	Carbon number	Solubility[a] (ppm)
<u>Alkanes</u>		
Methane	1	24
Ethane	2	60
Propane	3	62
n-Butane	4	61
n-Pentane	5	39
n-Hexane	6	9.5
2-Methylpentane	6	13.8
3-Methylpentane	6	12.8
2,2-Dimethylbutane	6	18.4
n-Heptane	7	2.9
n-Octane	8	0.66
n-Nonane	9	0.220
n-Decane	10	0.052
n-Undecane	11	0.0041
n-Dodecane	12	0.0037
		0.0029 (SW)
n-Teradecane	14	0.0022
		0.0017 (SW)
n-Hexadecane	16	0.0009
		0.0004 (SW)
n-Octadecane	18	0.0021
		0.0008 (SW)
n-Eicosane	20	0.0019
		0.0008 (SW)
n-Hexacosane	26	0.0017
		0.0001 (SW)
n-Triacontane	30	0.002
n-Heptacontane	70	10^{-5}[b]
<u>Cycloalkanes</u>		
Cyclopentane	5	156
Cyclohexane	6	55
Cycloheptane	7	30
Cyclooctane	8	7.9
<u>Aromatics</u>		
Benzene	6	1780
Toluene	7	515
o-Xylene	8	175
Ethylbenzene	8	152
1,2,4-Trimethylbenzene	9	57
iso-Propylbenzene	9	50
Naphthalene	10	31.3
		22.0 (SW)
1-Methylnaphthalene	11	25.8
2-Methylnaphthalene	11	24.6
2-Ethylnaphthalene	12	8.00
1,5-Dimethylnaphthalene	12	2.74
2,3-Dimethylnaphthalene	12	1.99
2,6-Dimethylnaphthalene	12	1.30
Biphenyl	12	7.45
		4.76 (SW)
Acenaphthene	12	3.47
Phenanthrene	14	1.07
		0.71 (SW)
Anthracene	14	0.075
Chrysene	18	0.002

[a] In distilled water, except where noted by (SW), indicating filtered seawater, usually corrected to a salinity of 35‰ (parts per thousand); ppm = parts per million-microgram per gram.
[b] Extrapolated

Source: Robotham and Gill (1989)

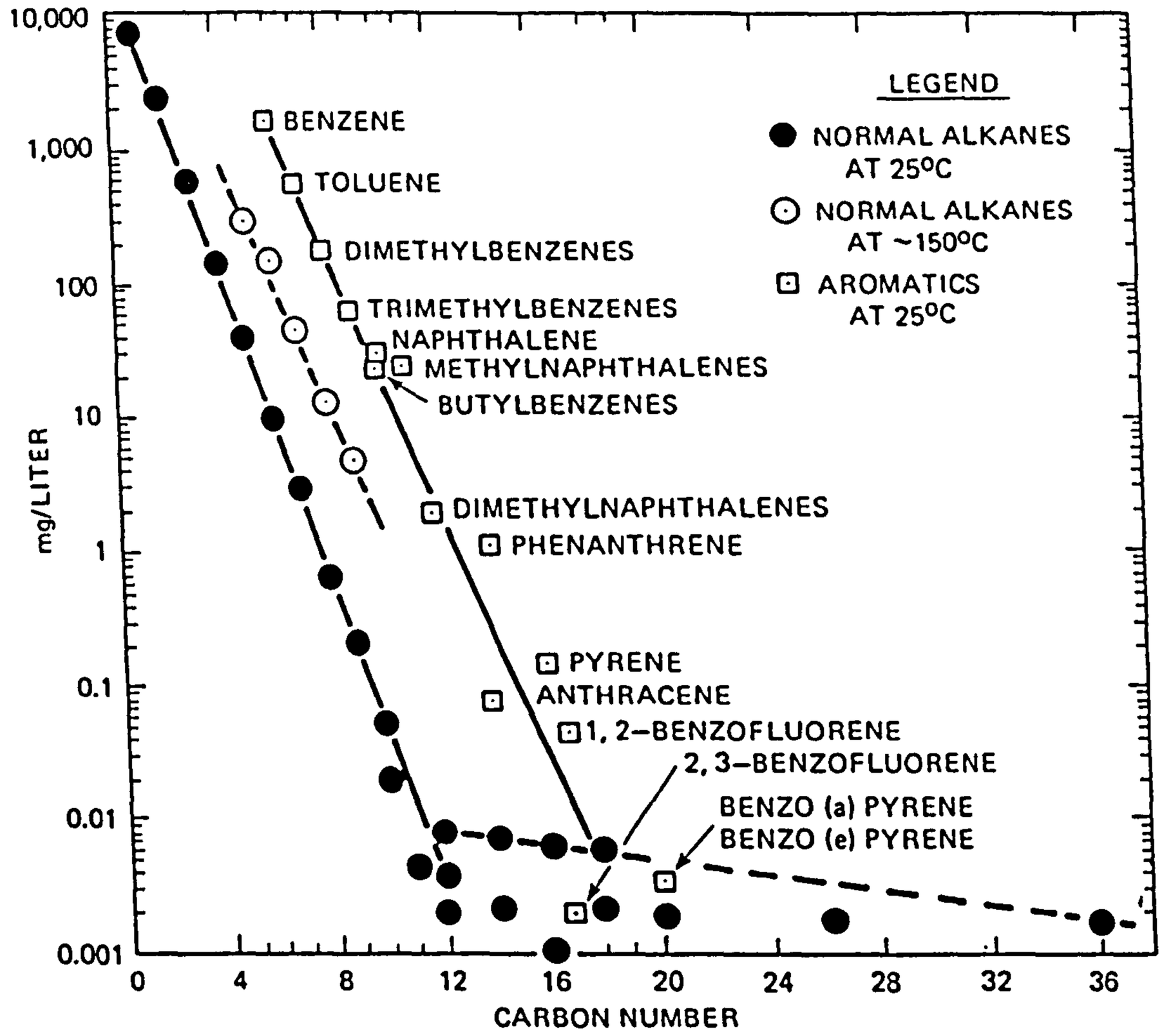

Figure 3-16 Graph of solubility against carbon number of selected hydrocarbons in water.

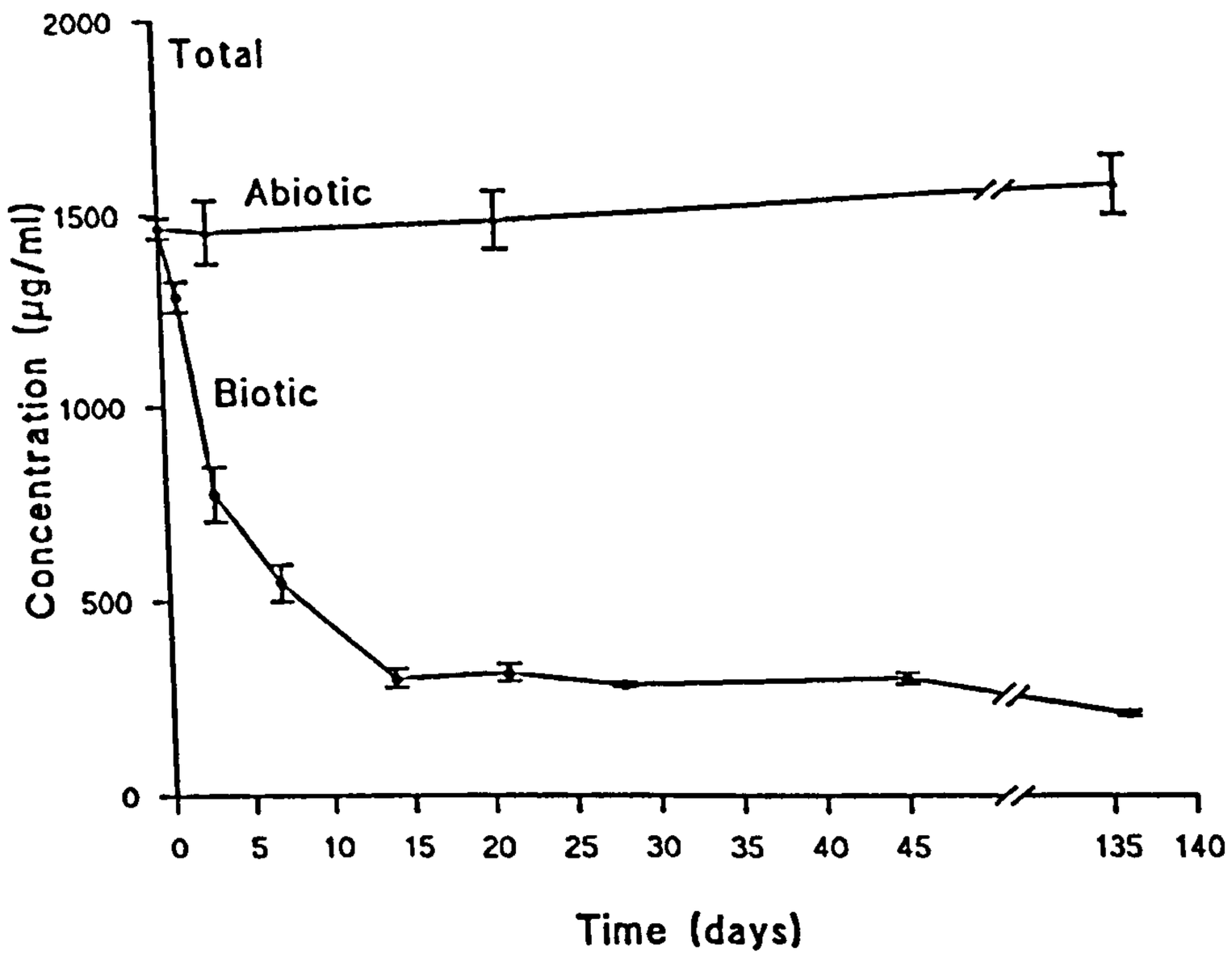

Figure 3-17 Graph showing the degradation of total aliphatic compounds over time.

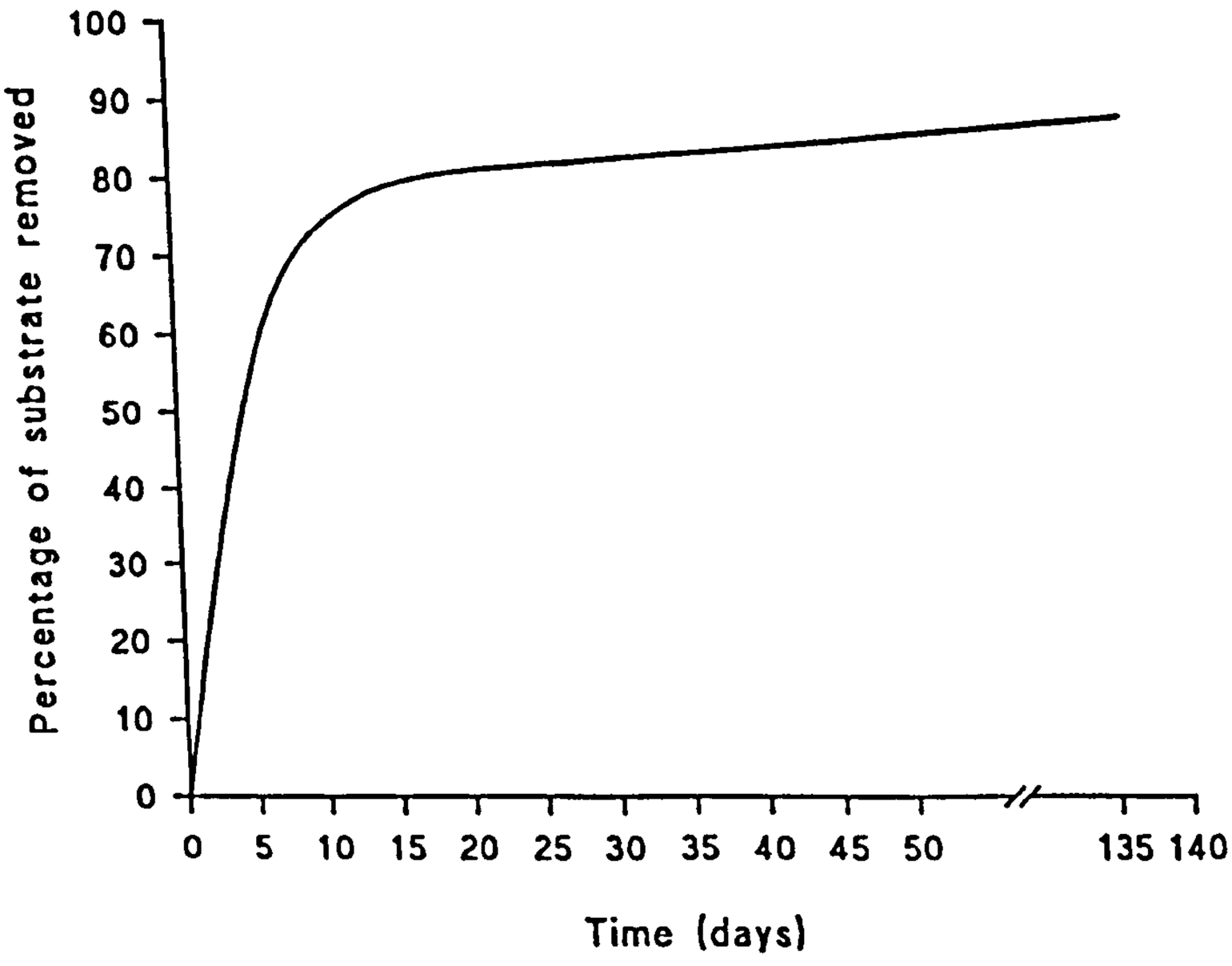

Figure 3-18 Percentage of removal of substrate over time.

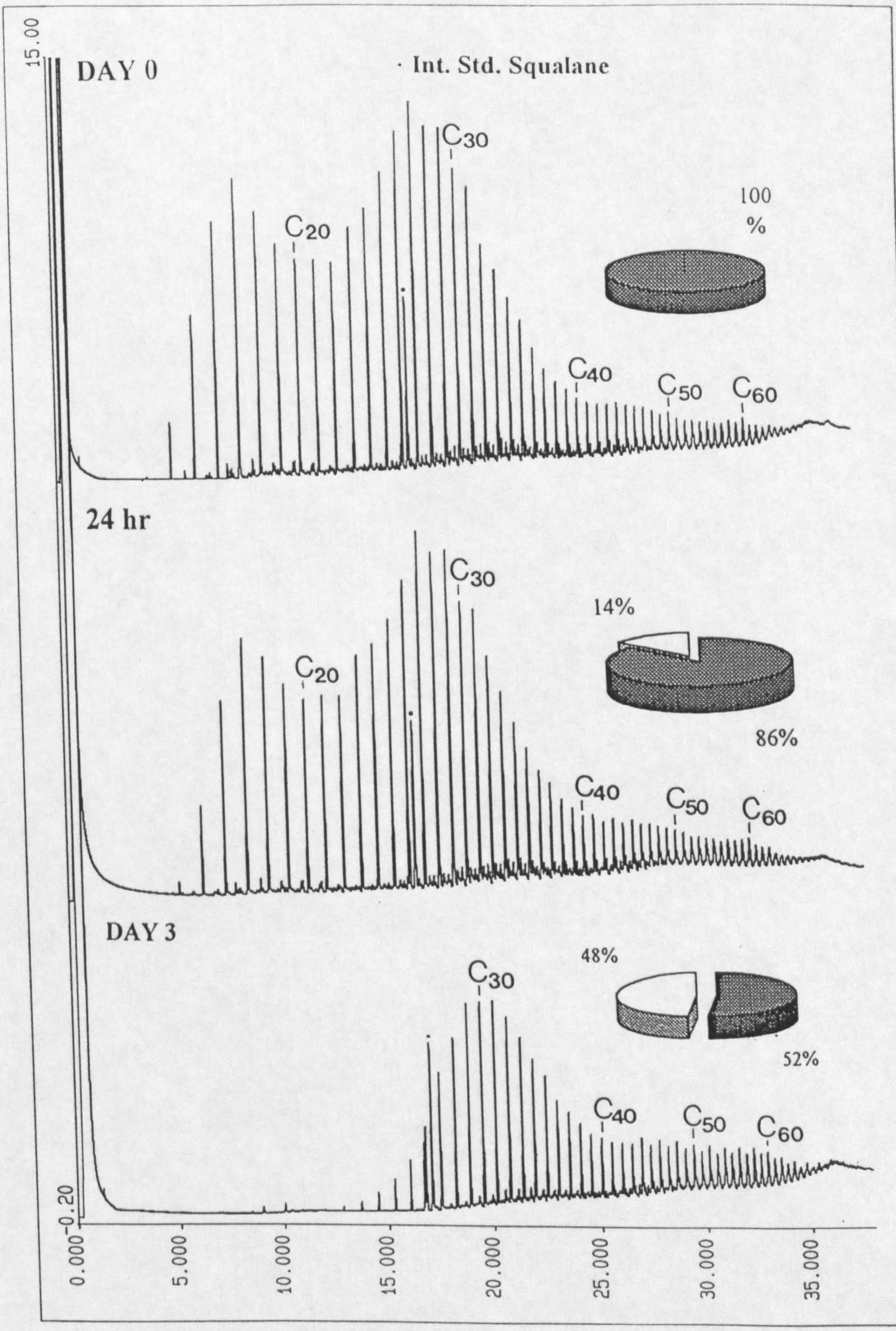

Figure 3-19 HTCGCs of degraded Indonesian oil.

continued overleaf .....

continued .....

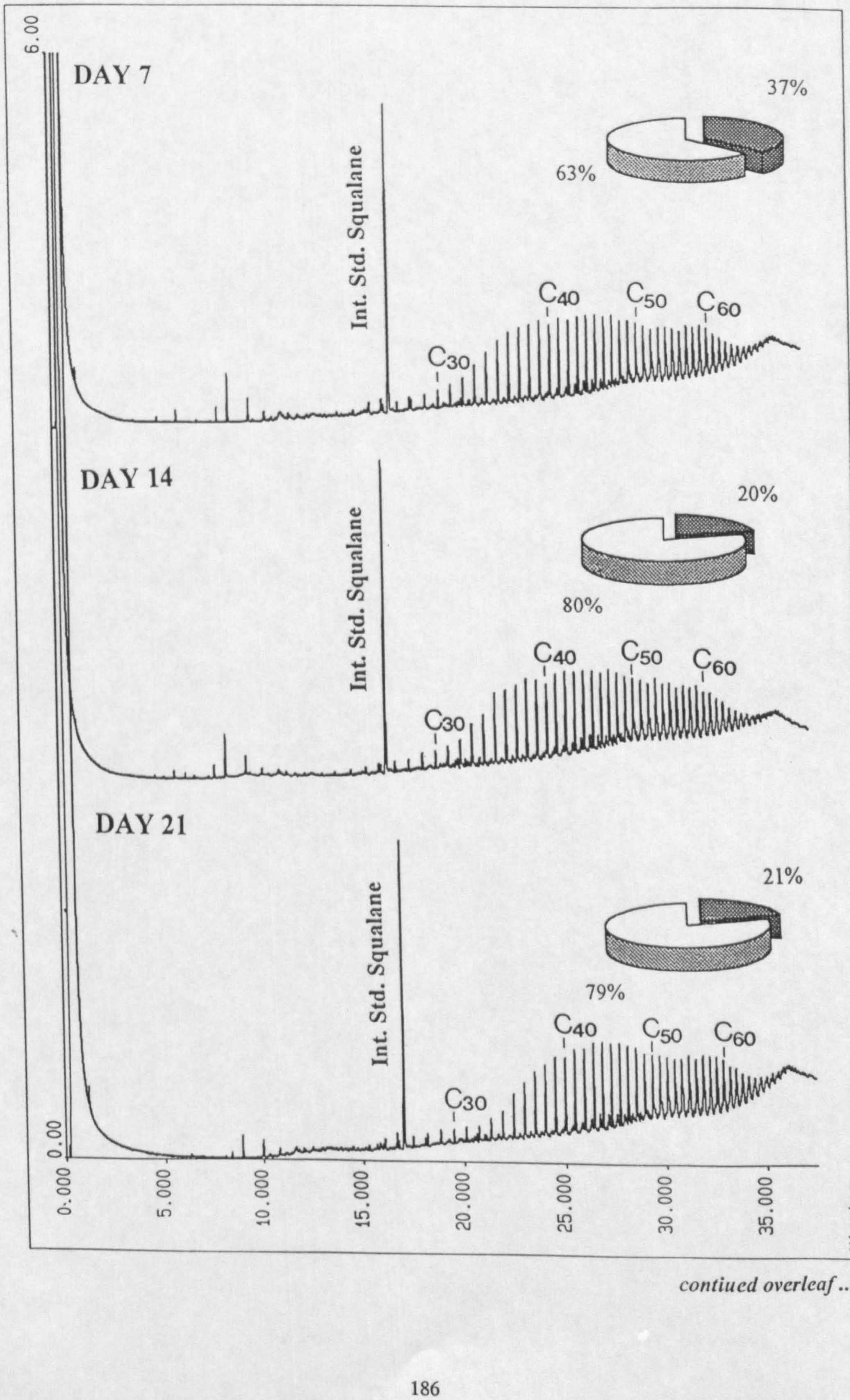

contiued overleaf .....

continued .....

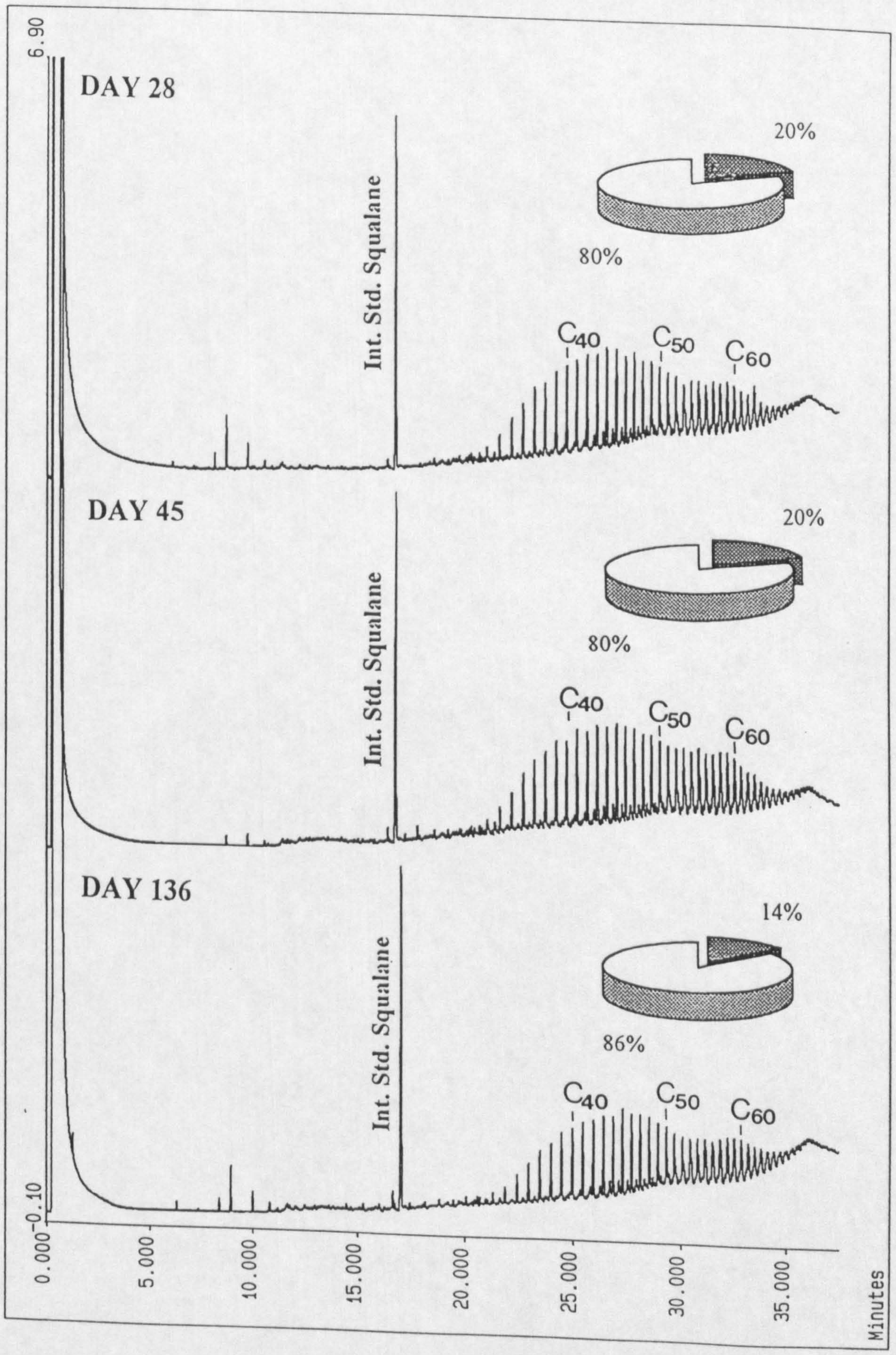
6.90
DAY 28
Int. Std. Squalane
20%
80%
C40
C50
C60
DAY 45
Int. Std. Squalane
20%
80%
C40
C50
C60
DAY 136
Int. Std. Squalane
14%
86%
C40
C50
C60
0.000
0.10
5.000
10.000
15.000
20.000
25.000
30.000
35.000
Minutes

Table 3-8 Results from the biodegradation of selected *n*-alkanes from the aliphatic fraction of a waxy Indonesian oil using *Pseudomonas fluorescens* (Texaco).

Days	n-C_{20}				n-C_{25}				n-C_{30}			
	Concentration in µg/ml											
	Biotic	[a]Err.	Abiotic	Err.	Biotic	Err.	Abiotic	Err.	Biotic	Err.	Abiotic	Err.
0	36.7	±0.6	36.7	±0.6	52.2	±0.4	52.2	±0.4	55.3	±0.7	55.3	±0.7
24hr	29.7	±2.8			44.6	±6.1			47.1	±3.4		
3	0	0	36.9	±1.0	6.1	±0.8	50.5	±1.4	14.2	±1.5	52.7	±1.0
7	0	0			1.5	±0.3			7.0	±1.1		
14	0	0	39.8	±2.0	0	0	50.8	±1.4	2.6	±0.5	51.3	±1.5
21	0	0			0	0			1.4	±0.1		
28	0	0			0	0			0	0		
45	0	0			0	0			0	0		
136	0	0	40.4	±1.3	0	0	52.1	±1.7	0	0	53.3	±1.6

Days	n-C_{35}				n-C_{40}				n-C_{45}			
	Biotic	Err.	Abiotic	Err.	Biotic	Err.	Abiotic	Err.	Biotic	Err.	Abiotic	Err.
0	25.3	±0.8	25.3	±0.8	11.6	±0.5	25.3	±0.8	9.8	±0.4	9.8	±0.4
24hr	23.7	±1.2			11.4	±1.2			8.7	±0.8		
3	18.4	±2.7	24.4	±0.6	11.3	±0.6	11	±0.5	9.9	±0.8	9.2	±0.5
7	14.0	±0.2			9.5	±0.3			8.4	±0.3		
14	7.0	±0.3			7.8	±0.3			7.7	±0.2		
21	6.4	±0.7	21.7	±1.5	7.9	±0.6	9.9	±0.4	7.9	±0.6	7.2	±0.9
28	3.0	±0.2			6.4	±0.2			8.4	±0.5		
45	2.1	±0.4			7.2	±0.5			8.8	±0.5		
136	1.4	±0.3	24.6	±1.0	4.8	±1.2	11.1	±0.9	6.3	±1.3	9.3	±0.3

Days	n-C_{50}				n-C_{55}				n-C_{60}			
	Biotic	Err.	Abiotic	Err.	Biotic	Err.	Abiotic	Err.	Biotic	Err.	Abiotic	Err.
0	7.9	±0.1	7.9	±0.1	4.8	±0.6	4.8	±0.6	5.5	±0.1	5.5	±0.1
24hr	6.4	±1.4			5.5	±1.4			6.1	±0.5		
3	8.8	±1	7.16	±0.3	9.8	±1.2	6.1	±0.6	7.9	±0.6	5.6	±0.3
7	6.5	±0.7			5.9	±0.2			4.9	±0.3		
14	5.9	±0.4			4.9	±0.7			3.9	±0.4		
21	5.5	±0.7	5.26	±0.9	5.4	±0.7	6.1	±2.2	5.3	±0.2	5.5	±0.5
28	6.5	±0.4			4.6	±0.2			3.3	±0.4		
45	7.6	±0.9			5.6	±0.2			5.4	±0.2		
136	6.5	±0.9	7.13	±0.7	5.3	±1.2	7.1	±0.7	5.4	±1.0	5.5	±0.3

a. Concentration expressed as the total extracted material dissolved in 1ml of solvent

b. Error expressed as the range of data (n=2).

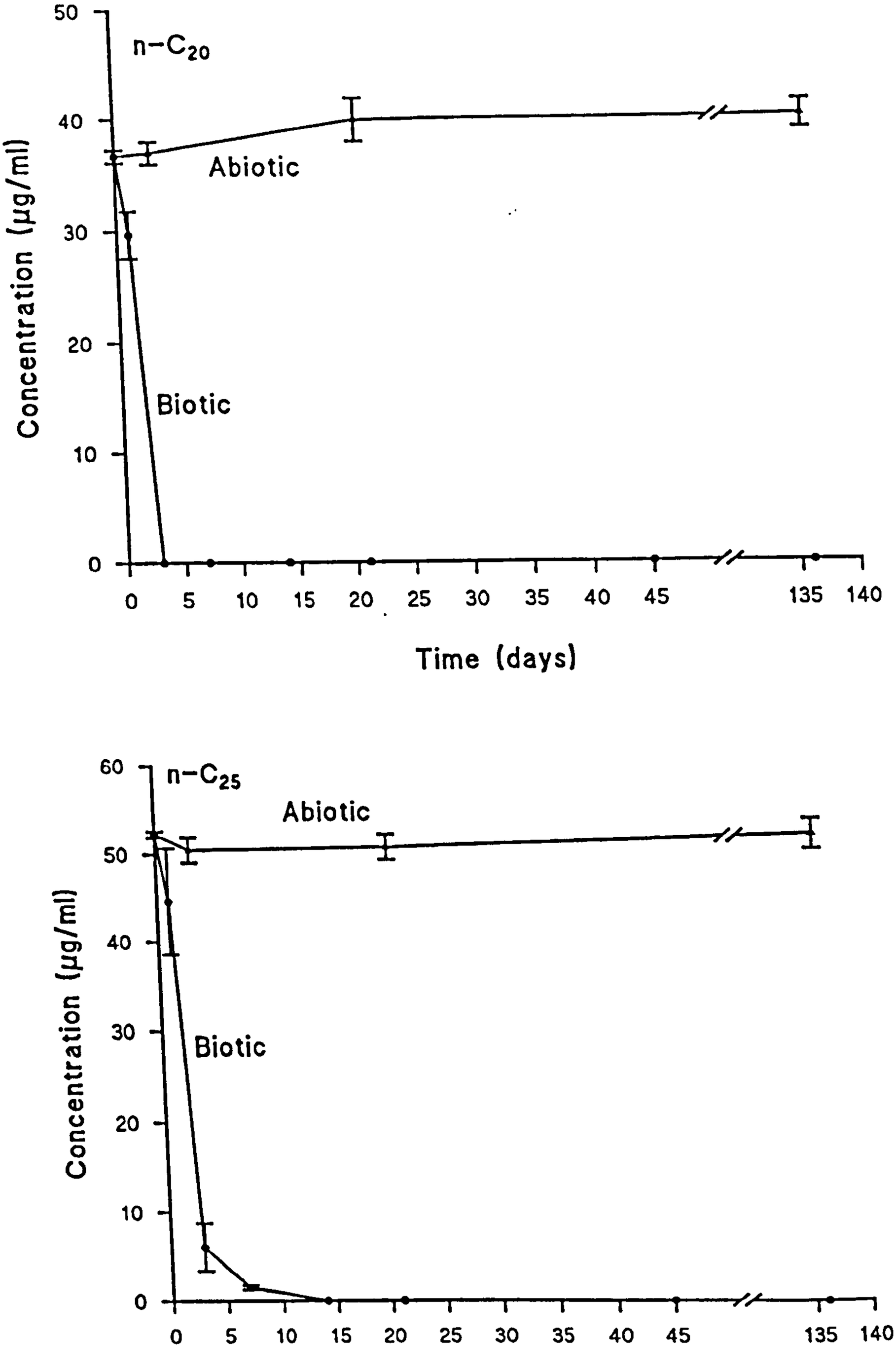

Figure 3-20 Removal with time of selected *n*-alkanes by the bacteria *Pseudomonas fluorescens* (Texaco).

Continued overleaf.....

continued.....

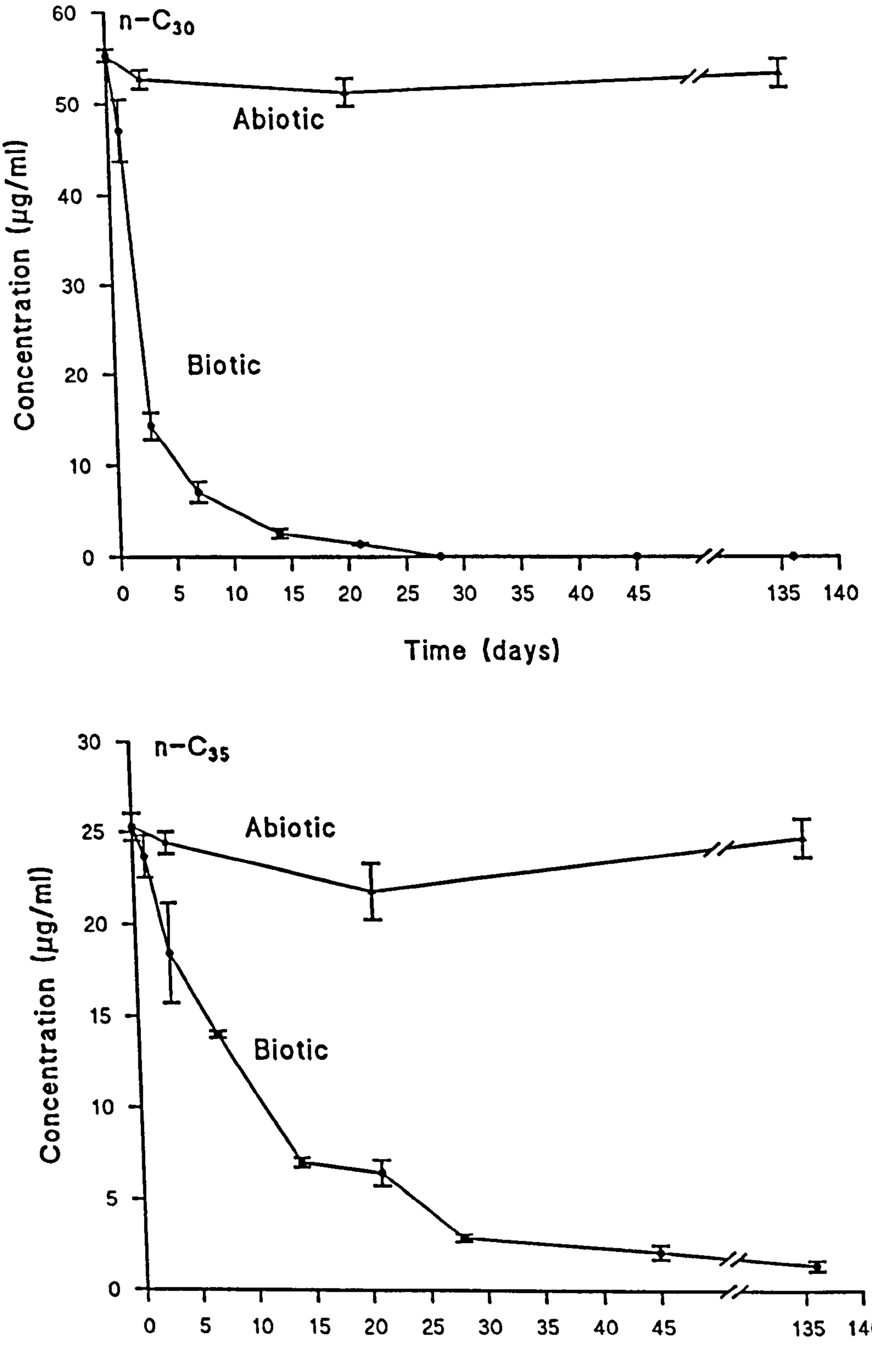

continued overleaf.....

continued.....

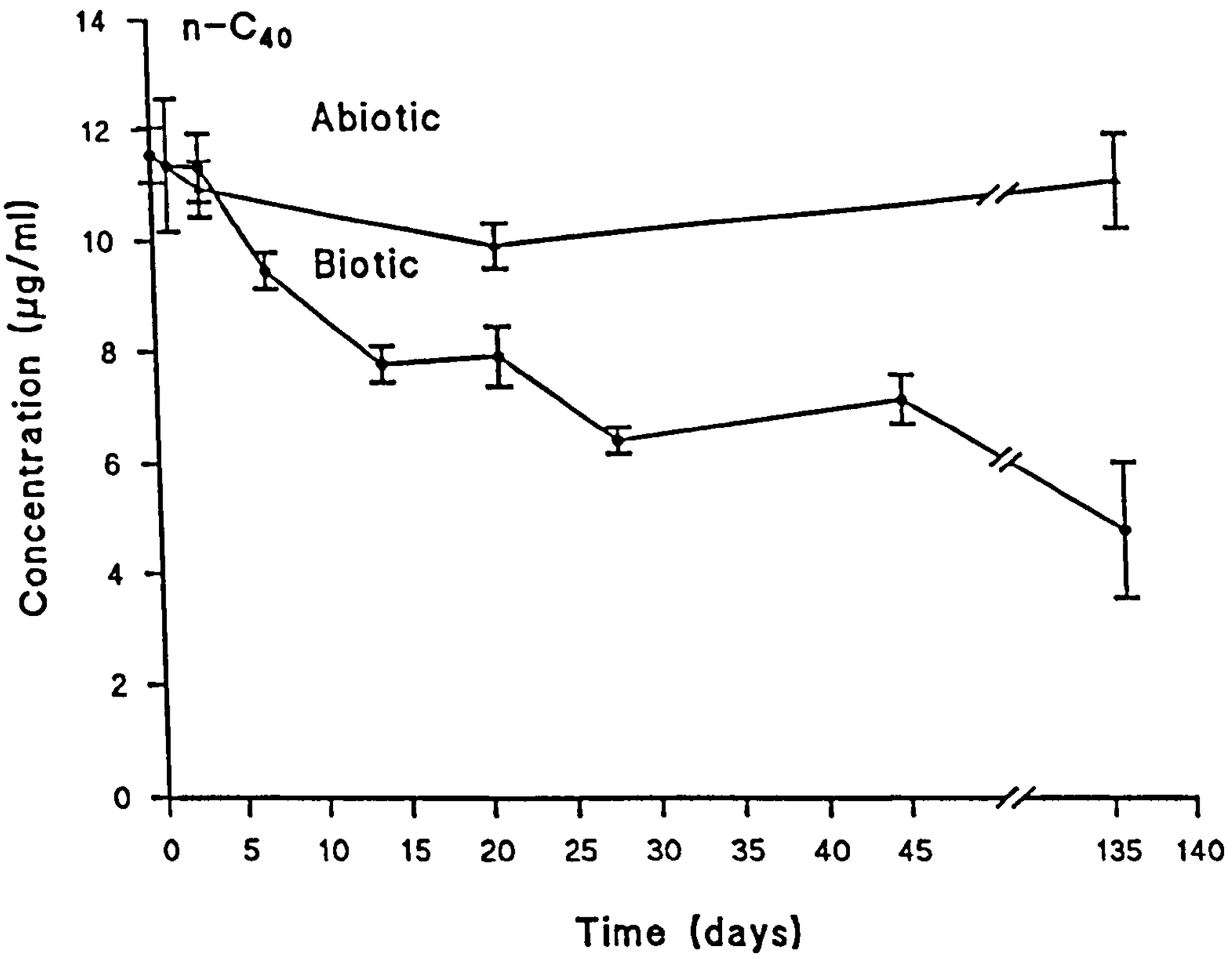

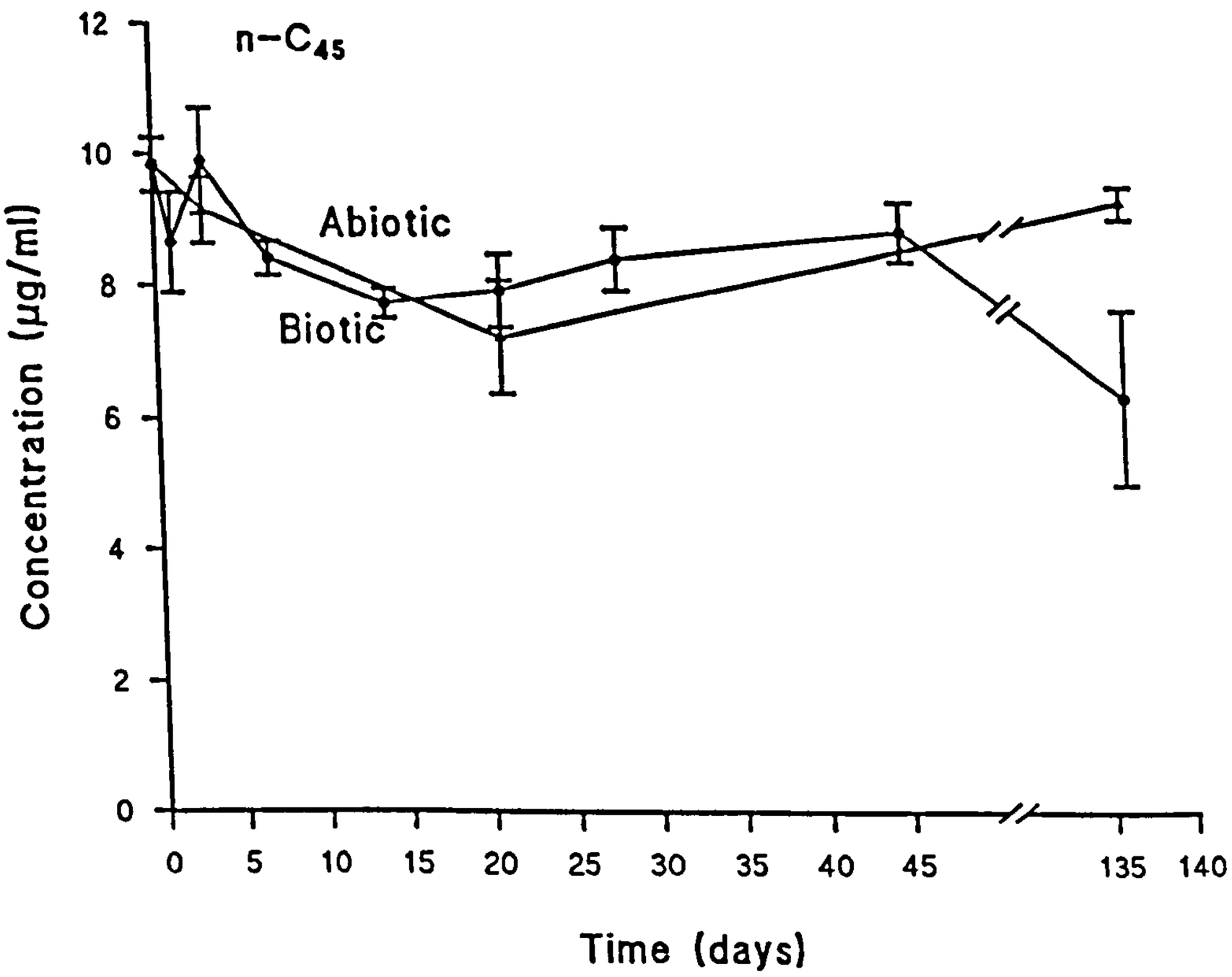

continued overleaf.....

continued.....

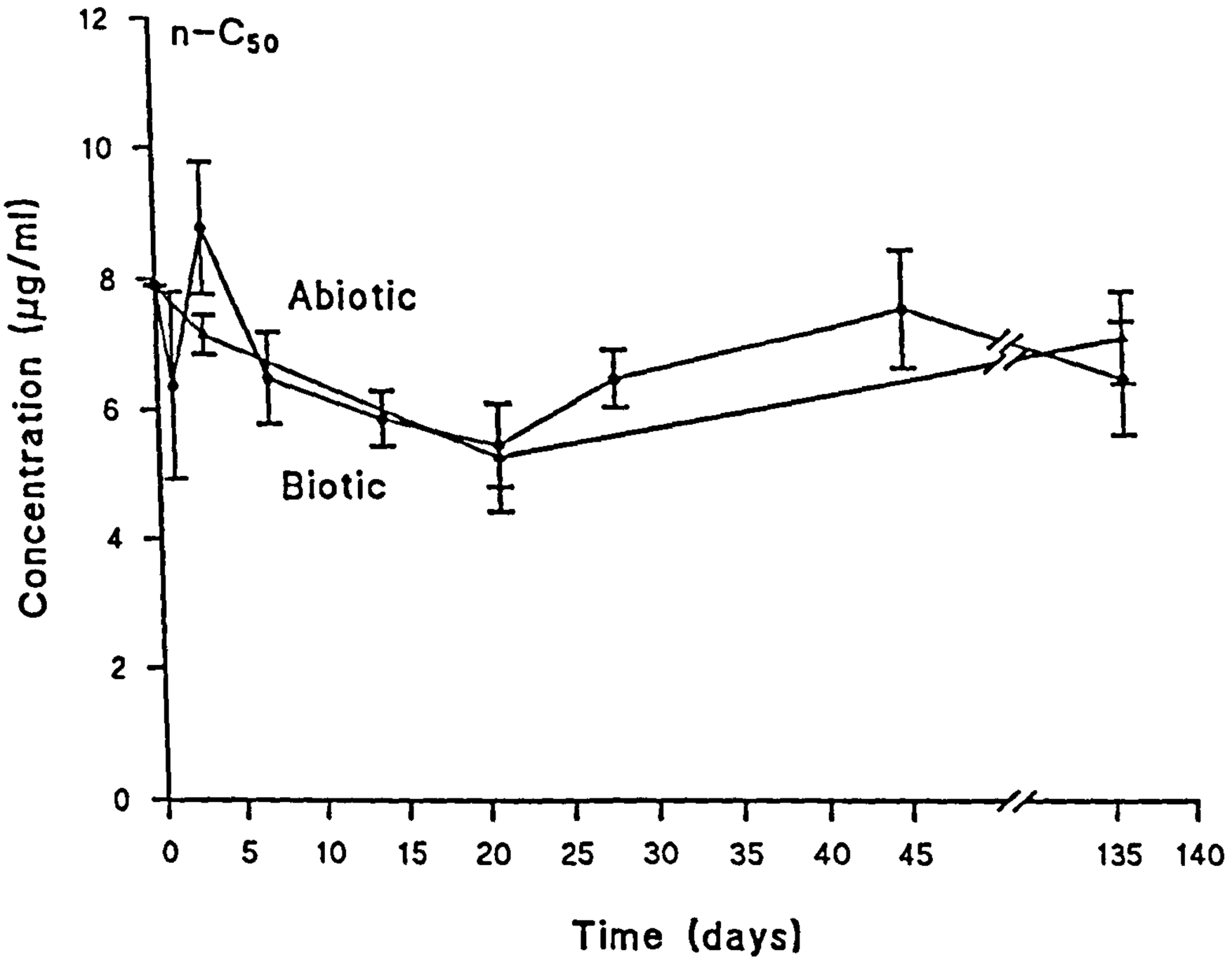

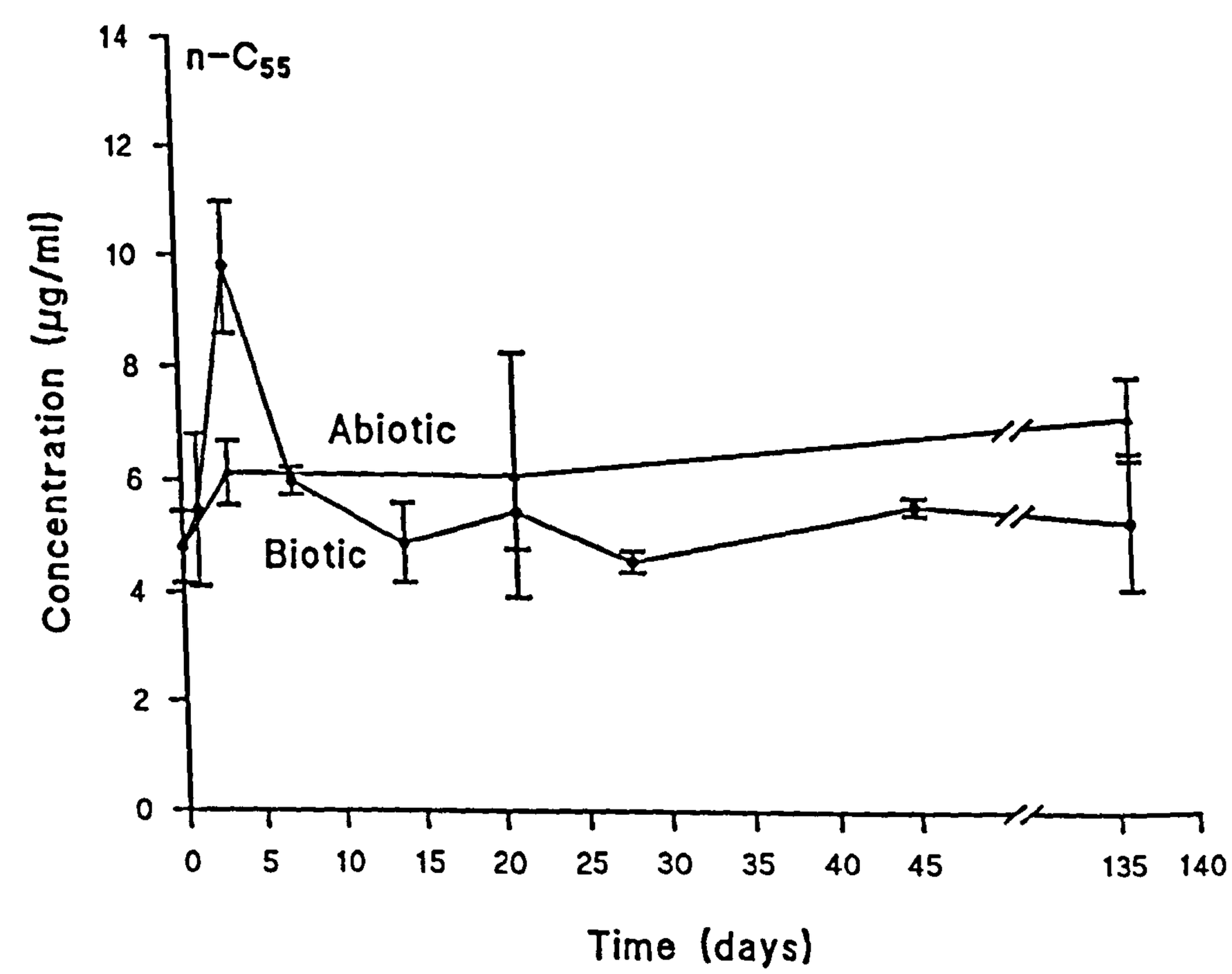

continued overleaf.....

continued.....

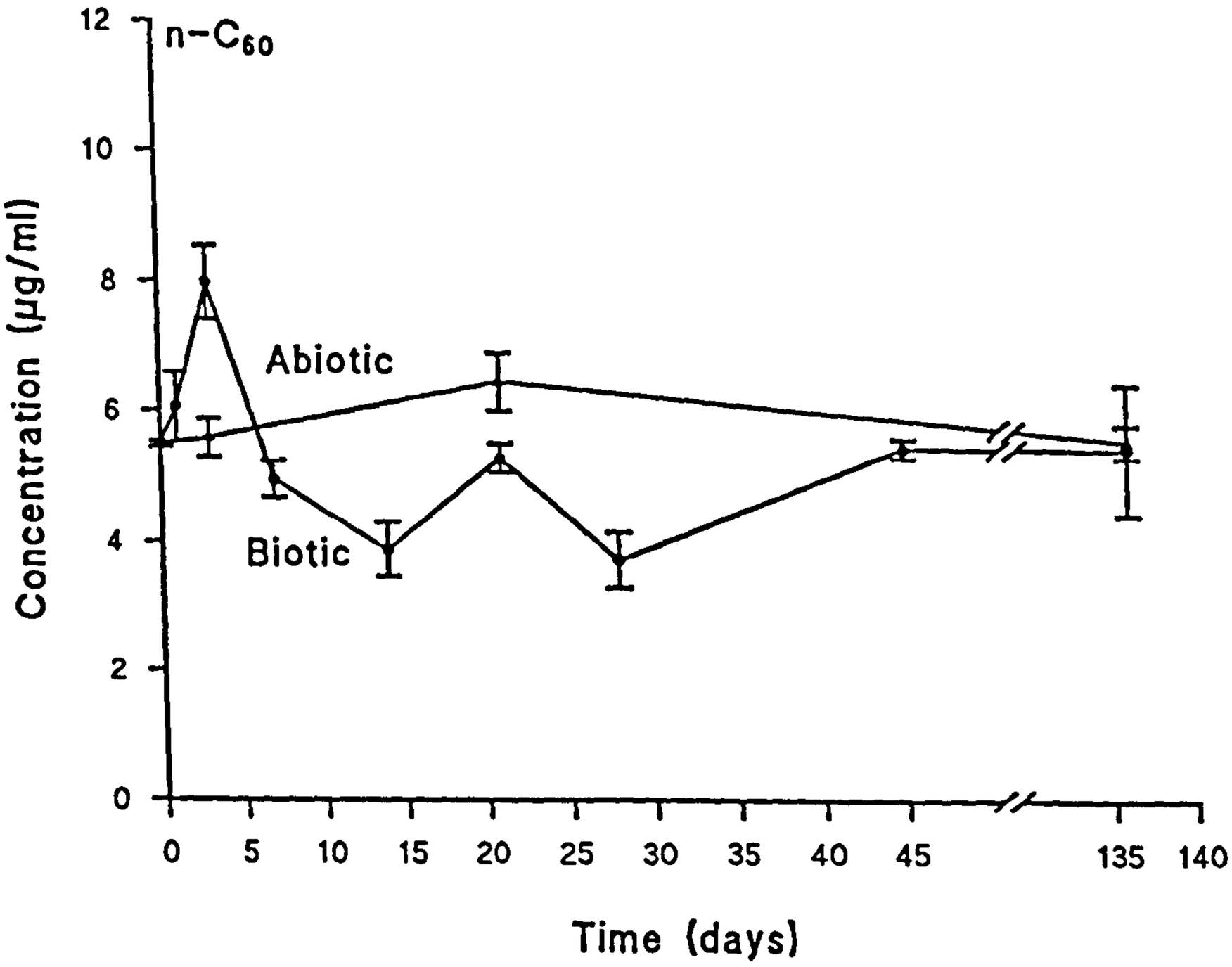
n-C60
Concentration (µg/ml)
12
10
8
6
4
2
0
Abiotic
Biotic
0
5
10
15
20
25
30
35
40
45
135
140
Time (days)

shown for *n*-triacontane (*n*-C_{30}) where a rapid degradation takes place within the first three days (74%) when the rate of degradation decreases until it finally disappears within 28 days. For *n*-pentatriacontane (*n*-C_{35}) the degradation is most dramatic up to 14 days (72%) and by 136 days of incubation only 5% remained. It appears that when negative growth of bacteria begins is when the *n*-alkanes $<$ *n*-C_{25} had been degraded (14 days). This negative growth also appears at the same time as the rate of removal of *n*-C_{30} starts to decline.

As expected, *n*-tetracontane (*n*-C_{40}) showed a much slower rate of decay with more than half (64%) still remaining at the end of the incubation period. No apparent degradation of pentatetracontane (*n*-C_{45}) appeared until after 45 days of incubation and at day 136 32% appeared to have been degraded. The results also showed that the degradation of the *n*-alkanes up to *n*-C_{35} occurred simultaneously, albeit at different rates. For the *n*-alkanes *n*-C_{40} and *n*-C_{45} there seemed to be an increasing delay before degradation started to occur (3 and 45 days respectively). This may indicate, especially in the latter, that as the amount of lower molecular *n*-alkanes dramatically decreased, the bacteria were forced to utilise the higher molecular *n*-alkanes and this may require some kind of enzymatic modification.

For the *n*-alkanes with chain lengths greater than C_{45} (*n*-C_{50}, *n*-C_{55}, and *n*-C_{60}) no degradation occurred, even after 136 days of incubation. This result agrees with that reported by **Setti et al. (1993)**, though **Hanstveit (1992)** showed extensive degradation (only qualitatively) of *n*-alkanes up to *n*-C_{50} within 28 days when the wax was adsorbed onto filters.

There have been many studies of the bacterial degradation rates of various substrate **(Monod, 1949; Simkins and Alexander, 1984; Battersby, 1990)** and it is assumed that the growth rate or the rate at which an organism utilises a substrate will fit a general rate law. The kinetics of biodegradation have been described by a variety of mathematical expressions, increasing in complexity as they attempt to accommodate the many variables which can affect the rate of biological removal of a substrate. These models are shown in Figure 3-21. For a study such as the present research, which

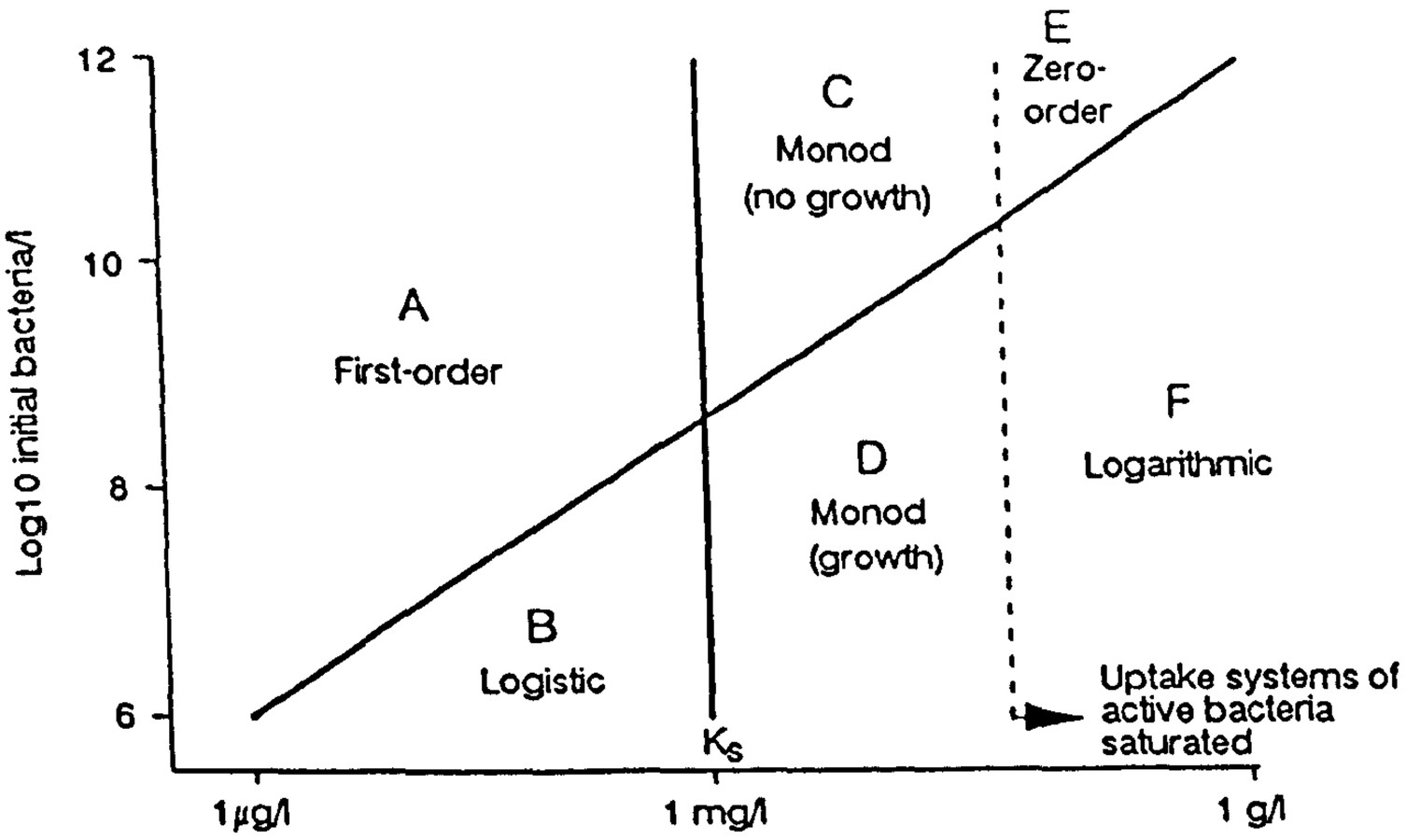

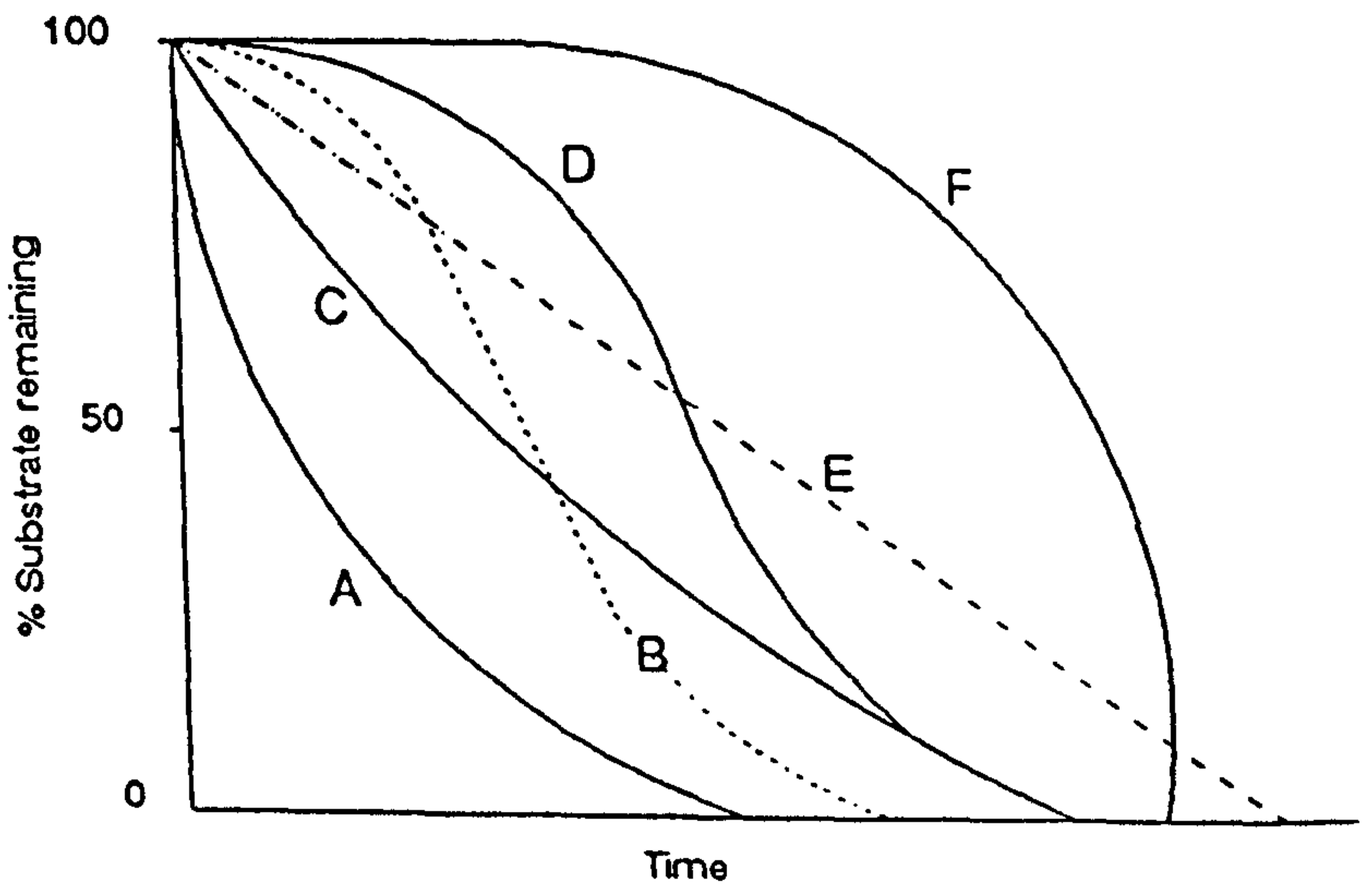

Figure 3-21 A) Kinetic models and B) Disappearance curves for a chemical degraded with time according to the kinetic models shown above (**Simkins and Alexander, 1984**).

monitors the decrease of a test substance (aliphatic wax) with a low initial concentration of substrate (15 mg/l) with high initial cell concentrations (3.5 x 10^8 per ml), the expectant rate law would be either Monod (no growth) or first order (**Simkins and Alexander, 1984**). The degradation curve obtained experimentally (Figure 3-22) does not match the six theoretical kinetic models shown in Figure 3-21. If the biodegradation is a first order reaction, as might be expected, then the rate of biodegradation will be proportional to the substrate concentration. **Battersby, (1990)** states that rate should be more properly described as a pseudo-first order reaction, because there are other factors affecting biodegradation. For instance, entry of the substrate into the cell, and the reaction will not entirely be dependent on concentration. Generally first order kinetics can be can be expressed as:

$$\frac{-d[C]}{dt} = k_{bio}[C]^n$$

Where

n = the order of the reaction

[C] = concentration of substrate

k_{bio} = biodegradation rate constant (Battersby, 1990)

Thus the rate will be the product of the rate constant and the substrate concentration. If ln of the concentration is plotted against time, the resultant curve should be a straight line (Figure 3-21 A). At first sight the data in Figure 3-22 does not appear to match the first order rate expression. However with a plot of between 0 and 14 days incubation (Figure 3-22 B) the data does show some linearity (r = 0.954) which may indicate first order rate with a degradation rate constant (k_{bio}) of 0.111 days and half life ($t_{1/2}$), (which is the time taken for half the original amount of substrate to be removed) for the first two weeks of incubation of 2.2 days.

At 14 days the rate changes dramatically and first order growth can no longer be assumed from the data available. An explanation may be that rate constants are usually applied to a single substrate, but the aliphatic fraction is a complex hydrocarbon mixture containing compounds which are easily degraded to those which are non-degradable. Solubility also affects degradation rate because as the compounds become

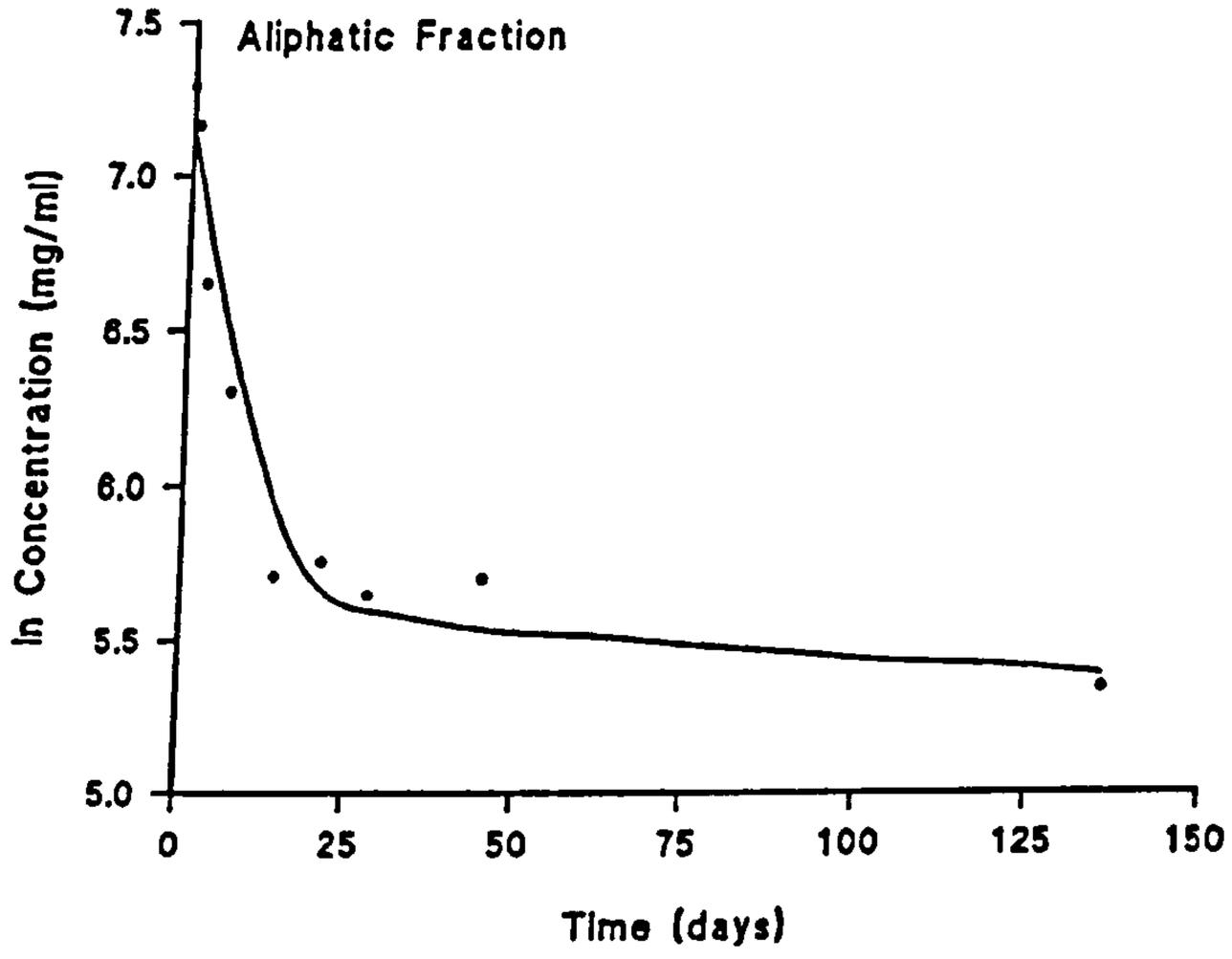

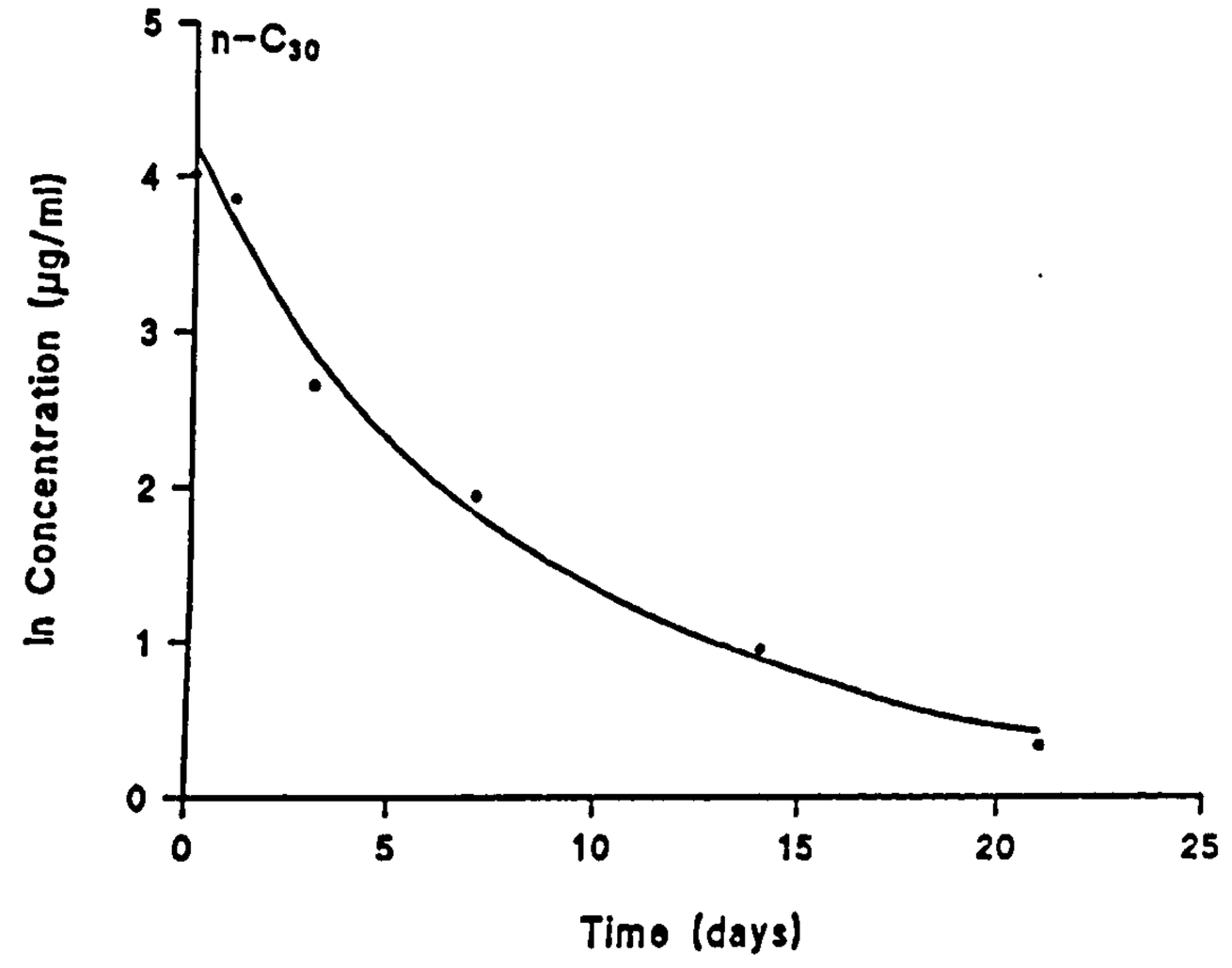

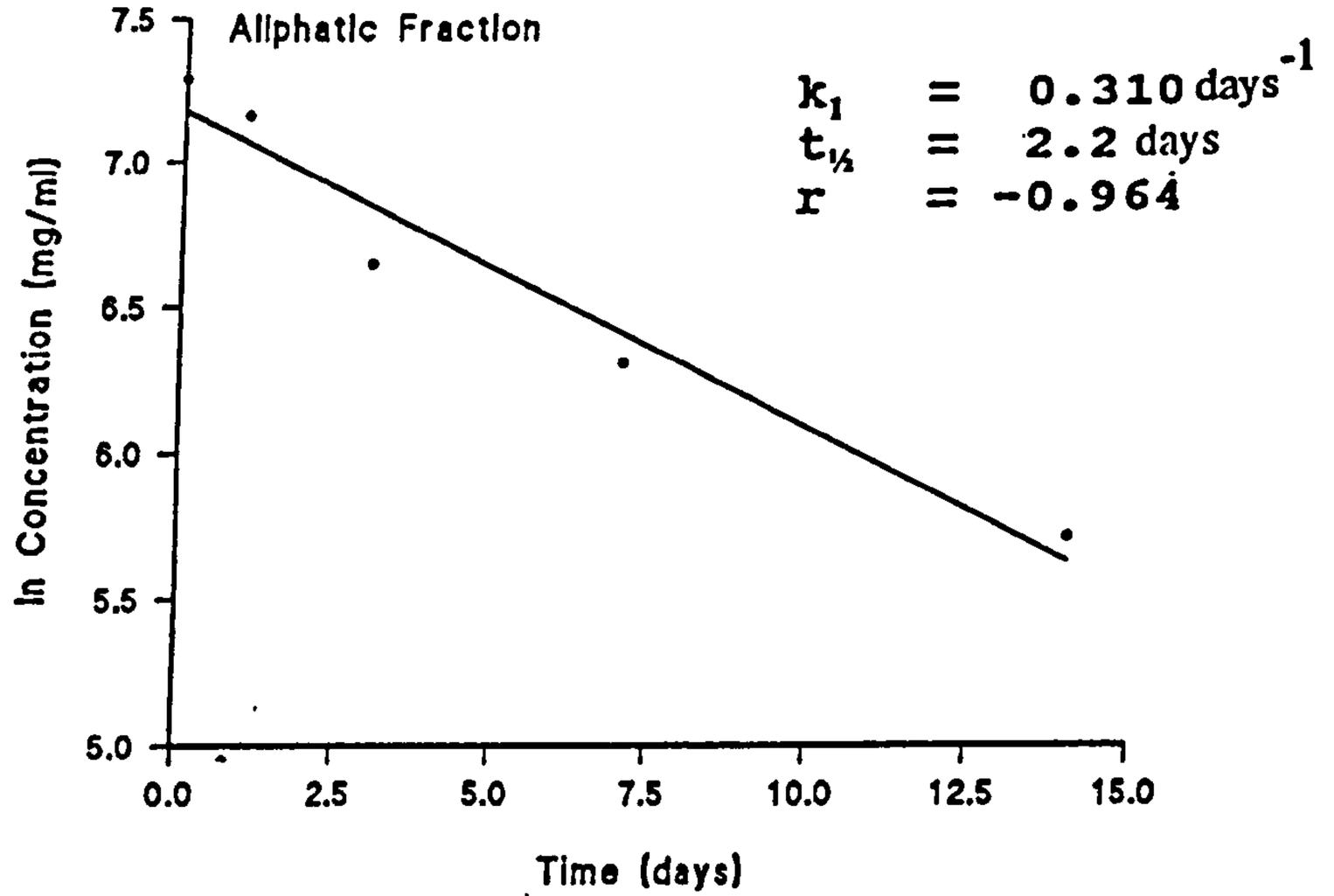

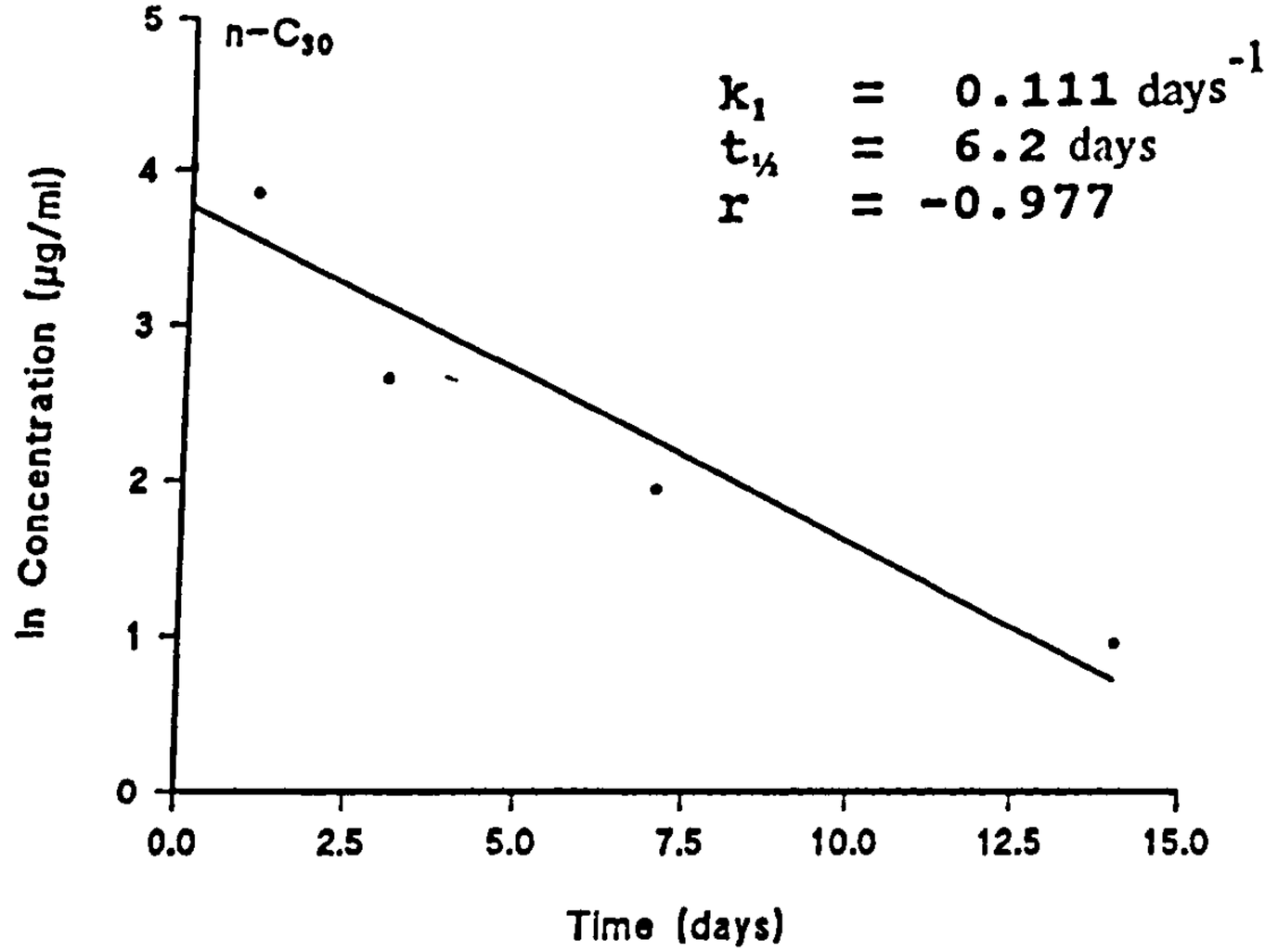

continued overleaf .....

Figure 3-22 First order rate curves for the biodegradation of the whole aliphatic wax and selected alkanes *n*-C_{30}, *n*-C_{35} and *n*-C_{40}.

Continued .....

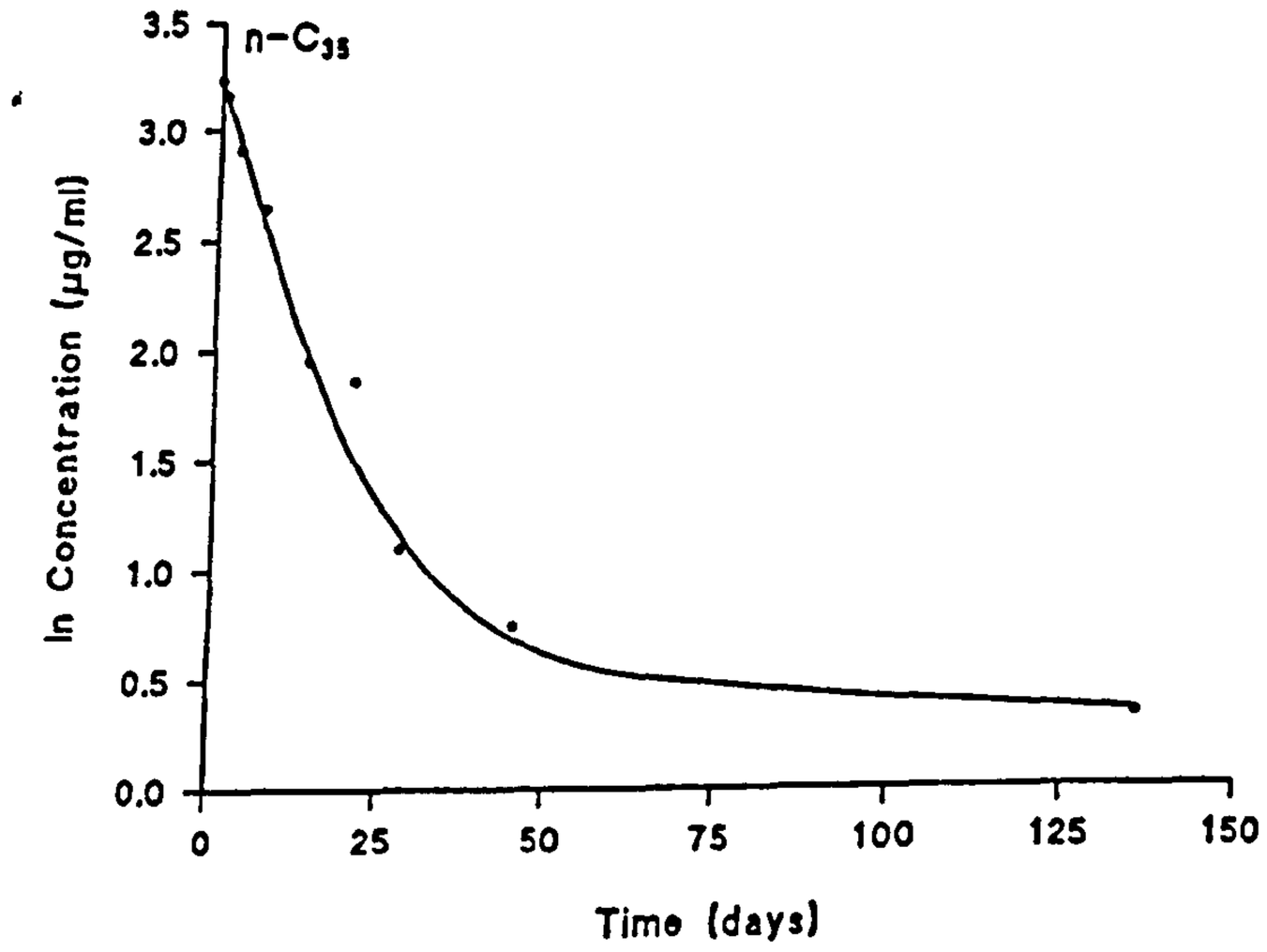
n-C35
ln Concentration (µg/ml)
3.5
3.0
2.5
2.0
1.5
1.0
0.5
0.0
0
25
50
75
100
125
150
Time (days)

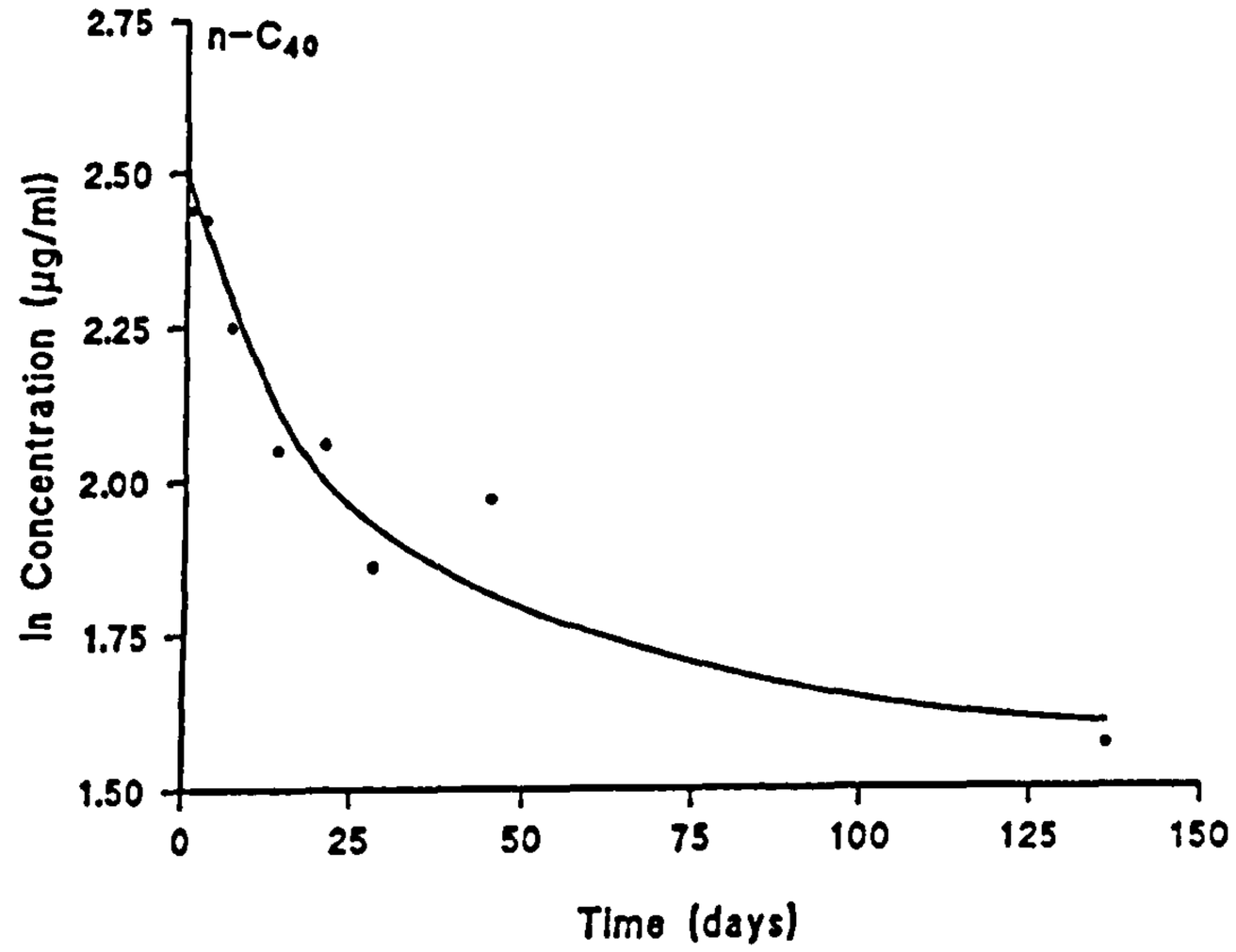
n-C40
ln Concentration (µg/ml)
2.75
2.50
2.25
2.00
1.75
1.50
0
25
50
75
100
125
150
Time (days)

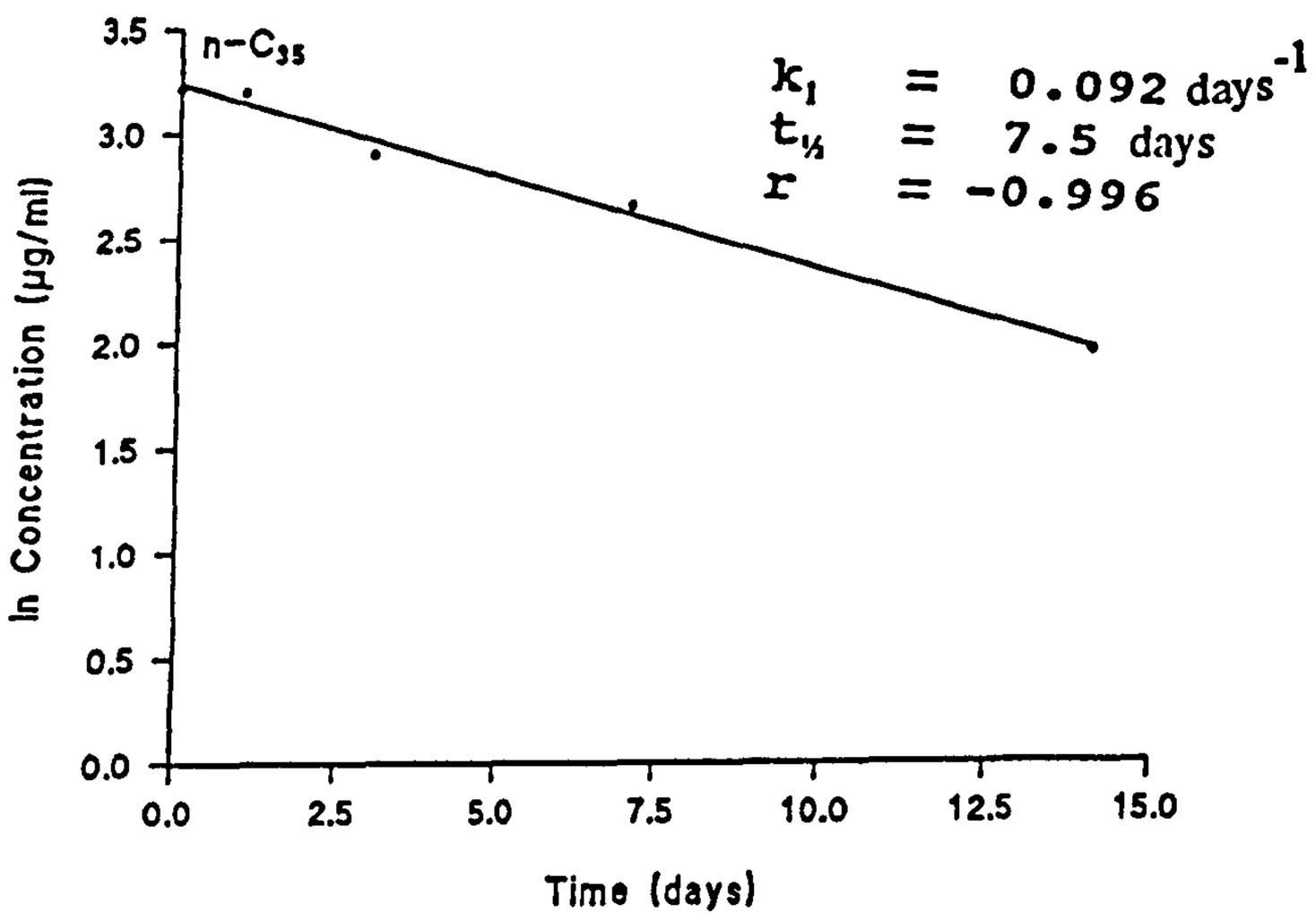
n-C35
k1 = 0.092 days-1
t½ = 7.5 days
r = -0.996
ln Concentration (µg/ml)
3.5
3.0
2.5
2.0
1.5
1.0
0.5
0.0
0.0
2.5
5.0
7.5
10.0
12.5
15.0
Time (days)

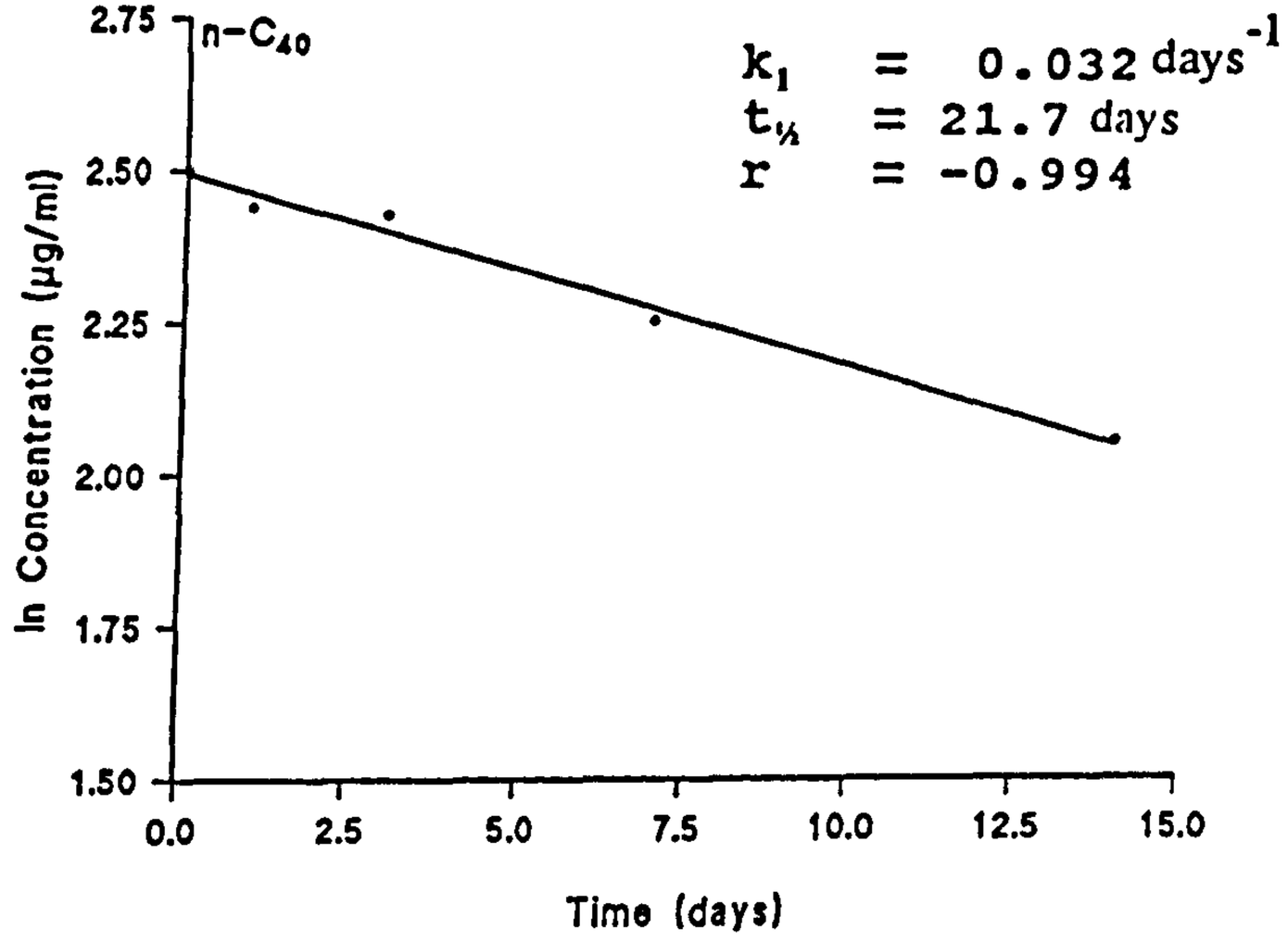
n-C40
k1 = 0.032 days-1
t½ = 21.7 days
r = -0.994
ln Concentration (µg/ml)
2.75
2.50
2.25
2.00
1.75
1.50
0.0
2.5
5.0
7.5
10.0
12.5
15.0
Time (days)

less soluble the free bacterial cells in solution will become limited in substrate and their growth rate will decline. First order rate kinetics will thus apply when the easily degradable compounds in the aliphatic fraction are not limited and there is ample scope for growth, for instance, in the exponential phase (**Monod, 1949**). As the concentrations of these compounds decreases the bacteria will start to metabolise the more difficult to degrade compounds, and so the rate of biodegradation will change.

Plots of log concentration against time for *n*-C_{30}, *n*-C_{35} and *n*-C_{40} are shown in Figure 3-22. Below triacontane the removal of the *n*-alkanes was too rapid to be observed by the sampling rate and above *n*-C_{40} the degradation was too low to be meaningful. The graphs (Figure 3-22) indicate that degradation for the first 14 days follows first order kinetics with linear correlation coefficients of -0.996 and -0.994 for *n*-C_{35} and *n*-C_{40} respectively. As expected, the rate of degradation also decreased with increasing carbon number ie. k_{bio} = 0.308 d^{-1} (*n*-C_{30}), 0.092 d^{-1} (*n*-C_{35}) and 0.03 d^{-1} (*n*-C_{40}) and $t_{1/2}$ increases from 6.2 days for *n*-C_{30} to 28 days for *n*-C_{40}. Again these reflect the biodegradability and the decreasing concentrations of the *n*-alkanes, $C_{30} > C_{35} > C_{40}$ and so forth.

It is interesting to compare these measured rates with those predicted from structure-activity relationships (**Tabak *et al.*, 1992; Tabak and Govind, 1993**). Using biodegradation respirometry data obtained for over seventy organic substances by **Urano and Kato (1968a,b)** as a training set, **Tabak *et al.*, (1992)** were able to devise both a simple linear and a more complex Monod model for the computation of k_{bio} of simple organic compounds. The linear method was later refined by use of a neural network but the computed values were in good agreement with their linear method. Table 3-9 shows the incremental values obtained by **Tabak *et al.*, (1992)** for their linear model for various structural components of organic compounds. Summation of these increments allows computation of k_{bio}. Thus for *n*-C_{20} alkane k_{bio} would be:

$$[2xCH_3] \times [18 \times CH_2] = -3.46\ hr^{-1}.$$

For the *n*-$C_{20\text{-}60}$ alkanes in the present study, values shown in Table 3-10 are obtained.

Group	Symbol	α_i
Methyl	CH_3	-1.37
Methylene	CH_2	-0.04
Hydroxy	OH	-1.71
Acid	COOH	-1.31
Ketone	CO	-0.51
Amine	NH_2	-1.46
Aromatic CH	ACH	-0.50
Aromatic carbon	AC	1.06

Table 3-9 Groups and their contribution values for first-order rate constants (Source: **Tabak *et al.*, 1992**).

Table 3-10 Experimental and predicted concentrations of *n*-alkanes in an Indonesian oil after 3 and 14 days biodegradation.

Carbon Number	[1]Relative concentration (%)	α_j	k_{bio} (days)	Amount of *n* -Alkanes Remaining			
				3 Days		14 Days	
				[2]Pred.	[3]Exp.	Pred.	Exp.
14	32.4	-3.220	-0.9589	1.8	0.0	0.0	0.0
15	94.6	-3.260	-0.9213	6.0	0.0	0.0	0.0
16	150.0	-3.300	-0.8852	10.5	0.0	0.0	0.0
17	174.3	-3.340	-0.8505	13.6	0.0	0.0	0.0
18	154.1	-3.380	-0.8171	13.3	0.0	0.0	0.0
19	135.1	-3.420	-0.7851	12.8	0.0	0.0	0.0
20	127.0	-3.460	-0.7543	13.2	1.5	0.0	0.0
21	124.3	-3.500	-0.7247	14.1	2.6	0.0	0.0
22	123.0	-3.540	-0.6963	15.2	5.1	0.0	0.0
23	144.6	-3.580	-0.6690	19.4	10.5	0.0	0.0
24	151.4	-3.620	-0.6428	22.0	17.9	0.0	0.7
25	173.0	-3.660	-0.6176	27.1	28.2	0.0	1.4
26	197.3	-3.700	-0.5934	33.3	46.2	0.0	2.5
27	213.5	-3.740	-0.5701	38.6	76.9	0.1	2.7
28	200.0	-3.780	-0.5477	38.7	112.8	0.1	3.4
29	198.6	-3.820	-0.5263	41.0	115.4	0.1	4.8
30	173.0	-3.860	-0.5056	37.9	111.5	0.1	5.5
31	159.5	-3.900	-0.4858	37.1	101.3	0.2	6.2
32	124.3	-3.940	-0.4668	30.6	89.7	0.2	8.2
33	109.5	-3.980	-0.4485	28.5	76.9	0.2	12.3
34	91.9	-4.020	-0.4309	25.2	67.9	0.2	15.1
35	81.1	-4.060	-0.4140	23.4	53.8	0.2	21.9
36	64.9	-4.100	-0.3977	19.7	46.2	0.2	22.2
37	50.0	-4.140	-0.3821	15.9	39.7	0.2	23.3
38	43.2	-4.180	-0.3672	14.4	33.3	0.3	25.3
39	39.2	-4.220	-0.3528	13.6	32.1	0.3	24.7
40	32.4	-4.260	-0.3389	11.7	30.8	0.3	22.6
41	29.7	-4.300	-0.3256	11.2	29.5	0.3	24.7
42	28.4	-4.340	-0.3129	11.1	28.2	0.4	24.7
43	28.4	-4.380	-0.3006	11.5	29.5	0.4	25.3
44	29.7	-4.420	-0.2888	12.5	25.6	0.5	24.7
45	27.0	-4.460	-0.2775	11.7	26.9	0.6	23.3
46	26.0	-4.500	-0.2666	11.7	25.6	0.6	23.3
47	24.3	-4.540	-0.2562	11.3	24.4	0.7	22.6
48	23.0	-4.580	-0.2461	11.0	25.6	0.7	19.9
49	21.6	-4.620	-0.2365	10.6	19.2	0.8	18.5
50	21.6	-4.660	-0.2272	10.9	20.5	0.9	17.8
51	17.6	-4.700	-0.2183	9.1	17.9	0.8	16.4
52	16.2	-4.740	-0.2097	8.6	17.9	0.9	18.5
53	16.2	-4.780	-0.2015	8.9	16.7	1.0	16.4
54	16.2	-4.820	-0.1936	9.1	17.9	1.1	16.4
55	14.9	-4.860	-0.1860	8.5	16.7	1.1	15.1
56	16.2	-4.900	-0.1787	9.5	17.9	1.3	15.8
57	16.2	-4.940	-0.1717	9.7	16.7	1.5	15.1
58	13.5	-4.980	-0.1650	8.2	15.4	1.3	15.1
59	14.9	-5.020	-0.1585	9.2	15.4	1.6	15.8
60	16.2	-5.060	-0.1523	10.3	16.7	1.9	15.1

1 Concentrations expressed relative to the height of the internal standard.

2 Predicted values (Tabak, 1992)

3 Experimental values.

The model (Figure 3-23) shows some qualitative agreement at day three but then the predicted values show much greater degradation of HMW *n*-alkanes ($>C_{40}$) than was actually observed. This is not surprising because the training set was limited and did not include compounds with greater than six carbon atoms whereas an oil is a mixture of hundreds of compounds many of them greater than C_6 and the degradation rate of each will be affected by the others. The results from this study have shown that very little degradation occurs after *n*-C_{40} while *n*-alkanes below *n*-C_{25} are degraded rapidly. The model predicts much higher rates of degradation of alkanes above C_{40}. Clearly the model needs to be refined with the training set including medium and HMW compounds. Nonetheless it does show how such structural activity relationships can be useful.

The above findings show that experimentally even after 136 days the bacteria did not noticeably degrade *n*-alkanes with more than 45 carbons under conditions in which the lower molecular weight *n*-alkanes ($<n$-C_{30}) were totally or extensively degraded. After three days of incubation (Figure 3-24, A) the HTCGC chromatographic profiles of the remaining aliphatic fraction already looked fairly similar to HTCGC of the tar balls collected by **McKirdy, (1994)** illustrated in Figure 3-24, B). The results indicate that within the first three days half of the aliphatic wax substrate had been degraded, although obviously the rate of degradation of these compounds might be much slower in the environment where there will be alternative carbon sources present and higher salinity and temperature will have the effect of slowing down biodegradation (**Mille *et al.*, 1991; Lyman *et al.*, 1982**). The rate of degradation will also depend on the bacterial community that is present because not all bacteria are efficient oil degraders. Nonetheless these studies support the argument that transport of naturally weathered waxy oils from Indonesia could be the source of some of the tar balls found in Australia

3.3.8 Electron microscopy

At the end of the incubation period of 136 days a small wax clump was removed and examined using scanning electron microscopy (SEM). Plates A and B shown in Figure 3-25 are of the same area but at a magnification of 7,000 and 9,500 times respectively.

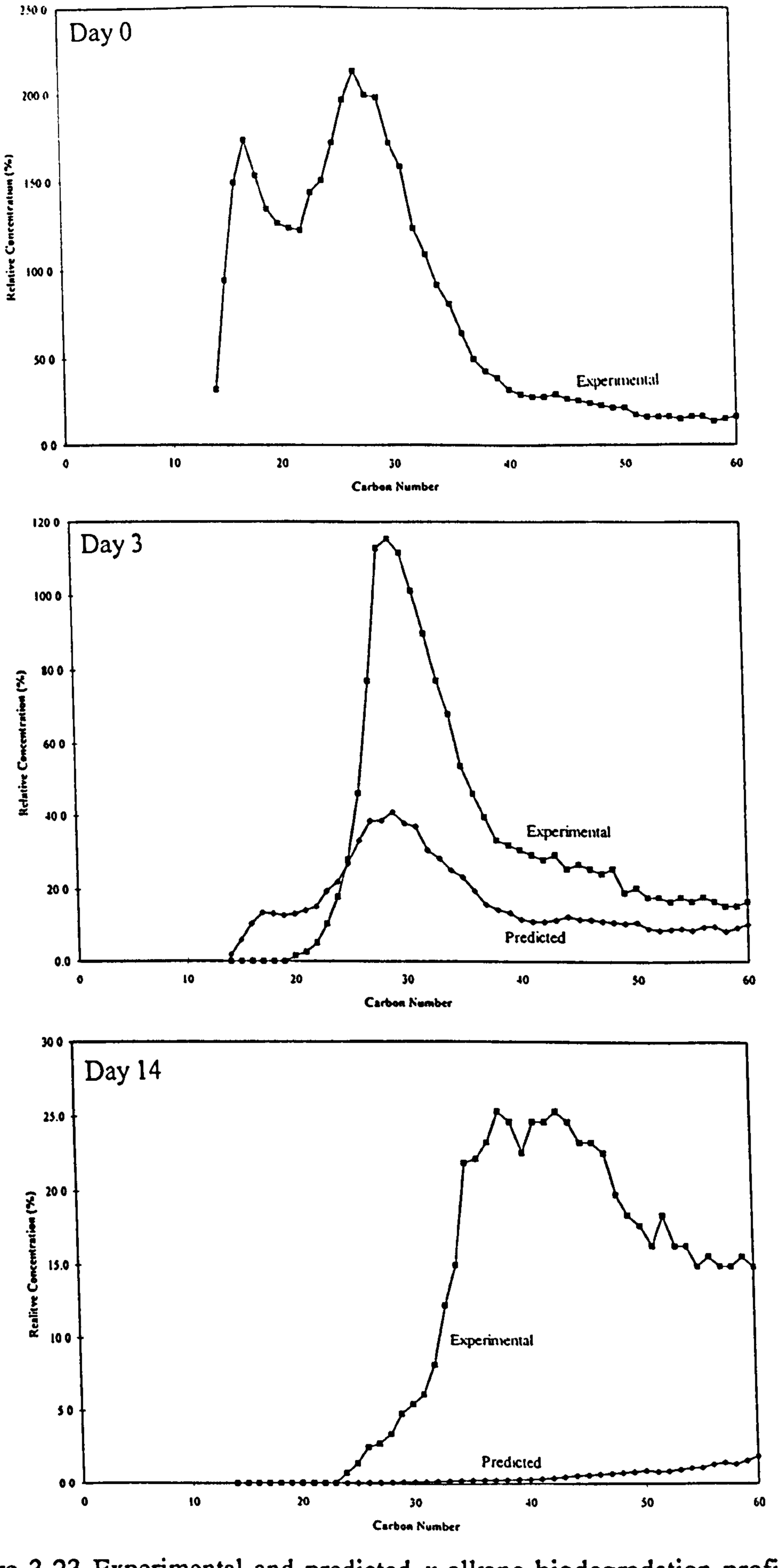

Figure 3-23 Experimental and predicted *n*-alkane biodegradation profiles of an Indonesian oil after 3 and 14 days.

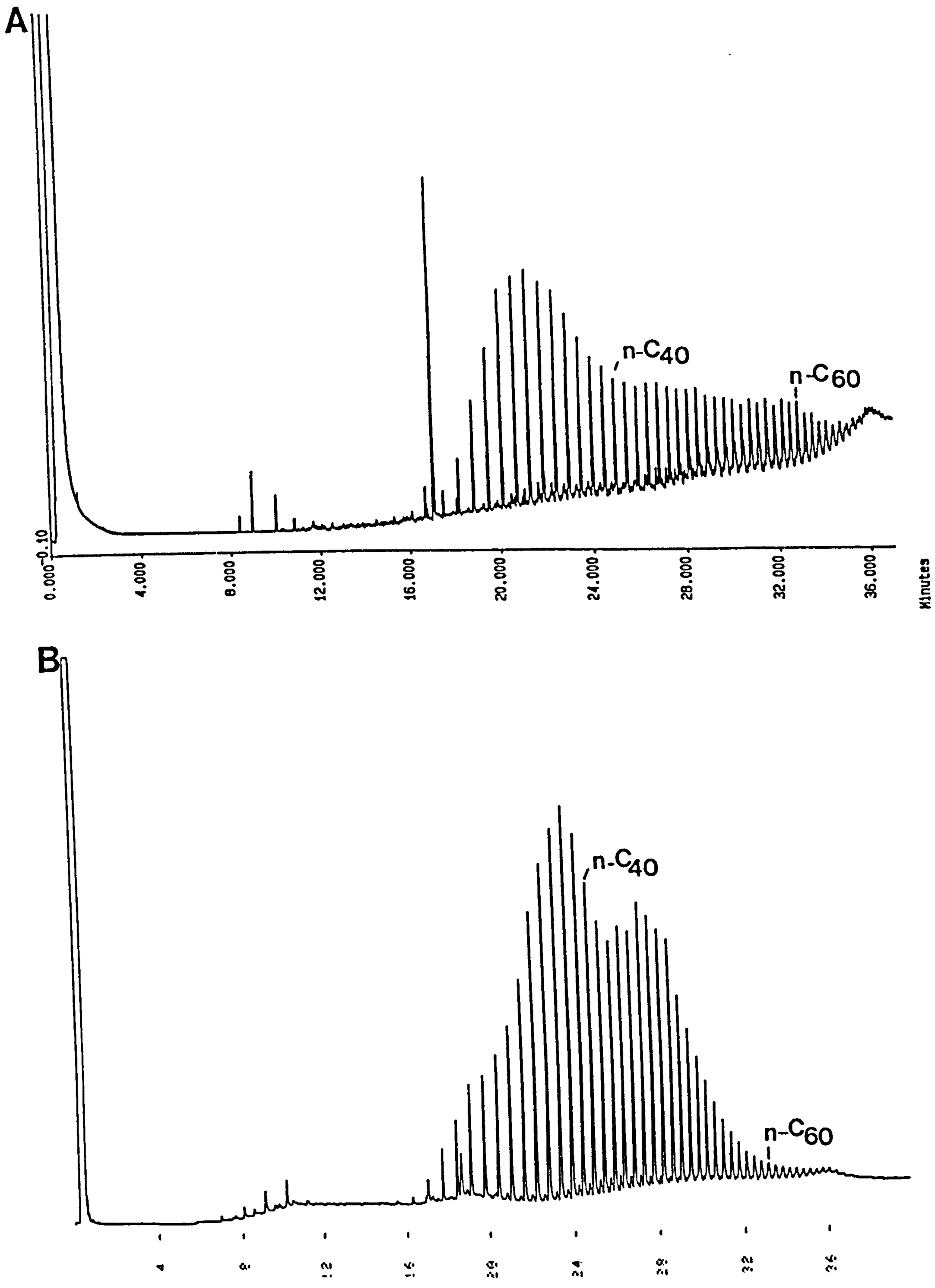

Figure 3-24 A) HTCGC of degraded aliphatic fraction of an Indonesian oil after three days incubation. B) HTCGC of tar ball collected by Padley (1991) from the South Australian coastline.

Figure 3-25 Plate A) SEM photograph of a wax clump after 136 days of incubation at x 7,000 magnification and Plate B) x 9,500 magnification.

A

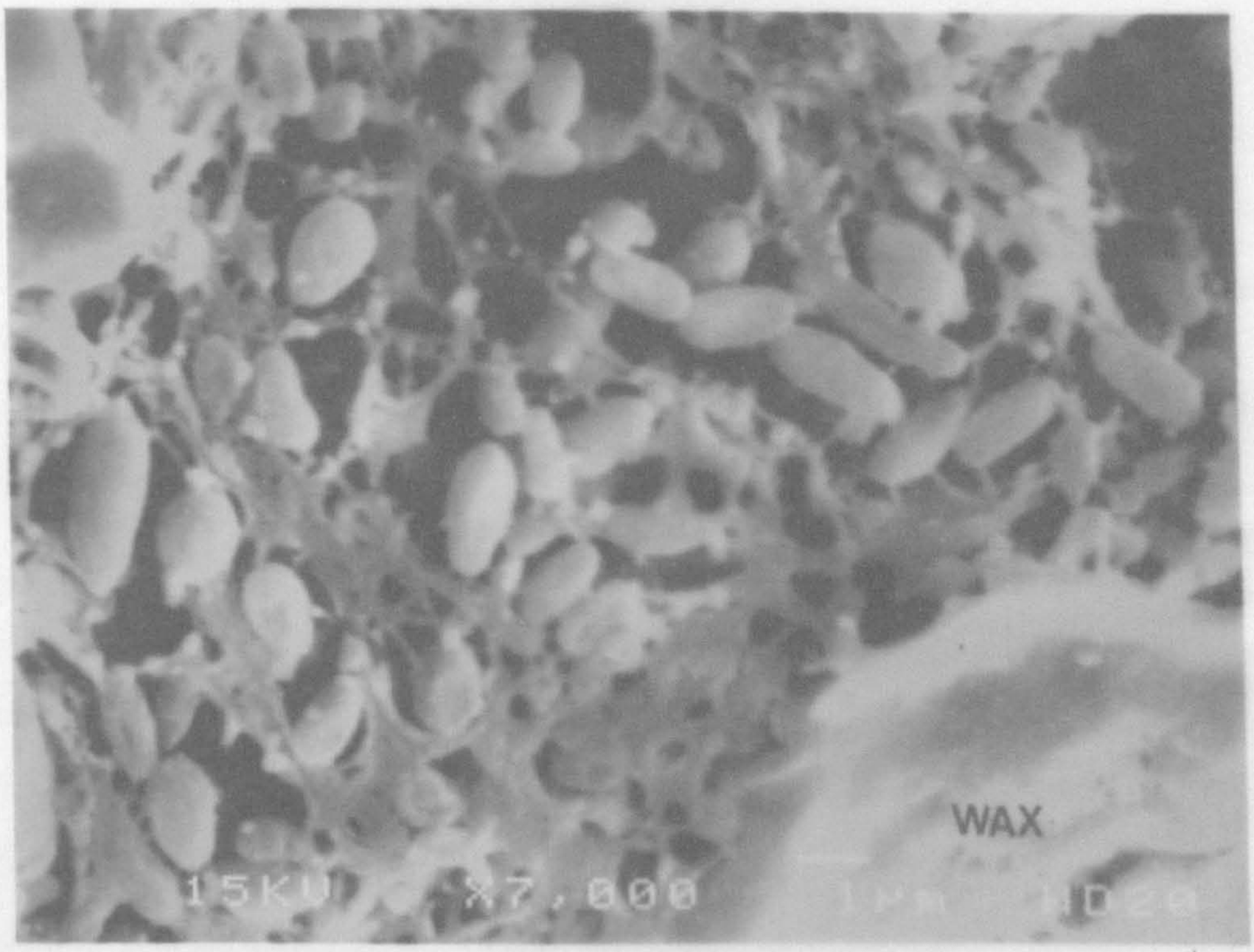

B

Figure 3-25 Plate A) SEM photograph of a wax clump after 136 days of incubation at x 7,000 magnification and Plate B) x 9,500 magnification.

The pictures show bacteria (gram negative rods b) about 1 μm in length, present within a loose spongy-stringy matrix c between the wax clumps. The bacteria (b) do not appear to be on the "wax" (a) (the material may be wax, degraded wax or extra-cellular material formed by the bacteria during incubation). This material appears as a white floc visible after several weeks into the experiment. The bacteria appear to be anchored to the main mass of material by small strands. The literature suggests (see Introduction) that many species of bacteria adhere to the surface of the hydrocarbon solids. These results suggest the bacteria are not directly in contact with the sample but are anchored in place close to it, and thus uptake will primarily be through solubilisation. Bacteria have been shown to produce extracelluar emulsifiers and enzymes to break down hydrocarbons and increase their solubility **(Reddy, 1992)**. It would appear advantageous for each bacterium to anchor close to the solid wax particles and then release solubilisation agents where they would be most effective. This material between the solid wax particles may be either extra-cellular material from a large number of bacteria or wax that has been degraded, leaving holes with the residual waxy material containing the heavy HMW weight alkanes that are resistant to microbial degradation.

3.3.9 Rapid Screening method to monitor solid *n*-alkane degradation

The above findings (3.3.7) suggest that *Pseudomonas fluorescens* (Texaco) is unable to degrade *n*-alkanes over *n*-C_{45}. However the fact that these compounds were not degraded could also be because the population of bacteria remaining late in the experiment were surviving on the small amount of LMW *n*-alkanes that remained and thus the bacteria had no need to begin to utilise the HMW *n*-alkanes. Also, bacteria may utilise the initial degradation products of LMW oxidation (such as primary alcohols) as carbon sources **(Singer and Finnerty, 1984)**.

By 136 days of incubation, other limiting factors, for example exhaustion of nutrients, may also be a contributing factor. *Pseudomonas fluorescens* (Texaco) like most microorganisms used in such studies, is a chemoorganotroph, which requires, in addition to an organic compound as a carbon and energy source, a hydrogen acceptor, inorganic ions (provided by the minimal media), and carbon dioxide. Any of these three

could be limiting factors, though the experiment was designed to avoid inorganic limitations by providing a large excess of nutrients. Another possibility is that further utilisation was prevented by the build up of toxic metabolites. Again this is unlikely because the concentration of these products would probably be very low in the culture flasks. Clearly whether or not *Pseudomonas fluorescens* (Texaco) is able to degrade HMW alkanes $>n$-C_{45} is still open to question.

On way to further investigate this question but in a qualitative manner is to use a method devised by **Kiyohara *et al.*, (1982)** to study the degradation of PAH's. The method involves inoculating the surface of a substrate-deficient mineral salts agar plate (*i.e.* an agar plate that does not contain any disodium succinate or glucose). A fine layer of the sample is then sprayed over the surface of the plate and the plate then incubated as normal. If the bacteria are able to metabolise the samples, colonies will grow, and as they grow, the sample around the colony will be metabolised and a "zone of clearing" will form.

The bacterium *Pseudomonas fluorescens* (Texaco) was cultured and separated from the cultural broth by centrifugation in phosphate buffer solution to remove any source of carbon from the culture broth, and streaked across the nutrient deficient agar plates. The plates were then sprayed separately with a single pure, n-C_{20}, n-C_{25}, n-C_{30}, n-C_{40}, n-C_{50}, and n-C_{60} alkane in a solution of hexane (50% wt/vol). Spraying of the waxes onto the plates was carried out using a modified Humbrol compressed air paint sprayer. The centre plastic tube was replaced by copper tubing and the large glass container replaced by a 10 ml glass vial to hold the sample. A major problem was solidification of waxes which caused blocking of the spray gun nozzle, particularly for the waxes with a melting point above 65-67°C (n-C_{30}). However, using the copper tubing meant that the spray gun could be heated to prevent the wax solidifying. A spray of a few seconds duration was found to be sufficient to cover a plate with a thin layer of wax. Although the plates took no more than a few seconds to dry there was concern that the solvent would render the plates sterile.

Figure 3-26 A & B shows a "deficient" agar plate and a nutrient agar plate after

Figure 3-26 Plate A) Inoculated substrate deficient agar plate showing negative growth of *Pseudomonas flourescens* (Texaco) after 36 hr incubation (37°C), and Plate B) inoculated nutrient agar plate showing positive growth after 24 hr incubation (37°C).

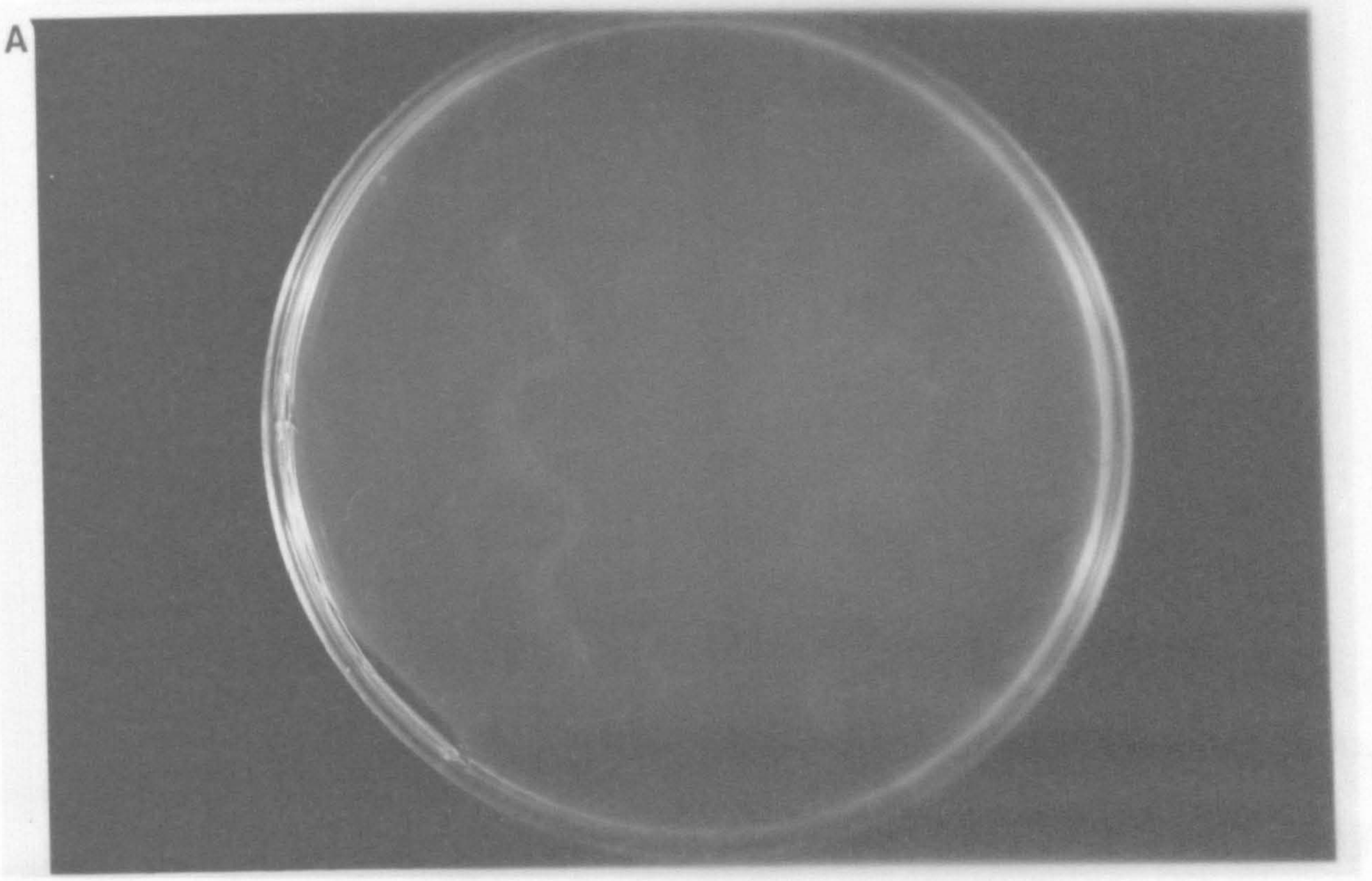

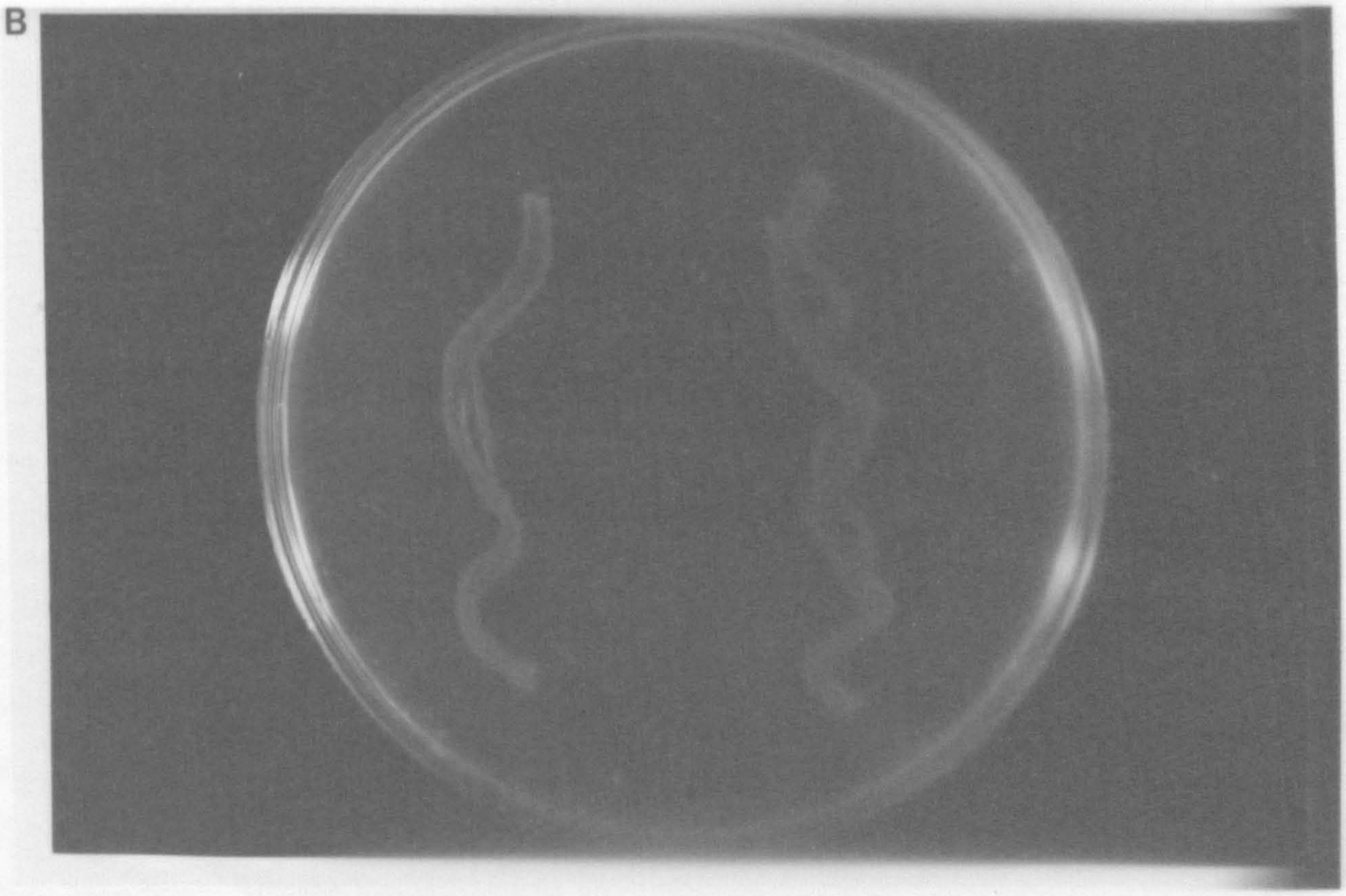

Figure 3-26 Plate A) Inoculated substrate deficient agar plate showing negative growth of *Pseudomonas flourescens* (Texaco) after 36 hr incubation (37°C), and Plate B) inoculated nutrient agar plate showing positive growth after 24 hr incubation (37°C).

inoculation with the *Pseudomonas* culture, both plates having been incubated for 36 hr. After incubation no growth was observed on the deficient plate but growth was apparent on the normal nutrient agar plate. The result shows that the bacteria were unable to grow on the plates that did not contain a substrate supplement. Figure 3-27 [A] shows a deficient plate that had been sprayed with *n*-triacontane (*n*-C_{30}). A thin layer of wax can be seen reflecting on the surface of the plate. Figure 3-27 [B] shows a similar plate that had been streaked with both bacteria and sprayed with n-C_{30}. Again both plates were incubated for 36 hr. In the case of the inoculated plate two zones of clearing can be seen where the plates had been streaked showing that the bacteria are capable of utilising triacontane as a carbon source. This was expected because *n*-C_{30} was shown to be significantly degraded in the previous experiments.

The results for the other *n*-alkane standards are shown in Table 3-11. Clearing was observed on duplicate test plates for *n*-$C_{20\text{-}30}$, and only on one of the test plates in the case of *n*-C_{40}. Above *n*-C_{40} no clearing was observed. Growth on only one of the plates sprayed with *n*-C_{40} might suggest spontaneous mutagenesis, or it may be because the bacteria on the other plate did not survive the wax spraying. Again these results confirm that the bacteria was not capable of degrading the HMW alkanes greater than *n*-C_{40}. The original culture had not been exposed to these HMW compounds in the presence of smaller utilisable alkanes and had not had the chance to undergo enzyme modification to deal with them.

A second experiment was carried out. This time the inoculum comprised the bacteria taken from the 136 day incubation culture from the experiment described in 3.3.6. The results are given in Table 3-11 (Exposed). Clearing zones were observed for all the *n*-alkanes even for *n*-C_{50} and *n*-C_{60}. In the case of *n*-C_{60} a zone of clearing was not observed until after three days of incubation rather than two days for the other *n*-alkanes, indicating the slow growth of the bacteria on the substrate.

This is thought be the first report of bacterial utilisation of *n*-C_{60} as a sole carbon source. The fact that growth was not observed for *n*-C_{50} and *n*-C_{60} using the original culture suggests that in the bacteria were gradual and required the presence of *n*-alkanes

Figure 3-27 Plate A) Abiotic nutrient deficient plate sprayed with pure triacontane C_{30} after 36 hr incubation at 37°C, and Plate b) inoculated with *Pseudomonas fluorescens* (Texaco) prior to being coated with wax.

A

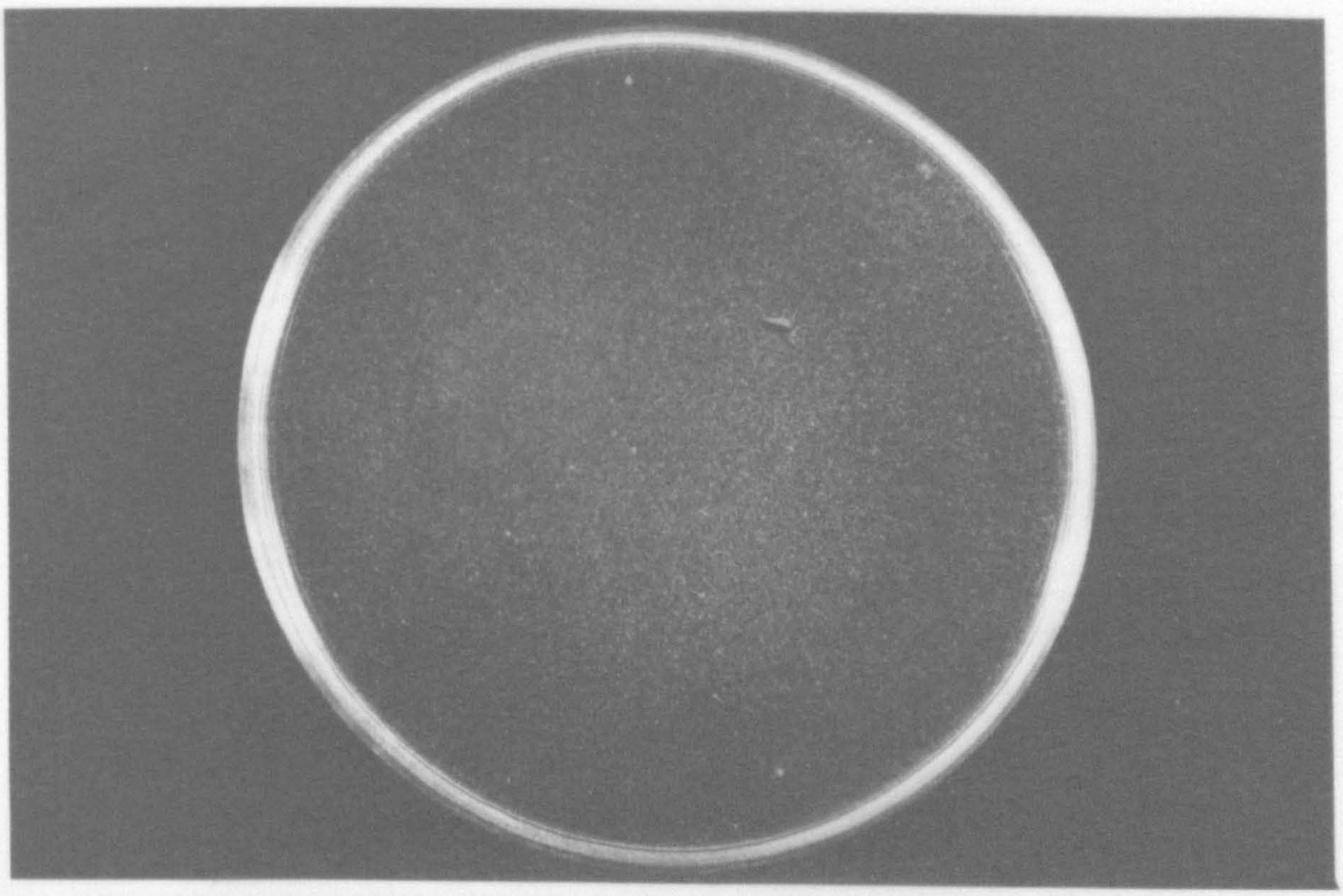

B

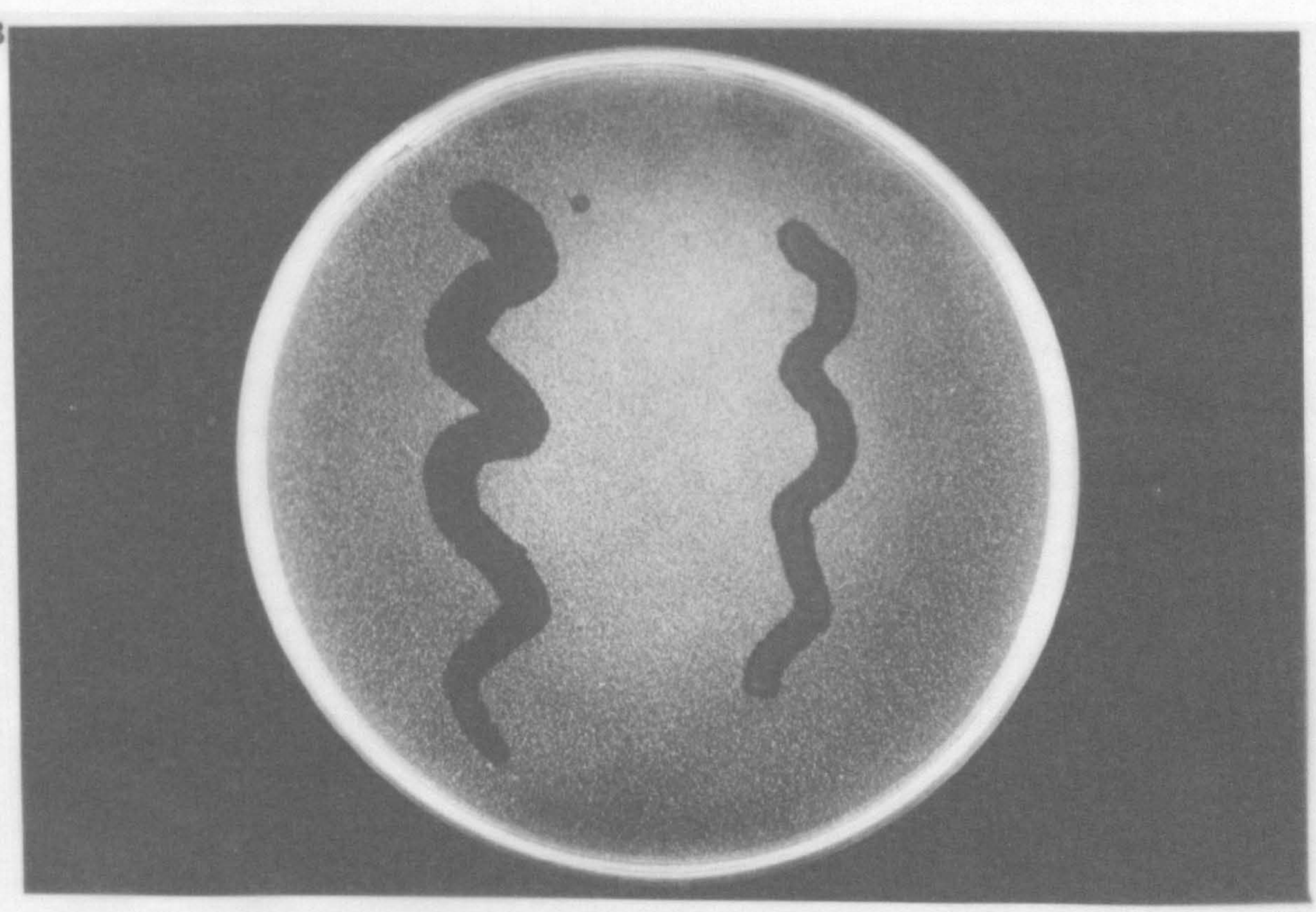

Figure 3-27 Plate A) Abiotic nutrient deficient plate sprayed with pure triacontane C_{30} after 36 hr incubation at 37°C, and Plate b) inoculated with *Pseudomonas fluorescens* (Texaco) prior to being coated with wax.

Table 3-11 Results from the rapid biodegradation screening method of pure solid *n*-alkane waxes using Pseudomonas Fluorescens (Texaco) after 36 hr incubation at 37°C.

n -Alkane	[a]Non-Exposed		[b]Exposed	
	Growth	UV fluorescence	Growth	UV fluorescence
C_{20}	[c]+/+	+/+	+/+	-
C_{25}	+/+	+/+	+/+	-
C_{30}	+/+	+/+	+/+	-/-
C_{40}	-/+	-/+	+/+	-/-
C_{50}	-/-	-/-	+/+	-/-
C_{60}	-/-	-/-	+/+	-/-
[d]Blank 1	-/-	-/-	-/-	-/-
[e]Blank 2	-/-	-/-	-/-	-/-
[f]Blank 3	-/-	-/-	-/-	-/-

a Bacteria grown from original culture

b Bacteria grown from culture exposed to wax after 140 days

c Replicate plates, + positive growth, - no growth

d Agar plate spread with bacteria alone

e Agar plate sprayed with wax alone

f Agar plate without wax or bacteria

with increasing chain lengths (so called acclimation). Organisms suddenly presented with the HMW alkanes were unable to utilise them.

3.3.10 Summary

Continuous liquid-liquid extraction proved a much more efficient and reproducible method of extracting HMW hydrocarbons from aqueous media than use of a separating funnel. Recovery of *n*-C_{60} was 93% with an RSD of under 5% compared with a separating funnel method which recovered only 50% and had a RSD of 20%.

Losses of HMW *n*-alkanes also occurred when using the traditional fractionation techniques of CC and TLC to isolate test substrate alkanes from a whole oil. This does not seem to have been reported previously probably because studies using conventional GC tend not to be concerned with the C_{40+} compounds. The limited number of qualitative HTCGC studies made previously mainly examined whole oil samples. Preferential adsorption of the more polar compounds of a whole oil onto activated alumina in an alumina/warm solvent slurry was found to leave in solution an aliphatic fraction rich in HMW alkanes. The absence of aromatics in solution was confirmed by UV spectroscopy and the presence of HMW alkanes above C_{60} by HTCGC.

By the end of a 136 day *in vitro* biological degradation trial of an aliphatic wax isolated from an Indonesian oil, only 14% remained non-degraded. HTCGC revealed the majority (80%) of material had been degraded in just under 14 days. Lower molecular weight *n*-alkanes *i.e.* *n*-alkanes with a carbon number of C_{20} and fewer were totally degraded within three days. Alkanes with carbon numbers *n*-$C_{20\text{-}25}$ were totally degraded within 14 days. At the end of the trial no biological degradation was observed for compounds greater than C_{45}. These results suggest a carbon number "cut off" for biological degradation somewhere between *n*-C_{40} and *n*-C_{45} under these conditions.

After 3 days HTCGC chromatograms of the *in vitro* biodegraded oil already matched those of tars collected from the coast line of South Australia. Although obviously this does not prove that the source of the tar balls is biodegraded Indonesian oils, combined with the results of **McKirdy (1994)** the findings of this study certainly support the

hypothesis that biodegraded Indonesian oils are plausible sources.

The use of a rapid screening biodegradation method proved conclusively that *Pseudomonas fluorescens* (Texaco) is capable of utilising *n*-alkanes up to C_{60} once acclimation of bacteria by HMW substrate has occurred. This is the first report of an organism able to utilise such HMW *n*-alkanes.

CHAPTER FOUR

EXPERIMENTAL DETAILS

This chapter describes the analytical and biological procedures used in this study.

4.1 General

All glassware was steeped in chromic acid (24 hr), soaked in a solution of "DECON 90" (2%) and thoroughly rinsed with distilled water and oven dried (110°C). After drying the glassware was sealed using clean aluminium foil to prevent re-contamination. The interiors of all glassware were rinsed three times with a small aliquot of solvent prior to immediate use.

The HPLC-grade solvents (dichloromethane, hexane, methanol, and cyclohexane) obtained from Rathburn Chemicals LTD (Walkerburn, Scotland) were found to be of acceptable purity. The purity was routinely monitored by first, rotary evaporating (Buchi, 40°C) solvent (100 ml) to near dryness, redissolving the residue in dichloromethane (1 ml) and analysis (0.5μl) by gas chromatography.

Deionised water (Milli Q) was further purified by solvent extraction. Water (1 l) was transferred to a separating funnel extracted with DCM (50 ml) and shaken for 5 minutes. The DCM layer was removed and the whole process was repeated twice with fresh solvent. Cotton wool was pre-extracted (Soxhlet, DCM, 36 hr).

Adsorbents, silica gel (BDH, 60-120 mesh) and aluminium oxide (BDH, Brockmann grade 1, neutral) used for chromatographic separations were pre-extracted (Soxhlet, DCM, 36 hr) and dried (40°C) prior to activation. De-activation of adsorbents was made by drying (12 hr, SiO_2 @ 185°C; Al_2O_3 @ 450°C), cooling in a desiccator, addition of water (pre-extracted Milli Q) followed by homogenisation by mechanical shaking (3-5 hr).

Molecular Sieve (BDH, 5Å ⅛-inch pellets), used for the removal of straight chain hydrocarbons, was prepared by solvent extraction (Soxhlet, DCM, 36 hr) followed by activation in a furnace (250°C for 12 hr and then 400°C for a further 36 hr) The sieve was allowed to cool and placed in a desiccator and stored prior to use.

Before preparing a saturated urea/methanol solution it was necessary to purify the urea crystals. This involved taking a saturated solution of urea in water (milli Q, 100ml) extracting three times with DCM (20ml), and removing the water by rotary

evaporation (Buchi, 60°C). The pure urea crystals were allowed to dry in a desiccator before being dissolved in hot methanol in sufficient quantity to produce a saturated solution.

Anhydrous sodium sulphate was prepared by drying pre-extracted sodium sulphate (Soxhlet, DCM, 36 hr) in an oven at 185°C for 24 hours and stored in a desiccator to prevent rehydration.

Thin-layer chromatography (TLC) plates were prepared using solvent (acetone) washed 20 x 20 cm glass plates coated with 0.5 mm (preparative) of silica gel (Merck kiesel gel type 60G). Following drying (120°C; 1 hr) all plates were pre-developed in ethyl acetate then reactivated prior to use (120°C; 12 hr)

4.2 Analysis of the C_{35+} fraction

4.2.1 Preparation of standards

Known weights (*ca.* 10 mg) of authentic *n*-alkanes (*n*-C_{20}, *n*-C_{40}, *n*-C_{50}, *n*-C_{60}, Fluka Chemicals Inc.) were weighed into a small vial (1.5 cm^3) and transferred to a volumetric flask (100 cm^3) with repeated washings with hot cyclohexane (60°C). The flask was placed into a water bath (50°C) and allowed to equilibrate. The flask was made up to the mark with hot cyclohexane (50°C) and shaken intermittently to ensure an homogeneous stock solution. From this a series of working standards was prepared by accurately pipetting into a series of clean vials (1.5 ml) the following amounts of stock solution;

1	2	3	4	5
50µl	100µl	150µl	200µl	250µl

The solvent was removed (N_2 blow down) and cyclohexane (1.00 ml) was accurately pipetted into each vial to give a range of working standard concentrations.

Prior to analysis by gas chromatography the samples were maintained at a constant temperature (60°C). This was achieved by fixing an aluminium block vial holder to a small laboratory hot plate. Before injecting the sample a small solvent plug and air gap was pulled into the syringe to ensure all the sample was transferred to the column.

A standard mixture of three glycerol esters; (tristearin, triarachidin, tribehenin) and *n*-hexacontane (C_{60}) was prepared using hot cyclohexane (see method above) to give 18 ng/μl, 13.6 ng/μl, 5.4 ng/μl, and 6.8 ng/μl respectively. A second standard mixture was also prepared containing *n*-pentacosane (C_{25}, 6.512 mg,), tristearin (C18:0, 4.47mg) and hexacontane (*n*-C_{60}, 1.598 ng) in hot cyclohexane (60°C), and from this a range of working was standards prepared.

4.2.2 Isolation of a high molecular weight fraction

A sample of condensate (*ca.* 5 g) was accurately weighed into stoppered glass centrifuge tube (50 cm^3), then centrifuged (2000 rpm, 30 min) and the supernatant collected using a micro-pipette. Fresh pentane (5 ml) was added and the pellet re-suspended by ultrasonication (10 min). The process of centrifugation and re-suspension was repeated four times. After the final removal of supernatant the remaining pellet was dried (N_2 blow down) and a final weight recorded. A portion of this waxy residue was transferred to a clean vial (1.5 ml), in cyclohexane (1 ml, warm sample-heater 60°C, 15 min) and analysed by HTCGC.

4.3 Analysis of the unresolved complex mixture (UCM)

4.3.1 Fractional distillation

A flow diagram illustrating the oxidation methodology is shown in Figure 4.1. Distillation cuts of the North Sea gas-condensate U were obtained using the Fischer Autodest 780 vacuum distillation rig courtesy of the PVT section, British Gas Research Station London. The rig is capable of operating at both atmospheric and reduced pressure with a maximum operating temperature of 220°C which at a pressure of 2 mm Hg corresponds to an atmospheric equivalent temperature (AET) of 420°C. The column efficiency was calculated prior to the distillation of the condensate using a test mixture of n-heptane/methylcyclohexane (50/50) and the Fenske equation;

$$N = \frac{\log(H/1-H)-\log(F/1-F)}{\log a}$$

where;

N = number of theoretical plates

a = relative volatility of n-heptane to methylcyclohexane

H = molar fraction of n-heptane in the reflux liquid

F = molar fraction of n-heptane in the flask liquid

The Fisher Autodest rig was found to have a column efficiency of 14.19 which is within the limits set by the ASTM D2892.

4.3.2 Determination of molecular weight

Several techniques exist for the determination of molecular weight but for most oils and condensates and their fractions, which generally have molecular weights in the range of 100-500 (*i.e.* C_7 to C_{35}), one of the simplest is that based on freezing point depression. The principle of the method is that the freezing point of benzene is lowered when it is contaminated with a small amount of oil. The temperature difference between the freezing point of the pure solvent and the contaminated solvent is a measure of the molecular weight per mole of a sample of the oil. Thus by calibrating the apparatus with a sample of known molecular weight, the observed value temperature difference can yield the average molecular weight of the oil sample.

For this analysis the Cryette A apparatus was calibrated using water saturated benzene. For the oil samples a solvent to sample ratio of 50:1 was used.

4.3.3 Molecular sieving (5A)

The method of molecular sieving was based on the techniques described by **Beryl (1961)** and **Dimmler and Strausz (1983)**. Prior to use the molecular sieve (BDH 5A) was activated as previously described. Condensate samples of *ca* 200 to 300 mg were dissolved in 150 ml of cyclohexane and transferred to a RBF (250 ml). Half the sieve necessary for the desired sieve:sample ratio of 100:1 was added and the mixture refluxed for 3 hr. The mixture was filtered and the sieve quickly washed four times with fresh aliquot of cold cyclohexane (150 ml). The filtrate was reduced *in vacuo* and dissolved in 50 ml of fresh cyclohexane. The remaining sieve (20.0 g) was added and the mixture refluxed again for a further 3 hr. The sample was filtered, the sieve washed with fresh solvent and the sample concentrated (Buchi, 40°C, N_2 blow down), and transferred to a vial. The weight was recorded.

4.3.4 Urea adduction

A known weight of condensate (*ca.* 50 mg) was transferred to a centrifuge tube (50 ml) and dissolved in a solution of hexane/acetone (2:1, 10 ml). A saturated solution of urea in methanol (*ca.* 10 ml) was added drop-wise while the solution was gently swirled. The solvent was removed (N_2 blow down) and the process repeated twice. Urea non adducts (UNA) were extracted by the addition of hexane (10 cm^3), sonication (30 sec), and centrifugation (2000 rpm, 10 min). The solvent supernatant was decanted and filtered through a cotton wool plug into a round bottom flask and the process repeated twice with fresh solvent. The collected extracts were combined, evaporated (Buchi, 40°C) and the UNA transferred to a vial and weighed.

Urea adducts (UA) were recovered by the addition of water (10 ml), heating (50°C, 10 min) and transferral to a separating funnel. The aqueous layer was extracted with hexane (3 x 10 ml). The extracts were combined, dried (anh. Na_2SO_4), concentrated (Buchi, 40°C, N_2 blow down), and transferred to a vial and weighed.

4.3.5 Chromium trioxide oxidations (CrO_3/AcOH)

The isolated UCM fractions were oxidised using chromium trioxide (CrO_3) according to the method developed by **Gough (1989)**. The sample (*ca.* 50mg) was transferred to the small double necked RBF in hexane and the solvent allowed to evaporate before addition of glacial acetic acid (10 ml). Argon (3ml/min) was purged through the apparatus for 10 min to remove the majority of the air from the system while the solution was pre-heated to 70°C and stirred. The oxidant was added (10:1 molar ratio) and the reaction allowed to continue for 60 minutes. The amount of oxidant needed was calculated from the average molecular weight of the samples determined by cryoscopy.

Once the reaction time had elapsed, the solution was cooled (ice bath) and transferred to a separating funnel with water (pre-extracted 10 ml) and DCM (10 ml). The mixture was shaken, allowed to settle, the organic phase removed and the aqueous phase re-extracted with DCM (2 x 10 ml). Combined organic washings were back washed (pre-extracted water, 2 x 10 ml), dried (Na_2SO_4) and the solvent removed by rotary evaporation (Buchi, 40°C). Hydrolysis was carried out by refluxing the sample in a 10% solution of KOH/methanol for 30 min. When cool, conc. HCl was added drop-

wise to the solution which was thus acidified to pH 1. Water was added (pre-extracted, 5 ml) and the total hydrolysed material extracted into DCM (3 x 10 ml). The washings were dried (anhydrous Na_2SO_4), solvent removed and the remaining products weighed. Prior to analysis by gas chromatography the sample was derivatised by refluxing the sample with BF_3/methanol (5ml) for 10 min to convert the acids to their methyl esters. The sample was extracted using DCM (3 X 10 ml) and the solvent removed (Buchi, 40°C; N_2 blow down). The remaining products were then analysed by gas chromatography.

4.3.6 Measurement of CO_2

The amount of carbon dioxide evolved during the chromic acid oxidation was determined using the method of **Standen *et al.* (1992)** modified by **Thomas (1995)**. The evolved gases were flushed from the reaction vessel with argon (*ca* $2cm^3$/min) through a pyridine/ethanol (1:1) trap to remove SO_2 into a double necked RBF containing standardised barium hydroxide ($Ba(OH)_2$) solution, thereby forming the insoluble carbonate ($BaCO_3$, (a)). The remaining hydroxide was titrated with standardised HCl (0.5 M) to the first end point (phenolphthalein indicator - pink to clear (b)) and then the total carbonate determined by taking the reaction to a second end point (screened methyl orange indicator - green to violet (c)).

(a) $Ba(OH)_2 + CO_2 \rightarrow BaCO_3 + H_2O$

(b) $Ba(OH)_2 + 2HCl \rightarrow BaCl_2 + 2H_2O$

(c) $BaCO_3 + 2HCl \rightarrow BaCl_2 + H_2O + CO_2$

Identical times and conditions were used to determine two blanks and corrections for the sample were based on the average blank titres. The efficiency of the CO_2 trap was determined by titration of $CaCO_3$ with HCL.

The amount of CO_2 could then be calculated using the following formula:

Titration value (L) x concentration HCl (M) x M.Wt. of CO_2

e.g., For Fraction 26

Phenolphthalein titre = 23.90 cm^3 (b)

Screened Methyl Orange titre = 25.50 cm^3 (c)

Amount of $CaCO_3$ converted to CO_2 = c - b = 1.6 cm^3

therefore;

$1.6 \times 10^{-3} \times 0.05 \times 44$ = 3.52 mg of CO_2

Efficiency Corrected (73%) = 4.82 mg of CO_2

Blank Corrected (1.8 mg) = 3.02 mg of CO_2

Weight of Fraction 26 mg = 46.3 mg

Percentage of CO_2 formed = 6.4%

4.4 Microbiological degradation

4.4.1 General

All work was carried out according to recognised aseptic techniques. This involved cleaning all bench space prior to use with an antiseptic solution. Glass pipettes were plugged with cotton wool, flamed and made sterile by heating in an oven (170°C, 90min). All other glassware was cleaned (Decon 90) and sterilised by autoclave (120°C, 30min) prior to use.

4.4.2 Reagents and inoculum

A minimal salt solution was prepared by dissolving the following salts; 5% NH_4Cl, 1% NH_4NO_3, 2% Na_2SO_4, 3% K_2HPO_4, 1% KH_2PO_4 and 0.1% $MgSO_4.7H_2O$, in 1 litre of deionised water (Milli Q) and sterilised by autoclave (120°C, 30min).

Phosphate buffer solution was prepared by dissolving five tablets of phosphate buffer (OXOID) in 1 litre of distilled water and centrifuging prior to use.

Nutrient agar (27g OXOID, 2g Agar) was dissolved in 1 litre of deionised water (laboratory grade) and heated in a steam bath for 1 hour and sterilised by autoclave.

The medium was melted in a steamer (60 min) and allowed to cool in a water bath (45°C) before pouring (5ml) into 3 inch petri dishes. After setting the agar, plates were stored under refrigeration.

4.4.3 Isolation of aliphatic wax

4.4.3 (a) Thin layer chromatography (TLC)

A flow diagram showing the steps taken in the biodegradation study is illustrated in Figure 4-2. TLC plates were prepared as described previously. The condensate sample (20 mg) was applied as a thin line across the bottom of the plate which was then developed with cyclohexane. Pentacontane was used as the reference compound. The band corresponding to the aliphatic hydrocarbons was by desorption with cyclohexane (*ca.* 10 ml). After removal of the solvent the extract was weighed.

4.4.3 (b) Column chromatography (CC)

The separation of the aliphatic hydrocarbons from the condensate was achieved by open column chromatography based on the method described by **Vogel (1978)**. Glass columns (70 cm x 2 cm i.d) were slurry packed (hexane) with silica gel (60-120 mesh, 5% de-activated, 30g). Condensate was applied in hexane (2 ml) and the column eluted with hexane (178 ml), dichloromethane (200 ml), and methanol (200 ml) to provide aliphatic, aromatic, and polar fractions, respectively. Following the removal of solvent (Buchi, 40°C and N_2 blow down) the weights of the isolated fractions were recorded.

4.4.3 (c) Adsorption onto alumina

The condensate sample (*ca* 100 mg) was transferred to a RBF (150 ml) into which cyclohexane (200 ml) was added. Initially 20 g of activated alumina was added and the mixture was shaken thoroughly (30 min). The sample was evaporated to dryness (Buchi 40°C). The consistency was still found to be sticky with oil-alumina adhering to the sides of the vessel. Fresh solvent (150 ml) and alumina (5 g) were added and the process was repeated. The final mixture had a dry non-sticky freely mobile consistency. Warm cyclohexane (55°C, 50 ml) was added to recover the non-adsorbed, less polar compounds, the solution filtered, the solvent removed (Buchi 40°C) and the final weight of material recorded.

4.4.4 Bacterial culture

Originally the bacterium known as *Pseudomonas fluorescens* (Texaco), a gram negative rod, was isolated from a metal working fluid waste by **Beech and Gaylarde, (1989).** A pure culture of *Pseudomonas fluorescens* (Texaco) was grown in an nutrient agar broth (13g OXOID, in 1 litre deionised water) for 24hr at 20°C. The carbon nutrient source was removed prior to use by centrifugation in phosphate buffer solution (1000 rpm). The supernatant was aspirated and the residual pellet re-suspended in phosphate buffer solution. This process was repeated a further three times.

4.4.5 Batch culture

Into each culture flask was accurately pipetted 1.00 ml of the solution of the aliphatic wax substrate in cyclohexane (1.5 μg/ml). The bottom inner surface of the flask was coated with the wax by gently swirling the solution. The solvent in the flasks was allowed to evaporate and 100 ml of minimal salts added. Into eighteen (two duplicate samples for each analysis) of the culture flasks was accurately pipetted 1.00 ml of the bacterial inoculum (biotic). Each flask was sealed using pre-extracted non-adsorbent cotton wool and incubated on an orbital shaker in the dark at room temperature. The flasks were incubated for a total period of 136 days. Samples were taken at day 0, after 24 hr, day 3, day 7, day 14, day 21, day 28, day 45, and day 136 of incubation. Two biotic cultures were set aside and used solely to measure bacterial growth. Flasks containing the substrate but with no bacteria were used as the control (abiotic) and incubated under the same conditions. A procedural bank was prepared by adding minimal salts and bacteria but without the condensate wax.

On each day of sampling two biotic and two abiotic cultures were tested for viability and bacterial contamination. This was carried out by streaking a sterilised loop of solution from the test cultures onto a nutrient agar plates. The plates were then incubated (24 h at 36°C) and visually checked for growth.

4.4.6 Measurement of bacterial population

An estimate of bacterial population was carried out using the drop count method developed by **Miles Misera (1938).** Serial dilutions of 10^{-5}, 10^{-6}, 10^{-7} and 10^{-8} were prepared using phosphate buffer solution. From each dilution 25 μl of solution was

delivered to a nutrient agar plate in the form of a small drop or lens. Two drops from each dilution were placed on a single plate, allowed to dry, inverted and then incubated at 36°C for 24 h. After incubation the colonies present in the drops were counted using a binocular microscope. The dilutions that produced between 10-20 colonies were used to calculate the number of bacteria in the original flask. The bacterial population in the count flasks was measured directly after the cultures had been inoculated (day 0) and then at the sampling times.

4.4.7 Continuous liquid-liquid extraction

Prior to use the liquid-liquid extractor was cleaned by extracting a sample of pre-extracted distilled water (100 ml) with cyclohexane for 24 h. The extractor apparatus was emptied and dried (110°C). The total contents of the culture flask were transferred to the liquid-liquid extractor. The interior of the flask was rinsed with warm cyclohexane (25 ml x 6, 55°C) and the washings poured into the central well of the extractor allowing the solvent to rise slowly up through the sample and overflow into the round bottom reflux flask. The sample was extracted for 24 h and the extract concentrated (Buchi 40°C, N_2 blow down), weighed, and finally analysed by HTCGC.

4.5 Instrumentation

4.5.1 Gas chromatography (GC)

Routine analyses were performed on a Carlo Erba Mega Series 5300 gas chromatograph (Fisons, Sussex, UK) fitted with a FID and the Carlo Erba Grob on-column injector system. Typically, DB1, wall coated open tubular (WCOT) fused silica columns (50 m x 0.32 mm) were used. The carrier gas was hydrogen (2 cm^3/min) and peak integration was made using the Shimadzu Chromatopac C-R3A integrator and the Philips PU4880 PC-based software.

Retention or a linear version of the Kovats indices (KRI) were calculated using the method described by **Poole and Schuette (1984)**:

Where;

$$KRI = 100z + 100\frac{t_R(Unknown) - t_R(z)}{t_R(z+1) - t_R(z)}$$

t_R = retention time

z = *n*-alkane with z carbon atoms emerging before the the compound of interest

z+1 = *n*-alkane with z+1 carbon atoms emerging after compound of interest

4.5.2 High temperature capillary gas chromatography (HTCGC)

A 12m x 0.32mm (id) aluminium-clad fused silica column coated with a HT5 (0.1 μm film thickness; SGE Scientific, Australia) was fitted into a Carlo Erba Mega Series 5300 SIM DIST gas chromatograph with on-column injection and a HT ceramic FID tip. The carrier gas was helium, set at a constant flow rate 3ml/min using the CP-CF 516 module. Integration was carried out using a Shimadzu Chromatopac C-R3A and the Phillips 4880 PC-based integration software.

4.5.3 High temperature capillary gas chromatography - electron impact mass spectrometry (HTCGC-MS)

Analysis of selected samples was performed on a Carlo Erba 5160 Mega series Finnigan 4500 quadrupole mass spectrometer. A 12m x 0.32mm, HT5 (SGE) aluminium-clad column was used. The oven was temperature programmed from 50°C-400°C at 10°C/min, and held at 400°C for 10 min. The mass spectrometer conditions were: ion source temperature: 380°C: ionising voltage 40 eV; spectra (50-1000 Dalton) were collected each second using a INCOS 2300 data collection system.

4.5.4 High temperature capillary gas chromatography - chemical ionisation mass spectrometry

Samples of authentic alkane standards and both the centrifuged solids of condensate U and a sample of polywax 1000 were analysed by chemical ionisation (CI) GC-MS using the system described above. The reagent gas was isobutane fed into the ion source at a pressure of -0.67 bar; the ionising voltage was 40 eV.

4.5.4 Gas chromatography - mass selective detection (GC-MSD)

GC-MSD was performed using a Hewlett Packard MSD GC-MS (series II) system (injector temperature, 250°C; auto injection, 0.5 μl; electron multiplier, 200 mV; scan rate, 1.72 cycles/s). Data were acquired using HP Chemstation software with the NBS54K spectral library. Chromatography was carried out using a 12 m x 0.2 i.d. mm HP1 (0.33 μm phase) capillary column.

4.5.5 Ultra violet spectroscopy (UV)

UV absorbance spectra for selected aromatic fractions were recorded using a Perkin Elmer Lambda 7 UV/Visible spectrometer. Both samples and solvent blank were measured in hexane.

CHAPTER FIVE

OVERALL CONCLUSIONS AND FUTURE WORK

General conclusions about the advances made by this study are given and suggestions for further research are proposed.

5.1 Conclusions

One of the main aims of this study was to assess the quantitative use of HTCGC for the analysis of the C_{30+} fraction of waxy gas condensates. High molecular weight (HMW) hydrocarbons (defined as C_{35+} compounds) are difficult to characterise by conventional analytical methods and very few studies have reported precise and reproducible quantification of such compounds in fossil fuels. In this study, a reliable, reproducible, quantitative HTCGC procedure was developed to allow the HMW fractions of fossil fuels such as waxy condensates to be measured.

Initially HTCGC injection was a major source of poor reproducibility. This was partly explained by the low solubility of HMW compounds such as hexacontane (C_{60}) in many common organic solvents used in GC. Warm (55°C) cyclohexane was the most efficient solvent for dissolving HMW compounds up to C_{60}. Hexacontane (C_{60}) was the largest pure *n*-alkane commercially available and so defines the upper limit of confidence for the quantitative analysis described in this thesis. Other factors were also important in producing good quantitative analysis, including the use of a dedicated high temperature chromatograph, a mass flow controller for the carrier gas and on-column injection.

Use of an auto-sampler with both a heated syringe and vial tray would be desirable but good results can be achieved manually if the sample is maintained at a constant temperature above the cloud point of the wax and the same procedure is carried out for each injection. To achieve this a simple modification, of adding an aluminium block vial holder to a small hot plate, proved very useful in maintaining a constant temperature.

Both a solvent plug and an air gap pulled into the syringe prior to the sample were needed to efficiently wash precipitated wax from the syringe onto the column. A fast injection speed (contrary to traditional on-column injection), is also advised. The injection method developed herein gave a RSD of under 5% for manual injection for the series of authentic *n*-alkanes C_{20} to C_{60}.

To the author's knowledge no study has reported the linearity of response or the limits of detection of these HMW compounds by HTCGC. This study has shown that the relative FID response was near unity for a series of *n*-alkanes C_{20-60} which produced linear response curves. Limits of detection were 0.8 ng (*n*-C_{20}) to 1.87 ng (*n*-C_{60}).

HMW internal standards suitable for HTCGC do not seem to have been mentioned previously in the literature. Tristearin meets most of the criteria of a good internal standard and has a FID response factor (1.1) close to that of the C_{20-60} *n*-alkanes. Response remained linear over the relevant concentration range and when co-injected with a waxy gas-condensate was adequately separated from C_{59} and C_{60} making accurate peak integration possible.

HTCGC analysis of two gas condensates derived from high temperature - pressure wells in the North Sea showed that 20% of the hydrocarbons were present in the C_{30+} fraction. In fact the carbon number range extended to above C_{80} in one condensate. Centrifugation of the waxes from cold pentane showed even longer chain aliphatic compounds are present in low concentrations. This is important to PVT analysis since small amounts of HMW compounds affect the way in which a reservoir fluid behaves during production from a reservoir. It is also a surprising result given that most condensates are regarded as low boiling point hydrocarbon liquids similar in composition to a gasoline fraction.

Good agreement for concentrations of compounds $\leq C_{30}$ was observed for HTCGC and gas chromatography of the same condensates. The advantage of HTCGC was that analysis could be extended up to C_{60} while still remaining within the confidence of the methodology.

Qualitative characterisation of the condensates by HTCGC-MS (EI) produced molecular ions for *n*-alkanes up to C_{42}. Other HMW compounds showed fragment ions characteristic of branched compounds but did not reveal much further information. HTCGC-MS (CI) produced molecular ion information for *n*-alkanes as large as *n*-C_{57} in a condensate sample and for *n*-C_{60} in Polywax 1000.

The discovery herein that 21% of the total gas-condensate was unresolved by gas chromatography is a new and perhaps surprising result. Certainly no account of this material has been taken in previous modelling of phase behaviour. Thus the UCM represents a chromatographic unknown that is quantitatively greater than that of the C_{30+} fraction in many condensates and oils.

Since the number of compounds present in the UCM was likely to be large the gas condensate was first fractionated by vacuum distillation to provide a series of smaller distillate cuts. By careful molecular sieving and urea adduction the UMCs could be isolated from the distillate cuts. Once isolated these were found to have contributed between 33% to 61% of the original distillate cuts. The GC integration method used for measuring the proportion of UCM was reproducible (RSD of 3.4%).

From CrO_3/AcOH oxidation 5% to 12% of UCM was converted to CO_2 whereas 65% to 94% was recovered as DCM soluble products. The remainder was thought to be water soluble acids ($<C_6$). The CO_2 losses have not been assessed in previous studies. The small percentage of CO_2 adds confidence to the inferences about the UCM composition drawn from the DCM solubles.

GC-MS of the DCM soluble oxidised products indicated that the condensate UCM was predominantly aliphatic. Straight chain *n*-monocarboxylic acids were identified as the major group of resolved oxidation products and accounted for 24% of the total condensate UCM and 19% to 48% of each distillate cut UCM. Since *n*-acids arise from oxidation of alkyl chains a third to a half of the resolved oxidation products must have come from alkyl substituted compounds originally in the UCM. The average carbon number of the alkyl chain was C_{12}. The ket-2-ones have a similar origin to the acids. Isoprenoid acids, keto acids and lactones present in the resolved oxidised compounds indicated the presence of branched and/or isoprenoid moieties within the UCM. GC-MS did not reveal any great differences in the products of the various distillate cut UCMs, although their relative amounts did vary.

Evidence from the resolved compounds identified in this study and from the literature, allow some conclusions to be drawn about the types of structures present within the

UCM. An illustration summarising the structures identified is shown in Figure 5-1. The mechanism of CrO_3/AcOH oxidation suggests that compounds identified would most likely have been attached at tertiary carbon centres or at benzylic positions (the most likely positions for chromic acid attack). For example, structure (I) and (IV) could have been formed from the oxidation of an alkyl benzene molecule and structures (V) and (VI) a monomethyl branched dialkyl substituted benzene (along with all the other possible isomers of that compound).

Polycyclic structures are missing from the figure since these were not observed in the resolved oxidation products. Such compounds are known to be present from before oxidation and from previous studies. If the unknown was a tetralin then addition of structure (I) would give an alkyltetralin while if the unknown was a alkyl tetralin joined to (III) it would form structures similar to those proposed by **Revill (1992)**. From the lack of such structures in the resolved oxidation products it can be concluded that these structures do not survive oxidation or remain unresolved in the oxidised UCM.

Branching of hydrocarbons is obviously a major factor in producing a UCM. The theoretical number of isomers of simple branched alkanes (15000 for the condensate UCM) could easily produce a UCM alone. Multiply branched, and cyclic structures would add to this. Clearly even modern high resolution GC could not resolve all of these compounds.

Although oxidation produced a significant amount of information about the compound structures in the gas condensate UCM, part of the oxidised products (19% to 63%) still remains unresolved and this requires further investigation. Such studies are under way **(Thomas, 1995 pers. comm. 1995)**.

Characterisation of the C_{30+} fraction by HTCGC and the UCM by oxidative degradation has significantly increased compositional information about this gas condensate and perhaps condensates in general. Prior to this study over 30% remained non-characterised, both qualitatively and quantitatively. The methods used in this study should be applicable to studies of other hydrocarbon mixtures.

To the author's knowledge there has been only one previous study of the biodegradation of $>C_{35}$ hydrocarbons in oils, One reason for this has been the difficulty associated with analysis of such compounds. This study has shown for the first time that use of liquid-liquid continuous extraction and analysis using HTCGC gives good recoveries and quantification of HMW compounds.

The problem of recovery of HMW alkanes from an aqueous media was exemplified by the recovery obtained for *n*-C_{60} using simple manual liquid extraction with a separating funnel. Typically 50.8% was recovered with a RSD of 20.6%. Liquid-liquid continuous extraction made a major improvement. Replicate analysis showed a recovery of 93% and RSD of only 5% for *n*-C_{60}.

Another important finding from this study was that a large proportion of HMW compounds greater than C_{40} were not efficiently isolated from oils by thin layer chromatography or column chromatography. This seems to have escaped attention previously, perhaps because few HTCGC studies have been made and most studies have used whole oil samples. An alternative method for isolating HMW aliphatic compounds was developed using the adsorptive properties of activated alumina to selectively remove the more polar compounds. The method involved using an alumina/warm hexane slurry and was successful in leaving only the aliphatic compounds in solution, including the HMW fraction. The method still needs further quantitative validation.

A biodegradation study of the aliphatic fraction isolated in the above manner from a waxy Indonesian oil and containing compounds with up to carbon number C_{70} with a known oil degrader *Pseudomonas fluorescens* (Texaco), showed that after only 14 days approximately 86% of the Indonesian oil had been degraded. However, degradation for a further 122 days did not apparently alter this value. HTCGC showed that *n*-alkanes up to C_{35} had been totally removed by the end of the study period but for the alkanes *n*-C_{35} to *n*-C_{45} the amount of degradation was much less suggesting increased resistance to degradation. No degradation was observed for compounds greater than *n*-C_{45}.

Published biodegradation rate models for aliphatic compounds did not match that of

the experimental data very closely suggesting that such models need to be refined for HMW compounds.

The final distribution of *n*-alkanes produced by 136 days degradation was similar to that of tar-balls collected from the shores of South Australia. At this stage only a visual comparison can be made and a more detailed study of a greater number of samples is needed but the data do not refute the suggestion from biomarker evidence that the source of some of the tars on the Australian coastline was waxy Indonesian oil.

The results from the biodegradation study and the literature suggest a limit for biodegradation (molecular weight "cut off") for *n*-alkanes around *n*-C_{45}. However, this study has shown by use of a rapid screening biodegradation assay technique, that the bacteria taken from the remaining cultures at the end of the study period were capable of growth on *n*-C_{60} as the sole carbon source. Because the original culture was not capable of growing on *n*-alkanes greater than *n*-C_{40} the bacteria must have acclimated to the HMW compound. Whether this is a genetic change or an irreversible or reversible enzymatic change is not known, but this is thought to be the first report of a bacterium capable of utilisation of *n*-C_{60} for growth. This result may have wide applications in the field of bioremediation of polluted environments (*e.g.* soil) where HMW residues are often concentrated.

5.2 Future Work

Suggestions for further work given here follow the three general topics covered by this study, namely, quantification of HMW compounds, UCM composition and biodegradation.

Extending HTCGC quantitatively to even higher carbon numbers ($>C_{60}$) requires higher molecular weight *n*-alkane standards. These are not yet commercially available but methods for synthesising *n*-alkanes with more than sixty carbon atoms have been reported in the literature **(Bidd, 1983)**. These could be used to verify the analytical limits of HTCGC.

HTCGC columns should be improved by increasing their resolving power at temperatures greater than 350°C. Future studies should assess the potential of microbore columns coated with high temperature stationary phases. Microbore (WCOT) columns, as their name suggests, have very small internal diameters (0.18 mm to 0.02 mm i.d). The main advantages of these columns are discussed by **Barker, (1995)** who concludes that the smaller internal diameter will increase column efficiency giving a high number of theoretical plates (for example a 10 m x 0.01 mm i.d. column has the potential of up to 100,000 theoretical plates) and that such columns exhibit increased sensitivity, decreased column bleed and require low carrier gas flow rates and hence have good compatibility with GC-MS.

For future studies of the UCM identifying single components may not be as important for PVT analysis as accurately quantifying the amount of the general types of structures present. This would require a much more accurate quantitative study. Such a study would require internal standards that would survive the oxidation step to characterise UCMs.

Alternative oxidants should also be sought, chromyl chloride (CrO_2Cl_2) is one example and ruthenium tetroxide, already used by **Revill (1992)** to examine the aromatic structures in UCMs from a biodegraded oil, and by others for coals (**Singleton *et al.*, 1985**) and kerogen (**Standen 1992 and references therein**), needs further investigation. Ruthenium tetroxide unlike chromic acid/AcOH does not require acetic acid as a reagent and so offers the advantage that the water soluble fraction could be examined for LMW acids and a total mass balance obtained. As shown from this study and the literature, oxidative degradation techniques still leaves a substantial proportion of the UCM unresolved and characterisation of the UCM_{ox} remains a major challenge **(Rowland and Revill, 1995).**

Further fractionation of the UCM should be investigated. The use of molecular sieves other than those used herein (5A and urea) should be applied to UCMs (**Dimmler and Strausz, 1983; Hoering and Freeman, 1984**; reviewed by **Ellis, 1994**). There are many zeolites now available with pore sizes between 3-10Å (**Ellis, 1994**) which are

capable of adducting more complex compounds **(Dimmler and Strausz, 1983).**

HPLC has also been used for fractionation of aromatic hydrocarbons from fossil fuels on a preparative scale and to separate aromatic compounds into ring size fractions **(Jones, 1986; Rønningsen and Skjevrak, 1990).** The aromatic UCM could be fractionated from the small distillate UCM and then be preparatively separated into aromatic ring fractions by such methods before analysis by high resolution GC-MS or oxidative techniques.

Tandem MS-MS could also be applied to UCM characterisation whereby both separation and identification is carried out in one instrument **(Holman, 1990).** The initial stage of mass analysis may be used to separate out the components on the basis of their mass (a form of mass chromatography) and once separated these ions are then analyzed by a second mass spectrometer. If applied to UCM of the distillate cuts or UCMs that have been further simplified by fractionation using molecular sieves and HPLC techniques mentioned previously, MS-MS may be useful in providing further information about structures present.

An improvement to the microbial degradation study would be a mass balance approach, whereby not just the remaining non-degraded alkanes, but also metabolites and respiration **(Aichinger *et al.*, 1992)** are measured. A more frequent sampling rate is required so that a better estimate of the rate of degradation could be obtained for the easily degradable LMW hydrocarbons.

The rapid screening method should be used to monitor the point at which the bacteria develop the capacity to degrade the higher *n*-alkanes. This study could be extended when more pure HMW *n*-alkanes become available. A biodegradation experiment should be carried out using the modified bacteria to see how the rate of degradation is altered. If the aliphatic wax is found to be degraded more rapidly and more extensively this may have useful implications for bioremediation. It would be interesting to investigate what physiological changes have happened to the *Pseudomonas* spp., whether these are genetic mutations or simple enzymatic modifications. If a genetic

change has taken place it may be possible to isolate the gene responsible and splice this to a more saline tolerant species for use in marine oil spill remediation.

REFERENCES

References

Abbot, D.J. (1995), Advances in simulated distillation. In Adlard, E.R., (ed), *Chromatography in the Petroleum Industry*. Elsevier Science B.V., Amsterdam, pp 41-52.

Adlard, E.R., (1995), *Chromatography in the Petroleum Industry*. Adlard, E.R. (ed), Elsevier Science B.V., Amsterdam, pp XV.

Ahmed, T. (1989), Hydrocarbon Phase Behaviour. *Contributions in Petroleum Geology and Engineering*, **7**, Gulf Publishing Company.

Aichinger, G., Grady, L. and Tabak, H.H. (1992), Apllication of respirometric biodegradability testing protocol to slightly soluble organic compounds. *Water Environmental Research*, **64**, **7**, pp 890-899.

Aldous, P. (1991), Gulf oil spill - Big test for bioremediation, *Nature*, **349**.

Ashford, J.D., Blount, C.G., Marcou, J.A., Ralph, J.M. and Skaalure, E.W. (1990), Annular packer fluids for paraffin control: model study and successful application. *Society of Petroleum Engineers Journal*, **19730**.

ASTM STANDARD D 2887 (1978), Boiling range distribution of petroleum fractions by gas chromatography. *Annual Book of ASTM Standards*.

ASTM STANDARD D 3710 (1987), Boiling range distribution of petroleum fractions by gas chromatography. *Annual Book of ASTM Standards*,

Atlas, R.M. (1991), Bioremediation of oil spills; promise and peril, *Program and Abstracts of the Second International Marine Biotechnology Reviews*, pp 174-176.

Atlas, R.M. and Bartha, R. (1992), *Microbial Ecology: Fundamentals and Applications*. Addison Wesley.

Baller, H. (1991), North Sea HP-HT wells require changes in drilling procedures. *Oil and Gas Journal*, **11**, pp 73-74.

Barker, A.D. (1987), Wax chromatography - the 80's crossroads. *Petroanalysis '87*, Crump, G.B. (ed), John Wiley & Sons Ltd, pp 159-757.

Barker, A.D. (1989), Problems with high temperature GLC. *Chromatography and Analysis*, pp 5-7.

Barker, A.D. (1995), Advances in simulated distillation. In Adlard, E.R. (ed), *Chromatography in the Petroleum Industry*. Elsevier Science B.V., Amsterdam, pp 55-90.

Bashall, A.D. (1992), Improving refining efficiency using high-temperature simulated distillation. *American Laboratory*, **19**, 5, pp-58-60

Beech, B. and Gaylarde, C.G. (1989), Adhesion of *Desulfovibrio desulfuricans* and *Pseudomonas fluorescens* to mild steel surfaces. *Journal of Applied Bacteriology*, **67**, pp 201-207.

Berg, R.J. and Hawkins, T. (1992), An improved FID design for capillary GC. *LC-GC*, **9**, 10, pp 10-14.

Bidd, I., Holdup, D.W., and Whiting, M.C. (1987), Studies on the synthesis of linear aliphatic compounds. Part 3: The synthesis of paraffins with very long chains. *Journal of the Chemical Society, Perkin Transactions 1*, pp 2455-2463.

Blomberg, L. and Wännaman, T. (1979), In situ synthesis of highly thermostable, non-extractable methylsilicone gum phases for glass capillary gas chromatography. *Journal of Chromatography*, **168**, pp 81-88.

Blum, W. and Damasceno, L. (1987), High temperature glass capillary gas chromatography using OH-terminated polysiloxane stationary phases. Separation of antioxidants and UV-stabilizers. *Journal of High Resolution Chromatography and Chromatography Communications*, **10**, pp 472-475.

Blum, W., Richter, W.J., and Eglinton, G. (1988), Glass capillary gas chromatography-mass spectrometry at high temperatures. Direct analysis of free base porphyrins and metal porphyrin complexes extracted from the Serpiano oil shale. *Journal of High Resolution Chromatography and Chromatography Communications*, **11**, pp 148-156.

Blum, W. and Eglinton, G. (1989), Preparation of high temperature stable glass capillary coated with PS-090 (20% diphenyl substituted CH_3OH-terminated polysiloxane) a selective stationary phase for direct analysis of metal-Porphryin complexes. *Journal of High Resolution Chromatography*, **12**, pp 290-293.

Blum, W. and Eglinton, G. (1989), Glass capillary gas chromatography-alkali flame ionisation detection at high temperatures. Direct analysis of free base petroporphyrins. *Journal of High Resolution Chromatography*, **12**, pp 621-623.

Brandenberger, S.G., Maas, L.W., and Dvoretzky, I. (1961), Determination of methyl groups in alkylbenzenes by chromic acid oxidation. *Analytical Chemistry*, **33**, pp 435-455.

Burwood, R. Cole, G.A., Drozd, R.J., Halpern, H.I., Penfield, I.E. and Sedivy, R.A. (1985), Carbon isotopec characterization of some North Alaska petroleums and potential source rock kerogen assemblages. In Magoon, L.B. and Claypool, G.E. (eds) *Alaska North Slope Oil/Rock Correlations Study*. The American Association of Petroleum Geologists, Tulsa, Oklahoma, pp 123-137.

Burwood, R. and Speers, G.C. (1974), Photooxidation as a factor in the environmental dispersal of crude oil. *Estuarine, Coastal and Marine Science*, **2**, pp 9-34.

Brooks, P.W., Eglinton, G., Gaskell, S.J., McHugh, D.J., Maxwell, J.R., and Philp, R.P. (1977), Lipids of recent sediments. Part II: Branched and cyclic alkanes and alkanoic acids of some temperate lacustrine and subtropical lagoonal/tidal-flat sediments. *Chemical Geology*, **20**, pp 189-204.

Butler, J.N., Morris, B. F. and Sass, J. (1973), Pelagic tar from Bermuda and Sargasso Sea. *Bermuda Biological Station Research Special Publication No 10*, 346.

Buyten, J. Duvekot, J. Peene, J. and Mussche, Ph. (1990), Improved metal Capillary column for high temperature gas chromatography. *Eleventh International Symposium on Capillary Chromatography*, Sandra, P. Redart, G. and Leuridan, M. (eds), Monterey, Lab. USA, pp 91-101.

Buyten, J. Duvekot, J. Peene, J. and Mussche, Ph. (1990), A capillary column for high temperature chromatography. *International Chromatography Laboratory*, **2**, pp 5-9

Cameotra, S.S., Singh, H.D., Hazarika, A.K. and Baruhah, J.N. (1990), Model of uptake of insoluble solid substrates by microorganisms. II: Uptake of solid *n*-alkanes by yeast and bacterial species. *Biotechnology and Bioengineering*, **XXV**, pp 2945-2956.

Cameotra, S.S. and Singh, H.D., (1990), Uptake of Volatile *n*-alkanes by *Pseudomonas* PG-1. *Journal of Microbiology Biotechnology*, **5**, 2, pp 47-57.

Carlsson, N.G., Karlsson, H. and Sandberg, A. (1992), Determination of oligosaccharides in foods, diets, and intestinal contents by high-temperature gas chromatography and gas chromatography/mass spectrometry. *Journal of Agriculture and Food Chemistry*, **40**, pp 2404-2412.

Carnahan, N.F. (1989), Paraffin deposition in petroleum production. *Journal of Petroleum Technology*, **41**, pp 1024-1025.

Chakravarty, M., Amin, P.M., Singh, H.D., Baraugh, J.N. and Iyengar, M.S. (1972). *Biotechnology and Bioengineering*, **12**, pp 61-65.

Clark, J.C. (1969), Elements of petroleum Reservoirs. *Society of Petroleum Engineers of the American Institute of Mining and Petroleum Engineers Inc.*

Clarke (1992), Oil Pollution, Chapter 3, *Marine Pollution. Third Ed.* Clarendon Press, Oxford, pp 28-52.

Clerc, R.J., Hood, A. and O'Neal, M.J. (1955), Mass spectrometric analysis of high molecular weight, saturated hydrocarbons. *Analytical Chemistry*, **27**, pp 868-875

Collins, C.H. and Patricia, M.L. (1984), Counting micro-organisms, Chapter 9. *Microbiological Methods, Fifth Ed.* Butterworths & Co. pp 128-145.

Connan, J. (1984), Biodegradation of crude oils in reservoirs. in Brooks, J. and Welte, D. (eds) *Advances in petroleum geochemistry, vol 1.* Academic Press, London, pp 299-335.

Corbin, C.J., Singh, J.G. and Ibiebele, D.D. (1993), Tar ball survey of 6 Eastern Caribbean countries. *Marine Pollution Bulletin*, **26**, 9, pp 482-486.

Cox, R.E., Maxwell, J.R., Ackman, R.G., and Hooper, S.N. (1972), Stereochemical studies of acyclic isoprenoid compounds. III. The stereochemistry of naturally occurring (marine) 2,6,10,14-tetramethylpentadecane, *Canadian Journal of Biochemistry*, **50**, pp 1238-1241.

CRC (1985), *Hand Book of Chemistry and Physics*. CRC Press, Inc.

Curtis, M. and Saner, A. (1974), Tar ball loadings on Golden Beach, Florida. U.S. *Department of Commerce, National Bureau of Standards Special Publications*, 409. pp 79-81.

Currie, T.J., Alexander R. and Kagi R.I. (1992), Coastal bitumens from Western Australia - long distance transport by ocean currents. *Organic Geochemistry*. **18**, pp 595-601.

Curvers, J. and van den Engle, P. (1989), Gas chromatographic method for simulated distillation up to a boiling point of 750°C using temperature programmed injection and high temperature fused silica wide-bore columns. *Journal of High Resolution Chromatography*. **12**, pp 16-23.

Damasceno, L.M.P., Cardoso, J.N., and Coelho, R.B. (1992), High temperature gas chromatography on narrow bore capillary columns. *Journal of High Resolution Chromatography*, **15**, pp 256-259.

Dawes, P and Cumbers, M. (1989), Capillary column design for high temperature GC. *LC-GC*, pp 109-111.

David, F. and Sandra, P. (1993), Characterisation of polymer additives using high temperature capillary gas chromatography: possibilities of atomic emission detection. *LC-GC*, **11**, 4, pp 283-287.

Del Rio, J.C., Philp, R.P. and Allen, J. (1992), Nature and geochemistry of high molecular weight hydrocarbons (above C_{40}) in oils and solid bitumens. *Organic Geochemistry*, **18**, 4, pp 541-555.

Dennis, J.V. (1959), Oil pollution survey of the U.S. Atlantic coast. *American Petroleum Institute Publication* No.**4054**.

Detsy, D.H. (1965), *Advances in Chromatography*, **1**, pp 218

Dimmler, A. and Strausz, O.P. (1983), Enrichment of polycyclic terpenoid, hydrocarbons from petroleum by adsorption on zeolite NaX. *Journal of Chromatography*. **270**, pp 219-225.

Douglas, A.G.; Blumer, M.; Eglinton, G. and Douraghi-Zadeh, K. (1970), Gas chromatographic-mass spectrometric characterisation of naturally-occurring acyclic isoprenoid carboxylic acids. *Tetrahedron Letters*, **22**, pp 1071-1092.

Eglinton, G. and Murphy M.T.J. (1969), *Organic Geochemistry-Methods and Results*. Springer-Verlag, Berlin.

Ellis, L. (1994) *Aromatic Hydrocarbons in Crude Oil and Sediments: Molecular Sieve Separations and Biomarkers*. Ph.D Thesis, Curtin University, Western Australia.

Evershed, R.P., Prescott, M.C., Goad, L.J. and Rees, H.H. (1987), High temperature gas chromatography-mass spectrometry of steroid derivatives. *Biochemical Society Transactions*, **15**, pp 175-179.

Evershed, R.P. and Prescott, M.C. (1989), Facile connection of aluminium clad capillary GC columns to a magnetic sector mass spectrometer. *Biomedical and Environmental Mass Spectrometry*, **18**, pp 503-506.

Evershed, R.P., Prescott, M.C., and Goad, L.J. (1990), High-temperature gas chromatography/mass spectrometry of triaglycerols with ammonia negative-ion chemical. *Rapid Communications in Mass Spectrometry*, **4**, 9, pp 345-347.

Evershed, R.P., Heron, C., and Goad, L.J. (1990), Analysis of organic residues of archaeological origin by high-temperature gas chromatography and gas chromatography-mass spectrometry. *Analysist*, **115**, pp 1339-1342.

Fayad, N.M. (1986), Identification of tar balls following the Norwruz oil spill. *Marine Environmental Research*, **18**, pp 155-163.

Fowler, M.G., Abolins, P., and Douglas. A.G., (1985), Monocyclic alkanes in Ordovician organic matter. *Organic Geochemistry*, **10**, pp 815-823.

Frior, R.L. and Phillips, R.J. (1989), Fused silica columns for high temperature simulated distillation. *Journal of High Resolution Chromatography*. **12**, pp 181-183.

Gallegos, E.J., Fetzer, J.C., Carlsson, R.M. and Pena, M.M. (1991), High temperature GC/MS characterisation of porphyrins and high molecular weight saturated hydrocarbons. *Energy and Fuels*, **5**, pp 376-381

Geeraert, E. and Sandra, P. (1984), On the potential of CGC in triglyceride analysis. *Journal of High Resolution Chromatography and Chromatography Communications*, **7**, pp 431-433.

Geeraert, E. and Sandra, P. (1985), Capillary GC of triglycerides in fats and oils using high temperature phenylmethylsilicone stationary phase. Part I. *Journal of High Resolution Chromatography and Chromatography Communications*, **8**, pp 100-105.

Geeraert, E. and Sandra, P. (1987), Capillary GC of triglycerides in fats and oils using high temperature phenylmethylsilicone stationary phase. Part II. The analysis of chocolate fats. *JAOCS*, **64**, 1, pp 100-105.

Gilby, G.W. (1983), The use of ethylene-vinyl acetate copolymers as flow improvers in waxy crude oil. *Chemicals in the Oil Industry*, special publications, Proceedings, Manchester.

Giles, J.J. (1987), The analysis of waxes and greases using high resolution gas chromatography. *Journal of the Forensic Science Society*, **27**, 4, pp 231-239.

Golik, A. (1982), The distribution and behaviour of tar balls along the Israeli coast. *Estuarine, Coastal and Shelf Science*, **15**, pp 267-276.

Golik, A. and Rosenberg, N. (1987), Quantitative-evaluation of beach stranded tar-balls by means of air photographs. *Marine Pollution Bulletin*, **18**, 6, pp 289-293.

Gough, M.A. (1989), *Characterisation of unresolved complex mixtures of hydrocarbons*. PhD Thesis, University of Plymouth.

Gough, M.A. and Rowland, S.J. (1990), Characterisation of Unresolved Complex Mixtures of Hydrocarbons in Petroleum. *Nature*, **344**, pp 648-650.

Gough, M. and Rowland, S.J. (1991), Characterisation of unresolved complex mixtures of hydrocarbons from lubricating oil feedstock. *Energy and Fuels*, **5**, 6, pp 869-874.

Gough, M.A., Rhead, M.M. and Rowland, S.J. (1991), Biodegradation studies of unresolved complex mixtures of hydrocarbons: Model UCM hydrocarbons and the aliphatic UCM. *Organic Geochemistry*, **18**, pp 17-22.

Grob, K. and Grob, G. (1976), A new, generally applicable procedure for the preparation of glass capillary columns. *Journal of Chromatography*, **125**, 3, pp 471-85.

Grob, K. (1978), On-column injection onto capillary columns. Part 2: study of sampling conditions;practical recommendations. *Journal of High Resolution Chromatography and Chromatography*, **1**, pp 263-267.

Grob, K. and Tschour, R. (1990), Optimal carrier gas velocities at high temperatures in capillary GC. *Journal of High Resolution Chromatography*. **13**, pp 193-194.

Hamilton, R. and Hamilton, S. (1987), Chapter Two, Stationary Phase. *Thin Layer Chromatography (Analytical Chemistry by Open Learning)*. John Wiley & Sons, pp 11-26.

Hansson, G.C., Bouhours, J. and Karlsson, H. (1991), Analysis of sialic acid-containing mucin oligosaccharides from porcine small intestine by high-temperature gas chromatography-mass spectrometry of their dimethylamides. *Carbohydrate Research*, **221**, pp 179-189.

Hanstveit, A. (1992), Biodegradability of petroleum waxes and beeswax in an adapted CO_2 evolution test. *Chemosphere*, **25**, 4, pp 605-620

Hertz, H.S., Andresen, B.D., Djuricic, M.V., Biemann, K., Saban, M. and Vitorovic, D. (1973), The isolation and identification of gamma-lactones in the acidic fraction in Aleksinac (Yugoslavia) shale bitumen. *Geochimica et Cosmochimica Acta*, **37**, pp 1687-1695.

Hinshaw, J.V. and Ettre, L.S. (1989), Aspects of high temperature capillary gas chromatography. *Journal of High Resolution Chromatography*, **12**, pp 251-255.

Hoffmann, C.F., Foster, C.B., Powell, T.G. and Summons, R.E. (1987), Hydrocarbon biomarkers from Ordovician sediments and the fossil algal *Gloecapsomorpha prisca* Zalessky 1917. *Geochimica et Chosmochimica Acta*, **51**, pp 2681-2697.

Holman, R.W. (1990) Tandem mass spectrometric applications in fuel science. *Journal of Coal Quality*, **9**, pp 120-124.

Hood, A. and O'Neal, M.J. (1959), Status of application of mass spectrometry to heavy oil analysis. *Advances in Mass Spectrometry*. Waldron, J.D. (ed), Academic Press, London.

Hood, A., Clerc, R.J. and O'Neal, M.J. (1959), The molecular structure of heavy petroleum compounds. *Journal of the Institute of Petroleum*, **45**, pp 168-173

Hoult, D.P. (1969), *Oil On The Sea*.

Huball, J. (1990), High temperature gas chromatography: A status report. *LC-GC*, **8**, 1, pp 12-16.

Jones, D.M., Douglas, A.G., Parkes, R.J., Taylor, J., Giger, W. and Schaffner, C. (1983), The recognition of biodegraded petroleum-derived aromatic hydrocarbons in recent marine sediments. *Marine Pollution Bulletin*, **14**, 3, pp 103-108.

Jones, D.M. (1986), *Biodegradation of geochemical markers in pollution studies*. PhD thesis, University of Newcastle Upon Tyne.

Kallio, R.E. (1982), Role of microorganisms in formation of heavy crude, in Meyer, R.F. Wynn, J.C. and Olson, J.C. (eds), *The Future of Heavy Crude and Tar Sands - Second International Conference*, pp 430-432.

Karcher, D. (1985), *Spectral Atlas of Polycylic Aromatic Compounds*. D. Reidal Publishing company.

Kemp, W. (1991), Ultraviolet and visible spectroscopy, Chapter Four. *Organic Spectroscopy, Third Edition*. MacMillan Education Ltd., pp 243-284.

Killops, S.D. and Al-Juboori M.A.H.A. (1990), Characterisation of the unresolved complex

mixture (UCM) in the gas chromatograms of biodegraded petroleum. *Organic Geochemistry*. **15**, pp 147-160.

Killops, S.D. and Readman, J.W. (1985), HPLC fractionation and GC-MS determination of aromatic hydrocarbons from oils and sediments. *Organic Geochemistry*. **8**, pp 247-257.

Kissin, Y.V. (1990), Catagenesis of light cycloalkanes in petroleum. *Organic Geochemistry*, **13**, pp 574-594.

Kiyohara, H., Nagao, K. and Yana, K. (1982), Rapid screen for bacteria degrading water-insoluble, solid hydrocarbons on agar plates. *Applied and Environmental Microbiology*, pp 454-457.

Kvenvolden, K.A., Hostettler, F.D., Rapp, J.B. and Carlson, P.R. (1993), Hydrocarbons in oil residues on beaches of islands of Prince William Sound, Alaska. *Marine Pollution Bulletin*, **26**, 1, pp 24-29.

Lawrence, F.J., Iyengar, J.I., Page, B.D. and Concher, H.B.S. (1983), Characterization of commercial waxes by high-temperature gas chromatography. *Journal of Chromatography*, **14**, 431, pp 404-418.

Lawrence, F.J. and Iyengar, J.I. (1983), Determination of paraffin wax and mineral oil on fresh fruits and vegetables by high temperature gas chromatography. *Journal of Food Safety*, **5**, pp 119-129.

Lewis, C.A. (1994), *Purpose written computer program for the calculation of isomers of simple branched alkanes*. University of Plymouth.

Lipsky, S.R. and McMurray, W.J. (1982), Performance of different types of crosslinked methyl polysiloxane stationary phases on fused-silica glass capillary columns. *Journal of Chromatography*, **236**, pp 61-69

Lipsky, S.R. and Duffy, M.L. (1986), High temperature gas chromatography: The development of new aluminium clad flexible fused silica glass capillary columns coated with thermostable nonpolar phases: Part 1. *Journal of High Resolution Chromatography and Chromatography Communications*, **9**, pp 376-381.

Lipsky, S.R. and Duffy, M.L. (1986), High temperature gas chromatography: The development of new aluminium clad flexible fused silica glass capillary columns coated with thermostable nonpolar phases: Part 2. *Journal of High Resolution Chromatography and Chromatography Communications*, **9**, pp 725-730.

Lipsky, S.R. and Duffy, M.L. (1986), Advances in capillary gas chromatography. *LC-GC*, **4**, 9, pp 899-906.

Literathy, P., Haider, S., Samhan, O., and Morel, G. (1989), Experimental studies on biological and chemical oxidation of dispersed oil in sea water. *Water Science and Technology*, **21**, pp 845-856.

Luke, L.A. and Ray, J.E. (1985), Simulated distillation of atmospheric residues using short pyrex capillary columns. *Journal of High Resolution Chromatography and Chromatography Communications*, **8**, pp 193-195.

Lyman, W.J., Reehl, W.F. and Rosenblatt, D.H. (1982), Rate of biodegradation, Chapter 9. *Handbook of Chemical Property Estimation Methods, Environmental Behaviour of Organic Compounds*. McGraw-Hill, Inc. pp 1-98.

Madani, C., Chambaz, E.M., Riguad, M. Durand, J. and Chenroux, J. (1976), New method for the preparation of highly stable polysiloxane-coated glass open tubular capillary columns and apllication to the analysis of hormonal steroids. *Journal of Chromatography*, **126**, 161-9.

Madani, C. and Chambaz, E.M. (1978), Glass open-tubular capillary columns with chemically bonded methyl-phenyl siloxane stationary phases of tailor made polarity. *Chromatographia*, **11**, 12, pp 725-729.

Madani, C. and Chambaz, E.M. (1981), High resolution glass capillary columns with chemically bonded stationary phases: Application to the gas chromatographic analysis of sterols and steroids in biological extracts. *JAOCS*, pp 63-70

Maskerinec, M.P. and Olerich, G. (1980), Thermally stable Dexsil-400 glass capillary columns. *Analytical Chemistry*, **52**, pp 588-591.

Melpolder, F.W., Brown, R.A., Washall, T.A., Doherty, W., and Headington, C.E. (1956), Composition of lubricating oil - use of newer separation and spectroscopic methods. *Analytical Chemistry*, **28**, pp 1936-1945.

McCormack, A.J., McCann, J.M., and Bohler, R.J. (1991), Determination of motor oil volatility using high-temperature gas chromatography. *LC-GC*, **4**, 2, pp 28-29.

McKirdy, D.M., Summons, R.E., Padley, D., Serafini, K.M., Boreham, C.J., and Struckmeyer, H.I.M. (1994), Molecular fossils in coastal bitumens from Southern Australia - signatures of precursor biota and source-rock environments. *Organic Geochemistry*, **21**, 3-4, pp 265-268

McLafferty, F.W. and Tureček, F. (1993), *Interpretation of Mass Spectra*, fourth edition. University Science Books, California.

Meinschein, W.G. and Kenny, G.S. (1957), Analyses of a chromatographic fraction of organic extracts of soils. *Analytical Chemistry*, **29**, 8, pp 1153-1161.

Middleditch, B.S. (1989), *Analytical Artifacts*. Elsevier, New York, USA.

Miles, A.A. and Misra, S.S. (1938), *Journal of Hygiene*, Cambridge, **38**, pp 732-738.

Miles, J. A. (1989), *Illustrated Glossary of Petroleum Geochemistry*. Oxford Science Publications.

Mille, G., Almallah, M., Bianchi, M., van Wambeke, F. and Bertrand, J. C. (1991) Effect of salinity on petroleum biodegradation. *Fresenius' Journal of Analytical Chemistry*, **339**, pp 788-791.

Miller, J. C. and Miller J. N. (1988), *Statistics for Analytical Chemical Second Edition*. Miller/Ellis Horwood Limited.

Moffatt, B. (1991), *Personal Communications*. PVT Research group, British Gas plc Research Centre, Loughborough, Nottinghamshire.

Monod, J. (1949), The growth of bacterial cultures. *Annual Review of Microbiology. Vol III*, pp 371-394.

Murphy, R.C., Djuricic, M.V., Markey, S.P. and Biemann, K. (1969), Acidic components of Green River shale identified by a gas chromatographic-mass spectrometry computer system. *Science*, **165**, pp 685-697.

Neto, F.R.D., Cardoso, J.N., Pereira, A.D. Fernandes, M.C.Z., Caetano, CA.O. and Machdo, A.L.D. (1994), Application of high resolution gas chromatography to the paraffinic deposits in petroleum production pipielines. *Journal of High Resolution Chromatography*. **17**, 4, pp 259-263.

Newley, T.M.J. and Merrill Jr., (1989), Pseudocomponent selection for compositional simulation. *Society of Petroleum Engineers Journal*, **19638**, pp 117-127.

Noel, F. (1988), Simulated distillation of petroleum distillates using capillary columns. *Journal of High Resolution Chromatography and Chromatography Communications*, **11**, pp 837-839.

Novotony, M., Ramon, S., and Albert, Z. (1971), High temperature gas chromatographic separations using glass capillary columns and carborane stationary phases. *Analytical Chemistry*, **44**, 1, pp 9-13

Okera, W. (1974), Tar pollution of Sierra Leone beaches. *Nature*, **252**, pp 682-685.

Padley, D., McKirdy D.M., Tewkesbury P.S. and Bye J.A.T. (1991), Coastal Bitumen Types and Stranding patterns in South Australia and Western Victoria. *Australian Organic Geochemistry Conference (Abstract)*. pp 11-12.

Patience, R.L., Rowland, S.J., and Maxwell, J.R. (1978), The effects of maturation on the configuration of pristane in sediments and petroleum, *Geochimica et Cosmochimica Acta*, **42**, pp 1871-1875.

Peaden, P.A., Wright, B.W. and Lee, M.L. (1982), The preparation of non-extractable methylphenylpolysiloxane stationary phases for capillary column gas-chromatography. *Chromatographia*, **54**, 7, pp 1090-1093.

Pedersen, K.S., Fredenslund, Aa., and Thomassen, P. (1989), Properties of oils and natural gases. *Contributions in petroleum geology and engineering*, Vol 5, Gulf Publishing Company.

Peters, K.E. and Moldowan, J.M. (1993), *The biomarker guide*. Pretice Hall, Inc.

Philp, R.P. (1985), *Fossil fuel biomarkers, applications and spectra*. Elsevier, Oxford.

Philp, R.P. (1994), High temperature gas chromatography for the analysis of fossil fuels: A review. *Journal of High Resolution Chromatography*, **17**, pp 398-406.

Pollock, G. E. (1972), Capillary gas chromatography with two new moderately high temperature phases. *Analytical Chemistry*, **44**, 3, pp 634-635.

Poy, F., Visani, S. and Terrosi, F. (1981), Automatic injection in high resolution gas chromatography - A programmed temperature vaporizer as a general-purpose injection system. *Journal of Chromatography*, **22**, 41, pp 81-90.

Pretorius, W.G., Ebdon, L. and Rowland, S.J. (1993), Development of a high temperature gas chromatography inductively coupled plasma mass spectrometry interface for the determination of metalloporphyrins. *Journal of Chromatography*, **646**, pp 369-375.

Quinlan, M. (1991), North Sea activity at record levels. *The North Sea*, pp 3-4.

Ratledge, C. (1978), Degradation of aliphatic hydrocarbons, Whatkinson, R. J. (ed) in *Developments in Biodegradation of Hydrocarbons*, Chapter 1, pp 1-111.

Ray, S.M., Oja, R.K., Jeffery, L.M. and Presley, B.J. (1974), A quantitative and qualitative study survey of oils and tars stranded on Galveston Island beaches. *Department of Transport, U.S. Coast Gaurd Report No GC-D-10-75.*

Reddy, P.G., Singh, H.D., Roy, P.K. and Barauh, J.N. (1982), Predominant role of hydrocarbon solubilization in the microbial uptake of hydrocarbons. *Biotechnology and Bioengineering*, **XXIV**, pp 1241-1269.

Revill, A. (1992), *Characterisation of Unresolved Complex Mixtures of Hydrocarbons by Degradative Methods*. PhD thesis, University of Plymouth.

Revill, A. (1992), Use of oxidative degradation followed by capillary chromatography-mass spectrometry and multidimensional scaling analysis to finger print unresolved complex mixtures of hydrocarbons. *Journal of Chromatography*, **589**, pp 281-286.

Robson, J. and Rowland S.J. (1990), Biodegradation of highly branched isoprenoid hydrocarbons: A possible explanation of sedimentary abundance. *Advances in Organic Geochemistry*, **13**, pp 691-695.

Rønningsen, H.P. and Skjevrak, I. (1990), Characterisation of North Sea petroleum fractions: Aromatic ring class distribution. *Energy & Fuels*, **4**, pp 608-626.

Rood, D. (1991), *A Practical Guide to the Care, Maintenance, and Troubleshooting of Capillary Gas Chromatography Systems*. Heidelberg: Hüthig, 1991.

Rose, M.E. and Johstone, R.A.W. (1982), *Mass Spectrometry for Chemists and Biochemists*. Cambridge University Books.

Rossini, F.D., Mair, B.J., and Streiff, A.J. (1953), *Hydrocarbons from Petroleum* (API Research project 6). ACS Monograph series, Reinhold, NY, USA.

Rowland, S. J. and Revill, A. T. (1995), Chapter 5; Chromatography in petroleum geochemistry. In *Chromatography in the Petroleum Industry*. Adlard, E. R. (ED) Journal of chromatography library series, **56**. pp 127-141. Elsevier Science B.V.

Sandra, P., and Verzele, M. (1977), Surface treatment, deactivation and coating in (GC)2 (glass capillary gas chromatography). *Chromatographia*, **10**, 8, pp 419-25.

Sandra, P (1990), High temperature capillary gas chromatography (HT-CGC): Possibilities and limitations. *Eleventh International Symposium on Capillary Chromatography*. Monterey, California, pp 21-25.

Sandra, P. and David, F. (1990), Microcolumn chromatography for the analysis of detergents and lubricants part 1. High temperature capillary gas chromatography (HT-CGC) and capillary supercritical fluid chromatography (CSFC). *Eleventh International Symposium on Capillary Chromatography*. pp 382-392.

Šepič, E., Leskovšek, H. and Marsel, J. (1994), Aerobic bacterial degradation of selected polyaromatic compounds and *n*-alkanes found in petroleum. (In Press).

Setti, L., Lanzarini, G., Pifferi, P.G. AND Spagna, G. (1993), Further research into aerobic degradation of *n*-alkanes in a heavy oil by a pure culture of a *Pseudomonas spp. Chemosphere*, Vol 26, **6**, pp 1151-1157.

Sewell, P.A. and Clarke, B. (1987), Chromatographic Separations. Kealey, D. (ED), *Analytical Chemistry by Open Learning*, John Wiley & Sons, New York, USA.

Schomburg, G., Belhau, H., Dielmann, R., Weeke, F. and Husmann, J. (1977), *Journal of Chromatography*, **142**, pp 87-95.

Shannon, L.V. and Chapman, P. (1983), Explanation for the vulnerability of the Arniston-Mossel bay region to pollution by oil and tar balls. *South African Journal of Science*, **79**, 4, pp 164-167.

Simkins, S. and Alexander, M. (1984), Models for mineralization kinetics with the variables of substrate concentration and population density. *Applied and Environmental Microbiology*, **47**, 6, pp 1299-1306.

Singer, M.E. and Finnerty, W.R. (1984), Microbial metabolism of straight chain and branched alkanes, Atlas, R.M. (ed). *Petroleum Microbiology*, Macmillan Publishing Company, pp 1-59.

Smith, L. (1991a), Oil and gas projects head for a climax. *The North Sea*. pp 8-10.

Smith, L. (1991b), Ambitious targets planned for Bruce. *The North Sea*. pp 12-11.

Standen, G. (1992), *Carbon Skeletal Typing of Sedimentary Organic Matter*. Ph.D Thesis University of Bristol.

Tabak, H.H., Gao, C., Desi, S. and Govind, R. (1992), Development of predictive structural-biodegradation relationship models with use of respirometrically generated biokinetic data. *Water Science Technology*, **26**, 3, pp 763-772.

Tabak, H.H. and Govind, R. (1992), Prediction of biodegradation kinetics using a nonlinear group contribution method. *Environmental Toxicology and Chemistry*, **12**, pp 251-260

Takla, M. (1992), Embla, first HT/HP oil development. *EUROIL*, pp 78-77.

Termonia, M., Munari, F., and Sandra, P. (1987), High oven temperature-cold on-column injection for automated CGC analysis of high molecular weight compounds such as triglycerides. *Journal of High Resolution Chromatography and Chromatography Communications*, **10**, pp 263-268.

Thomas, K.V. (1995), *Characterisation and Environmental Effects of Unresolved Complex Mixtures of Hydrocarbons*. Ph.D thesis University of Plymouth.

Thompson, J.S. and Ryanski, A.F. (1992), Simulated distillation of wax samples using supercritical fluid and high temperature gas chromatography. *Journal of High Resolution Chromatography*. **15**, pp 227-235.

Thompson, S. and Eglinton, G. (1978), Composition and sources of pollutant hydrocarbons in the Severn Estuary. *Marine Pollution Bulletin*, **9**, 133-136.

Tipler, A. and Johnson, G. (1990), Optimization of conditions for high temperature capillary gas chromatography using split-mode programmable temperature vaporizing injection system. *Journal of High Resolution Chromatography*, **13**, pp 365-370.

Tissot, B.P. and Welte, D.H. (1984), *Petroleum Formation and Occurrence*. Springer-Verlag, New York, USA.

Toth, T. and Garay, F. (1994), Separation of novolac resin oligermers and related industrial materials by high temperature capillary gas chromatography. *Journal of High Resolution Chromatography*, **17**, 3, pp 177-179.

Testianu, S., Zilloli, G., Sironi, A., Saravalle, C., Munari, F., Galli, M. Gaspar, G., Colin, J.M. and Jovelin, J.L. (1985), Automated simulated distillation of heavy petroleum fractions up to 800°C TBP by capillary gas chromatography. Part 1 possibilities and limits of the method. *Journal of High Resolution Chromatography and Chromatography Communications*. **8**, pp 771-781.

Tremonia, M., Munari, F. and Sandra, P. (1987), High oven temperature - cold on-column injection for the automated CGC Analysis of High molecular weight compounds such as triglycerides. *Journal of High Resolution Chromatography and Chromatography Communications*, **10**, pp 263-268.

Tříska, J., Kuraš, M., Vodička, L. and Šafář, M. (1984), Determination of the composition of a high-boiling condensate from natural gas by gas capillary gas chromatography. *Fresenius' Z. Analytical Chemistry*, **318**, pp 407-409.

Tulloch, A.P. (1973), Comparison of some commercial waxes by gas liquid chromatography. *Journal of the American Oil Chemists Society*, **50**, pp 367-371.

Tuttle, R.N. (1983), High-pour-point and asphaltic crude oils and condensates. *Journal of Petroleum Technology*, **35**, pp 1192-1197.

United Nations Environmental Programme (1980), Summary of reports on the scientific results of MED POL, Part 1. *UNEP/IG 18/INF 3*. pp 202.

Urabe, Y. and Takamizawa, K. (1994), The determination of the homologous purity of higher normal alkanes up to dohectane with capillary gas chromatography. *Polymer Journal*, **26**, 3, pp 283-289.

Urano, K. and Kato, Z. (1986a), Evaluation of biodegradation ranks of priority organic compounds. *Journal of Hazardous Materials*, **13**, 2, pp 147-159.

Urano, K. and Kato, Z. (1986b), A method to classify biodegradabilities of organic-compounds. *Journal of Hazardous Materials*, **13**, 2, pp 147-159.

Venosa, A.D., Haines, J.R., Nisamaneepong, W., Govind, R., Pradhan, S. and Siddique, B. (1992), Efficacy of commercial products in enhancing oil biodegradation in closed laboratory reactors. *Journal of Industrial Microbiology*, **10**, pp 3-23.

Vogel, A. (1981), *Textbook of Practical Organic Chemistry: Fourth Edition*, Longman, London.

Warth, A.H. (1956), *Chemistry and Technology of Waxes*, 2nd edition.

Whitson, C.H. (1983), Characterizing hydrocarbon plus fractions. *Society Of Petroleum Engineers Journal*, August, pp 683-694.

Wolff, G.A., Preston, M.R., Harriman, G. and Rowland, S.J. (1993), Some preliminary observations after the wreck of the oil tanker Braer in Shetland. *Marine Pollution Bulletin*, **26**, 10, pp 567-571.

Wood, P.S. (1969), High temperature gas chromatography of lipids. *Column*, **3**, 2, pp 7-9.

Yangming, Z. and Zhongyi, Z. (1991), Distribution characteristics of alkylcyclohexanes in lower palaeozoic strata on the northern margin of the Tarim Basin, China. *Chinese Journal of Geochemistry*, **10**, pp 80-87.

Yon, D.A., Maxwell, J.R. and Ryback, G. (1982) 2,6,10,-trimethyl-7-(3-methylbutyl)-dodecane, a novel sedimentary biological marker compound. *Tetrahedron Letters*, **23**, pp 2143-2146.

Zeng, Y.D. and Uden, P.C (1994), High-temperature gas-chromatography-atomic emission detection of metalloporphyrins in crude oils. *Journal of High Resolution Chromatography*, **17**, 4, pp 223-229.

Zilber, K., Rosenberg, E., and Gutnick, D (1980), Incorporation of ^{32}P and growth of pseudomonad UP-2 on *n*-tetracosane. *Applied and Environmental Microbiology*, **40**, 6, pp 1086-1093.

APPENDIX A

Conferences attended and presentations given.

CONFERENCES AND PRESENTATIONS

1. 13th International Symposium on Capillary Chromatography, 13-16, May 1991, Riva del Garda, Italy.
2. British Association: "Science '91", Polytechnic South West, Plymouth, August 28, 1991.
3. 15th International meeting on Organic Geochemistry, September 16-20, 1991, Manchester, U.K.
4. Geological Society Petroleum Group meeting, 2-3 June, 1992, Geological Society, Burlington House, London. Poster Presentation.
5. Annual meeting of the British Organic Geochemistry Society, Newcastle, 1992, Poster Presentation.
6. Annual meeting of the British Organic Geochemistry Society, 20-23 July, 1993, Plymouth. Poster Presentation.
7. "HTCGC of Waxy Gas-Condensates", Oral presentation, British Gas plc, Research and Technology Division. 1991, London Research Station.
8. "HTCGC of Waxy Gas-Condensates", Oral presentation, University of Plymouth. 1991, Plymouth, England.
9. "HTCGC of Waxy Gas-Condensates", Oral presentation, University of Plymouth. 1992, Plymouth, England.
10. "Biodegradation of waxy oils", Oral presentation, University of Plymouth. 1993, Plymouth, England.

APPENDIX B

Lectures attended, associated study and visits.

LECTURES AND VISITS

1. Royal Society: Analytical Division (South West), lectures, 1991-1994.
2. NERC/Joel Mass Spectrometry Facility, September 1991, University of Swansea, Wales.
3. Weekly seminars at University of Plymouth, 1991-1995, Plymouth.
4. Fortnightly seminars at Plymouth Marine Laboratory, 1991-1995, Plymouth, England.
5. SERC (CRAC) Graduate School, 16-21 July, 1992, University of York, York.